SKB

TECHNICAL REPORT 89-19

Characterization of fracture zone 2, Finnsjön study-site

Editors: K. Ahlbom, J.A.T. Smellie
Swedish Geological Co, Uppsala

Augusti 1989

SVENSK KÄRNBRÄNSLEHANTERING AB
SWEDISH NUCLEAR FUEL AND WASTE MANAGEMENT CO

BOX 5864 S-102 48 STOCKHOLM
TEL 08-665 28 00 TELEX 13108-SKB

CHARACTERIZATION OF FRACTURE ZONE 2, FINNSJÖN STUDY-SITE

August 1989

CHARACTERIZATION OF FRACTURE ZONE 2, FINNSJÖN STUDY-SITE

PART 1

OVERVIEW OF THE FRACTURE ZONE PROJECT AT FINNSJÖN, SWEDEN

K. Ahlbom and J.A.T. Smellie

Swedish Geological Company, Uppsala, Sweden

August 1989

OVERVIEW OF THE FRACTURE ZONE PROJECT AT FINNSJÖN, SWEDEN.

K. AHLBOM and J.A.T. SMELLIE.

Swedish Geological Company, Box 1424, 751 44 Uppsala, Sweden.

Abstract.

At the Finnsjön site, central Sweden, a 100 m wide low angle fracture zone in granodiorite, Zone 2, has been studied by means of borehole investigations. This has included core and geophysical logging as well as hydraulic tests and groundwater sampling. Zone 2 was developed 1.6 - 1.7 Ga as a ductile shear zone at a depth of ca.10-15 km and repeated reactivation has occurred during Precambrian time and later. Today, the upper boundary of the zone is defined in nine boreholes at depths ranging from 100-295 m. Pumping tests have demonstrated that the upper part of the zone is highly water conductive with a transmissivity in excess of 10-3 m2/s. From tracer tests the equivalent single fracture conductivity was calculated to be 0.03-0.2 m/s. This extremely high transmissivity and conductivity over such a large areal extent can be speculated to be the result of recent opening of Zone 2 during the last inland ice period.

In-situ measurements of the natural groundwater flow show that the flow is high (67-90 $m^3/m^2 \cdot year$) at the upper boundary of Zone 2, while near-stagnant conditions occur at the lower boundary, and in the relict saline water beneath the zone. Isotope data suggest a complex origin to the saline water. The hydraulic head measurements as well as the groundwater chemistry strongly suggest that the low angle Zone 2 acts as a hydraulic barrier preventing groundwater from percolating downward through the zone.

These studies have helped to focus on repository safety assessment problems which hitherto had been oversimplified for the benefit of performance models. Furthermore, the results have shown that these low angle large-scale fracture zones are likely to be even more important controls than steep zones, when considering bedrock stability, rock stress regimes, and lateral groundwater flow patterns. Quantification of such phenomena should provide an invaluable input into the various safety assessment performance codes for model validation and siting criteria for a repository.

1. Introduction.

The safety of a repository for spent nuclear fuel in crystalline rock is strongly related to groundwater flow, groundwater chemistry and migration of radionuclides. These factors are in turn dependent on the amount and distribution of groundwater flow in the bedrock. When assessing the safety of a repository it is therefore necessary to locate and characterise the pathways for groundwater flow. Fracture zones are in this respect important since they constitute the main pathways for groundwater in crystalline rock, and also constitute the potential planes of future displacements on different rock blocks boundaries. The distribution and geometry of fracture zones will also determine the lay-out of a repository.

In the safety assessment analyses made for the KBS-studies in Sweden (KBS-3, 1983), the repository was assumed to be situated in a structurally demarcated rock unit of relatively low hydraulic conductivity, at least 100 m from the nearest highly conductive disconformity or major fracture zone which would provide direct access to the biosphere. Within this rock unit or 'block' the groundwater was expected to flow slowly from places of higher to lower potential via a system of minor fractures and fissures, thus providing maximum surface area for the retardation of, for example, those potentially dangerous actinides which may have been released during breakdown of the engineered barriers containing the spent fuel. Rapid groundwater transport of residual actinides to the biosphere is assumed to occur when the large-scale fracture zones/lineaments which bound the rock unit/block are intercepted. It is therefore obvious that fracture zones and their geometry will strongly affect the overall performance of a repository. What is worrying, however, is the presently prevailing general lack of understanding of the hydraulic, mechanical, chemical and retardation properties of these zones. This was exemplified in the past by the KBS-studies which made the over-conservative assumption that the fracture zones are completely open to groundwater flow, resulting in an unrealistic rapid radionuclide transportation between the repository and the biosphere. Since then the complexities of water flow have been increasingly demonstrated, for example, it is only recently that the concept of channeling, i.e. water flow within fracture planes along a discrete system of anastomosing channels, has come to the fore. Although of no surprise to the geological fraternity, the impact of such a concept in safety assessment considerations is far-reaching and must be given serious consideration (Abelin et al., 1985). For example, in a disposal concept based on flow distribution along discrete channels, there exists the possibility that the majority of canisters will not come into contact with the groundwater circulation; a minority, however, will be subjected to increased contact with the groundwater flow. To date, the impact of channeling on repository safety assessment analysis has not yet been fully evaluated.

Generic studies of fracture zones have therefore been initiated by the Swedish Nuclear Fuel and Waste Management Company (SKB) to further quantify the safety performance of the geosphere barriers. These studies comprise two main projects, characterisation of fracture zones in tunnels, and, borehole studies of a fracture zone at the Finnsjön site, central Sweden.

The tunnel study aims to evaluate the considerable amount of data regarding fracture zones that are available from Swedish underground projects (Palmqvist and Stanfors, 1987). Fracture zones are classified into different types and the hydraulic characteristics of each type are discussed. In the characterisation, emphasis is given to evidence of hydraulic channeling (Neretnieks et. al., 1987).

In this report a series of papers discussing the Fracture Zone Project at Finnsjön are presented. The project involves a series of in situ borehole studies in order to understand and quantitatively describe the hydraulic, geochemical and migrational properties of one specific fracture zone. The project has also provided the opportunity to test and evaluate new drilling and groundwater sampling techniques which are new to the SKB programme of site characterisation.

This introductory paper aims to present an overview of the results of the project hitherto, and a discussion of the possible implications to repository safety assessment.

2. The Fracture Zone Project at Finnsjön.

The Finnsjön site is located in central Sweden, about 140 km north of Stockholm (Fig. 1). The site has a flat topography with differences in altitude of less than 15 m. The area is covered to 85% by Quaternary sediments, mainly till.

The last inland ice disappeared from the area around 10000 years ago whereafter the region was subjected to the marine transgressions of the Yoldia (ca. 8500-9500 years ago) and the later Litorina (ca. 2500-7500 years ago). Between ca. 2300 - 800 years ago uplift of the Finnsjön area above sea-level occurred. The present rate of isostatic uplift is approx. 6 mm/year.

The Finnsjön site was investigated mainly from 1977-1978 to assess its suitability to host a repository for reprocessed nuclear waste; ancillary studies continued at the site until 1982. This investigation included 8 cored boreholes, down to 700 m depth, and extensive borehole geophysical, geochemical and hydraulical measurements. Due to the tectonic complexity of the area, coupled with a tight time schedule at that juncture

of the SKB programme, no further work or detailed interpretation was possible. However, a few years later, the hydrogeological character of the area, together with its geographical position, made it a suitable choice for further detailed studies of water flow in a fractured rock medium.

The present fracture zone study at Finnsjön commenced in 1985 and has included the drilling of three cored boreholes and three percussion drilled boreholes. The project is divided into four components:

- preliminary characterisation
- detailed characterisation
- predictive modelling of tracer transport and hydraulic interference tests
- tracer tests

The two first components have been completed (Ahlbom et al., 1986, 1988; Andersson et al., 1988) and the third and fourth components have recently been started. The final report for the project is planned for 1990.

3. Characterisation of Fracture Zone 2.

Earlier tectonic studies in the Finnsjön area (Ahlbom et al., 1986) defined and characterised three major fracture zones, Zones 1-3, two of which have been studied in detail (Fig. 1). The Brändan fracture zone (Zone 1; width of about 20 m and striking NNE with a dip of 75 degrees to the east) is topographically expressed as a minor gully traceable for more than 500 m, and from surface geophysical measurements to extend for at least 1 km. A low angle fracture zone (Zone 2; trending north with a dip of 16 degrees to the southwest) is defined only from borehole data.

3.1 Selection and geometry

The low angle fracture zone, Zone 2, was selected for two main geoscientific reasons: a) that the hydraulically active character of Zone 2 should permit studies of retardation properties using tracer tests under natural groundwater flow conditions, and, b) that new techniques should be evaluated for the detection and characterisation of sub-horizontal fracture zones. Since the project was restricted to borehole studies, it was also considered advantageous to select a low angle zone since this would facilitate the use of near-vertical boreholes.

Zone 2 is defined by eight boreholes located within an area of approx. 500 m x 500 m in the northern part of the Finnsjön site. The fracture zone is almost planar within this area, with the upper boundary located between 100 to 240 m below the ground surface. Zone 2 strikes N 28 W with the upper zone boundary dipping some 16 degrees to the southwest. The location

of the lower surface is somewhat uncertain. In general, Zone 2 is interpreted to have a width of about 100 m. Outside this area, Zone 2 is interpreted to occur in borehole KFI07 at a depth of 295 m. However, at this distance the zone cannot be followed as a continuous plane. Instead, faulting on later formed and steeply dipping fracture zones appears to have displaced Zone 2. The zone has not been identified in the deep (700 m) cored boreholes located southeast of the steeply dipping Zone 1 (Fig. 1). A cross-section of Zone 2 is presented in Figure 3.

3.2 Geology

The geologic evolution and character of the Finnsjön site and Zone 2 is presented by Tirén (this volume). A short summary is presented below.

Within the Finnsjön area the predominant rock is a greyish, medium-grained and foliated granodiorite; minor amounts of pegmatite, metabasite and aplite also occur. The granodiorite is bordered to the east by a reddish young granite and to the northeast by a layered gabbro. Metavolcanic rocks occur to the west and to the south of the site. With the exception of the young granite, all rock units have been deformed during the Svecokarelian orogeny (ca. 1.85 Ga). At this time the granodiorite was transformed into a gneiss now characterised by a steeply dipping and uniform foliation.

Zone 2 was formed more than 1.6-1.7 Ga as a some hundred metres wide ductile shear zone at a depth of ca. 10-15 km, and considered to be the product of repeated shear movements. The deformation has resulted in the frequent occurrence of mylonites, cataclastic rocks and high frequency of sealed fractures. Late reactivation of Zone 2 seems to occur preferentially along the upper boundary of the zone. The granodioritic bedrock above the zone is relatively unfractured and unaltered, while the rock below the zone contains inliners of fault rocks and is generally characterised by a higher degree of fracturing.

A somewhat surprising observation is that the fracture frequency is low, on average 5 fr/m, within Zone 2, which is only slightly greater than in the country rock. In contrast, the frequency of sealed fractures is greater in most parts of the zone, with infillings mostly of hydrothermal origin. According to Tullborg and Larson (1982) and Tiren (this volume), the sequence of fracture infilling, from oldest to youngest, is:

* Epidote and calcite (associated with mylonitic and cataclastic processes).
* Prehnite and calcite/quartz.
* Haematite, laumontite, prismatic calcite and quartz.
* Chlorite and calcite.

Most of the fractures are considered to be initiated early in the geologic history and reactivated several times. Geological dating using Rb-Sr indicate ages of 1.6-1.5 Ga for epidote and 1.25-1.1 Ga for prehnite (Wickman et al., 1983). Fractures which are potentially young, i.e. no evidence of reactivation and lacking hydrothermal minerals, are rare.

3.3 Hydraulic character.

A great number of hydraulic tests have been made to characterise Zone 2 and the near-vicinity. A summary of these tests is presented below. Detailed discussions regarding the hydraulic properties of Zone 2 and groundwater flow are presented by Andersson et al.(this volume).

Single-hole injection tests for many of the boreholes showed a general decrease in hydraulic conductivity with depth for the bedrock above Zone 2 (Fig. 2). This decrease is sharply interrupted by Zone 2, where the hydraulic conductivity increases by one to four orders of magnitude to values between 10^{-6}-10^{-5} m/s (measured in 20 m sections). Using much smaller packer intervals, 2 m and 0.11 m respectively, the latter only in borehole BFI02, provided a unique opportunity to investigate the hydraulic properties in detail along these sections. The 0.11 m tests indicated that the most conductive parts of Zone 2 merely consist of a few very narrow subzones with a width of only about 0.5 m in the boreholes. The uppermost of these subzones, which coincides with the upper boundary of Zone 2, proved to be highly conductive. This subzone can be correlated in all boreholes within the studied area.

Towards the bottom of the zone several alternating thin intervals of very high hydraulic conductivity exist; more than 10^{-4} m/s was measured in 20 m sections. These conductive intervals are separated by bedrock with low hydraulic conductivity. Below the zone the conductivity is in general low, 10^{-10}-10^{-9} m/s, but several minor sections with high conductivity still occur.

Given the narrow widths of the subzones, the hydraulic properties of Zone 2 should preferably be expressed in terms of transmissivity rather than average hydraulic conductivity of longer test sections. The transmissivity of each subzone was estimated at $1\text{-}4 \cdot 10^{-3}$ m^2/s. The hydraulic conductivity in the vertical direction of Zone 2, assuming an equivalent porous medium between the upper and lower part of the zone, was estimated at about 10^{-6} m/s. Zone 2 thus shows a pronounced vertical anisotrophy.

3.4 Groundwater flow

Registration of the groundwater head indicates that in the western and deeper part of the Zone 2, groundwater from the overlying bedrock infiltrates into the upper, highly conductive part of the zone. This water is then discharged within the zone to its eastern part where the groundwater head is higher than that of the adjacent bedrock. Gustafsson and Andersson (this volume) have demonstrated this groundwater flow pattern using tracers under natural hydraulic gradient conditions between borehole KFI11 in the western part, and borehole HFI01 in the eastern part of the Zone 2 (Figs. 2 and 3). The distance between the boreholes is approx. 400 m and the tracers have been transported along this distance in about one month. The equivalent single fracture conductivity of the upper part of Zone 2, calculated from this tracer test, is between $3 \cdot 10^{-2}$ - $2 \cdot 10^{-1}$ m/s.

The groundwater flow was also measured in situ in two boreholes by using a borehole point dilution probe (Gustafsson, 1986; Gustafsson and Andersson, this volume). The point dilution technique is the only method available where estimation on natural groundwater flow rates does not have to rely on measuring "capacity to flow" (i.e. hydraulic conductivity) and "cause of flow" (i.e. hydraulic gradient) separately.

The results showed that the natural groundwater flow in Zone 2 is concentrated along its upper boundary; the obtained values in the two boreholes were 67 and 90 $m^3/m^2 \cdot$year respectively. In the lower parts of Zone 2, no flow could be measured in the tested sections of high hydraulic conductivity. This indicates that no driving force, i.e. no hydraulic gradient, is present below the upper boundary of Zone 2. In the bedrock above Zone 2, the groundwater flow is in general moderately high, with high values recorded from 0-50 m depth, and lower values from 50-230 m depth.

Taking into consideration the hydraulic and groundwater flow properties of Zone 2, estimates of the total groundwater discharge at the eastern rock boundary (approx. 1000 m wide) was found to range from 150 000-340 000 m3/year. However, when compared to a rough estimate of 500-5000 m3/year derived from groundwater recharge to the zone, an extremely high discrepancy exists. The recharge calculation was based on inadequate hydraulic data from the vertical to sub-vertical fractures in the Finnsjön area, i.e. those which provide the most rapid recharge flow to Zone 2. A two-fold increase in recharge volume is required to show agreement between all three hydraulic estimations. An annual precipitation of 685 mm is inadequate, and so it is assumed that the measured groundwater flow in Zone 2 is a combination of both precipitation and regional flow

sources. Agreement with all three estimates results in an aperture width of 1.4 mm for an equivalent single fracture.

3.5 Groundwater chemistry

All boreholes intersecting Zone 2 show a strong increase in groundwater salinity at the upper boundary of Zone 2. The salinity increases from fresh water above Zone 2 to 5500 mg/l Cl- below the upper boundary of Zone 2. At increasing depths, the salinity remains uniformly high. The origin of the saline water is complex, and involves mixing of waters from several sources (Smellie and Wikberg, this volume). In general, however, the saline water can be regarded as an old relict water, at least in comparison with the fresh water above Zone 2. This is in agreement with the groundwater flow determinations which indicate near stagnant conditions where the saline water is encountered.

A schematic model showing the main structural and hydraulic characteristics of Zone 2 is presented in Figure 3. In the model the main part of the groundwater transport is assumed to take place in the upper, most conductive part of the zone. Below Zone 2 there may be some circulation of saline water towards the zone, as indicated in the figure, but the flow-rate is probably very low when compared to the fresh water above the zone.

4. Summary and Discussion.

Investigations of Zone 2 at the Finnsjön site show a long tectonic history of reactivation, most of which occurred during Precambrian time. Today, most of the early initiated fractures are sealed and the frequency of potentially open fractures are low for the major part of Zone 2. Taking into consideration previous experience from other site specific studies in crystalline bedrock environments, and bearing in mind the limited number of fractures in the zone, and the wide areal distribution of the boreholes, either a low hydraulic conductivity, or, strongly variable conductivity between the different boreholes, was expected for Zone 2. It was therefore somewhat surprising that the hydraulic conductivity was high in all nine boreholes at the upper boundary of Zone 2. Moreover, the depth of intersection of Zone 2 could be accurately predicted within the investigated northern part of the Finnsjön site of areal extent 500x500 m. One is without doubt dealing here with a large-scale, uniform, and open low angle fracture zone, of much greater dimensions and hydraulic potential than could have originally been envisaged.

The question arises whether Zone 2 may be regarded as representative for other low angle fracture zones in crystalline rock. Although several such fracture zones have been encountered in other study sites in Sweden, only one has been subjected to hydraulic interference testing. This zone, located in Forsmark close to the Finnsjön area, recorded a transmissivity about two orders of magnitude lower than for Zone 2 (Carlsson et al., 1986). Examples from the Underground Research Laboratory (URL) site in Manitoba, Canada (Davidson, 1984; Davidson and Guvansen, 1985) show that the hydraulic conductivity varies strongly within each of the three encountered low angle fracture zones. Values between 10-4m/s to 10-10m/s have been reported. In conclusion, therefore, the few available data regarding the hydrological properties of low angle fracture zones do not permit any conclusive insight into how general and representative the hydraulic properties of Zone 2 at Finnsjön really are.

One plausible explanation for the generally uniform high hydraulic conductivity of Zone 2 can be a recent opening of the zone. Talbot (1989) argues that high hydrostatic pressure beneath an inland ice sheet might hydraulically open existing large-scale horizontal or low angle fracture zones at the ice sheet margins. Since the last ice cover over Sweden is estimated to have had a maximum thickness of 3 km, this type of opening could have occurred down to a maximum depth of 1 km. Recent hydraulic fracturing stress measurements in Finnsjön (Bjarnason and Stephansson, 1988) revealed the predominance of a horizontal stress field at depths equivalent to Zone 2. This may explain why Zone 2 has remained open since ice melt. Because of the short time-period since the last glaciation, no significant reactivation/alteration or fracture infilling process, that could otherwise have sealed parts of the fracture system, would have occurred.

In support of the hydraulic conductivity values, tracer tests and groundwater flow measurements both show a large and rapid movement of groundwater along the upper boundary of Zone 2. Below this boundary measurements indicate more or less stagnant groundwater conditions; this is supported by the presence of old relict saline water at depth in this part of the bedrock.

The upper boundary of Zone 2 therefore acts as an efficient structural/hydraulic boundary to the bedrock groundwater cells of circulatory movement. As a result, the downward moving fresh water preferentially spreads out along the upper, more conductive levels of Zone 2, rather than continue to deeper levels to mix and flush out the older saline waters. Similarly, any movement at greater depths in the saline water will tend to be upwards until the highly conductive levels are reached. Zone 2 is therefore a horizon along which groundwaters of con-

siderable contrasting age and chemistry come into contact and partially mix with one another. Furthermore, this mixing has produced a highly supersaturated water resulting in the precipitation of calcite, thus partly forming a `seal' which in turn further enhances the physico-chemical boundary between these two groundwater environments.

As pointed out by Tiren (this volume), the general occurrence of low angle zones in cratonic areas has been generally underestimated. Further evidence from Sweden (e.g. Forsmark, Dannemora, and Lansjärv in Norrbotten), Finland (Hästholmen), and particularly at the Underground Research Laboratory (URL) in Canada, show that highly permeable low angle fracture zones tend to be the norm rather than the exception. It would appear that such low angle fracture zones are likely to be even more important controls than steep zones on bedrock stability, rock stress regimes and the lateral flow of groundwater (Talbot, 1989). There is an acute need to recognise such zones from the surface.

What are the ramifications of these studies at Finnsjön for safety assessment considerations? Let us first tackle the general concept of groundwater flow by channeling. There is no doubt that in the majority of cases in crystalline bedrock groundwater does not flow uniformly across a fracture plane. An anastomosing network of channels or pathways, which continuously change in shape and direction coeval with fracture reactivation or mineral precipitation, most probably serve to conduct the water through the fracture zones. Thus, intersection of a hydraulically conductive fracture zone in one borehole may not be reflected in a closely adjacent borehole, even though the same zone has been penetrated. This is a common situation which has frustrated many a tracer test.

However, what does one find at Finnsjön? One finds a large-scale, low angle, highly conductive fracture zone, which shows a fast response from both hydraulic and tracer tests over distances of up to 400 m, and, irrespective where this zone is intercepted by drilling, the same upper part of the zone has similar hydraulic properties. This uniformity of character would strongly argue against channeling in this particular case; it is highly unlikely that the same system of channels could be intercepted over such a large area. It is more plausible, as these present studies indicate, that the fracture Zone 2 is quite simply open and highly permeable over its areal extent. As this is the probable case, then the radionuclide retardation potential of such a fracture zone should be affected. For example, fast flow coupled with increasing dilution should result in a reduction of radionuclide retardation effects. It will therefore be interesting when the third and fourth components of this project (e.g. selective tracer testing along Zone 2) are completed this year (1989).

These studies have also shown that the salt groundwater environment below the physico-chemical barrier imposed by Zone 2 is characterised by near-stagnant water flow conditions, and is clearly an old relict water of marine origin with modifications due to rock-water reactions. To locate a repository below this zone would, therefore, effectively shield the installation from the deep circulation of groundwater (possibly marginally oxidising) from above. This would appear to offer many advantages. The question is, however, for how long? Reoccurring glacial periods, and even the changes created in construction of the repository itself (during and after), may detrimentally influence the groundwater flow system and those groundwater chemical conditions which at the moment prevail within and below the fracture zones.

One can go one step further and speculate on the siting of a repository between two parallel sets of sub-horizontal zones; such tectonic phenomena are not uncommon. Locating a repository under these conditions would be even more ideal, with the hydraulic gradients being controlled by conducting fractures both above and below, with near-stagnant conditions being preserved between the fractures.

Hydrochemical studies have shown that the Finnsjön saline groundwaters, in common with many Finnish examples, have been the product of isostatic instability in the Fennoscandia Shield area due to repeated glacial events during recent geological time. Periods of uplift alternating with marine transgressions have resulted in the periodic flushing out of both fresh and saline water types within the bedrock. Within the time scales envisaged for repository safety (at least 100 000 years), similar events can be expected to occur in the future. In such instances, the presence of low angle zones may serve to minimise a change to more dynamic groundwater conditions, although ultimately changes in groundwater chemistry will be inevitable.

Excavation and construction of the repository may influence the adjacent hydraulic and chemical environment. This might initially be a constructive influence because of the groundwater head difference above and below Zone 2. Penetration through the zone, as shown from the borehole studies, will encourage an upward hydraulic gradient thus flushing the repository area free from any residual oxidants etc. introduced during construction, and at the same time preventing any downward movement of fresh, possibly marginally oxidising water, from higher levels. Furthermore, an upward hydraulic circulation in the near-vicinity of the repository may also result from thermal gradients arising from the emplacement of the spent fuel, estimated to be 70-100 degrees C. In the long-term, however, these artificially induced hydraulic gradients may eventually introduce recharge groundwaters from higher

levels in sufficient quantities to detrimentally influence the groundwater chemistry around the repository.

To conclude, these studies at Finnsjön have helped to focus on problems which hitherto had been oversimplified for the benefit of repository performance assessment models. The results have shown that these low angle, large-scale fracture zones, are likely to be even more important controls than steep zones when bedrock stability, rock stress regimes, and lateral groundwater flow patterns, have to be taken into consideration. However, there still remains the problem of extrapolating surface geological data to depths below such low angle zones, where considerable tectonic movement may have occurred. For example, traditional methods in surface mapping and geophysical measurements cannot be effectively employed. This means that information relating to such depths is restricted to borehole data.

Quantification of many of these phenomena, some of which is presented in this volume, should provide an invaluable input into the various safety assessment performance codes for model validation and siting criteria for a repository.

REFERENCES.

Abelin, H.I., Neretnieks, I., Tunbrant, S. and Moreno, L., 1985. Migration in a single fracture: Experimental results and evaluation. Final Rep., Stripa Project, Stockholm.

Ahlbom K., Andersson P., Ekman L., Gustafsson E., Smellie J. and Tullborg E-L., 1986., Preliminary investigations of a fracture zone in the Brändan area, Finnsjön study site. SKB Tec. Rep. (TR 86-05), Stockholm.

Ahlbom K., Andersson P., Ekman L. and Tirén S., 1988., Characterization of fracture zones in the Brändan area Finnsjön study site, central Sweden. SKB Status Rep. (AR 88-09), Stockholm.

Andersson, J-E., Ekman, L., Gustafsson, E, Nordqvist, R. and Tiren, S.A., 1988. Interference tests within the Brändan area, Finnsjön study site. SKB Tec. Rep. (In prep.).

Andersson, J-E., Andersson, P. and Gustafsson, E., 1989. Effects of gas-lift pumping on hydraulic borehole conditions at Finnsjön, Sweden. (This volume).

Andersson, J-E. and Nordqvist, R., 1989. Hydraulic testing and modelling of a low angle fracture zone at Finnsjön. (This volume).

Bjarnason, B. and Stephansson, O., 1988. Hydraulic fracturing stress measurements in borehole Fi06 Finnsjön Study Site, central Sweden. SKB Tec. Rep. (Submitted for publication).

Davison, C.C., 1984. Hydrogeological characterisation at the site of Canada's Underground Research Laboratory. In: Proceedings of the IAH International Symposium on Groundwater Resource Utilization and Contaminant Hydrogeology, Montreal, Canada. May 21-23, 1984.

Davison, C.C. and Guvanasen, V., 1985. Far-field hydrogeological monitoring at the site of Canada's Underground Research Laboratory. In: Proceedings of the 17th International Association of Hydrogeologists Congress on the Hydrogeology of Rocks of Low Permeability. Tuscon, Arizona, Jan. 7 -12.

Gustafsson, E., 1986. Determination of groundwater flow using a point dilution technique. SKB Status Rep. (AR-86 -21), Stockholm. (In Swedish).

Gustafsson, E. and Andersson, P., 1989. Groundwater flow conditions in a low angle fracture zone at Finnsjön, Sweden. (This volume).

KBS-3, 1983. Final storage of spent nuclear fuel - KBS-3. SKBF/KBS, Stockholm (5 Volumes).

Neretnieks, I., Abelin, H. and Birgersson, L., 1987. Some recent observations of channeling in fractured rocks - its potential impact on radionuclide migration. Proc. of DOE/AECL Conference on Geostatistical, Sensitivity, and Uncertainty Methods for Ground Water Flow and Radionuclide Transport Modelling. (Ed. Bruce Buxton). Battelle Press, Ohio.

Palmqvist, K. and Stanfors, R., 1987. The Kymmen power station TBM tunnel: Hydrogeological mapping and analysis. SKB Tec. Rep. (TR 87-26), Stockholm.

Smellie, J.A.T. and Wikberg, P., 1989. Hydrochemical investigations at Finnsjön, Sweden. (This volume).

Talbot, C.J., 1989., Problems posed to a bedrock radwaste repository by gently dipping fracture zones. Abstract. Winter meeting of the Geological Society of Sweden. Stockholm University (January 31).

Tiren, S.A., 1989., Geological setting and deformation history of a low angle fracture zone at Finnsjön, Sweden. (This volume).

Tullborg, E-L. and Larson, S-Å. 1982., Fissure fillings from Finnsjön and Studsvik, Sweden. Identification, chemistry and dating. SKBF/KBS Tec. Rep. (TR 82-20), Stockholm.

Welin, E., Kähr, A-M. and Lundegårdh, P.H., 1980: Rb-Sr isotope systematics at amphibolite facies conditions, Uppsala region, eastern Sweden. Precambrian Res., 13, 87-101.

Wickman, F.E., Åberg, G. and Levi, B., 1983: Rb-Sr dating of alteration events in granitoids. Contrib. Mineral. Petrol., 83, 358-362.

Wiman, E., 1930: Mineralized fissures and the succession of fissure fillings. Bull. Geol. Inst. Uppsala, 23.

Figure Texts.

Figure 1: Simplified map of the Finnsjön site showing borehole locations and major fracture zones. Section A-A´, illustrated in Figure 3, is also shown.

Figure 2: Results of point dilution measurements in borehole BFI02 compared with the hydraulic conductivity.

Figure 3: Transverse hydrogeological section (A-A´) showing a tentative model of groundwater flow during unperturbed conditions. Location of section A-A´ is shown in Figure 1.

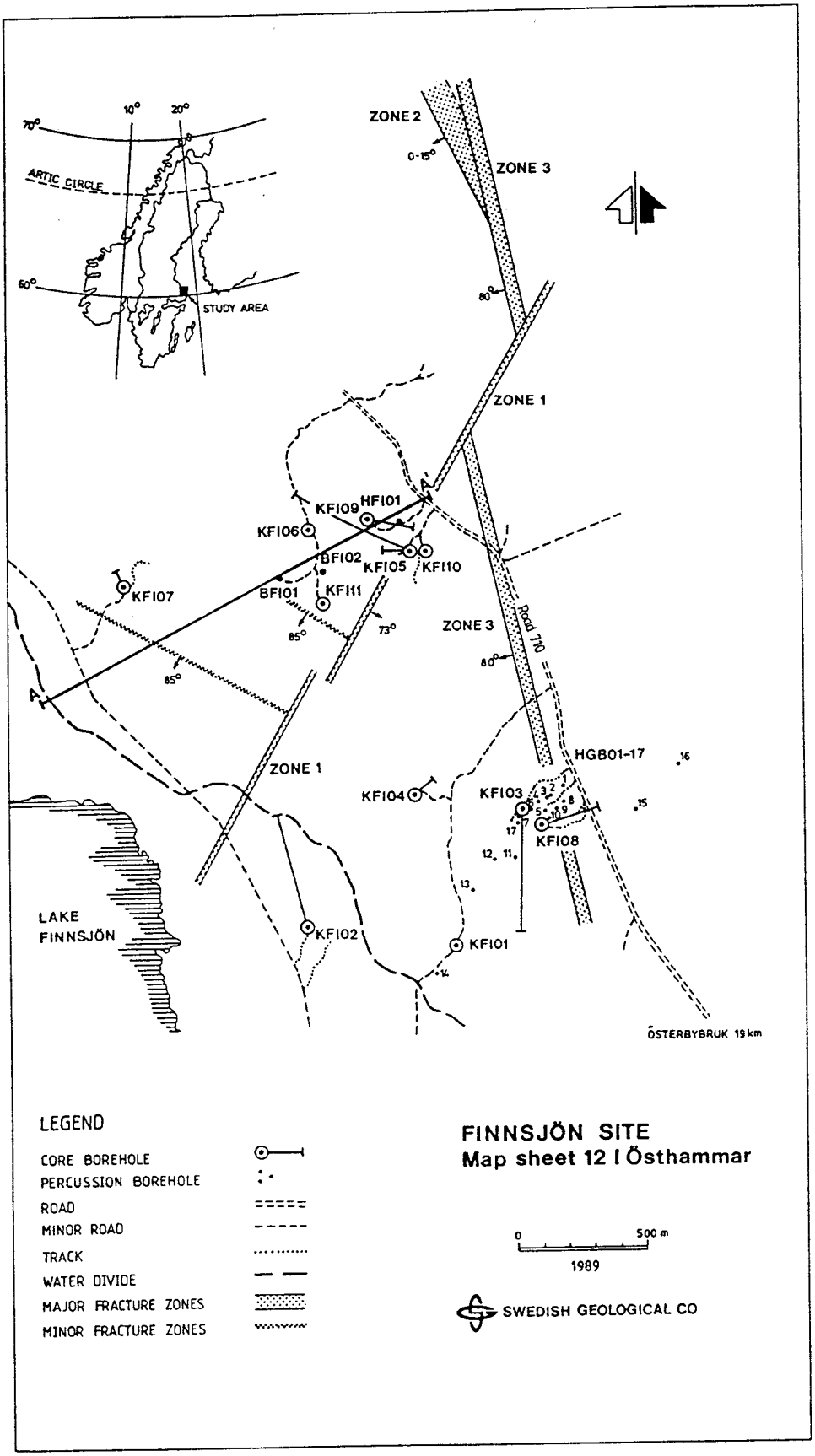

Figure 1: Simplified map of the Finnsjön site showing borehole locations and major fracture zones. Section A-A´, illustrated in Figure 3, is also shown.

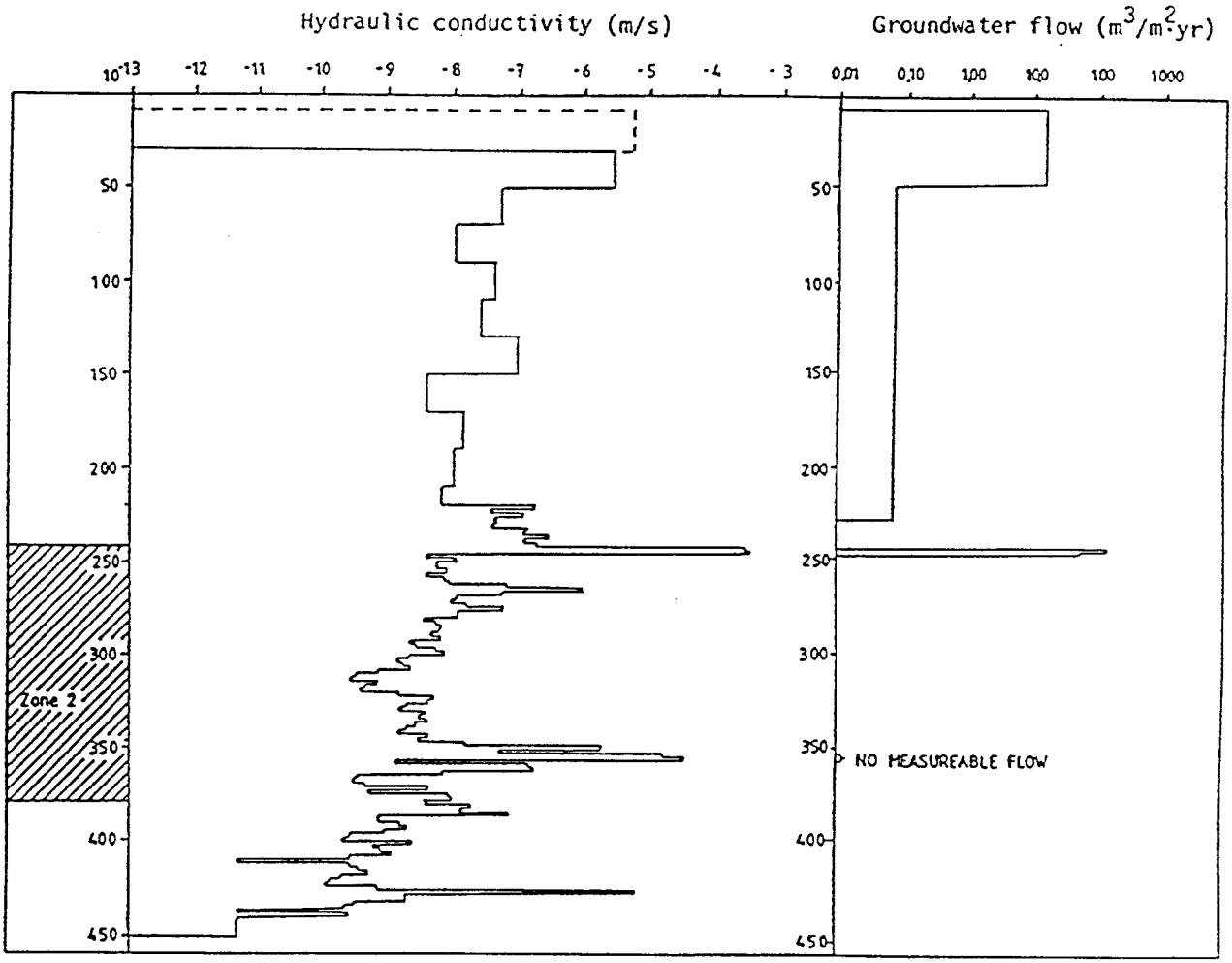

Figure 2: Results of point dilution measurements in borehole BFI02 compared with the hydraulic conductivity.

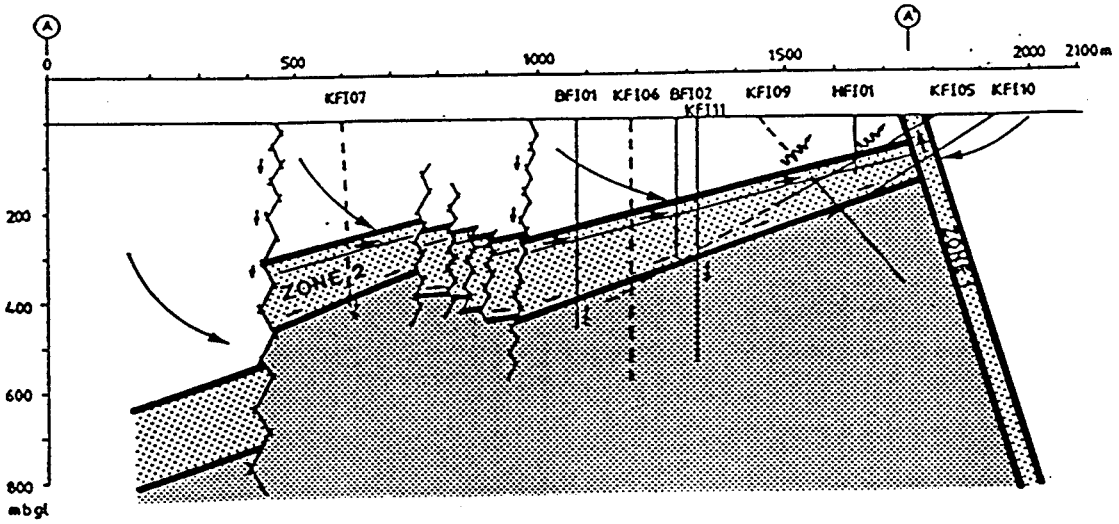

FRACTURE ZONES:

Major fracture zones Zone 1 and Zone 2 — ZONE 1.2

Minor fracture zones

SALINE AND NON SALINE WATER:

Non-saline water

Transitional water (1500-5000 mg/l Cl^-) within the major zones

Saline water (av. 5500 mg/Cl^-)

UPPER CONDUCTIVE ZONE:

Zone within large waterflow (av. 1500 mg/l Cl^-) within the major fracture zones

BOREHOLES:

Located in front of projected profile

Located behind projected profile

FLOW LINES:

Major flow lines

Minor flow lines

Recharging groundwater

HYDRAULIC HEAD:

Direction of major gradient

Direction of minor gradient

Figure 3: Transverse hydrogeological section (A-A´) showing a tentative model of groundwater flow during unperturbed conditions. Location of section A-A´ is shown in Figure 1.

CHARACTERIZATION OF FRACTURE ZONE 2, FINNSJÖN STUDY-SITE

PART 2

GEOLOGICAL SETTING AND DEFORMATION HISTORY OF A LOW ANGLE FRACTURE ZONE AT FINNSJÖN, SWEDEN

Sven A. Tirén

Swedish Geological Company, Uppsala, Sweden

August 1989

GEOLOGICAL SETTING AND DEFORMATION HISTORY OF A LOW ANGLE FRACTURE ZONE AT FINNSJÖN, SWEDEN.

Sven A. Tirén

Swedish Geological Co (SGAB), Box 1424, S-751 44 Uppsala, Sweden.

Abstract.

In 1984 the Swedish Nuclear Fuel and Waste Management Co (SKB) initiated detailed investigations of the geological, geophysical, hydrological, and geochemical character of a fracture zone.

For this purpose, a low angle, SSW-dipping fracture zone in a foliated granodiorite of Svecokarelian age (ca. 1.8 Ga), within the sub-Cambrian peneplain of northeastern Uppland, central, eastern Sweden, was identified and investigated by extensive drilling. The initial formation of this zone, which is estimated to have taken place ca. 1.7 Ga ago as a result of ductile deformation, was followed by shearing during ductile-brittle transitional conditions, and subsequently by brittle deformation. It formed as a thrust in a 20-30 km WNW-ESE trending strike-slip fault zone. The fracture zone is approx. 100 m wide with an anastomosing shear pattern and it is displaced by subvertical faults. Late reactivation of the zone has occurred preferentially in the upper part of the zone, which is now open, permitting water transport.

The palaeo-flow paths, indicated by bedrock alteration and fracture infillings, show that the hydraulic flow system in the rock mass has become increasingly more restricted during geological time, and now dominantly occurs along descrete zones which were initiated more than 1.7 Ga ago, and since then have been repeatedly reactivated. The most intense penetrative

fracturing, associated with hydrothermal activity, occurred more than 1.0 Ga ago.

Fractures and fracture zones most likely to conduct water, i.e. forming transport pathways between a repository and the biosphere, will tend to be those with a long and complex tectonic history.

1. Introduction

The Swedish Nuclear Fuel and Waste Management Company (SKB) has performed site selection studies for a repository of spent nuclear fuel since 1977. The Finnsjön site (Fig. 1), situated in the southern part of a 20-30 km wide right-lateral WNW-ESE trending Precambrian shear zone within the sub-Cambrian peneplain of northeastern Uppland, in central, eastern Sweden, has been a target area for such detailed investigations. During the period 1979-1982, surface and subsurface geological and hydrological site selection studies were performed. The hydrogeological character of the area, together with its geographical position, made it suitable for further detailed studies of water flow in fracture zones. These later studies, which commenced in 1984, where restricted to a fracture zone, Zone 2, in the Brändan area of the Finnsjön site (Figs. 1, 3), and involved a comprehensive evaluation of the geology and hydrogeology.

Zone 2 is well defined by nine boreholes drilled within an area of approximately 1200 m x 500 m. In this area the fracture zone is gently dipping, N30W/15SW, with an almost planar upper surface located between 100 to 240 m below the ground surface (exception of KFI07; Fig. 2). The location of the lower surface of the zone is less well-defined, although, the zone generally has a thickness of about 100 m. The extension of Zone 2 towards the northeast and southwest is displaced by steep faults.

Zone 2 is mainly comprised of a series of narrow sections (up to 2-5 m wide) characterised by increasing fracturing and hydraulic conductivity (10^2 to 10^6 times). Breccias and rocks displaying catacalstic to mylonitic transitional fabrics are commonly associated with the fracturing. The frequency of sealed fractures in the zone is high in all the examined cores

but the frequency of coated fractures varies. All boreholes penetrating Zone 2 display high hydraulic conductivities (10^{-5} to 10^{-3} m/s) in restricted sections of the zone, while other sections have conductivities similar to the country rock (10^{-10} to 10^{-6} m/s; Andersson et al., this volume).

This paper sets out to describe the regional and local geological setting of Zone 2 with reference to the zone and its palaeohydrological history. Much of the presented data are from Tirén et al. (1985), Ahlbom et al. (1986, 1988), Andersson et al. (1988), and Munier and Tirén (1989). The implication of such data for repository safety analysis concepts is outlined by Ahlbom and Smellie (this volume).

2. The geology of the Finnsjön site

2.1 Major rock types

The bedrock of the Brändan area is dominated by a grey granodiorite containing elliptically-shaped grabbroic xenoliths (average elongation 4:1); the longest axis (i.e. average 9 cm) is oriented along the regional foliation (N60W/subvertical; Fig. 4). The grey granodiorite is mineralogically uniform with a grain size range of 0.5 - 3.0 mm. The mineral composition is quartz (25-31 vol. %), plagioclase (An_{35}, 30-34 vol. %), microcline (14-21 vol. %), hornblende (9-12 vol. %), biotite (7-11 vol. %) and accessory minerals such as sphene, apatite and opaque minerals. The mean chemical composition for the granodiorite is presented in Table 1. The granodiorite has been affected by regional metamorphism, deformation, and hydrothermal alteration along specific generations of shear zones and fractures. The oldest pegmatites, trending NNE with subvertical dips and NW with a gentle southwesterly dip; (Fig. 4), are associated with the granodiorite and exhibit a textural zonation (coarser grains in the central parts). The pegmatites are very rich in plagioclase, and minor amounts of garnet (diameters <0.2 mm) generally occur close to the country-rock contacts.

The granodiorite has been intruded by at least two subvertical sets of dolerite dykes, trending WNW and N-S respectively, and by young aplites/pegmatites, subparallel to the older sets of pegmatites (Fig. 4). The young acid dykes are associated with the intrusion of a pinkish granite.

2.2 Geological evolution

2.2.1 Period 2.0 - 1.8 Ga

The geological evolution of the Brändan area (Fig. 5) extends back to an early stage of the Svecokarelian orogeny (ca. 1.9 Ga) when first gabbroic rocks and later a large sequence of granodioritic rocks intruded a sequence of ca. 2.0 Ga old sediments and volcanites (Lundqvist, 1979). At the end of this period dolerite dykes were intruded.

The present mineralogy of the granodiorite is the result of metamorphic reactions ca. 1.83 $\pm$ 0.01 Ga ago (Rb-Sr whole-rock age; Welin et al., 1980) when the primary mineralogy was largely destroyed. Inclusion trails of quartz in hornblende and fishes of white mica in biotite indicate that the granodiorite was more fine-grained and had an earlier pronounced foliation. The present foliation is defined by mineral alignment of hornblende and biotite. Biotites, which have been rotated into the foliation, have recrystallized, and additional biotite has grown along the foliation. Post foliation non-kinematic growth of feldspar and quartz has resulted in: a) an increase in the overall grain-size (from 0.5 to 3.0 mm), b) the formation of a stable grain configuration (tripple junctions), and c) a rock of gneissic appearance.

2.2.2 Period 1.8 - 1.6 Ga

Ductile shears, $1.8 > x > 1.7$ Ga (i.e. younger than the old dolerite dykes and older than young aplite pegmatites; see Fig. 4 for orientation of the latter), formed as a thrust in a strike-slip fault regime (apparent maximum stress in NE-SW), produced a decrease in grain-size together with a distortion of the foliation, and have locally transformed the granodiorite

via shear zones to fine-grained, banded mylonites. This signifies the early formation stage of gently dipping shear zones in the area (e.g. Zone 2). This ductile deformation was followed by a transitional semi-ductile deformation, representing deformation at a higher crustal level. The age of these early cataclastic rocks (nomenclature according to Sibson, 1977), is not known.

According to a regional synthesis by Lundqvist (1979), unfoliated red granites where intruded ca. 1.7 Ga causing alteration of the granodiorite and locally reactivating existing zones of weakness. The configuration of epidote infilled fractures (epidote dated by Rb-Sr to ca. 1.5 - 1.6 Ga by Wickman et al., 1983, probably formed at approx. 200-300°C according to Turner, 1981) indicates an apparent maximum stress from NNW-SSE (Munier and Tirén, 1989). Epidote has formed in the rock coevally with the alteration of biotite and hornblende to chlorite.

The most pronounced effect, however, of the intrusion of the red granites was the hydrothermal alteration of the bedrock adjacent to water-conductive shear zones and fractures, producing a distinct red colouration due to the dispersion of Fe-oxyhydroxides. Transport of hydrothermal fluids, as indicated by this red colouration of the wall rock, occurred preferentially along major semiductile shear zones.

In a broader regional context this period corresponds in time to an Andino-type orogeny, ca. 1.8 - 1.6 Ga (Nyström, 1982) which was active some 150 km to the west, and to the intrusion of the Rapakivi granites (ca. 1.6 Ga; Vaasjoki, 1977) in the Åland archipelago in Finland some 100 km to the east. The region between the Andino-type orogeny and the Rapakivi granites, (i.e. eastern, central Sweden) is characterized by the above-mentioned 1.7 Ga red granite massifs, an alkaline

intrusion (1.6 Ga; Doig, 1970), block faulting, and extensive erosion.

2.2.3 Period 1.2 - 0.9 Ga

The next period of deformation to influence the Brändan area is contemporaneous with the Sveconorvegian orogeny ca. 1.2 - 0.9 Ga, and resulted in the reactivation of shear zones, block faulting, and fracturing of the host rock. Fracture infillings of prehnite (dated by Rb-Sr to ca. 1.1 Ga by Wickman et al., 1982, suggesting a temperature of 150-200°C according to Turner, 1981) are typical, and the configuration of these fractures indicates an apparent NNE-SSW orientation of the axis of maximum compression (Munier and Tirén, 1989).

The fractures are often discoloured red, and those with apertures of approx. 0.1-3.0 mm are often accompanied by hydrothermal aureoles approximately 0.5-12 cm in width. Within these aureoles most of the plagioclase (andesine) has been altered to red coloured pseudomorphs, comprising aggregates of fine-grained albite (?), sericite, and Ca-minerals. Feldspar has formed on the fracture walls prior to sealing by prehnite. Older fractures (e.g. NW-shears) have locally been reactivated when intersected by NE-oriented fractures; this is indicated by the red colouration of the fracture walls and infillings of prehnite. In Zone 2 prehnite occurs as a matrix constituent within repeatedly brecciated mylonites, cataclasites and calcite infillings. Fragments of these calcite infillings display intense internal deformation. This has resulted in grains which are densely twinned and locally split along deformation twin planes into flakes (thickness-length ratio up to 30:1). Those which have not been recrystallized are commonly rotated into a shear foliation, often parallel to the fractures which can be observed as

unbrecciated veins containing older calcite. Fractures overprinting the prehnite-infilled fractures are rare outside the hydrothermal aureoles of the regional fracture zones. This indicates that the transport of fluid in the rock at the end of this period (ca. 1.0 Ga ago) was controlled by the regional fracture zones. This is supported by infillings of pinkish red laumontite (suggesting a temperature of approx. 100-200°C according to Turner, 1982) restricted to Zone 2. Most of the laumontite-rich fractures in Zone 2 are shear fractures, oblique to the orientation of the zone (cf. Blès & Feuga, 1986), indicating an anisotropic flow condition with increased flow at right angles to the shear direction.

The regional distribution of epidote as a fracture infilling, followed by prehnite and later laumontite, indicates a regional evolution with successive elevation of the bedrock to higher crustal levels.

2.2.4 Period 0.9 - 0.6 Ga

At this time Zone 2 is displaced by a N30E/75SE trending zone (Zone 1; Fig. 3 and Table 2), in which Fe-oxyhydroxide percipitation is typical. Transport pathways have been opened up in Zone 2 adjacent to Zone 1. This is indicated by a random scatter of Fe-oxyhydroxide infilled fractures in Zone 2 close to Zone 1; away from Zone 1 these infilled fractures become more regularly distributed along distinct levels in Zone 2 and their frequency decreases. This suggests that the transport of water became more restricted, occurring within distinct levels of Zone 2. The present flow of water also occurs preferentially within these levels now defined by shear fractures (coated with Fe-oxyhydroxides) parallel to the orientation of the zone (Fig. 9), especially within the uppermost part of Zone 2 (Andersson et al., this volume).

This period was characterized by major uplift and peneplanization, resulting in the sub-Cambrian peneplain (> 0.6 Ga ago) which roughly coincides with the ground surface of today. A sequence of Cambrian-Ordovician epicontinental sediments (> 500 m?) were deposited on the sub-Cambrian peneplain. In Uppland only some downfaulted remnants of this pre-existing sedimentary cover have been preserved along regional fault zones.

2.2.5 Period 0.6 Ga - 10 000 B.P.

The present ground surface, roughly coinciding with the peneplain, displays a systematic arrangement of rotated lensoidal blocks (up to several hundred square kilometres large with the ground surface tilted up to 2°) which indicates listric faulting and the existence of a deeply located, subhorizontal detachment surface. This block rotation predates the latest glaciation (<10 000 B.P.). It took place during a period of regional extension, possibly deformation associated with the deposition or faulting of the Cambro-Ordovician sediments. Minor post-glacial movements may have occurred, and may still be occurring, during isostatic recovery (at present approx. 6 mm/year; Bergqvist, 1977).

2.2.6 Zonated and late fracture infillings

Calcite, which is a common infilling constituent in Zone 2, has been precipitated along fractures and redistributed (stylolites) throughout a considerable period of geologic time (i.e. for more than 1.5 Ga). Calcite infillings, with zonations demarcated by 4-5 repeated dustbands in recrystallized polygonal calcite, comprise an older type, (>1.5 Ga). Late (age unknown) idiomorphic undeformed aggregates of calcite

occur in voids. Dust zoned quartz is observed in undeformed idiomorphic quartz aggregates in minor voids (up to some 5 mm^2 large) in the upper porous part of Zone 2. Calcite infillings of late glacial age above Zone 2 (^{14}C-dating; Tullborg and Larson, 1984) indicate minor movements in the bedrock during glaciation.

2.2.7 Variation in stress directions

The direction of the largest principal stress has changed during the geological history of the area. During the late stage and decline of the Svecokarelian orogeny (ca. 1.8 Ga) the principal stress changed from NE-SW to NNW-SSE (ca. 1.6 Ga). Fractures infilled with prehnite of Sveconorvegian age (ca. 1.0 Ga) indicate a subsequent clockwise rotation of the larger principal stress to NNE-SSW.

At present the largest principal rock stress in the Brändan area is horizontal down to a depth of approx. 500 m, where the vertical stress component becomes the intermediate principal stress (Bjarnason and Stephansson, 1988). The maximum horizontal stress is NW-SE, normal i.e. to the Mid Atlantic Ridge. This stress configuration is in agreement with the general stress pattern in the Fennoscandian Shield (Stephansson et al., 1986).

3. Fracture morphology and local rock blocks

3.1 Introduction

A fracture is a surface along which the cohesion of the rock has been lost. The term is neutral and is neither related to the size of the structure or any displacement along or normal to the fracture surface. A local rock block is defined here as a rock volume outlined by fracture zones, persistent for more than 500 m and having a width of more than 10 m (cf. Fig. 3).

3.2 Fractures

3.2.1 Fracture sets

Surface mapping has been concentrated to the central part of the Brändan area, the Brändan Block (Fig. 3). The morphology of the outcrops reflects the fracture pattern, i.e. an orthogonal fracture system with fracture sets oriented N30-70W/subvertical, N30-70E/subvertical and NW/gently SW dipping (Fig. 6a). If fractures within outcrops are considered, the gently southwest dipping fracture set becomes diffuse (Fig. 6b) and the relative occurrence of the NE fractures increases.

The NW-trending fractures, formed in foliation flexures (Fig. 7a), are relatively extensive and locally traceable for more than 500 m (borehole radar investigations). These fractures often follow tectonic discontinuities which are characterized by ductile to semi-ductile deformation and usually associated with mylonites, boudinaged or sheared meta-dolerites and quartz veins, and infillings of epidote.

The NE-trending fractures are the most frequent and generally arranged en echelon (stepping fractures). They penetrate the local rock blocks, but fractures within the rock blocks belonging to this set have generally not been reactivated. They are characteristically hydrothermally altered and infilled with prehnite. They comprise two sets: N30E and N50-70E, both subvertical. The former fracture set has blind terminations while the latter set often has connected fracture endings (Fig. 7b). The trace length of individual NE fractures is relatively short, generally less than 3 m.

The gently SW dipping (0-15°) fractures may form planar fracture surfaces larger than 40 x 8 m. The original character of these fractures which demarcate the outcrop surfaces has been affected by weathering, in general to a depth of a centimetre in post glacial time (i.e. during the last 10 000 years). However, some fracture surfaces exhibit a red colouration, probably indicating contact with hydrothermal fluids.

An additional set of fractures trending NE and dipping moderately (30-60°) toward the SE (Fig. 8) are common southeast of the Brändan Zone (Zone 1; Fig. 2) in the Gåvastbo Block. These fractures are coated with pinkish laumontite (fine grained hematite staining) which is typical for Zone 2.

3.2.2 The effect of the present stress regime on the fracture system

The present axis of maximum stress, horizontal and oriented NW-SE (Bjarnasson and Stephansson, 1988), puts the NW fractures under tension, the NE fractures under compression, and the gently SW dipping fractures under oblique slip conditions.

3.3 Fracture zones

3.3.1 Sets of fracture zones

Three sets of fracture zones dominate the network of fractures in the Brändan area: N30E/steep, N60W/steep and N20W/10-20SW (Fig. 3 and Table 2). The fracture zone network broadly conforms with the system of fractures outlining the morphological shape of the outcrops. The semi-regional Brändan fracture zone (Zone 1, N30E/75SE) is approximately 20 m wide and traceable for more than 2.5 km. Local zones trending N30E are few and tend to be shorter than 500 m. The trace lengths of the N60W and N20W fracture zones are relatively long, more than 300 m. Zone 2 (N28W/16SW), not exposed in the Brändan area, extends westwards (down dip) for more than 500 m.

3.3.2 The effect of the present stress regime on the fracture zones

The stress pattern in northern Uppland is similar to that measured in the Brändan area and the influence of rock stress on the fracture zones should be analogous to that on the fractures (cf. above). There is, however, a small change in the orientation of maximum horizontal stress across Zone 2, from N45W above to N53W below the zone associated with a weakly indicated stress discontinuity (Bjarnasson and Stephansson, 1988). Stress measurements across an analogous zone at Forsmark, approximately 15 km to the east of the Finnsjön area, (Fig. 1), recorded a major stress field discontinuity, showing an increase towards depth in the order of 20 MPa across the zone (Carlsson and Christansson, 1986).

3.4 Nature of Zone 2

Zone 2 was first characterized by an early ductile deformation with the local development of mylonites and cataclasites (Fig. 9). This was followed by hydrothermal alteration (resulting in red colouration of the fracture walls), brecciation, and finally the formation of different generations of infilling minerals sealing the fractures and the establishment of the present water flow system within the zone.

3.4.1 Fractures

All logged fractures in drillcores from the Brändan area are not orientated. As a result, the fracture survey performed on rock outcrops formed the basis for a semi-quantitative analysis of the fracture populations in the three vertical boreholes (KFI06, 07 and 11); the fractures were grouped into three classes according to their dips (0-19°, 20-69° and 70-90°; Fig. 9). Vertical-subvertical as well as gently-subhorizontal fractures are present in outcrops within the Brändan Block (Fig 3); inclined fractures ranging from 20°-69° are rare (cf. Fig. 6). Small scale structures displayed in outcrops are used as indicators of the mesoscopic deformation pattern in Zone 2.

The fracturing in Zone 2 is inhomogeneous with an average of less than 5 fractures/m, ranging up to 35 fractures/m in single one metre sections. The fracturing in the rock above Zone 2 is much less, averaging approximately 1 fracture/m, while there is no contrast in fracturing between Zone 2 and the rock below. However, in the later case there is a change in fracture characteristics (orientations and infillings).

The upper boundary of Zone 2 is distinct or transitional. On a semi-regional scale it is a planar, tectonic discontinuity. It is distinct where the border is defined by gently dipping fractures, and it is transitional where it is defined by splays of moderately inclined zones, penetrating upwards from Zone 2 into the Brändan Block. Locally, the lowermost parts of the Brändan Block also exhibit an increase in vertical, often open, rough fractures.

Fracturing in Zone 2 is heterogeneous, comprising a central section of highly intense deformation, and a section with relative sound rock separated by minor, fractured sections. Although the occurrence of fractures with different dips (vertical, moderate, and gently dipping; Fig. 9) shows distribution variations, the fracture patterns show some general features. Vertical fractures are rare in sections with a high frequency of gently dipping fractures. These sections are bordered or coincide with sections exhibiting a high frequency of moderately dipping fractures. Both the moderately dipping fractures and the vertical fractures contribute to the vertical transport of water into and within Zone 2, while the gently dipping fractures control the lateral transport of water along Zone 2.

3.4.2 Geophysical character

Zone 2 is geophysically characterized by a general decrease in resistivity as compared to the rock above and below (Fig. 10). This difference is caused by the influence of saline water together with a general increase in porosity. The normal resistivity log indicates that Zone 2 is composed of zones of intense fracturing enveloping less deformed rock. The temperature log shows that the uppermost part of Zone 2 contains hydraulically active fractures, and the salinity log

shows a rapid increase in salinity below the uppermost water-conductive fractures, which are characterised by fresh water. The decrease in salinity below Zone 2 in borehole KFI11 (Fig. 11) is assumed to represent relict flushing water which is less saline. A general moderate increase in natural radiation (fracture minerals), together with a decrease in normal resistivity, indicate sealed fractures just below the uppermost, water-conductive part of Zone 2. This suggests that the total section of fractured rock earlier transported ground water over its entire width, while present water transport occurs along a very narrow zone.

3.4.3 Hydraulic properties

The style of deformation and the nature of the wall-rock alteration and fracture infillings indicate that through time, the water flow system in the rock has become more and more restricted to discrete zones (Fig. 9). The most water-conductive sections coincide with a high density of gently inclined, open fractures (dipping 10-20^{o}). These conductive sections are narrow, in most cases some decimetres or centimetres wide.

The highest hydraulic conductivity measured in the cored boreholes coincides with a fault breccia, less than 0.5 dm thick, situated at the uppermost part of an approximately 1 m thick section, characterized by fractures (fracture frequency less than 8 fractures/m) subparallel to Zone 2 (Figs. 9 and 11). This section occurs in the uppermost part of Zone 2 within an approx. 30 m altered unit, comprising other minor sections (up to 5 m thick) with a high density of sealed fractures (e.g. at 227 m in borehole KFI11; Fig. 9).

3.4.4 Model

From the constructed model (Fig. 12), based on the configuration of tectonic discontinuities in a shear regime (c.f. Hancock, 1985; Blès and Feuga, 1986; Sylvester, 1988), Zone 2 is presented as an anastomosing network of minor shear and fracture zones, enveloping "lozenges" (oblique-angled parallelograms) of mildly deformed rock. Zone 2 is a planar shear zone from which minor, moderately inclined zones (splays), project upwards into the overlying rock block. Tension fractures are formed at the root-zone of the splays and the splays are offset by vertical shears parallel to the direction of displacement.

3.4.5 Rock stresses

According to Bjarnasson and Stephansson (1988) the orientation of the present stress field with the axis of maximum compression oriented NW-SE, and with a horizontal stress greater than the vertical stress, will result in oblique thrust fault conditions in Zone 2. The change in orientation of the maximum horizontal stress across Zone 2 from N48W above to N53W below Zone 2, will result in a torsion effect on the fracture system.

3.5 Local rock blocks

The most obvious rock block boundary is the Brändan Zone (N30E/75SE, approx. 20-30 m wide) which is considered as a high order discontinuity along which late displacement (oblique slip) has occurred (Zone 1; Figs. 2, 3 and Table 2). The rock block west of the Brändan Zone is the Brändan Block and to the east is the Gåvastbo Block.

The northern block boundary of the Brändan Block lies outside the area investigated in detail, and parallels the orientation of a gabbro to the north (Zone 4; Fig. 3 and Table 2). The western boundary of the Brändan Block is partly defined by a N20W trending zone, dipping approximately 15° to the southwest. At the surface this zone is relatively wide (the lateral width is approximately 200 m, outlined by Zones 14 and 15; Fig. 3). The southern part of the zone is offset by a N60W fault with a downthrow to the south. The N60W fault (Zone 10; Fig. 3) constitutes the southern border of the Brändan Block. An additional fracture zone must be engaged to define the complete western boundary of the Brändan Block; possibly the morphologically expressed N30E zone just outside the Brändan area. The lower limit of the Brändan Block is the gently inclined Zone 2.

The Brändan Block is thus a polyhedron with three sets of subparallel surfaces (Fig. 13), and has a low average density of internal fractures (< 1 fracture/m; core KFI11).

Zone 2, which is a wedge-shaped unit (acute angle approximately 5°), is located below the Brändan Block. The N60W and N30E block boundaries of the Brändan Block are faults that truncate and displace Zone 2, which is also distorted by the reactivation of minor N60W faults. The rock block below Zone 2 has an average fracture density (approximately 3.2 fractures/m; core KFI11) equal to the fracture density of Zone 2 (approximately 3.5 fractures/m; core KFI11).

The Gåvastbo Block, southeast of the Brändan Block, has a triangular surface expression, outlined by N30E, N60W and N20W trending faults. The configuration of fractures, fracture density, and types of fracture infilling minerals in the Gåvastbo Block, differ significantly in comparison with those of the Brändan Block, and resemble those of Zone 2. The lower

limit of the Gåvastbo Block is defined by a surface dipping gently westwards (10-20°W) which outcrops along the Gåvastbo Zone and is displaced by the Brändan Zone. Ground geophysical, electric measurements indicate that the Gåvastbo Block comprises a more fractured rock block than does the Brändan Block (Ahlbom et al., 1986).

4. Occurrence of gently dipping fracture zones

The general occurrence of low angle fracture zones in cratonic areas, typified here by the Fennoscandian Shield which is dominated by granitoids and gneisses, has generally been underestimated.

Underground information from site investigations and mines, e.g. the Finnsjön site, Forsmark (SFR, 1986) and the Dannemora mine (Lager, 1986) in northeastern Uppland (Fig. 1), has demonstrated the existence of major horizontal to low angle fracture zones in these areas. The orientation of the zones differs slightly, varying from subhorizontal to a gentle dip southwards. At Forsmark, infillings of blue-green chlorite are typical for the more water conductive sections, while Fe-oxyhydroxides tend to dominate in the Finnsjön site. In the Dannemora mine, situated in a tight subvertical synformal structure comprised of volcanites, iron ore and tidal sediments, all downfolded in a granodioritic gneiss, a subhorizontal fault, transecting the synform, has displaced the upper block approx. 400 m northwards (Lager, 1986). Seismic reflection measurements in the Finnsjön area (Dahl-Jensen and Lindgren, 1987) have recorded a broad band of coherent energy at a depth of more than 1500 m, which may represent an additional zone at greater depth. Furthermore, it is notable that the low angle faults in northeastern Uppland are not

related to lithological units or contacts of lithological units, but transect the lithological units.

As a general observation, it can be thus stated that in the overwhelming majority of areas in Sweden, where subsurface investigations have been performed during the last ten years (Kamlunge, Gideå, Svartboberget, Gravberg, Stripa mine, Kråkemåla, Simpevarp area, and Sternö) the occurrence of horizontal to low angle fracture zones has been demonstrated. Late-glacial to post-glacial movements have been recorded on faults in northern Sweden (Lundqvist and Lagerbäck, 1976 and Lagerbäck, 1988). Talbot (1986) interpreted these faults to be gently dipping to subhorizontal.

Comparison with other shield areas reveal similar features. For example, at Hästholmen, location site of the Loviisa nuclear power station, central southernmost Finland, low angle zones are related to primary layering in a sequence of rapakivi granite types (Anttila, 1986). Further examples from Finland have been described from a 120 km long N-S trending tunnel which supplies fresh water to Helsinki. Here the bedrock consists of Proterozoic migmatites and granitoids containing several low angle (8-10^{o}) fracture zones, with a long tectonic history (Suominen 1985). These zones are open to water flow, if not infilled with clay, at depths of 30-130 m. Furthermore, in the Canadian shield, fracture surveys at four sites and in the Sudbury mine display a general occurrence of low angle fractures and fracture zones. Characteristically these zones predate most of the vertical faulting.

Investigations (surface survey, drillings and shafts) at the Underground Research Laboratory (URL), performed by the Atomic Energy of Canada Limited (AECL), have resulted in detailed descriptions of the structural framework of the Lac

du Bonnet granitic batholith in Manitoba (e.g. Everitt and Brown, 1986). At URL there occur three major low angle fracture zones which are 25-50 m wide and with a mutual separation of 100-150 m. These zones, with associated splays, demarcate tabular rock blocks each reflecting their own fracture characteristics. Except for the fracturing associated with the low angle faulting, the intra-block fracturing in these three blocks includes non-systematic fractures and local fracture fabrics related to the lithological composition of the blocks; the lithology is distinct for each block. An interesting observation is the frequent occurrence of vertical fractures, locally restricted to bedrock levels above the central low angle zone. Typical alteration and fracture infillings, notably Fe-oxyhydroxides and late clay minerals, together with a general pervasive reddening of the wallrock, characterize these low angle fracture zones.

The structural character of the low angle zones at URL is therefore closly analogous to Zone 2 in the Finnsjön site. Thus, the relatively common occurrence of such fracture zones must therefore be regarded in a much wider perspective, as a major control on mass groundwater transport in crystalline rocks and underground rock excavations.

5. Summary and discussion

The bedrock of the Brändan area is composed of a homogeneous, foliated granodiorite dated to ca. 1.8 Ga. Transecting the foliation of the granodiorite are dykes of mafic and acid composition. Adjacent to the investigated area there are two major rock bodies, an older gabbro to the northeast and a younger reddish granite (ca. 1.7 Ga) to the southeast, which may have influenced the fracture configuration in the Brändan area. Gently SW dipping and

subvertical N30E and N60W fracture zones divide the bedrock into tabular units and rock blocks. This configuration of discontinuities was established more than 1.0 Ga ago.

The formation of tectonic discontinuities in the relatively homogeneous granodiorite is revealed by small scale structures. The regional foliation, which is N60W/subvertical, is cut by early plagioclase-rich pegmatites, presumably associated with the granodiorite, and old dolerite dykes (ca. 1.8 Ga). The early pegmatites, NE/subvertical and NW/gently dipping SW, are locally folded and have an axial plane foliation parallel (approx. N60W/ 80-90 SW) to ductile shear zones. The more pronounced shear zones are characterized by mylonites, locally with intrafolial folds, and by strongly sheared metadolerites. The metadolerites are deformed and transposed into these shear zones. The ductile shears, sub-parallel to the foliation and the early pegmatites, form a pseudo-ortogonal system of discontinuities. Zone 2, characterized by early ductile deformation, is parallel to the gently dipping discontinuities of this system. Late aplites and pegmatites of the younger red granite (1.7 Ga) intruded this system. These are relatively frequent and occur in two sets: one vertical trending NE and one subparallel to Zone 2.

The intrusion of the young granite deformed the granodiorite by fracturing, reactivation of discontinuities, and resulting in hydrothermal alteration along these fractures. Infillings of epidote (ca. 1.6 Ga) are characteristic for the semi-brittle shear zones.

The most frequent types of fractures in the Brändan area are synchronous with the Sveconorvegian orogeny (1.2 - 0.9 Ga) and formed with the maximum compression axis oriented in NNE. These normally trend N10-70E with step to vertical dips, are infilled with prehnite (ca. 1.1 Ga), and are probably

associated with the deformation on the Brändan zone, Zone 1 (Fig. 2).

Subsequent fracturing occurred preferentially along regional fracture zones resulting in reactivation, accompanied with infillings of laumonite and hematite (ca. 1.0 Ga) and later Fe-oxyhydroxides (unknown age) and calcite.

All mineral infillings indicate temperatures in excess of 100°C and were formed during periods of block faulting and extensive erosion, prior to the formation of the sub-Cambrian peneplain more than 0.6 Ga ago.

Extensional deformation of the craton in early Cambrian time was accompanied by a transgression of the Cambrian sea, block-faulting and sedimentation (cf. clastic Cambro-Ordovician dykes; Bergman, 1982, and faulting of the Cambro-Ordovician sediments in the Baltic sea; Floden, 1980, 1984). The Cambro-Ordovician sediments in northeastern Uppland are now eroded and the present ground surface is roughly coinciding with the sub-Cambrian peneplain, reflecting the limited block-faulting which is analogous to that of the crystalline basement of the Baltic Sea.

The low angle Zone 2 was formed initially as a ductile shear zone more than 1.7 Ga ago in a regional strike-slip shear regime (the Östhammar Fault Zone; Fig. 1), followed by semi-ductile and brittle deformation. The upper surface of Zone 2 is planar, orientated N28W/16SW, and traceable for more than 600 m. The configuration of Zone 2 outside the Brändan Block is uncertain, but most probably it is displaced by the subvertical faults delimiting the Brändan Block.

The width of Zone 2 is in the order of 100 metres but the late deformation, accompanied by the transport of water, has

become increasingly more restricted to certain minor sections in the zone; fractured sections, open to water flow, vary from less than a decimetre to some metres in width. Age determinations (^{14}C-method; Tullborg and Larson, 1984) of the calcite infillings in fractures above Zone 2 indicate the mixing of saline and fresh groundwaters during the last glaciation, or more recently. This is also supported by hydrochemical studies in the region (Smellie and Wikberg; this volume).

In summary, the framework of conducting fractures in the Svecokarelian crystalline rocks of northeastern Uppland is governed by a fracture configuration that was already well established more than 1.0 Ga ago, with some of the discontinuities initiated as ductile shear zones more than 1.7 Ga ago. However, formation of new fracture configurations occurred during a period of almost 0.7 Ga as the area became a craton. Subsequently, deformation was accommodated by existing zones of weakness. This study elucidates that fractures with a long complex geologic history also provide the most likely hydraulically active zones in the future.

Acknowledgements

The author is indebeted to Dr. Otto Brotzen (Danderyd), Dr. Sven Åke Larson (Göteborg) and Dr. Per-Gunnar Andreasson (Lund) for reading and improving the manuscript. I am especially grateful to Dr. John Smellie (Uppsala) and Dr. Monica Beckholmen (Uppsala) for fruitful discussions and constructive critisism during the investigation and the preparation of the paper. Margit Svensk is thanked for the typeing and Annika Wettervik for the drawings.

The project was initiated and sponsored by the Swedish Nuclear Fuel and Waste Management Co; Stockholm. Their continuous support throughout the study is greatfully acknowledged.

REFERENCES

Ahlbom, K., Andersson, P., Ekman, L., Gustavsson, E. and Smellie, J., 1986: Preliminary investigations of fracture zones in the Brändan area, Finnsjön study site. SKB Tec. Rep. (TR 86-05), Stockholm.

Ahlbom, K., Andersson, P., Ekman, L. and Tirén, S., 1988: Characterization of fracture zones in the Brändan area, Finnsjön study site, central Sweden. SKB Status Rep. (AR 88-09), Stockholm.

Ahlbom, K., and Smellie, J.A.T., 1989: Overview of the fracture zone project at Finnsjön, Sweden (This volume).

Andersson, J-E., Ekman, L., Gustafsson E., Nordqvist, R., and Tirén, S., 1988: Interference tests within the Brändan area, Finnsjön study site. SKB Tec. Rep. (TR 88-XX), Stockholm.

Andersson, J-E., Ekman, L., Nordquist, R., and Winberg, A. 1989: Hydraulic testing and modelling of low-angle fracture zones at Finnsjön, Sweden, (This volume).

Anttila, P., 1986: Loviisa power station, final disposal of reactor waste: Geological and hydrological conditions of the island of Hästholmen. Nucl. Waste Comm. of the Finl. Power Comp. Rep. YJT-86-5, Helsinki.

Bergman, L., 1982: Clastic dykes in the Åland Islands, SW Finland, and their origin. Geol. Surv. Finland, Bull. 317, 7-33.

Bergqvist, E., 1977: Post-glacial land uplift in northern Sweden. Some remarks on its relation to the present rate of uplift and the uncompensated depression. Geol. Fören. Stockholm Förh., 99, 347-357.

Blès, J-L., and Feuga, B., 1986: The fracture of rocks. North Oxford Academic, 1-132.

Bjarnasson, B., and Stephansson, O., 1988: Hydraulic fracturing stress measurements in Borehole Fi 6 Finnsjön study site, central Sweden. CENTEK PUBLISHER/Division of Rock Mechanics, Luleå University of Technology, 1-40.

Carlsson, A., and Christiansson, R., 1986: Rock stress and geological structures in the Forsmark area. In Stephansson, O. (editor), Proc. Int. Symp. on Rock Stresses and Rock Stress Measurements, Stockholm, Sept 1-3. CENTEK PUBLISHERS; 457-465.

Dahl-Jensen, T., and Lindgren, J., 1987: Shallow reflection seismic investigation of fracture zones in the Finnsjön area, method evaluation. SKB Tec. Rep. (TR 87-13), Stockholm.

Doig, A., 1970: An alkaline rock province linking Europe and North America. Can. J. Earth Sci., 7, 22-28.

Everitt, R., and Brown, A., 1986: Subsurface geology of the Underground Research Laboratory, an overview of recent developments. At. Energy Can. Ltd., Pinawa, Man., Tec. Rec. (TR-375).

Flodén, T., 1980: Seismic strategraphy and bedrock geology of the central Baltic. Stockholm Contrib. Geol., 35, 1-240.

Flodén, T., 1984: Der Strukturbau im Seegebiet von Sweden. Zeitschrift für Angevandte Geologi, Bd 30, 1-16.

Gorbatschev, R., Lindh, A., Solyom, Z., Laitakari, I., Aro, K., Lobach-Zhucheko, S.B., Markov, M.S., Ivliev, A.I., and Bryhni, I. 1987: Mafic dyke swarms of the Baltic Shield. In Hall, C., and Fahrig, W.F. (eds), Geol. Ass. Can., special paper 34, 361-372.

Hancock, P.L., 1985: Brittle microtectonics: principles and practice. Jour. Struct. Geol., 7, 437-457.

Johansson, Å., 1988: The age and geotectonic setting of the Småland - Värmland granite-porphyry belt. Geol. Fören. Stockholm Förh. 110, 105-110.

KBS-3, 1983: Final storage of spent nuclear fuel. Swedish Nuclear Supply Co, SKBF (present SKB).

Lager, I., 1986: The Dannemora iron ore deposit. In Lundström, I., and Papunen, H. (Eds): Mineral deposits of southwestern Finland and the Bergslagen Province, Sweden. Excursion guide nr 3.7. IAGOD Symposium, 1986. Geol. Surv. Sweden, SGU Ca 61, 26-30.

Lagerbäck, R., 1988: Postglacial faulting and paleoseismicity in the Landsjärv area, northern Sweden. SKB Tec. Rep. (TR 88-25), Stockholm.

Lundqvist, J., and Lagerbäck, R., 1976: The Pärve Fault: a late-glacial fault in the Precambrian of Swedish Lapland. Geol. Fören. Stockholm Förh., 98, 45-51.

Lundqvist, Th., 1979: The Precambrian of Sweden. Geol. Surv. Sweden, SGU C 768, 1-87.

Munier, R., and Tirén, S.A., 1989: Geometry and kinetics of deformation zones in the Finnsjön area, central Sweden: A deformation system controlled by five sets of shear zones. Thesis, Uppsala University, 1-34.

Nyström, J-O., 1982: Post-Svecokarelian Andinotype evolution in central Sweden. Geol. Rundsch., 71, 141-157.

Olkiewicz, A., and Arnefors, J., 1981: Berggrundsbeskrivning av undersökningsområdet vid Finnsjön i norra Uppland. SKB Status Rep (AR 81-35), Stockholm.

Rudberg, S., 1954: Västerbottens berggrundsmorfologi. Geographica, 25, 1-457.

Sibson, R.H., 1977: Fault rocks and fault mechanisms. Journal of the J. Geol. Soc. Lon., 133, 191-213.

SFR, 1986: Geologisk beskrivning av zoner kring slutförvaret by R. Christiansson. Swedish Nuclear Fuel and Waste Management Co, (SKB), Disposal of low- and Intermediate-Level Waste for Reactor Operation (SFR), Progress Report SFR 86-02, 1-25.

Stephansson, O., Särkää, P., and Myrvang, A., 1986: State of Stress in Fennoscandia. In Stephansson, O. (editor), Proc. Int. Symp. on Rock Stresses and Rock Stress Measurements, Stockholm, CENTEK PUBLISHERS; Luleå University of Technology, 21-32.

Stålhös, G., 1988: Berggrundskartan 12 I Östhammar NV. Geol. Surv. Sweden, SGU Af 166.

Suominen, V., 1985: Repeated crushing and solidafication along joints in the Finnish Proterozoic bedrock, as observed in the Päijänne tunnel. In Stephansson, O. (editor), Proc. Int. Symp. on Fundamentals of Rock Joints, Björkliden, 15-20 sept. 1985, CENTEK PUBLISHER, Luleå University of Technology; 65-69.

Sylvester, G.S., 1988: Strike-slip faults. Geol. Soc. Am. Bull, 100, 1666-1703.

Talbot, C., 1986: A preliminary structural analysis of the pattern of post-glacial faults in northern Sweden. SKB Tec. Rep. (TR 86-20), Stockholm.

Tirén, S., Ahlbom, K., and Ståhle, A., 1985: Investigations of fracture zones in the Brändan area, northern Uppland, Sweden: Geological and hydrogeological characterization. In Stephansson, O. (editor), Proc. Int. Symp. on Fundamentals of

Rock Joints, Björkliden, 15-20 September 1985, CENTEK PUBLISHER, Luleå University of Technology, 57-64.

Tullborg, E-L., and Larson, S-Å., 1982: Fissure fillings from Finnsjsön and Studsvik, Sweden. Identification, chemistry and dating. SKB Tec. Rep. (TR 82-20), Stockholm.

Tullborg, E-L., and Larsson, S-Å., 1984: Stable isotopes of fissure filling calcite from Finnsjön Uppland, Sweden. Lithos, 17, 117-125.

Turner, F.J., 1981: Metamorphic petrology 2nd ed. Mc Graw-Hill, New York, 1-524.

Vaasjoki, M., 1977: Rapakivi granites and other postorogenic rocks in Finland: their age and the lead isotopic composition of certain associated galena mineralizations. Geol. Surv. Finland, Bull., 294, 1-64.

Welin, E., Kähr, A-M., and Lundegårdh, P.H., 1980: Rb-Sr isotope systematics at amphibolite facies conditions, Uppsala region, eastern Sweden. Precambrian Res., 13, 87-101.

Wickman, F.E., Åberg, G., and Levi, B., 1983: Rb-Sr-dating of alteration events in granitoids. Contrib. Mineral. Petrol., 83, 358-362.

Wiman, E., 1930: Studies of some Archean rocks in the neighbourhood of Uppsala, Sweden, and their geological position. Bull. Geol. Inst. of Uppsala, 23, 1-170.

Wiman, E., 1942: Studies of the morpho-tectonics of the Mälardepression, Sweden. Bull. Geol. Inst. of Uppsala, 29, 287-303.

Table 1: Mean chemical analyses of the granodiorite (Olkiewicz and Arnefors, 1981). Brändan area, Sweden (n = 12).

Element	x (Weight %)	s (Weight %)
SiO_2	65.5	1.2
TiO_2	0.45	0.05
Al_2O_3	13.6	0.7
Fe_2O_3	1.5	0.2
FeO	3.3	0.3
MnO	0.10	0.02
CaO	3.6	0.9
MgO	1.9	0.2
Na_2O	2.7	0.3
K_2O	3.6	0.2
$H_2O>105^oC$	1.3*	
$H_2O<105^oC$	0.2*	
P_2O_5	0.11*	
CO_2	0.05*	
F	0.09*	
S	<0.03	0.03
Ba	0.09	0.04

* n = 1 s - standard deviation

Table 2.1: Fracture zones in Brändan area (c.f. Fig. 3.)

Zone No	Orient	Width (m)	Trace length (m)	Fracture frequency range (fr/m)	Remote sensing	Surface mapping	Ground geophysics	Borehole	Borehole radar	Block boundary
1	N30 E/75 SE	20-30	>2 500	20-50	x	x	x			Brändan Block Gåvastbo Block Zone 2 Unit
2	N28 W/16 SW	100-150		<32				Fi 5-7, 10-11 BFi 1-2	Fi 5-7, 10-11 BFi 1-2	Brändan Block
3	N26 W/80 W	>25	>3 000		x	x		Fi 8	Fi 8	Gåvastbo Block
4	N50 W/80SW	<20	1 000		x					Brändan Block
5	N60 W/80 SW	<10	800		x					
6	N60 W/80 SW	5	700	0,5-5		x	x	HFi 1	HFi 1	
7	N60 W/90		450		x				BFi 1-2	
8	N60 W	<10	>900		x	x				
9	N60 W	<10	350		x	x				
10	N60 W/85 S		>1 000		x	x				Brändan Block Gåvastbo Block
11	N60 W		800		x					
12	N30 E/85 NW		400		x	x			BFi 1	
13	N23 W/19 S	<5	1 000	<5			x	Fi 6, 11		
14	Ns/15 W	<65	>1 600		x	x		Fi 7		Brändan Block
15	NS/15 SW		>1 600		x	x		Fi 7		

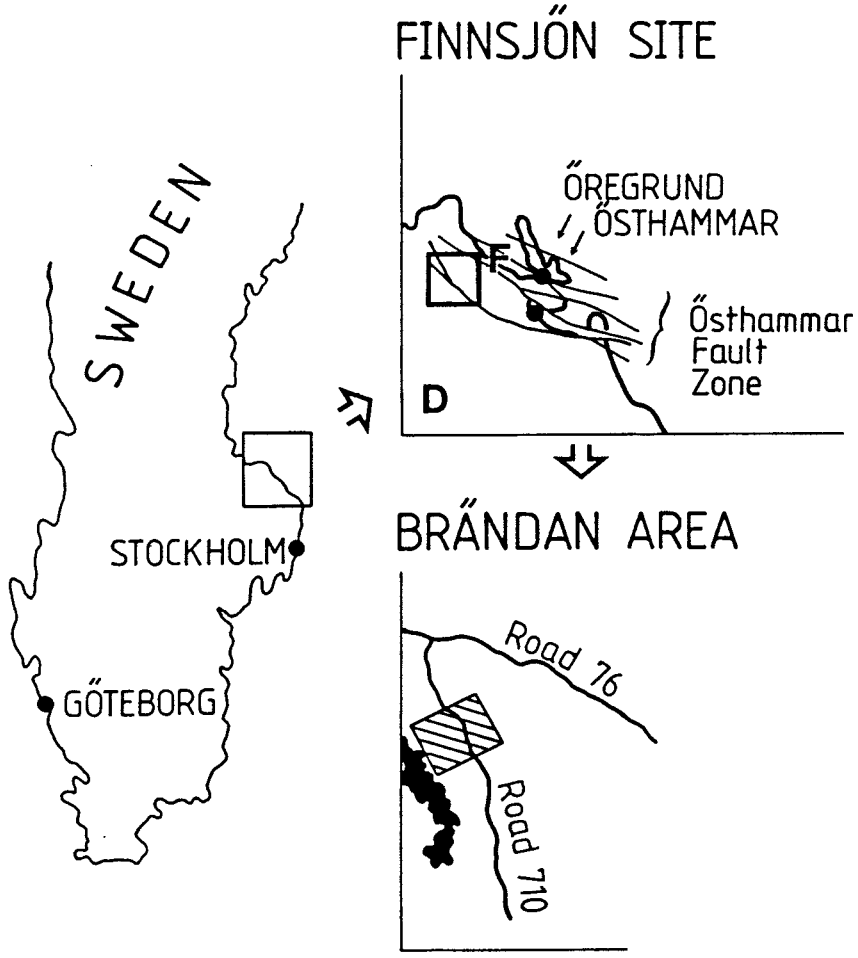

Figure 1: Location of the Finnsjön site and the Brändan area, central, eastern Sweden. F = Forsmark and D = Dannemora. The Östhammar Fault Zone is outlined on the map of Sweden.

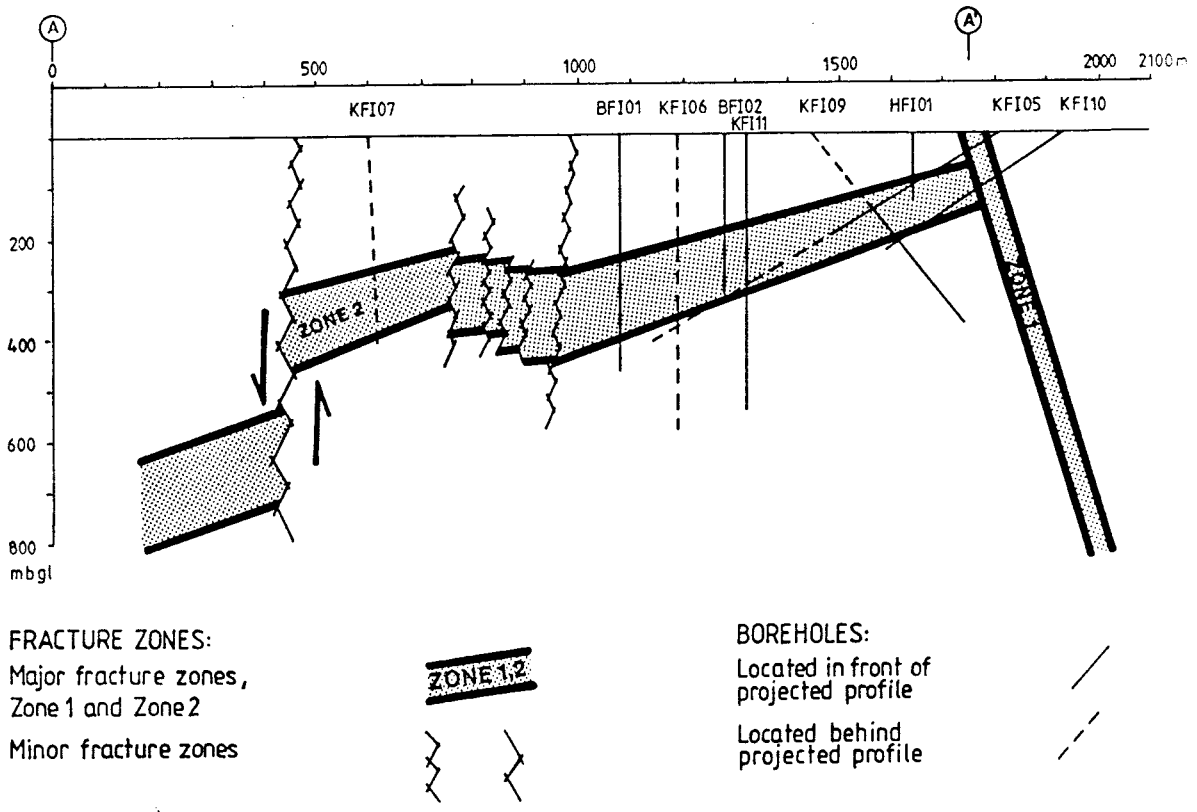

Figure 2: Vertical section through the low angle fracture zone (Zone 2) in the Finnsjön site. The location of the projected section A-A´ is shown in Figure 3.

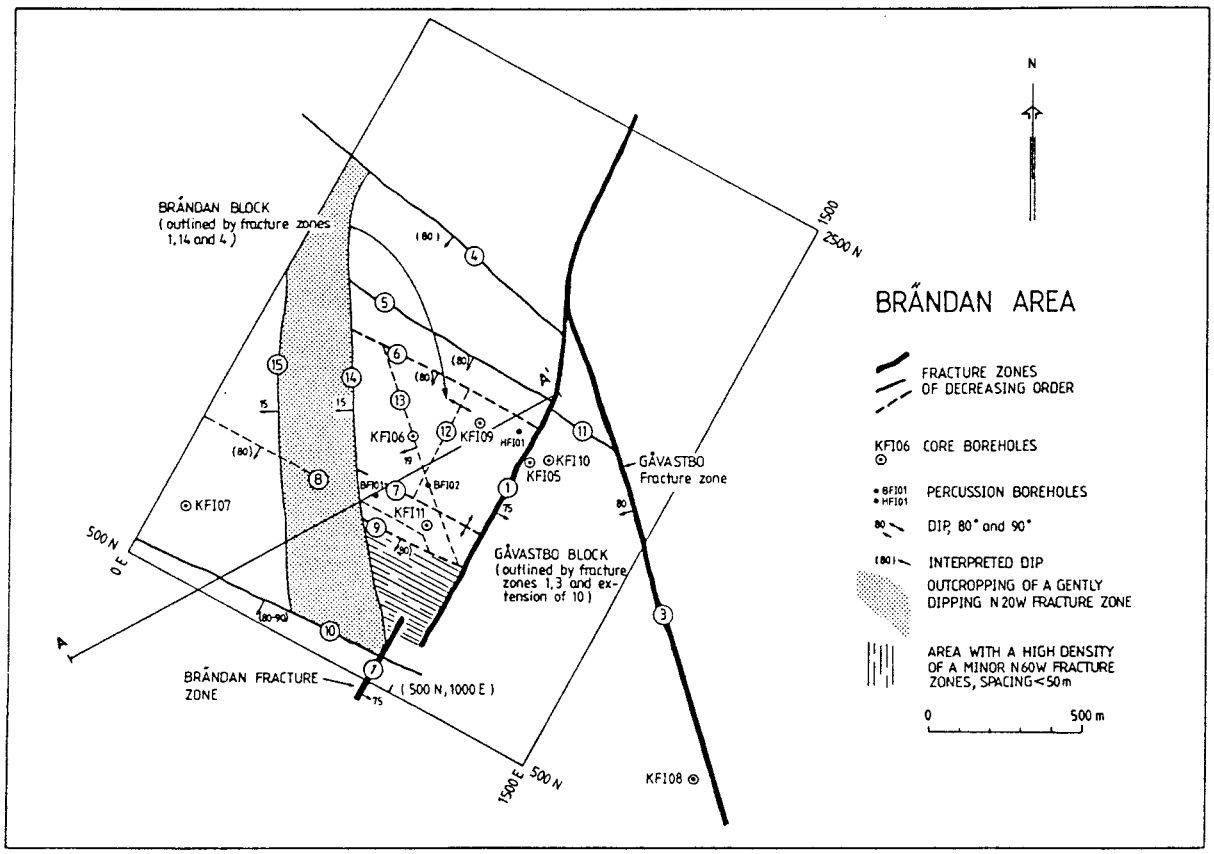

Figure 3: Map of fracture zones in the Brändan area, northeastern Uppland. Fracture zones are listed in Table 2 according to their numbers. Foliation is uniform in the area (N60-70W/80-90NE). The gently SW dipping zone shown on the map is a minor zone parallel to Zone 2. Projected section A-A´ illustrated in Figure 2, is also shown.

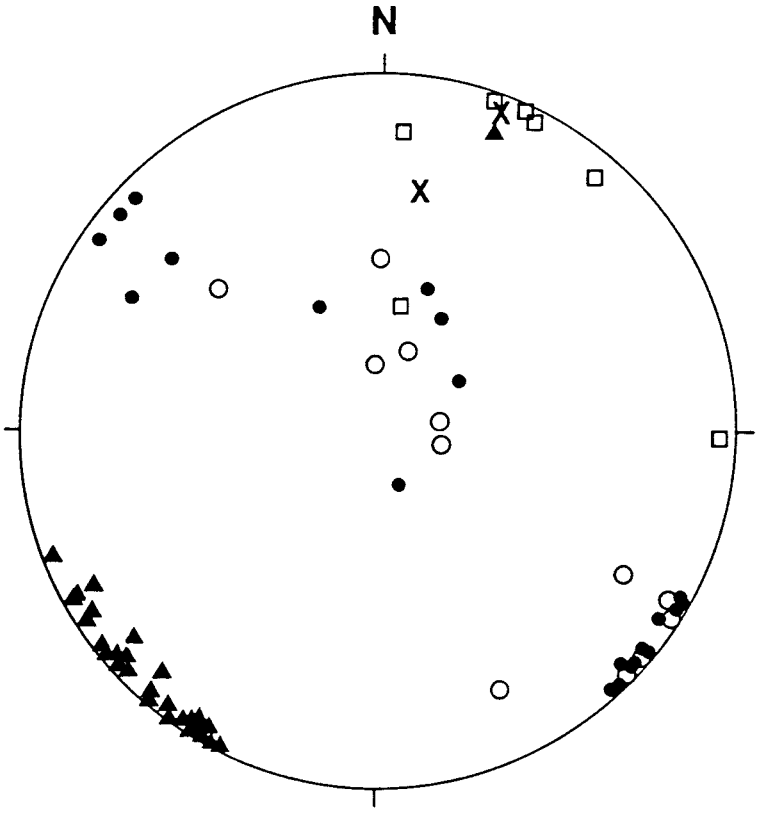

Figure 4: Orientation of dykes plotted on a Schmidt net, lower hemisphere projection. Dots represent pegmatites associated with the granodiorite (n = 21), rings represent pegmatites and aplites associated with the younger granite (n = 12), crosses are dolerites (n = 2), squares are metadoleritic layers (n = 5), and triangles are the foliation (n = 28).

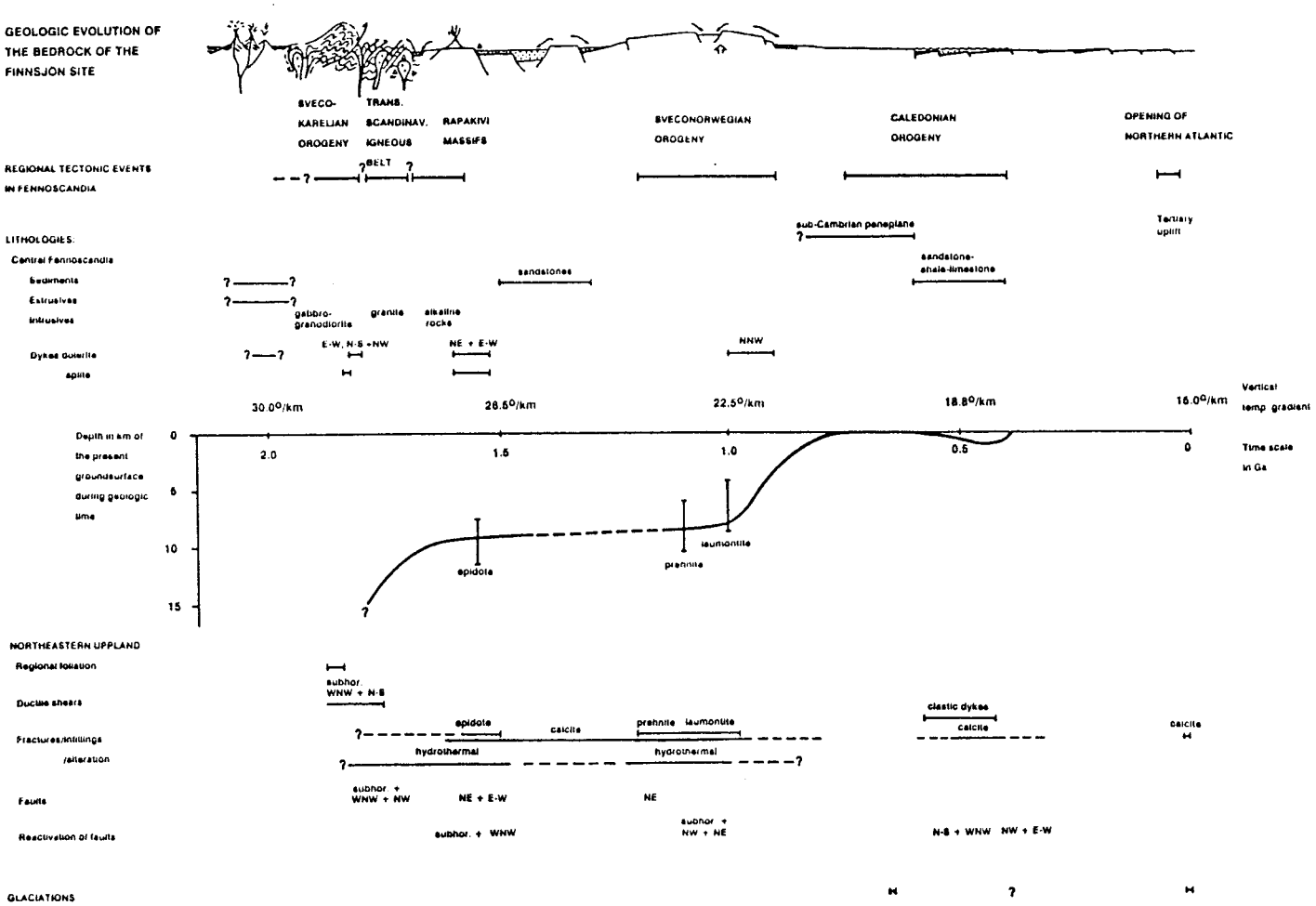

Figure 5: Geologic evolution of the Finnsjön site with references to regional geologic events. Main data sources: Wiman (1930, 1942), Rudberg (1954), Vaasjoki (1977), Lundqvist (1979), Welin et al. (1980), Olkiewicz and Arnefors (1981), Tullborg and Larson (1982, 1984), Bergman (1982), Wickman et al. (1983), Gorbatschev et al. (1987), Ahlbom et al. (1988), Stålhös (1988), Munier and Tirén (1989).

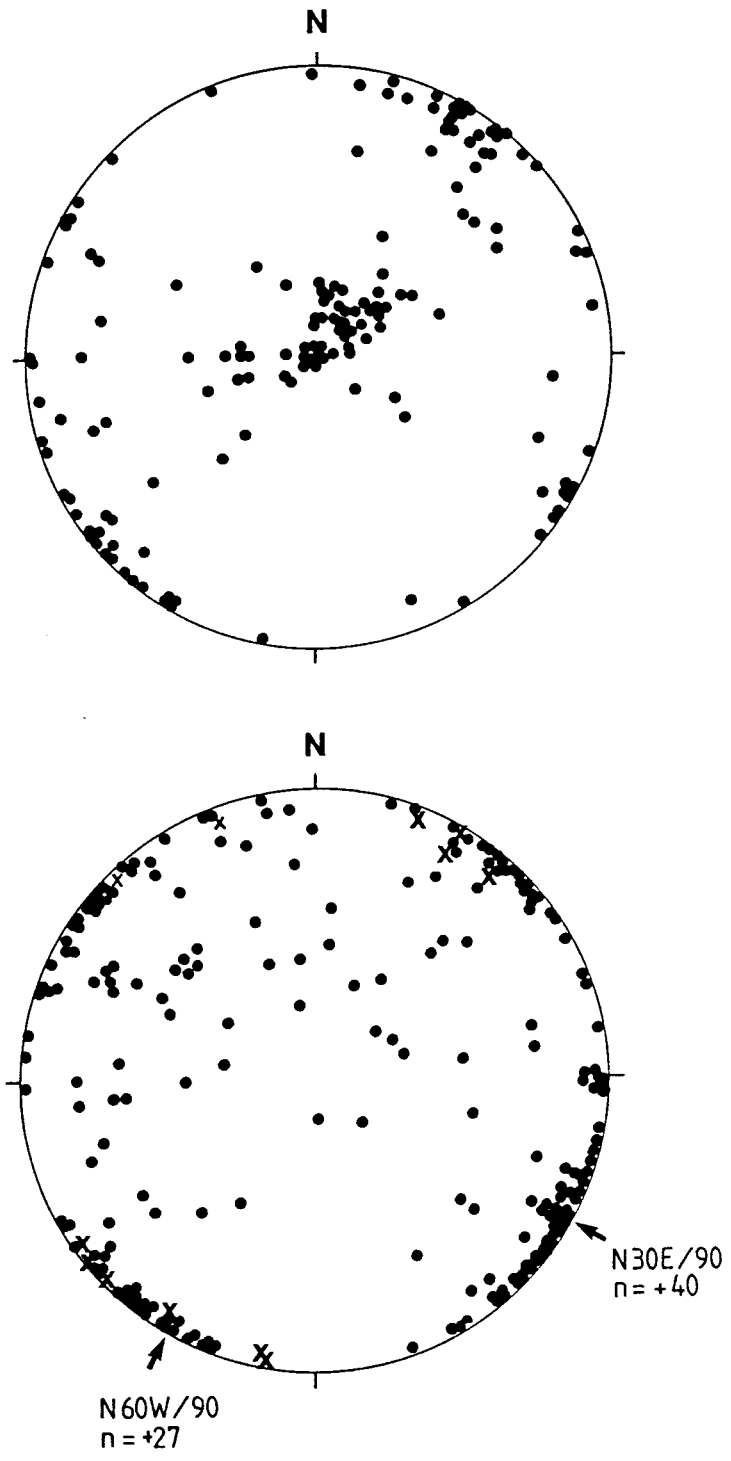

Figure 6: Orientation of fractures in the Brändan Block plotted on a Schmidth net; lower hemisphere projection.
a. Fractures outlining the outcrops (n = 154).
b. Fractures in outcrops. Dots represent "ordinary" fractures (n = 266) and crosses represent mylonitic shears (n = 14).

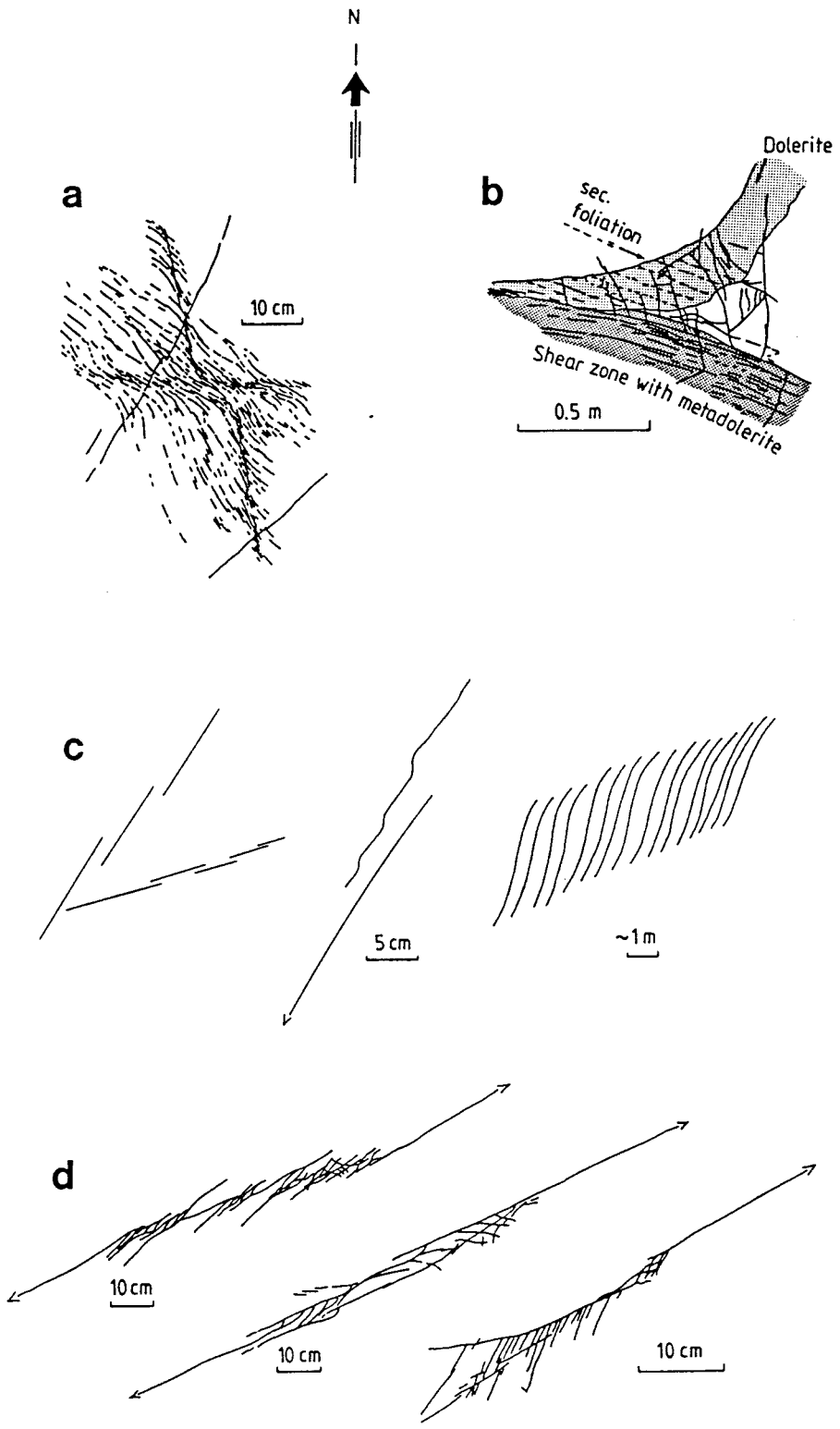

Figure 7: Examples of ductile shear zones and fractures present in the Finnsjön site.
a: NW ductile shears
b: N30E en echelon fractures
c: Interconnections of N70E fractures

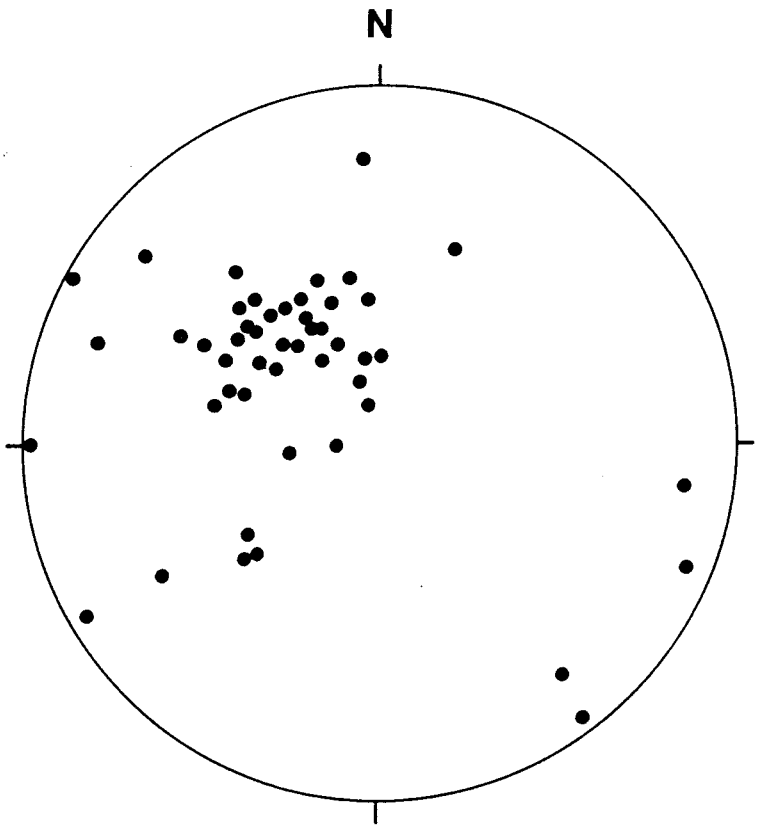

Figure 8: Orientation of laumontite coated fractures (n = 49) in the Gåvastbo Block plotted on a Schmidt net; lower hemisphere projection.

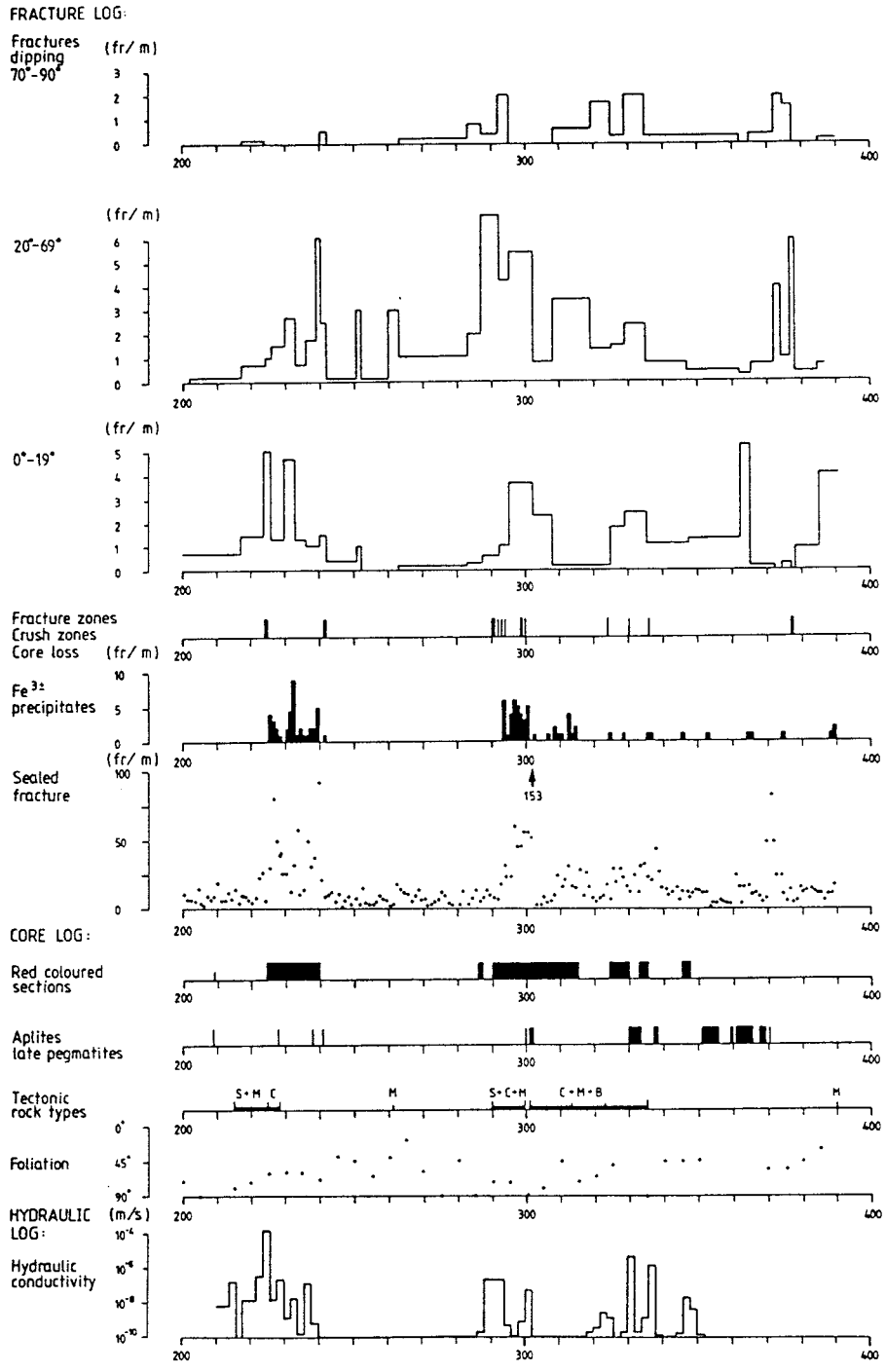

Figure 9: Composite geologic log and hydraulic conductivity across Zone 2; borehole KFI11, section 200-390 m. (S = ductile shear, M = mylonite, C = cataclasite and B = breccia. Arrows = slickenside striation. Foliation: 0° = horizontal and 90° = vertical). For discussion of hydraulic properties of Zone 2, see Andersson et al. (This volume).

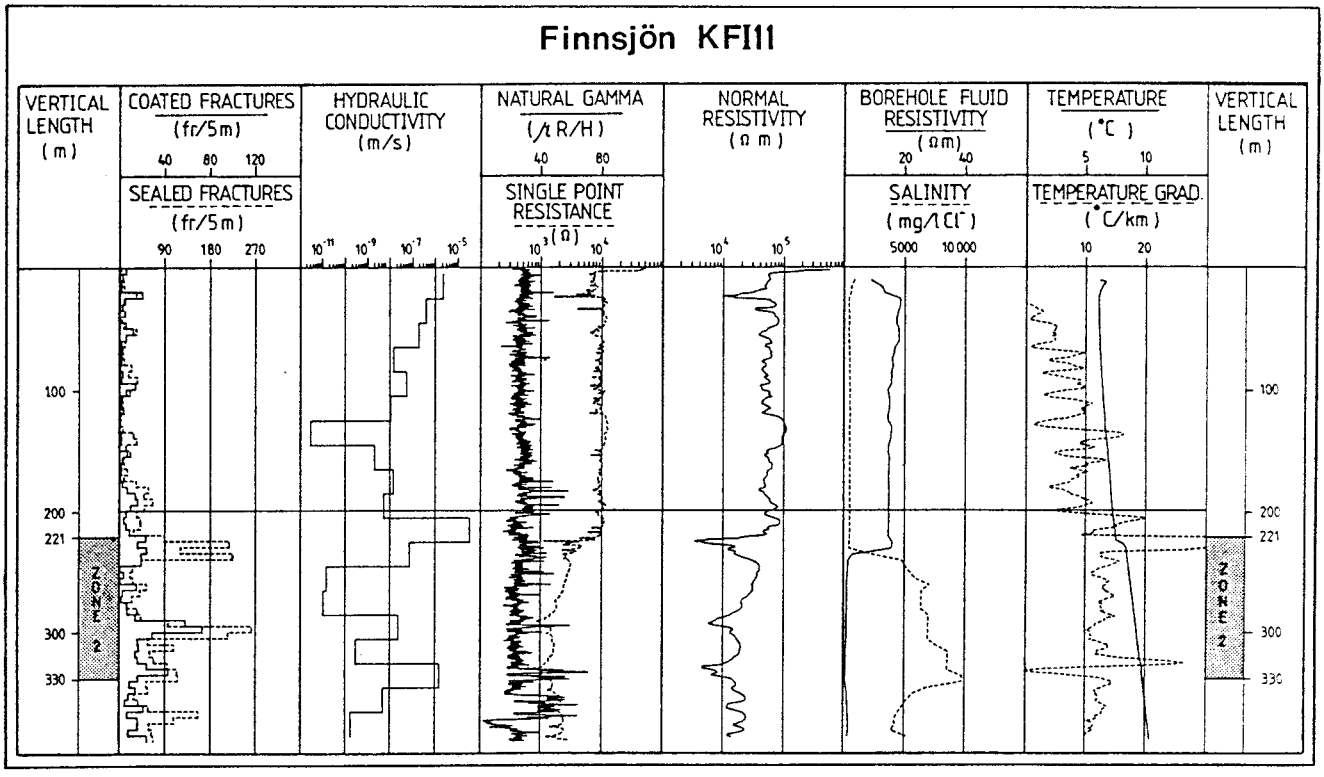

Figure 10: Composite geophysical log of borehole KFI11.

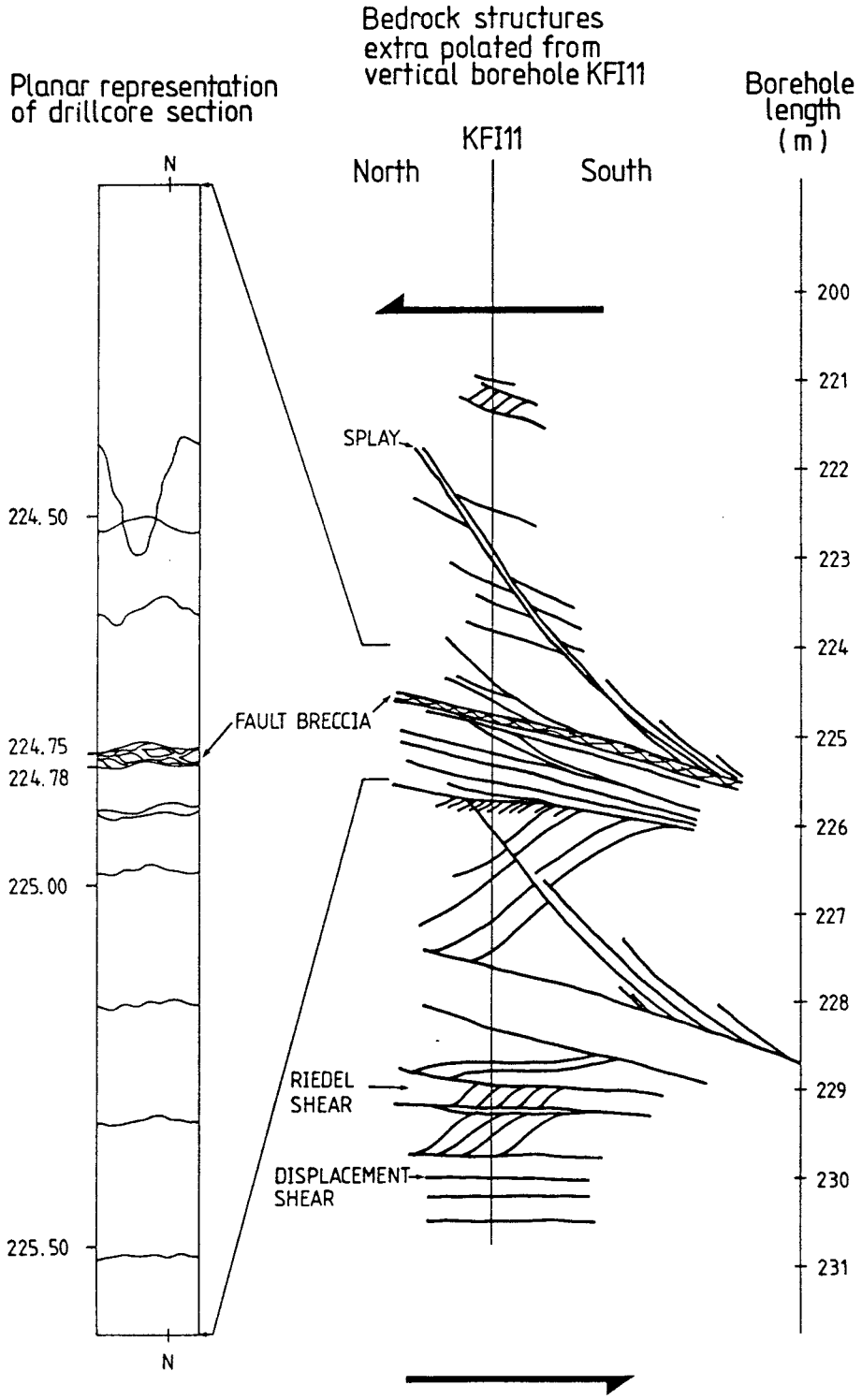

Figure 11: Tentative fracture model of the uppermost section of Zone 2. It is worth noting that the breccia is incohesive and the loose fragments removed from the borehole ranged in size from 0-3 cm; some were striated and prismatic.

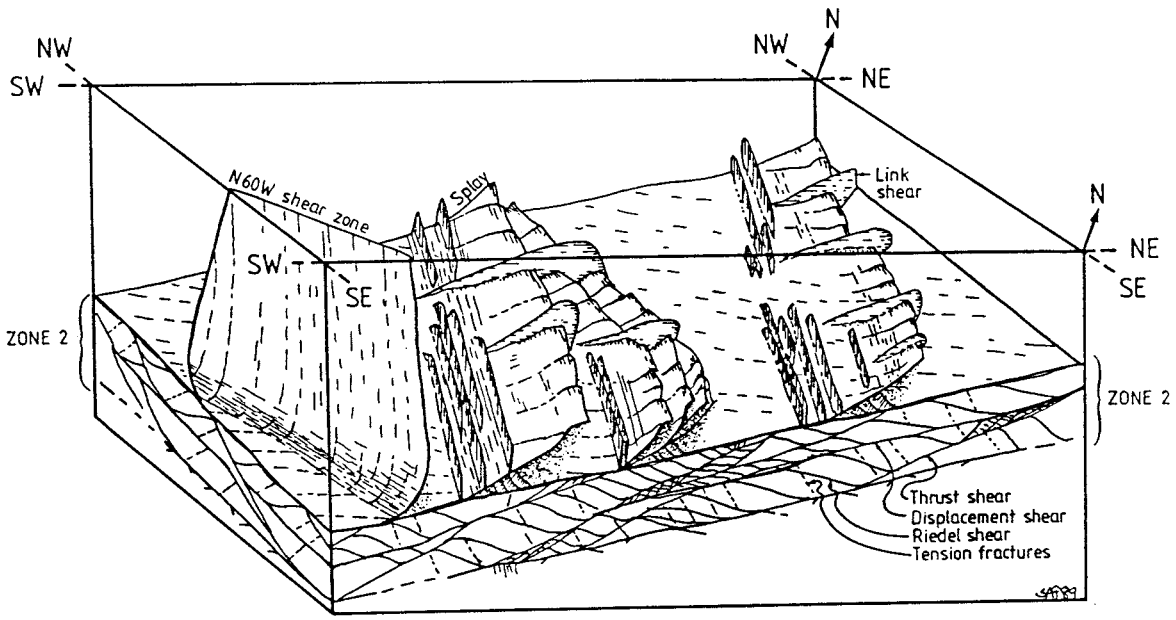

Figure 12: Tentative fracture model of Zone 2 formed in a thrust regime with maximum compression to the NE. Vertical and horizontal scales are similar.

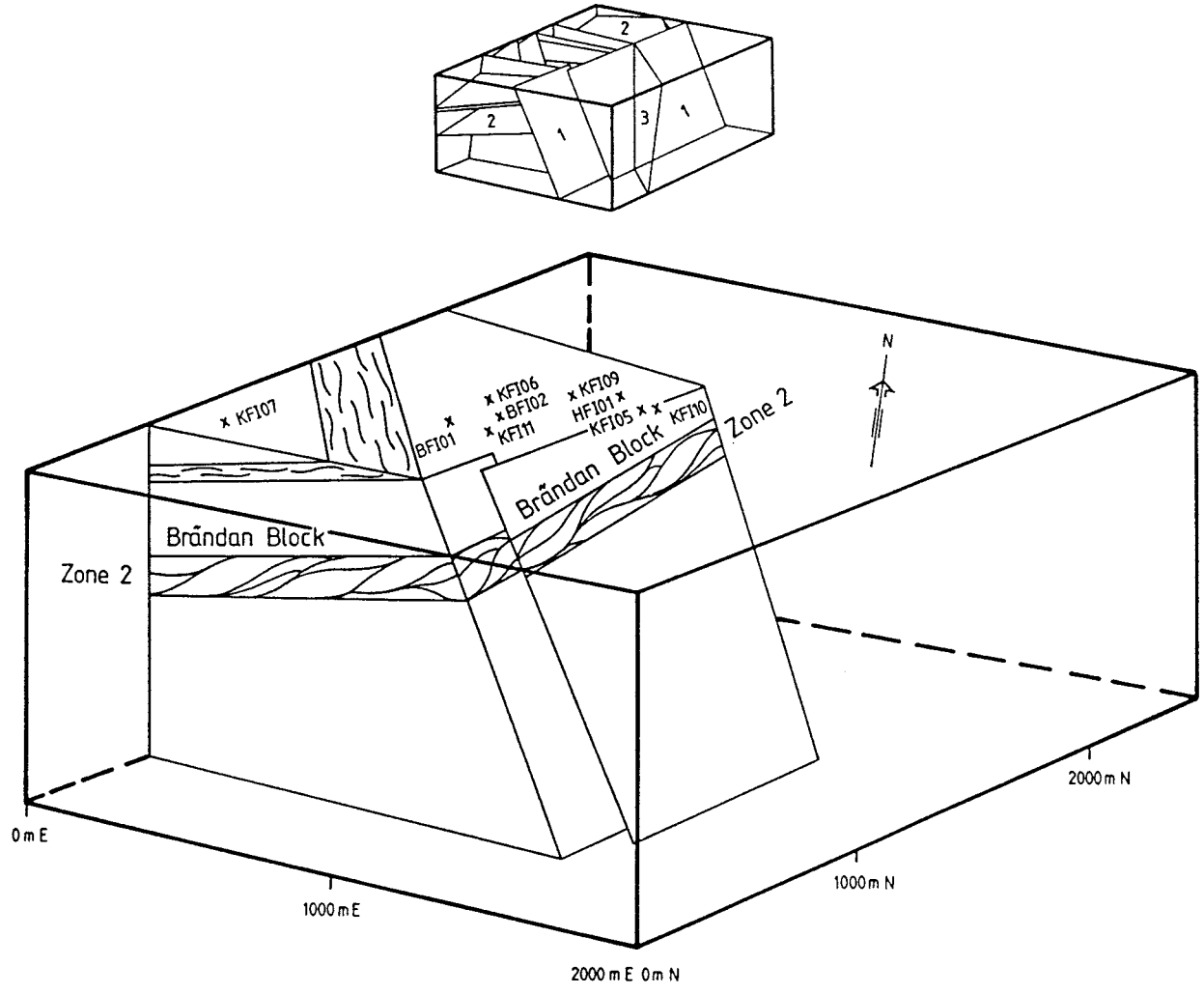

Figure 13: Brändan Block and Zone 2, the Brändan area, northeastern Uppland.

HYDRAULIC TESTING AND MODELLING OF A LOW-ANGLE FRACTURE ZONE AT FINNSJÖN, SWEDEN

J-E. ANDERSSON[1], L. EKMAN[1], R. NORDQVIST[1] and A. WINBERG[2]

[1]Swedish Geological Company, Box 1424, S-751 44 Uppsala (Sweden)
[2]Swedish Geological Company, Pusterviksgatan 2, S-413 01 Göteborg (Sweden)

Abstract

This paper describes the hydraulic characteristics of a gently dipping fracture zone in crystalline rock at the Finnsjön test site in Sweden. The information is derived from single-hole injection tests of different packer spacings, including very detailed tests in 0.11 m sections in a few borehole segments. In addition, preliminary interference tests were carried out during drilling of borehole BFI01. Subsequently, detailed interference tests were performed by pumping in different parts of the zone and monitoring pressure changes in multiple-section observation boreholes.

The results of the hydraulic testing show that the fracture zone is composed of 2-5 narrow, highly conductive subzones in the boreholes, the uppermost subzone consistently located close to the upper boundary of the zone. This subzone can be correlated over several hundreds of metres along the zone.

There are evidences of hydraulic anisotropy of the zone, both in the lateral and vertical directions. The interference tests showed that the fracture zone is delimited by semi-permeable boundaries, probably consituted by steeply dipping fracture zones. The results of the hydraulic testing were used to simulate the pressure responses obtained in the observation boreholes by a numerical model.

1. Introduction

The hydraulic characteristics of a gently dipping fracture zone (Zone 2) are described, together with its hydraulic interaction with the adjacent rock. The results from an analysis of the geology and tectonics (Tirén, this volume) together with hydrogeologic interpretations are integrated into a numerical model of the Finnsjön study site and the Brändan area in particular.

Hydrogeologic interpretation is mainly based on results from single-hole tests and interference testing including hydraulic head measurements. The results of the single-hole tests including estimations of the conductive fracture frequency are presented by Andersson et al. (1988a and c). In addition, tracer and dilution tests were performed in boreholes transecting Zone 2. The results from the latter tests were used in conjunction with the hydraulic head conditions to estimate the natural groundwater flow within Zone 2 (Gustafsson and Andersson, this volume).

Preliminary interference tests and hydraulic head measurements were carried out during drilling of borehole BFI01. After the drilling of borehole BFI02, detailed interference tests were performed in different isolated parts of this borehole with pressure responses measured in multiple-section observation boreholes. The preliminary tests are reported by Ahlbom et al. (1987) and the detailed interference tests by Andersson et al. (1988b).

In Figure 1 a location map of the Finnsjön area, including the Brändan area is shown. A schematic cross section through the Brändan area is presented in Figure 2.

2. Single-hole testing

Single-hole water injection tests have been carried out during different phases since 1977 at the Finnsjön study site. Test

results from boreholes used in the Fracture Zone Project have been reported by Ahlbom et al. (1986, 1987), Andersson et al. (1988a) and Ekman et al. (1988). Table 1 compiles information on the boreholes used, section lengths, intervals measured and year of testing for the single-hole tests. The test sequences before 1985 were not specifically performed within the Fracture Zone Project, but used for comparison with recent tests. The table shows that, in general, the single-hole tests were performed using both long and short test sections (20 m and 2 or 3 m, respectively). A few 2 m-sections in BFI02 were further tested along 0.11 m sections. The prime objective of the testing was to characterize Zone 2 in detail by identifying and measuring hydraulically significant borehole intervals.

In conjunction with the single-hole tests, special studies in some of the boreholes were also undertaken to investigate various items of interest. For example, a comparative study of tests performed with two different equipment systems in borehole KFI10, and a study on the effects of gas-lift pumping as a means to clear a borehole from drilling debris etc. (Andersson et al., 1987 and this volume). Furthermore, an analysis of the conductive fracture frequency within Zone 2 and adjacent parts of the bedrock, including a comparison of previous and renewed tests in 3 m and 2 m sections respectively in boreholes KFI05, KFI06 and KFI07, was reported by Andersson et al (1988a). A special study was also performed in borehole BFI02 (along a limited number of intervals) using a very short packer spacing of 0.11 m (Ekman et al., 1988).

2.1 Test methods and interpretation

The 2m-tests were performed using two types of equipment systems: the pipe string equipment system and the umbilical hose system (Almén et al., 1986a). The tests with short packer spacing were generally performed as constant head, steady-state injection tests. An injection head (H_0 = 200 kPa) was applied for a period of approx. 15 min, after which the pressure recovery was registered (approx. 15 min). In the most

conductive test sections rather low injection heads (a few kPa) were achieved depending on the flow capacity of the actual equipment system used. In test sections of particular interest, e.g. highly conductive intervals in Zone 2, transient injection tests of longer duration were employed to obtain more information on the hydraulic conditions and more reliable values on the hydraulic parameters. In these tests the injection and recovery periods had a duration of 2 hours.

In one of the large-diameter boreholes, BFI02, single-hole injection tests were also performed in very short test sections within some of the hydraulically most interesting 2 m sections previously tested. To facilitate these measurements, a new single-hole testing tool was developed (Ekman et al., 1988). This tool has an overall length of 3.4 m with a total inflation length of 3 m (Fig. 3). Centrally located is a perforated stainless steel sleeve, the perforation serving as orifices for the pipe string. The length of the test section is in this case governed by the packer inflation pressure, the elasticity of the rubber and the difference in diameter between the borehole and the deflated packer. The diameter of the packer is 150 mm. Together with the geometry of BFI02 the resulting effective section length becomes 0.11 m. Downhole testing was preceeded by a surface and subsurface testing programme where the geometrical and mechanical character of the test equipment, including packer creep and head losses in the tool due to friction, were established. Packer inflation and deflation periods during the very detailed tests were approx. 15 minutes, whereas an injection period of 5 minutes was used.

The steady-state tests, constituting the majority of the 2 m and 0.11 m tests, were normally evaluated according to the following expression (Zeigler, 1976):

$$K_{SS} = \frac{Q_P}{H_o \, L} \cdot C \qquad (1)$$

where K_{ss} = steady-state hydraulic conductivity (m/s)
Q_p = flow rate during final stage of injection (m^3/s)
L = length of test section (m)
H_o = injection head (m)

The constant C which takes into account the flow geometry of the test is defined by Moye (1967) as:

$$C = \frac{1 + \ln\left[\frac{L}{2 \cdot r_w}\right]}{2 \cdot \pi} \qquad (2)$$

where r_w is the radius of the borehole in metres.

The definition of the constant C assumes flow in a homogeneous porous medium. Thus, the validity of the constant C is questionable for tests in fractured crystalline rock with isolated flow paths (Doe and Remer, 1982). The C-value used for the 0.11 m tests was the same as for the 2 m-tests because the calculated value for a 0.11 m section length (and thus the K_{ss}-value) according to Eqn. (2) turned out to be unrealistically low in comparison to transient evaluation.

The transient tests were evaluated in accordance with the actual flow geometry of the tests (Andersson and Persson, 1985). The theory and methodology of the transient tests is described by Almén et al. (1986b).

2.2 Results

The results of the 2 m-tests in boreholes within the Brändan area reveal large contrasts in hydraulic conductivity within Zone 2, ranging from minimum values of 10^{-10} m/s (lower measurement limit) up to about 10^{-3} m/s. Between two and five highly conductive subzones were identified in each borehole; two of the subzones were consistently located along the upper and lower boundaries of the zone. The results from the 20 m- and 2 m-sections in BFI02 are presented in Figure 4a. To facilitate comparison of the tests, the transmissivity

(T = K L) of the sections is plotted in the figure. The results indicate an apparent, rather smooth transmissivity profile from the 20 m-sections above the zone. This pattern is altered significantly when the resolution in the section length is increased one order of magnitude within the zone. Two interpreted subzones in borehole BFI02 are indicated with (steady-state) transmissivities about 8 x 10^{-4} m^2/s. This value is considered as the upper measurement limit of the actual equipment system used for the 2 m-tests.

Detailed measurements along 0.11 m test sections incorporating some of the subzones were performed over a total length of 8 m in borehole BFI02 (Table 1). In Figure 4b the results of the 0.11 m measurements in the two successive 2 metre sections incorporating the uppermost subzone (sections 202-204 m and 204-206 m) are presented in terms of transmissivity. The figure shows several interesting features; firstly, the sum of transmissivities calculated from the two 2 m-tests are in good agreement with the cumulative transmissivity obtained from the 0.11 m tests over the same 4 m interval (202-206 m). In fact, the uppermost subzone only consists of a few 0.11 m sections which govern the total transmissivity of the entire 4 m interval (and a major part of Zone 2).

The increase in resolution (scale) of the testing thus provided the possibility to more accurately define the "true hydraulic width" of the uppermost subzone, which was estimated at about 0.4 m. The main flow path within the subzone may be even narrower. The transmissivity values show a gradual increase towards the central part of the subzone. In addition, the fact that the subzone was located at the limit of two 2 m-test sections, thus tended to obscure the narrow width of the subzone in the 2 m-tests. If a longer section length had been used for testing (e.g. 20 m), an even more false impression of the true width of the subzone may have resulted.

The single-hole tests in the other boreholes within the Brändan area show the same general pattern for Zone 2, i.e. comprising a few highly conductive intervals (subzones). The

very detailed tests in BFI02 revealed that the width of the subzones is in the order of decimeters. This is also consistent with the core mapping which indicates a limited number of narrow zones with intense fracturing and deformation (Tirén, this volume). In general, between two and five subzones are present within the major extent of Zone 2; the total thickness of Zone 2 is more than 100 m. In all boreholes the hydraulic conductivity within the upper boundary of Zone 2 contrasts markedly with the overlying rock (two to three orders of magnitude). In most boreholes a large hydraulic conductivity contrast is also present between the lower boundary of Zone 2 and the underlying rock (Ahlbom et al., 1987).

As shown by the interference tests these features are laterally consistent over several hundreds of metres. Possible vertical interconnections between the subzones were not investigated during the single-hole testing campaign but instead during the interference testing (see Section 4.2). In summary, the single-hole tests show that the hydrogeological character of Zone 2 mainly consists of long intervals of low- to intermediate-conductive rock, separated by a few highly conductive narrow subzones.

3. Conductive fracture frequency

The conductive fracture frequency (CFF) implies the hydraulically conductive portion of the total number of (coated) fractures mapped over a given length in a borehole or an underground opening. This entity has previously been estimated employing statistical techniques (Carlsson et al., 1984; Osnes et al., 1988), using information on mapped fracture properties (Winberg and Carlsson, 1987) and finally by multivariate analysis of integrated borehole data (Andersson and Lindqvist, 1988). Based on results from single-hole tests in detailed sections (2 and 3 m) in the cored boreholes within the Brändan area, the conductive fracture frequency within Zone 2 and of the adjacent rock was calculated using statistical methods.

The statistical techniques, utilizing information from hydraulic tests and core logs, yield an estimate of the probability that one fracture is conductive. A hydraulic conductivity equal to the lower measurement limit is in this context regarded as non-conductive. Combined with the average frequency of coated fractures in the studied domain an estimate of CFF can be obtained. Statistical homogeneity and independence is assumed in the rock volume studied. The details of the analysis is presented in Andersson et al. (1988a).

Essential input data regarding the total frequency of coated fractures are provided by Ahlbom et al. (1985) and Tirén and Arnefors (1987). The CFF has been calculated for the entire Zone 2, the adjacent rock mass above (denoted B1), and below (B2) the zone. Three subparts of the zone have been defined; an upper (A1) and a lower (A3) more conductive part and the remainder of the zone (A2). The former two correspond respectively to the more fractured and more conductive portions of the zone consistently observed in the detailed hydraulic testing along its upper and lower boundary.

Data from recent testing in boreholes KFI05, KFI06, KFI07, KFI09, KFI10 and KFI11 (2 m sections) have been used in the analysis (data set 1). Since hydraulic measurements in 3 m sections were made previously (see Table 1), and existing old core mapping is available for boreholes KFI05, KFI06 and KFI07, a unique opportunity exists to make a comparison between calculated values of CFF based on new (data set 1) and old data (data set 2) for these boreholes. The results of the calculations are compiled in Tables 2 and 3 and Figure 5.

The results show that Zone 2 has a CFF of around 1 fracture/m which is of the same order as the calculated CFF of the surficial rock mass above the zone and twice that of the bedrock below the zone. The CFF value for Zone 2 should be compared with an average frequency of coated fractures in the zone of 5.2 fractures/m. The lack of entries for subparts A1 and B2 in the case of boreholes KFI05-07 (data set 1) are due to a lack of convergence in the calculations and lack of data,

respectively. The two extreme values calculated for data set 2, subparts A1 and B1, are due to a total lack of no-flow sections and influences of very surficial data, respectively.

Comparison between the analyses of the old and new data sets reveal that the calculated CFF, based on data set 2, is 1.2-1.4 times higher when discounting the above mentioned extreme values. This is in agreement with that expected from the measurement limits of the two sets, i.e. 2 x 10^{-10} m/s (except KFI05, 2 x 10^{-9} m/s) and 7.5 x 10^{-10} m/s (KFI09-KFI11, 1x10^{-10} m/s) for the old and new data sets, respectively. A lower measurement limit may be conceptualized by adding more minor conductive fractures to the measured quantity, i.e. the hydraulic conductivity, which in turn would entail an increase in the portion of conductive fractures.

Possible leakage around packers, particularly in the case of the tests performed in KFI05, KFI06, KFI07 (data set 2), tends to overestimate the difference. This fact is moderated by a contemporaneous underestimation in average fracture frequency in the case of data set 2 (compare Tables 2 and 3). The respective sizes of the confidence limits reflect the variance in the estimator. The greater the amount of data (n_m), the higher the values of P and N (m=1,...,N) used, the smaller the variance and the narrower the confidence limit obtained.

The calculated values of the conductive fracture frequency (CFF) are compatible with the overall results of the single-hole hydraulic testing. The results indicate that only 10-40 % of the mapped coated fractures are hydraulically active, the actual figure being closely related to the lower measurement limit of the hydraulic testing equipment used.

4. Interference testing

During the drilling of borehole BFI01 the groundwater head was registered in isolated sections of the other boreholes within the Brändan area (c.f. the hydraulic head measurements

described by Gustafsson and Andersson, this volume). Since water was flushed out of borehole BFI01 by compressed air at a fairly constant rate during the drilling periods, these periods could be regarded as (preliminary) drawdown tests. Between the drilling periods the groundwater head in the boreholes was allowed to recover. Subsequently, more sophisticated interference tests were carried out by pumping from different parts of Zone 2 in borehole BFI02 and monitoring the head changes in isolated sections of boreholes within Zone 2 and in a few open boreholes outside the zone. The interference tests during drilling of BFI01 and after drilling of BFI02 are described separately.

4.1 Tests during drilling of BFI01

In the preliminary interference tests carried out during drilling of BFI01, the groundwater head was in general registered in five isolated sections in the observation boreholes; two sections above and two below the central section which normally comprised the entire Zone 2. The uppermost observation section in the boreholes corresponded to the groundwater table. In those boreholes intersected by Zone 1 (Fig. 2) this zone was also isolated by packers. The packer configuration in the observation boreholes was identical during all drilling steps and the duration of each drilling step was rather short, varying from a few hours up to about 13 hours. The duration of the drilling steps, the discharge rate, and rate of penetration during drilling of borehole BFI01, are shown in Figure 6. The dotted line denotes the cumulative flow rate during drilling and the solid line denotes the average volume discharged per penetrated metre. A detailed account of the drilling protocol is described by Ahlbom et al. (1987).

Drilling steps 1 and 2 both terminated above Zone 2; during these steps no significant responses to the flushing (pumping) were observed in any of the observation boreholes. In contrast, when the upper part of Zone 2 (at about 250 m) was penetrated during step 3, very pronounced and rapid responses occurred in

all borehole sections within the Brändan area, confirming Zone 2 as a prime conductor within the area. It also confirms the large contrast in hydraulic conductivity between the zone and the overlying rock indicated by the single-hole tests (see Section 2). Even the most distant observation sections in Zone 2 responded within a few minutes after penetration of the zone (see below). The discharge rate from BFI01 (by air flushing) was considerably increased to about 25 m^3/h (6.9 l/s) by the penetration of the upper conductive horizon of Zone 2 (see Fig. 6).

Drilling step 4 was terminated when the lower conductive horizon of Zone 2 was penetrated at about 350 m. During penetration of this horizon the discharge rate again increased significantly (see Fig. 6). Between the upper and lower horizons of Zone 2 the discharge rate appeared to be rather stable. However, with the measuring technique used (cumulative discharge), only major conductive horizons can be identified (Smellie et al., 1987). During drilling step 5 the final stage of which penetrated the rock below Zone 2, no registration of head changes in the observation boreholes was made. Step 6 was drilled entirely in rock below Zone 2 and, as can be seen from Figure 6, the discharge rate increased somewhat, indicating a certain contribution of water from the interval below Zone 2 (Ahlbom et al., 1987).

Once the top of Zone 2 was penetrated, the repsonses in the observation borehole sections were very similar, i.e. during drilling steps 3 (final part), 4 and 6. As an example of the pressure response, the recovery after drilling step 6 in borehole KFI11 is shown in Figure 7. The rapid responses obtained in those sections representing Zone 2 in all observation boreholes within the Brändan area after penetrating the upper part of Zone 2, may be regarded as primary (or direct) responses. Since the head change in the entire Zone 2 was only measured in one section in each borehole, no detailed picture of the response pattern in the vertical direction of the zone could be established (cf. Section 4.2).

The observation sections above and below Zone 2 generally show somewhat more delayed and attenuated responses (secondary or indirect responses). The latter responses are likely to initially be propagated along Zone 2 (like the primary responses) and then become diverted by subvertical fractures to the surrounding sections in the observation boreholes, or possibly by conduits along the boreholes (Ahlbom et al., 1987). The uppermost section in each observation borehole, representing the groundwater table, always reacted slower than the other sections due to borehole storage effects.

According to the qualitative interpretation of the reponses in the observation borehole sections discussed above, quantitative analysis of the (average) hydraulic properties of Zone 2 was performed (Ahlbom et al. 1987. High values on the hydraulic conductivity of Zone 2 were calculated from the responses in the observation sections encompassing the zone (primary responses). Apparent (high) values were also calculated from the (secondary) responses in the surrounding sections using the same methods. However, according to the qualitative interpretation, these values may not be representative of the hydraulic conditions between these sections and the pumping borehole, but instead dominated by the properties of Zone 2. This conclusion is also confirmed from the results of the single-hole tests along these intervals in the observation boreholes (Ahlbom et al., 1987). The single-hole tests generally resulted in much lower values on the hydraulic parameters in these sections than indicated by the interference tests.

The responses in Zone 2 were evaluated according to the theory for radial flow in an aquifer of infinite areal extent, both using time-drawdown and distance-drawdown analyses. Thus, Zone 2 was treated as one hydraulic unit in the analyses. Both the drilling (pumping) phase and the recovery phase after drilling were analysed. However, due to the short duration of the drilling steps no firm conclusions about the actual outer hydrogeological boundaries of Zone 2 could be deduced from the tests. The transmissivity and storativity calculated for Zone 2

from different boreholes and drilling steps range from about $5x10^{-4}$ m^2/s to 10^{-3} m^2/s and from $4x10^{-7}$ to $5x10^{-5}$, respectively.

The detailed interference tests subsequently carried out in borehole BFI02, which were of longer duration, demonstrated the presence of (closed) outer boundaries of Zone 2 (see below). Since the interpretation of the preliminary interference tests did not account for (closed) hydrogeological boundaries, the transmissivity values calculated for Zone 2 were thus in general somewhat underestimated, whereas the storativity values calculated were accordingly overestimated (c.f. Section 4.2). The preliminary interference tests during drilling of BFI01 thus only provided rough estimates of the hydraulic properties of Zone 2.

The calculated values of the hydraulic parameters from the different drilling steps were very similar and showed that the hydraulic properties of Zone 2 totally dominate the borehole responses once the upper part of the zone was penetrated. The results also indicate a good vertical hydraulic connection within Zone 2 as evidenced by the similar responses obtained during drilling step 3 (when only the uppermost part of the zone was penetrated) and during step 6 when the entire zone was penetrated.

A rough estimate of the possible anisotropy in the lateral direction of Zone 2 was made from the calculated rate of propagation of the pressure pulse from BFI01 in different directions. The approximative times of first response were calculated for some borehole sections. This time (t_e) is here defined as the time after start of drilling (pumping) corresponding to a head change of 0.02 m in the observation sections. Knowing the distance (r) between BFI01 and the observation sections along Zone 2, the mean velocity (v) of the propagation of the pressure pulse may be estimated in different directions (assuming one-dimensional flow), simply by dividing the distance by the response time. The vectors of the estimated mean velocity in different directions from BFI01 along Zone 2

are illustrated in Figure 8. The figure shows that the estimated rate of propagation of the pressure pulse (in the horizontal direction) is very high, particularly towards the boreholes KFI09 and KFI10. A certain degree of anisotropy in the zone is indicated since the mean velocity from BFI01 towards the boreholes KFI11 and particularly KFI06 is considerably lower, although these two boreholes are located closer to the pumped borehole. This fact may also be explained by local heterogeneities between the boreholes (see below).

4.2 Detailed interference tests in BFI02

4.2.1 Design and performance

After the drilling of borehole BFI02, three separate interference tests were performed in this borehole by pumping in different parts of Zone 2 (upper part, lower part and the entire zone, respectively). The primary objectives of the detailed interference tests were to determine the hydraulic properties of Zone 2 in more detail, both in the lateral and vertical directions, and to investigate the outer hydrogeological boundaries of Zone 2. Moreover, possible hydraulic connections of the most permeable horizons of Zone 2 between boreholes, and the hydraulic interaction between the zone and the over- and underlying rock, were to be investigated. The design, performance and results of the detailed interference tests are presented by Andersson et al., (1988b).

By the design of the interference tests, the results of the single-hole tests and the preliminary interference tests together with associated numerical simulations were utilized (see Section 5). As discussed above, the dominating hydraulic features of Zone 2 in the pumping borehole BFI02 (and the other boreholes) comprised the uppermost and lowermost parts of the zone. It was therefore decided to pump these parts individually and subsequently the entire Zone 2. A schematic illustration of

the packer configuration used in BFI02 for the different tests is shown in Figure 9.

In the observation boreholes KFI05, KFI06, KFI09, KFI10, KFI11, HFI01 and BFI01 a varying number of high-conductive horizons were isolated by packers. The packers were installed in low-conductive rock encompassing the high-conductive horizons to minimize the risk of pressure by-pass near the boreholes. In the observation boreholes nearest to the pumping hole, double packers were used at the top and bottom of each high-conductive horizon for an effective hydraulic isolation. In addition, in most of the observation boreholes, one section above Zone 2 and one section below the zone was isolated by packers. In all packed-off boreholes the variations of the groundwater table at the top of each borehole were monitored during the interference tests. The observation intervals in the packed-off boreholes, together with their distances (in space) to the pumped borehole intervals in BFI02 (during interference test 2), are listed in Table 4. Moreover, the vertical position of the observation sections within Zone 2 and the upper and lower boundaries of Zone 2 in the boreholes as interpreted from the single-hole tests, are included in Table 4. Note that borehole HFI01 does not fully penetrate Zone 2. Borehole KFI05 was not used during interference test 2. The peripheral boreholes KFI01, KFI02, KFI04, KFI07, KFI08 and HGB02 were used as open observation boreholes in the interference tests (see Fig. 1).

In borehole BFI02 a submersible pump was installed in the pumped interval to maintain a constant discharge rate. The groundwater pressure in this interval, and above and below, was measured by pressure transducers. In the pumped interval and below this the pressure was transmitted via hydraulic tubes to the transducers. The groundwater pressure in the packed-off observation boreholes was monitored by a multi-packer system (Piezomac) described by Almén et al., (1986a). The water discharge from the pumping borehole was controlled automatically. The groundwater flow rate, together with the electric conductivity, temperature, atmospheric pressure and

chemistry of the discharged water, was monitored continuously at the well site. All the automatic measuring devices were connnected to a data acquisition system. In addition to the automatically registered data, manual registrations of the groundwater table were also undertaken in all boreholes (including the peripheral boreholes). The active sections in BFI02, together with the discharge rates and duration of the drawdown and recovery phases of the different interference tests, are listed in Table 5. Test 3 was divided into test 3A and 3B. By the end of test 3A the automatic flow regulation system failed and the flow rate increased from 500 l/min to about 700 l/min. After recovery the test was restarted (3B) using a manual flow-rate control.

Before the start of interference test 2, tracers were injected into certain observation sections within Zone 2 (boreholes KFI06, KFI11 and BFI01) in order to investigate possible anisotropic conditions in different directions from BFI02. Furthermore, by the end of the pumping phase of test 2, an additional tracer was injected below the lower packer in BFI02 to check for possible short-circuiting of water around the packer. No short-circuiting was detected. The tracer experiments are discussed by Gustafsson and Andersson, (this volume).

4.2.2 Qualitative interpretation

Firstly, some general results, common to all three interference tests, can be deduced. Secondly, differences between the tests are discussed qualitatively, and finally a preliminary quantitative interpretation of the interference tests is presented. Since interference test 2 (in the uppermost part of Zone 2) had the longest duration (Table 5) it is discussed in more detail than the other tests. The distances from the midpoint of the pumped interval in borehole BFI02 to the midpoints of each observation section during interference test 2 are shown in Table 4. By the calculation of the distances, the deviation of the boreholes was taken into

consideration. Figure 1 shows that the subvertical boreholes KFI06, KFI11 and BFI01 are located at similar distances (approx. 150-190 m) but in different directions from BFI02. The other observation sections (within Zone 2) are located at about 250-350 m from BFI02.

The observed head changes in the different sections of borehole KFI11 and in the more distant borehole KFI09 during interference test 2 are shown in logarithmic graphs in Figures 10 and 11, and represent the near-region and distant-region responses, respectively. Figure 10 shows that the near-region responses are markedly distinct for different borehole sections. The section exhibiting the most rapid and largest head change is likely to represent the primary pathway from the pumped section in BFI02 (primary response). In test 2 the primary response in KFI11 occurs in the uppermost part of Zone 2 (section 4). The other borehole section(s) responses in KFI11 should then represent more diffuse pathways, resulting in somewhat more delayed and attenuated (secondary) responses in the lower parts of Zone 2. The primary response section(s) in each observation borehole during interference test 2 is marked with a point in Table 4. Figure 10 also shows that the section above the zone responds rapidly whereas the section below the zone responds more slowly. However, it is uncertain if a sufficient hydraulic isolation was obtained between Zone 2 and the sections above and below the zone in order to obtain representative pressure responses in these sections.

Figure 11 shows that the more distant-region responses in borehole KFI09 are less separated from each other. No pronounced primary response section occurs in this borehole but all sections within Zone 2 respond similarly to the secondary responses in KFI11. The section above (and also below) Zone 2 responds more slowly.

Figures 10 and 11 indicate that the induced (primary) pressure wave propagates very rapidly from BFI02 to the observation boreholes (cf. KFI11). This demonstrates a high transmissivity (and hydraulic conductivity) in the lateral direction of Zone

2. On the other hand, the non-uniform responses between sections in the same boreholes, particularly in the near-region, indicate a decreased hydraulic conductivity in the vertical direction of Zone 2. The differences in head change between sections in the vertical direction of Zone 2 seem to be persistent in most boreholes both in time and with distance, although the differences decrease with the distance from BFI02. Despite the lower hydraulic conductivity in the vertical direction of Zone 2, vertical hydraulic interaction does exist within the zone. This is also supported by an increase in electric conductivity of the discharged water during interference test 2, indicating a significant contribution of water from the lower, more saline parts of Zone 2.

During interference test 2 the primary responses in the observation sections almost exclusively occurred in the uppermost (pumped) part of Zone 2. This indicates that the high-conductive uppermost horizon is continuous and can be correlated over large distances (cf. Section 2). Accordingly, during interference test 1 the primary responses generally occurred in the lowermost horizon of Zone 2, which also seems to be persistent with distance. Borehole BFI01 is an exception; in this case the primary response occurred in the uppermost part of Zone 2 during both tests 1 and 2. This may indicate deviating (hydro)-geological properties of this borehole and BFI02. In general, all interference tests carried out between the sections above and below Zone 2 responded much slower than the sections within the zone.

The primary drawdown response (most rapid response section) in each borehole during interference test 2 are shown in semilogarithmic graphs in Figures 12a and b. The graphs clearly show that the shape of the primary response curves is very similar in all boreholes. In BFI02 the drawdown is delayed up to about 8 minutes due to technical reasons. While the actual primary drawdown differs somewhat between the near-region observation boreholes, it is almost identical in the distant-region boreholes. The rate of drawdown is virtually the same in most of the boreholes, independently of the distance to BFI02.

Thus, within the investigated area, the rate of drawdown is (nearly) constant at all points, i.e. the hydraulic gradient is constant. This fact indicates that Zone 2 is bounded by hydraulic boundaries in the lateral direction. This is further confirmed by the steep shape of the head change versus time curves at intermediate times shown in Figures 10 and 11, suggesting that Zone 2 is surrounded by barrier boundaries (Earlougher 1977). This is consistent with the geological interpretation which describes Zone 2 as a triangular shaped area (Tirén, this volume). Figures 12a and b also show that the primary drawdown responses in the near-region observation boreholes (KFI06, KFI11 and BFI01) generally deviate somewhat from the other boreholes (independently of the distance to BFI02). This may be a reflection of local heterogeneities between these boreholes and BFI02 (Gustafsson and Andersson; this volume).

By the end of interference test 2 the drawdown curves in Figures 10 and 11 flatten out and an approximate steady-state is reached indicating a major (external) source of recharge to Zone 2. The location of this recharge source is not known but it may derive from other fracture zones within the area. For example, water may possibly be transmitted along Zone 1 which extends southwest towards Lake Finnsjön (Fig. 1). Other fracture zones may also be potential recharge sources to Zone 2.

During interference test 3 the entire Zone 2 was pumped below a single packer. Simple balance calculations based on the resulting electric conductivity of the discharged water indicate that approximately the same quantities were discharged from the upper and lower parts of Zone 2 during test 3. As an example of a near-region response the drawdown in borehole KFI11 during test 3A is shown in Figure 13. Since the flow rates during test 2 and test 3A (up to approx. 13.5 hours) were the same, Figures 10 and 13 are directly comparable up to this time. The latter figure shows, as expected, that the response curves in KFI11 are more compressed during test 3A when the entire zone is pumped. In the distant region observation

boreholes the drawdowns are very similar during the initial part of test 2 and test 3A. The response pattern (order of response among sections) and the primary response section in each observation borehole are very similar for tests 2 and 3.

To summarize, the near-region responses (drawdowns and response patterns) within Zone 2 differ significantly between the interference tests, whereas the distant-region responses are very similar in all three tests. In the peripheral observation boreholes significant responses were obtained in the boreholes KFI04, KFI07, KFI08 and HGB02 (Fig. 1). During interference test 3B drawdowns of approx. 0.7 m, 1.6 m, 0.8 m and 0.7 m respectively, were measured in these (open) boreholes. The distances to BFI02 from these boreholes are about 920 m, 800 m, 1310 m and 1260 m, respectively. Small drawdowns (about 0.1 m) were also measured in the boreholes KFI01 and KFI02, located 1400-1500 m from BFI02. The significant responses measured in most of the peripheral observation boreholes outside Zone 2 indicate a certain hydraulic communication across the outer boundaries of the Zone 2, possibly via other fracture zones. Thus, the outer hydraulic boundaries of Zone 2 may be regarded as semi-permeable.

4.2.3 Quantitative interpretation

A preliminary quantitative (time-drawdown) interpretation of the interference tests, in particular tests 1 and 2, based on the theory for a leaky auqifer system by Hantush (1967) has been carried out. Both the single-hole and interference tests have documented the uppermost and lowermost parts of Zone 2 as being highly conductive and persistent in most of the boreholes. Accordingly, these horizons are treated as high-conductive subaquifers within Zone 2 separated by a fictive low-conductive layer, representing the postulated decrease in hydraulic conductivity in the vertical direction (Fig. 14). One of the subaquifers is assumed to be pumped while the other remains unpumped and vice versa. For example, in test 1 the

lowermost part of Zone 2 is regarded as the pumped aquifer while the uppermost part of the zone is treated as the unpumped aquifer. An alternative approach would be to treat Zone 2 as one aquifer with hydraulic conductivity anisotropy in the vertical direction.

Figure 15 illustrates an example of theoretical type curves for such a leaky aquifer system of infinite areal extent. Thus, the type curves do not take the bounded nature of Zone 2 into account. The evaluation of the hydraulic parameters must therefore be based on prior conditions when the effects of the boundaries have not become appreciable. In addition to the time-drawdown analysis described above, distance-drawdown analyses of the primary responses were also performed. The former analyses provided estimates of the transmissivity (and hydraulic conductivity) and storativity of the two subaquifers from the near-region observation boreholes. The latter analysis gave estimates of the total transmissivity and storativity of the entire Zone 2 from the distant-region observation boreholes. The interpretation using analytical methods was accompanied by numerical predictions of observation borehole responses based on the preliminary interference tests in BFI01 and numerical simulations of the detailed interference tests in BFI02. The numerical predictions and simulations are presented in Section 5.

The transmissivity of the uppermost and lowermost parts of Zone 2 was estimated at about $1\text{-}2\times10^{-3}$ m^2/s both for test 1 and 2. These values are in good agreement with the values obtained from the single-hole tests (see Section 2). The corresponding storativity values from the near-region observation boreholes differ between the tests. From test 1 the storativity of the lowermost part of Zone 2 was estimated at $4\text{-}6\times10^{-6}$. From test 2 the storativity of the uppermost part of Zone 2 ranges from 6×10^{-7} to 2×10^{-6}. In both tests, apparantly higher storativity values were calculated from BFI01 indicating deviating hydrogeological conditions between this borehole. From the distant-region observation boreholes the transmissivity and storativity of the entire Zone 2 were estimated at 2.5 -

3.5×10^{-3} m^2/s and $1\text{-}2 \times 10^{-5}$ m^2/s, respectively, both from the time-drawdown and distance-drawdown analyses.

From the separation of the data curves for the pumped and unpumped aquifers a rough estimation of the hydraulic conductivity in the vertical direction of Zone 2 may be made. Assuming a thickness of the fictive low-conductive layer of 50 m, the equivalent average vertical hydraulic conductivity of this layer may be estimated at about $1\text{-}2 \times 10^{-6}$ m/s. This estimate is consistent with rough estimates of the leakage rate between the subaquifers during tests 1 and 2, based on simple balance calculations from the change in electric conductivity (salinity) during the tests, knowing the initial concentrations in each subaquifer.

5. Numerical modelling

5.1 Objectives and approach

Numerical flow modelling was performed in order to, if possible, obtain an accurate description of the geological and hydrogeological conditions that governs groundwater flow in the Finnsjön area. Two specific objectives could be identified:

- Use the groundwater flow model to verify geological interpretations and hydrologic evaluation of interference test data.

- Use the groundwater flow model to predict results from future tracer tests.

In this text, only the first objective will be considered. The approach taken was to use available geological and hydrogeological data as input to the flow model. The model results could then be compared to actual field observations from the interference tests. By analyzing the discrepancies between the calculated and measured results, the flow model could be updated by adjusting hydraulic parameters. This calibration

process was repeated in an iterative manner until a satisfactory agreement between model results and field observations was achieved.

The numerical modelling described here consists of two distinctive phases, before and after the interference tests. The first phase was aimed at the prediction of drawdown distributions in the investigation area based on somewhat limited data. The second was to study the discrepancies between predicted and measured interference test results, and improve the model performance by an updated calibration. The updated model was calibrated for test 3B only, and therefore only the prediction for test 3B will be discussed here.

The groundwater flow is assumed to take place in a porous saturated medium with constant density of the fluid, and is governed by the equation (Freeze and Cherry, 1979) :

$$\frac{\partial}{\partial x}\left(T_x \frac{\partial h}{\partial x}\right) + \frac{\partial}{\partial y}\left(T_y \frac{\partial h}{\partial y}\right) - Q = S \frac{\partial h}{\partial t} \qquad (3)$$

where h = hydraulic head (m)
T = transmissivity (m^2/s)
Q = fluid sources or sinks (m^3/s)
S = storativity

Eqn. (3) was solved numerically by the two-dimensional finite element simulation code SUTRA, version 1284-2D; (Voss, 1984).

5.2 Predictive modelling prior to interference tests

The predictive modelling of the hydraulic interference tests was performed in a vertical profile, assuming radial symmetry around the pumped borehole, BFI02. The computational domain and its assumed hydraulic parameter distribution is shown in Figure 16, where Zone 2 appears as more or less permeable subzones between depths of approximately 150 and 250 metres. The parameter values are primarily obtained from single-hole water injection tests. In addition, some model calibration was

carried out based on very limited drawdown data (from borehole KFI09) from pumping during drilling of borehole BFI01 (see Section 4.1). Fluid discharge was distributed along the left boundary in accordance with the extent of the pumped section for each test.

Predicted versus measured drawdown time series (primary responses) in two of the observation holes for test 3B are compared in logarithmic diagrams in Figures 17 and 18. Also included are predicted responses above Zone 2, shown as solid lines without symbols. Examination of Figures 17 and 18 reveals two striking discrepancies between predicted and measured results. Firstly, the magnitude of the total drawdowns are relatively accurately predicted only for the borehole (HFI01) farthest away from the pumped hole. At shorter distances (KFI11), predicted drawdowns are significantly higher than measured. Secondly, the general shape of the predicted drawdown curves in all the boreholes does not conform to the measured.

The fact that total drawdowns (when approaching steady-states) are not accurately predicted at all distances, may be seen as failure of the prediction model to describe the shape of the cone of depression created by the pumping. In this case, the actual slope of the cone was considerably less then predicted. This might explained by the fact that the values of transmissivity within Zone 2 used for the predictive modelling were too small (c.f. Section 4.1). The difference in shape of the drawdown curves is taken as an indication that the physical geometry of the modelled region is not sufficiently detailed. Apparently, the hydrogeological boundaries of the model region are more complex than what the relatively simple model geometry accounts for.

The conclusions from the predictive modelling indicated that a more detailed description of the hydrogeological boundaries was required to improve the model performance with respect to prediction of hydraulic heads during pumping tests. Furthermore, hydraulic parameters within Zone 2 needed to be revised.

5.3 Model calibration after interference tests

In order to obtain an updated and improved groundwater flow model for the Brändan area, more detailed geological features were incorporated into the model (Tirén; this volume). This resulted in a computational domain as shown in Figure 19, where the fracture zone is modelled as a sub-horizontal plane. Zone 2 is generally surrounded by less transmissive rock mass and appears as a triangular shape in the middle of the figure. Two vertical fracture zones, the Brändan and Gåvastbo zones, are also represented as physical entities. Boundaries to Zone 2 are either no flow or semi-permeable. It can be noted that boundary conditions for the entire computational domain are either no flow or constant hydraulic head.

Groundwater recharge is modelled as lateral inflows to the computational domain through constant head boundaries. Thus, no areal vertical leakage from the rock mass above or below Zone 2 is considered. If this term is significant, it would cause some error in the model calculations. However, it is judged that possible areal reacharge does not affect calculations significantly concerning Zone 2 and the boreholes of interest.

It was decided to model the entire Zone 2 rather than separate subzones, since the results from the interference tests indicated that three-dimensional effects within Zone 2 may be important when pumping in only one of the subzones. Thus, test 3B is the test actually modelled in this case. The hydraulic parameters for the updated model were determined by trial-and-error calibration of the numerical model, supported by analytical aquifer analyses of the interference tests (see Section 4.2).

The resulting parameter distribution and the resulting computed drawdown distribution is shown in Figures 20 and 21, respectively. The transmissivity value for Zone 2 is 3.5×10^{-3} m^2/s, which is somewhat higher than was used in the previous modelling. Comparison of measured and modelled drawdown curves in observation holes HFI01 and KFI11 are presented in Figures

22 and 23. This was considered, by visual inspection, to be the best fit attainable with this particular model. For most boreholes, computed and measured responses are practically identical, the main exception being borehole BFI01, where modelled steady- state drawdowns are somewhat larger than measured. This can not be modelled without significantly altering the geological description of the fracture zone, or introducing some local heterogeneities which may or may not be artificial. Some attempts to improve model performance by assuming a general horizontal anisotropy in Zone 2 were made, but without conclusive results (Andersson et al., 1988b).

It should be pointed out that the calibration described here is not verified, that is, tested during a different hydraulic event (for example pumping in a different borehole). Thus, there is significant uncertainty as to the uniqueness of the obtained hydraulic parameters and flow geometry. An additional factor of uncertainty is that spatial data are somewhat sparse. However, the flow modelling has proven to be extremely valuable for understanding the flow conditions in the Brändan area, as well as for verification of geological and hydrogeological interpretations.

6. Summary and conclusions

The studies in the Brändan area have provided basic data with regard to the geological and hydrogeological disposition of the studied fracture zone in particular, and fracture zones in general. The detailed hydraulic testing provided data for a conceptual model used in the evaluation of the interference and tracer tests. The results clearly demonstrate the heterogeneous nature of the studied fracture zone. Thin, highly conductive conduits occur intermittently, separated by wider intervals of more competent rock of low to intermediate conductivity. The uppermost and lowermost parts of the zone consistently showed increased hydraulic conductivity in all boreholes. The single-hole tests also indicated a large

contrast in hydraulic conductivity between the zone and the over- and underlying rock.

The very detailed hydraulic testing clearly demonstrates that the decrease in section length with about two orders of magnitude, from 20 m to 2 m and 0.11 m, increases the resolution in the estimation of the effective hydraulic width of identified hydraulic features accordingly.

The calculated values of the conductive fracture frequency (CFF) are compatible with the results of the detailed hydraulic testing. The results indicate that only 10-40% of the mapped coated fractures are hydraulically active, the actual figure being closely related to the lower measurement limit of the hydraulic testing equipment used. The CFF and the fracture size distribution, together with possible channelling along individual fracture planes, control the interconnectivity of the rock and the amount of wetted surface area available. The latter is an important parameter in the retardation of radionuclide migration in crystalline rock (Neretnieks, 1987).

During the preliminary interference tests whilst drilling borehole BFI01, no significant pressure response was obtained in the observation boreholes until the uppermost part of Zone 2 was penetrated. At this occasion, rapid and pronounced responses were obtained in all observation boreholes. The responses were very similar during all drilling steps through Zone 2 once its uppermost part was penetrated, although the total discharge rate increased at the deeper parts of the Zone. The preliminary interference tests demonstrated the high transmissivity in the lateral direction of Zone 2 and possible flow patterns within and adjacent to the Zone. Due to the short duration of the tests during drilling, no reliable information on the nature of the outer hydrogeologic boundaries of Zone 2 could be deduced.

The detailed interference tests in BFI02 showed that different borehole response patterns were generated in the near and distant regions from the pumping borehole, in particular when

the uppermost and lowermost part of the zone was pumped separately. When the entire zone was pumped the multiple-response curves obtained from the boreholes were less separated from each other. In the near-region the flow pattern was dominated by the primary responses, corresponding to the most rapid flow path between the pumping borehole and the actual observation borehole. These flow paths may be strongly influenced by local heterogeneities between the boreholes, e.g. restricted flow channels, stratification etc. The secondary responses in the boreholes (in the near-region) are in general more delayed and attenuated, representing more averaged flow conditions.

In the distant region no dominating (primary) response occurs in the boreholes but instead the responses in all borehole sections within Zone 2 almost coincide. The secondary responses in the near and distant regions were very similar in all tests. These responses are believed to represent the averaged (long-term) hydraulic properties of the entire zone, whereas the primary responses in the near-region should represent the short-term behaviour of the system. This interpretation is supported by the fact that the long-term drawdown behaviour in all boreholes was very similar between the different tests, whereas the short-time behaviour in boreholes close to the pumping borehole varied considerably between tests.

The interference tests have confirmed that the upper and lower subzones of Zone 2 have a high hydraulic diffusivity (high transmissivity and low storage). The transmissivity of each subzone was estimated at about 2.5×10^{-3} m^2/s from the time-drawdown analysis. The calculated storage coefficients corresponding to the primary responses in the subzones are generally small, ranging from about 6×10^{-7} to 7×10^{-6} in the near-region boreholes KFI11 and KFI06 during test 1 and test 2. The lowest storage values were obtained from test 2 indicating particularly low-porosity flow paths in the uppermost subzone close to BFI02.

From the distance-drawdown analysis for the most distant observation boreholes, the representative (long-term) transmissivity of the entire Zone 2 was estimated at about $3x10^{-3}$ m^2/s and the storage coefficient at about $2x10^{-5}$. From the observed drawdown differences in sections in the same boreholes, the leakage coefficient was estimated at about $1-5x10^{-8}$ s^{-1}. Assuming a thickness of about 50 m of the fictive semi-permeable layer between the subzones, these values correspond to an equivalent hydraulic conductivity in the vertical direction of Zone 2 of about $1x10^{-6}$ m/s. However the actual flow transfer within Zone 2 is likely to be controlled by discrete fractures which locally may have much higher hydraulic conductivity.

The theory used for the analytical interpretation of the interference tests proved to be useful. An alternative approach would be to treat the entire Zone 2 as a layered aquifer with vertical anisotropy of the hydraulic conductivity. Interference test 1 and 2 may then be analyzed by theory for a partially penetrating well in an anisotropic aquifer. Since the two approaches are similar, the results would also be expected to be similar. However, the latter approach would possibly provide a more representative value of the hydraulic conductivity in the vertical direction of Zone 2.

Although the responses above and below Zone 2 generally are more slow and attenuated compared to those within Zone 2, they indicate a certain hydraulic interaction between Zone 2 and the over and underlying rock. However, tests 2 and 3 showed a slower response above the zone in the boreholes BFI01 and BFI02, indicating good hydraulic isolation towards the overlying rock in these boreholes. During interference test 2 a considerable leakage was estimated from the lower parts of Zone 2 (and possibly also from the rock below the zone) to the upper (pumped) part of the zone.

The interference test responses clearly show that Zone 2 hydrogeologically is bounded by outer deliminations. These boundaries are probably constituted by other fracture zones as

suggested by Tirén (this volume). According to this interpretation the geometry of Zone 2 may be characterized by a triangular-shaped area. However, interference test 2 showed that a steady-state was reached by the end of the test indicating major inflows to Zone 2 during pumping, possibly from adjacent fracture zones across the boundaries, e.g. the Brändan Zone (Zone 1), or other more distant zones.

Observations of the groundwater levels in open boreholes outside Zone 2 showed that significant drawdowns occurred at long distances (about 1.5 km) from BFI02 during the interference tests. This indicates certain hydraulic interactions between Zone 2 and adjacent areas, possibly via fracture zones.

The responses of the detailed interference tests were compared to those predicted from a previous model, and to simulations based on an updated model taking into account the results of the present interference tests. The relatively simple predictive model, based on the single-hole injection tests and limited pumping test data, did not prove to yield satisfactory predictions of hydraulic heads during the transient pumping tests. This was attributed to a lack of detailed hydrogeological description of the fracture zone, mainly the outer boundary conditions, and inaccurate hydraulic parameter description for Zone 2.

A considerably improved description of the flow conditions in the fracture zone was obtained by the updated calibrated model. The fact that the shape of the measured drawdown curves are accurately reproduced, indicate that the flow geometry is described correctly. The calibrated model failed to reproduce exactly the drawdowns in the boreholes adjacent to the pumped hole. This is interpreted to be an effect of local heterogeneities in the rock material. The numerical flow modelling work has proved to be of considerable value in assisting analytical aquifer analyses and gaining a general understanding of the factors governing flow in the fracture zone. The calibrated model will be used to predict future

tracer tests and ideally, also serve as a verification tool for the model.

The present series of interference tests have demonstrated the usefulness of conducting such tests by pumping and recording pressure changed in multiple-borehole sections. This provided detailed studies of the propagation of the pressure waves created in the pumping borehole and the associated flow pattern within Zone 2. The results of the present interference tests may provide a basis for future developments of models for flow in fractured crystalline rock. Although Zone 2 within the Brändan area may appear unique in a geological and hydrogeological sense, fracture zones with similar properties are likely to be encountered in other areas. Combined use of hydraulic (interference) tests and tracer tests is recommended in future investigations.

Finally, the question arises whether Zone 2 may be regarded as representative for other fracture zones in crystalline rock with similar geological and hydrological character. Several gently dipping fracture zones in crystalline rock have been encountered in other study sites in Sweden. However, only one of these zones has been subjected to hydraulic interference testing. For this zone, located in the Forsmark area in eastern, central Sweden, the transmissivity was estimated at about 10^{-5} m^2/s, i.e. about two orders of magnitude lower than that calculated for Zone 2 at Finnsjön (Carlsson et al., 1986). Single-hole tests have, however, indicated higher transmissivities for gently dipping fracture zones at other study sites, e.g. Klipperås at about 800 m depth (Gentzschein, 1986).

Hydraulic information from gently dipping fracture zones is also available from the Canadian investigation programme at Chalk River, Ontario. A narrow subhorizontal fracture zone (Zone No. 1) in monzonitic gneiss recorded an estimated transmissivity of 4×10^{-6} m^2/s (Raven, 1986); the anisotropy ratio between horizontal to vertical hydraulic conductivity was

estimated at 10-170 from hydraulic interference tests (Raven, 1986).

In the Finnish site investigation programme several subhorizontal fractured and weathered zones were encountered in massive rapakivi granite. Increased hydraulic conductivity in the upper and lower fractured zones showed these to be the most hydraulically significant. From single-hole tests the arithmetic mean of hydraulic conductivity was estimated at about 10^{-5} m/s and $5x10^{-6}$ m/s for the upper and lower zones, respectively (Anttila, 1986). The thickness of the upper fracture zone varies between 3 and 6 m in the boreholes, whereas the lower fracture zone varied between 4 and 17 m (Anttila, 1986). The mean transmissivity of the upper and lower fracture zones is thus $3\text{-}6x10^{-5}$ m^2/s and $2\text{-}8.5x10^{-5}$ m^2/s, respectively.

REFERENCES

Ahlbom, K., Melkersson, K. and Stråhle, A., 1985. Core logging and technical data for boreholes KFI05, KFI06, KFI09 and KFI10. SKB Stat. Rep., (AR 87-06), Stockholm.

Ahlbom, K., Andersson, P., Ekman, L., Gustafsson, E., Smellie, J.A.T. and Tullborg, E-L., 1986. Preliminary investigations of fracture zones in the Brändan area, Finnsjön study site. SKB Tec. Rep., (TR 86-05), Stockholm.

Ahlbom, K., Andersson, P., Ekman, L. and Tirén, S., 1987. Characterization of fracture zones within the Brändan area, Finnsjön study site. SKB Stat. Rep., (AR 88-09), Stockholm.

Ahlbom, K., 1989. Overview of the Fracture Zone Project at Finnsjön Sweden. (This volume).

Almén, K-E., Andersson, O., Fridh, B., Johansson, B-E., Sehlstedt, M., Hansson, K., Olsson, O., Nilsson, G. and Wikberg, P., 1986a. Site investigation - equipment for geological, geophysical, hydrogeological and hydrochemical characterization. SKB Tec. Rep., (TR 86-16), Stockholm.

Almén, K-E., Andersson, J-E., Carlsson, L., Hansson, K. and Larsson, N-Å., 1986b. Hydraulic testing in crystalline rock. A comparative study of single hole test methods. SKB Tec. Rep., (TR 86-27), Stockholm.

Andersson, J-E. and Persson, O., 1985. Evaluation of single hole hydraulic tests in fractured crystalline rock by steady-state and transient methods. SKB Tec. Rep., (TR 85-19), Stockholm.

Andersson, J-E., Andersson, P. and Ekman, L., 1987. Water injection tests in borehole KFI10 at the Finnsjön test site. Comparison of tests performed with two different equipment systems. The effects of gas-lift pumping on hydraulic parameters. SKB Stat. Rep., (AR 87-33), Stockholm.

Andersson, J-E., Ekman, L. and Winberg, A., 1988a. Detailed investigations of fracture zones in the Brändan area, Finnsjön study site. Single hole water injection tests in detailed sections. Analysis of the conductive fracture frequency. SKB Stat. Rep., (AR 88-08), Stockholm.

Andersson, J-E., Ekman, L., Gustafsson, E., Nordqvist, R. and Tirén, S., 1988b. Interference tests within the Brändan area, Finnsjön study site. SKB Tec. Rep., (In prep).

Andersson, J-E., Ekman, L. and Winberg, A., 1988c. Detailed hydraulic characterization of a fracture zone in the Brändan area, Finnsjön, Sweden. Paper presented at the 4th Canadian/ American Conference on Hydrogeology: Fluid flow, Heat transfer and Mass transport in Fractured rocks. Banff, Alberta, Canada, June 21-24, 1988.

Andersson, J-E., and Lindqvist, L. 1988. Prediction of hydraulic conductivity and conductive fracture frequency from integrated geodata. SKB Tec. Rep. (In prep).

Anttila, P., 1986. Geological and hydrogeological conditions of the island Hästholmen, Loviisa, Nucl. Waste Comm. of the Finn. Power Comp., Rep. YJT 86-05, Helsinki.

Carlsson, L., Winberg, A. and Rosander, B., 1984. Investigations of hydraulic properties in crystalline rock. Mat Res Soc Symp Proc Vol 26, Boston, Elsevier.

Carlsson, L., Winberg, A. and Arnefors, J., 1986. Hydraulic modelling of the final repository for reactor waste (SFR). - Compilation and conceptualization of available geological and hydrogeological data. SKB/SFR Progress Report SFR, (86-03), Stockholm.

Doe, T. and Remer, J., 1982. Analysis of constant-head well tests in nonporous fractured rock. Proceedings of the 3rd International Well-testing Symposium, Berkeley, California.

Earlougher, R.C., 1977. Advances in well test analysis. Monograph Series, Soc. Pet. Eng. of AIME, Dallas.

Ekman, L., Andersson, J-E., Andersson, P., Carlsten, S., Eriksson, C-O., Gustafsson, E., Hansson, K. and Stenberg, L., 1988. Documentation of borehole BFI02 within the Brändan area, Finnsjön study site. SKB Stat. Rep. (In prep).

Freeze, R.A. and Cherry, A. 1979. Groundwater. Prentice-Hall.

Gentzschein, B., 1986. Hydrogeological investigations at the Klipperås study site. SKB Tec. Rep., (TR 86-08), Stockholm.

Gustafsson, E. and Andersson, P., 1989. Groundwater flow conditions in a low-angle fracture zone at Finnsjön, Sweden. (This volume).

Hantush, M.S., 1967. Flow to wells in aquifers separated by a semieprevious layer. J. Geophys. Res. 72 (6) pp 1709-1720.

Moye, D.G., 1967. Diamond drilling for foundation exploration. Civil Eng. Trans. Inst. Eng. Australia, pp 95-100.

Neretnieks, I., 1987. Chanelling effects in flow and transport in fractured rocks - Some recent observations and models. Proceedings from the GEOVAL Symposium in Stockholm, April 1987.

Osnes, J.D., Winberg, A. and Andersson, J-E., 1988. Analysis of well test data - Application of probabilistic models to infer hydraulic properties of fractures. SKB/OWTD joint report (In prep).

Raven, K.G., 1986. Hydraulic characterization of a small groundwater flow system in fractured monzonitic gneiss. Report AECL-9066.

Smellie, J.A.T., Gustafsson, E. and Wikberg, P., 1987. Groundwater sampling during and subsequent to air-flush rotary

drilling: hydrochemical investigations at depth in fractured crystalline rock. SKB Stat. Rep., (AR 87-31), Stockholm.

Tirén, S. and Arnefors, J., 1987. Core logging and technical data for boreholes KFI05, KFI06, KFI09 and KFI10. SGAB IRAP 87409.

Tirén, S., 1989. Geological setting and deformation history of a low-angle fracture zone at Finnsjön Sweden. (This volume).

Voss, C., 1984. A finite-element simulation model for saturated-unsaturated fluid-density-dependent groundwater flow with energy transport or chemically reactive single species solute transport. U.S. Geological Survey, Water Resources Investigations Report 84-4369, 1984.

Winberg, A. and Carlsson, L., 1987. Calculations of conductive fracture frequency and description of skin effects around tunnels in the rock cavern area, SFR, Forsmark. Report in Swedish prepared for SKB, June 1987.

Zeigler, T.W., 1976. Determination of rock mass permeability. Technical Report S-76-2, U.S. Army Engineer Waterways Experiment Station, Vicksburg, Missisippi.

Table 1: Compilation of single-hole tests performed in the Fracture Zone Project at the Finnsjön study site.

Bore-hole	Inclination	Section length (m)	Interval measured (m)	Test type	Year of testing	Remarks
KFI05	50°	3	50-743	SS	1979	
		2	142-318	SS	1986/87	Zone 2
KFI06	90°	3	61-679	SS	1979	
		2	192-292	SS	1987	Zone 2
KFI07	85°	3	18-543	SS	1979	
		2	263-364	SS	1987	Zone 2
KFI09	60°	20	10-350	T	1985	
		2	109-262	SS	1986	Zone 2
KFI10	50°	20*	10-230	T	1985	
		5*	70-105	T	1985	
		5*	205-235	T	-"-	
		2	60-224	SS	1986	Zone 2
KFI11	90°	20	6-386	T	1986	
		2	210-358	SS	1986/87	Zone 2
HFI01	90°	10	4-124	SS	1985	
		2	34-44	SS	1985	
			104-114	SS	-"-	(Zone 2)
BFI01	90°	20	30-450	T	1987	
		2	220-448	SS	1987	
BFI02	90°	20	10-210	T	1987	
		2	200-284	SS	1988	Zone 2
		0.11	201.89-206.07	SS	1987	Zone 2
		-"-	211.89-214.09	-"-	-"-	-"-
		-"-	257.89-262.18	-"-	-"-	-"-

* The tests were repeated at three different occasions for comparative purposes.

SS = steady-state test
T = transient test

Table 2 Probability 1-P (one fracture is conductive) and the total number of data (M) used in the analysis of the two data sets from fracture Zone 2 and adjacent rock mass in the Brändan area, Finnsjön.

Bedrock unit	Data Set 1				Data Set 2	
	All		KFI05-07		KFI05-07	
	1-P	M	1-P	M	1-P	M
A	0.19	263	0.14	127	0.30	113
A1	0.25	50	-	28	1.00	20
A2	0.18	122	0.15	57	0.27	54
A3	0.15	91	0.15	42	0.38	39
B1	0.29	79	0.13	33	0.80	177
B2	0.21	34	-	-	0.32	322

Table 3 Conductive fracture frequency (CFF) and confidence limit (δ) based on the two data sets from fracture Zone 2 and adjacent rock mass in the Brändan area.

Bedrock unit	Data Set 1				Data Set 2	
	All		KFI05-07		KFI05-07	
	CFF	$\pm$ δ	CFF	$\pm$ δ	CFF	$\pm$ δ
A	0.98	0.22	0.90	0.46	1.15	0.38
A1	1.43	0.72	-	-	4.60	-
A2	0.62	0.19	0.65	0.31	0.75	0.30
A3	1.06	0.47	1.29	1.01	1.85	1.29
B1	1.02	0.33	0.47	0.31	1.44	0.20
B2	0.56	0.25	-	-	0.76	0.12

Table 4 The observation borehole intervals during the interference tests together with their distance to the midpoint of the pumped sections in BFI02 (during interference test 2) and position within Zone 2. The upper and lower boundaries of Zone 2 in the boreholes are also shown. M = manual registration. Intervals marked with (*) correspond to primary response section(s) in the boreholes during interference test 2.

Borehole	Observation section (no)	Interval (m)	Distance to BFI02 (m)	Part of Zone 2	Zone 2-interval (m)
KFI05	5	0-162	309	above	
	4	163-189	245	upper	
	3	227-240	217	middle	162-290
	2	241-296	206	lower	
	1	297-751	293	below	
KFI06	M	0-165	-	above	
	5	166-201	189	above	
	4	202-227*	189	upper	
	3	250-259	195	middle	214-269
	2	260-279	200	lower	
	1	293-691	345	below	
KFI09	M	0-100	-	above	
	5	101-118	286	above	
	4	119-151*	288	upper	
	3	152-188*	294	middle	134-214
	2	189-230	302	lower	
	1	231-376	339	below	
KFI10	5	0- 75	391	above	
	4	76-134	331	Zone 1	
	3	139-158*	294	upper	
	2	159-193	272	middle	142-210
	1	194-255*	234	lower	
KFI11	M	0-135	-	above	
	5	200-216	153	above	
	4	217-240*	155	upper	
	3	285-304	177	middle	222-338
	2	327-340	200	lower	
	1	341-390	222	below	
HFI01	3	0- 50	367	above	
	2	51- 81*	349	above	
	1	82-129*	338	upper	108-
BFI01	M	0-218	-	above	
	5	219-238	165	above	
	4	239-250*	168	upper	
	3	261-270	174	upper	241-356
	2	345-364	221	lower	
	1	364-459	265	below	

Table 5 Active borehole sections in BFI02 together with discharge rates and duration of the different phases of the interference tests.

Test no	Phase	Active section (m)	Discharge rate (l/min)	Duration (days)
1	Drawdown	246-270	500	3.7
1	Recovery	246-270	-	5.2
2	Drawdown	193-217	500	7.8
2	Recovery	193-217	-	10.2
3A	Drawdown	193-289	500-700	0.9
3A	Recovery	193-289	-	0.8
3B	Drawdown	193-289	700	4.0
3B	Recovery	193-289	-	8.2

Figure 1 Location map of the Finnsjön test site.

Figure 2 Cross section (A-A´) through the Brändan area, Finnsjön test site.

Figure 3 Description of the test equipment used for the injection tests in 0.11 m test sections.

Figure 4 a) Transmissivity distribution versus borehole length in 20 m sections (above Zone 2) and 2 m sections (within Zone 2) in borehole BFI02.

b) Transmissivity distribution of the uppermost subzone of Zone 2 in 0.11 m sections in borehole BFI02.

Figure 5 Estimated conductive fracture frequency of different rock units at the Finnsjön test site using new and old borehole data sets.

Figure 6 Discharge rate and rate of penetration recorded during drilling of borehole BFI01, Finnsjön. Broken line represents the cumulative discharge rate. Solid line represents the average volume discharged per penetrated metre.

Figure 7 Recovery of groundwater head in different sections of borehole KFI11 after drillstep 6 during drilling of borehole BFI01.

Figure 8 Vectors of the mean velocity of the propagation of the pressure pulse in different directions during drilling of borehole BFI01.

Figure 9 Schematic illustration of the equipment assembly and packer positions together with the numbering of the observation sections in the pumping borehole BFI02 during the detailed interference tests.

Figure 10 Drawdown responses in multiple-sections of observation borehole KFI11 during interference test 2 (uppermost subzone) in a logarithmic graph.

Figure 11 Drawdown responses in multiple-sections of observation borehole KFI09 during interference test 2 (uppermost subzone) in a logarithmic graph.

Figure 12 Drawdown of primary responses in the boreholes during interference test 2 (uppermost subzone) in a semi-logarithmic graph.

a) boreholes BFI02 (pumping borehole), BFI01, KFI06 and KFI11.

b) boreholes KFI09, KFI10 and HFI01.

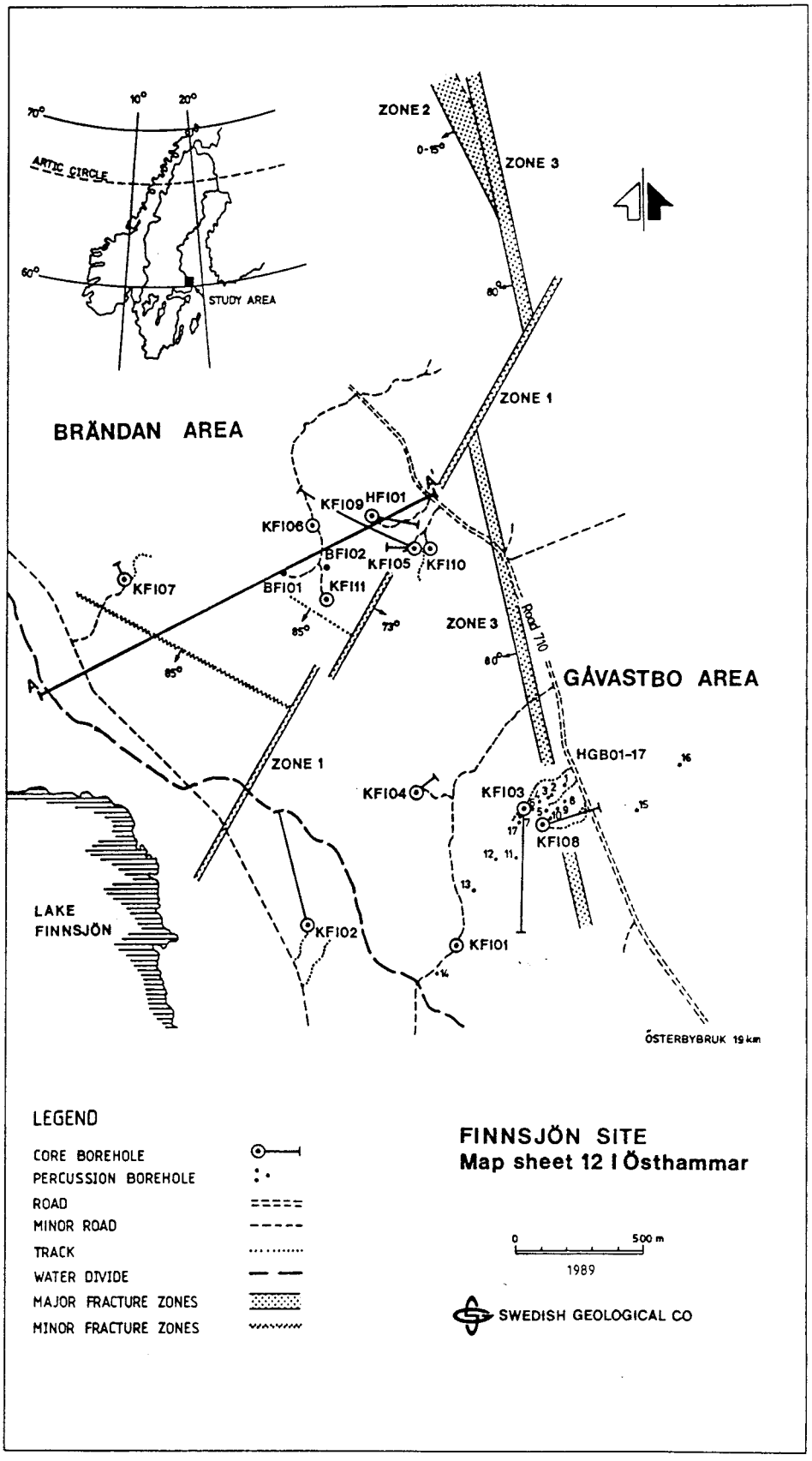

Figure 1 Location map of the Finnsjön test site.

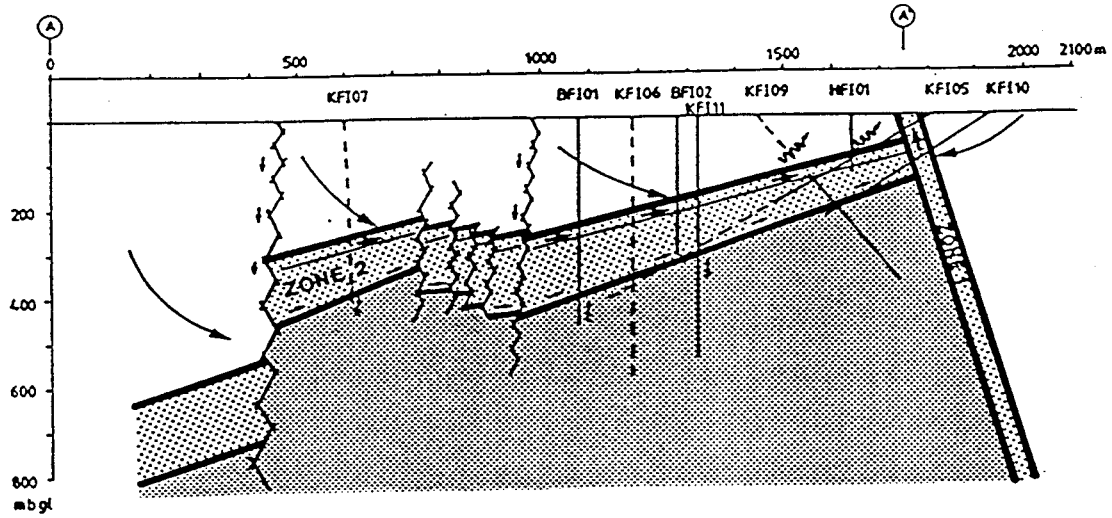

FRACTURE ZONES:

Major fracture zones Zone 1 and Zone 2 — ZONE 1,2

Minor fracture zones

SALINE AND NON SALINE WATER:

Non-saline water

Transitional water (1500-5000 mg/l Cl^-) within the major zones

Saline water (av. 5500 mg/l Cl^-)

UPPER CONDUCTIVE ZONE:

Zone within large waterflow (av. 1500 mg/l Cl^-) within the major fracture zones

BOREHOLES:

Located in front of projected profile

Located behind projected profile

FLOW LINES:

Major flow lines

Minor flow lines

Recharging groundwater

HYDRAULIC HEAD:

Direction of major gradient

Direction of minor gradient

Figure 2 Cross section (A-A´) through the Brändan area, Finnsjön test site.

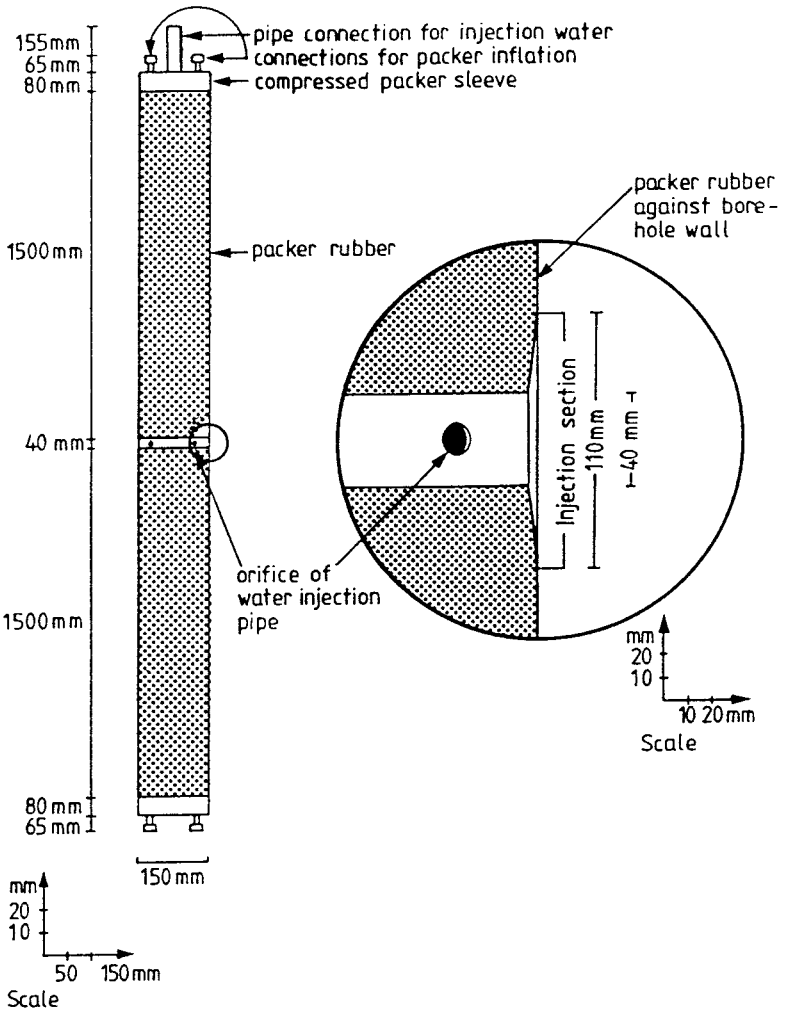

Figure 3 Description of the test equipment used for the injection tests in 0.11 m test sections.

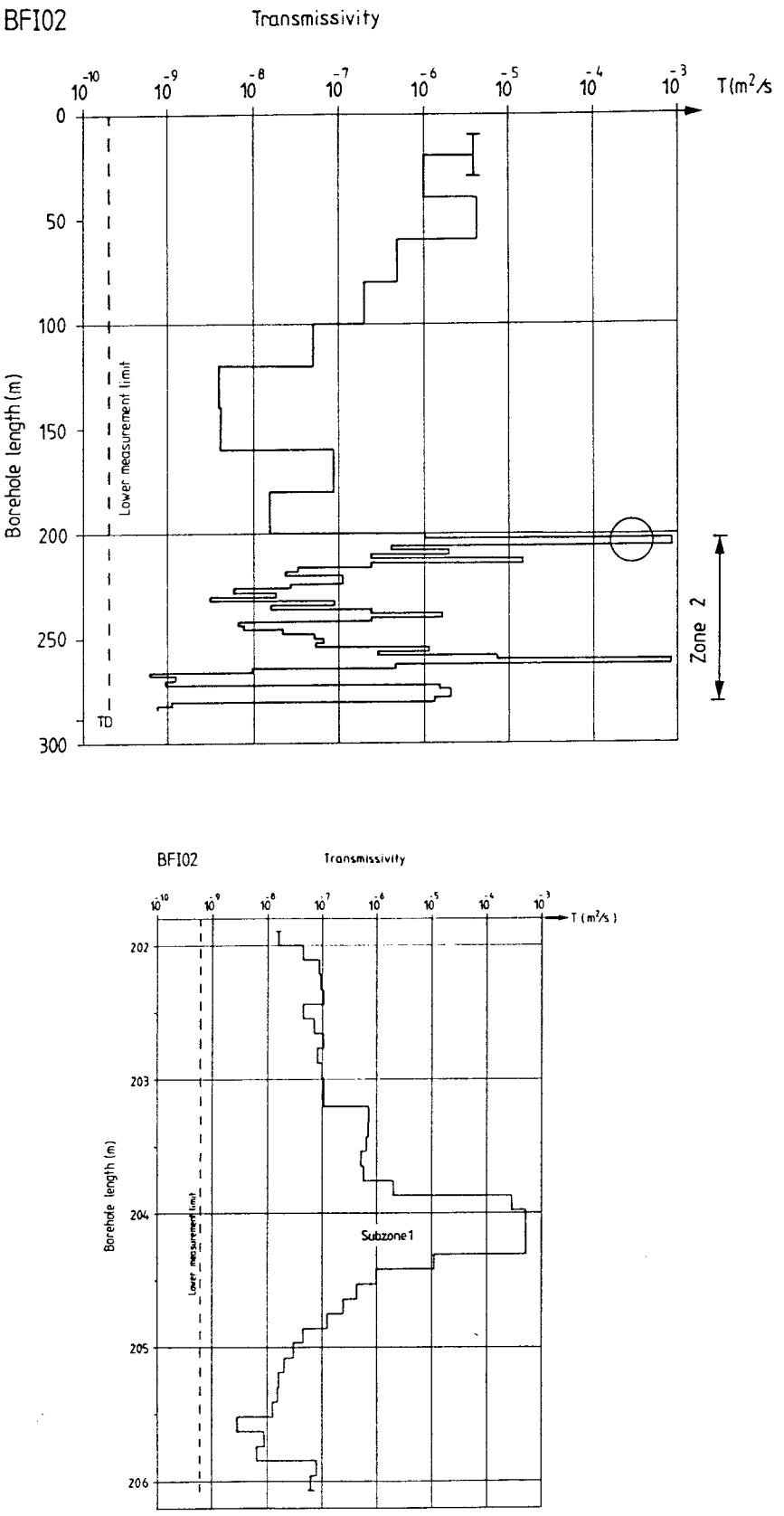

Figure 4 a) Transmissivity distribution versus borehole length in 20 m sections (above Zone 2) and 2 m sections (within Zone 2) in borehole BFI02.

b) Transmissivity distribution of the uppermost subzone of Zone 2 in 0.11 m sections in borehole BFI02.

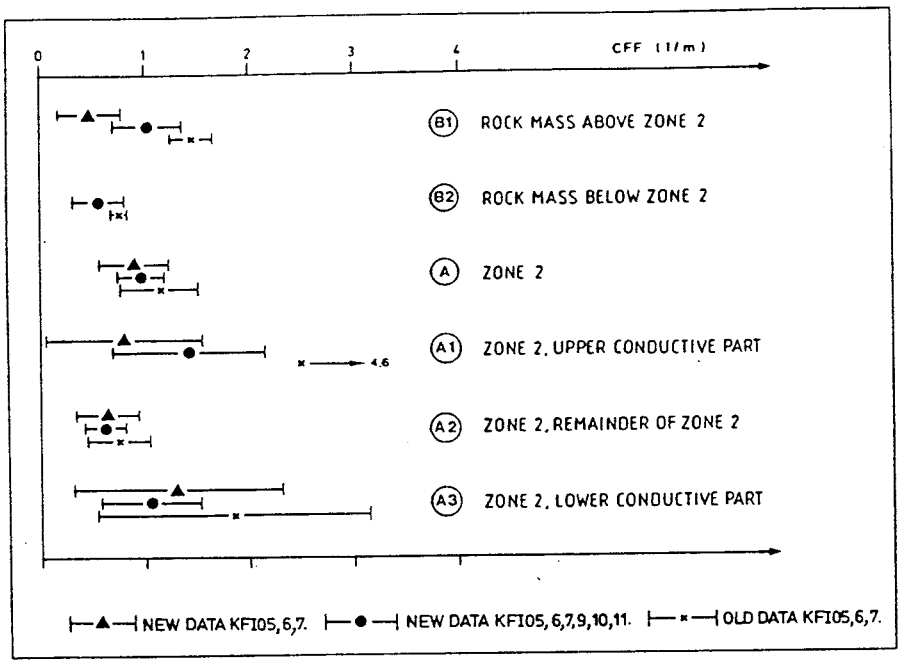

Figure 5 Estimated conductive fracture frequency of different rock units at the Finnsjön test site using new and old borehole data sets.

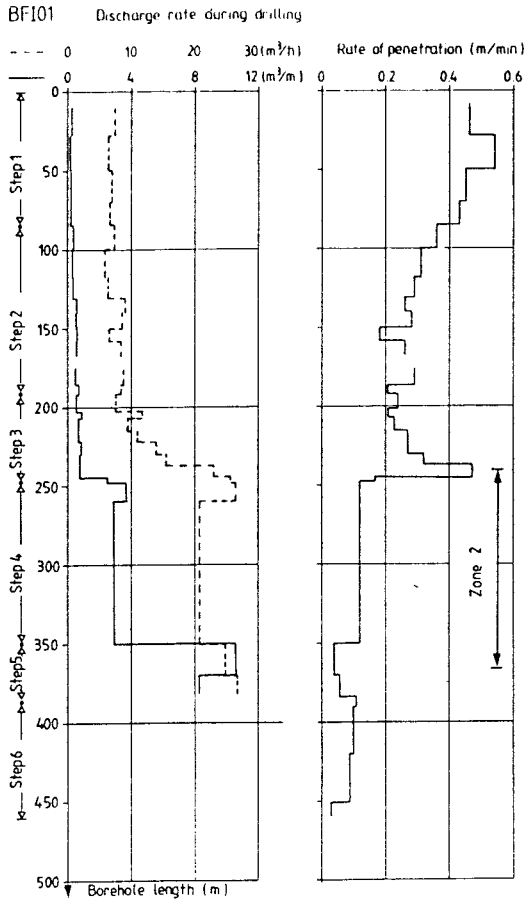

Figure 6 Discharge rate and rate of penetration recorded during drilling of borehole BFI01, Finnsjön. Broken line represents the cumulative discharge rate. Solid line represents the average volume discharged per penetrated metre.

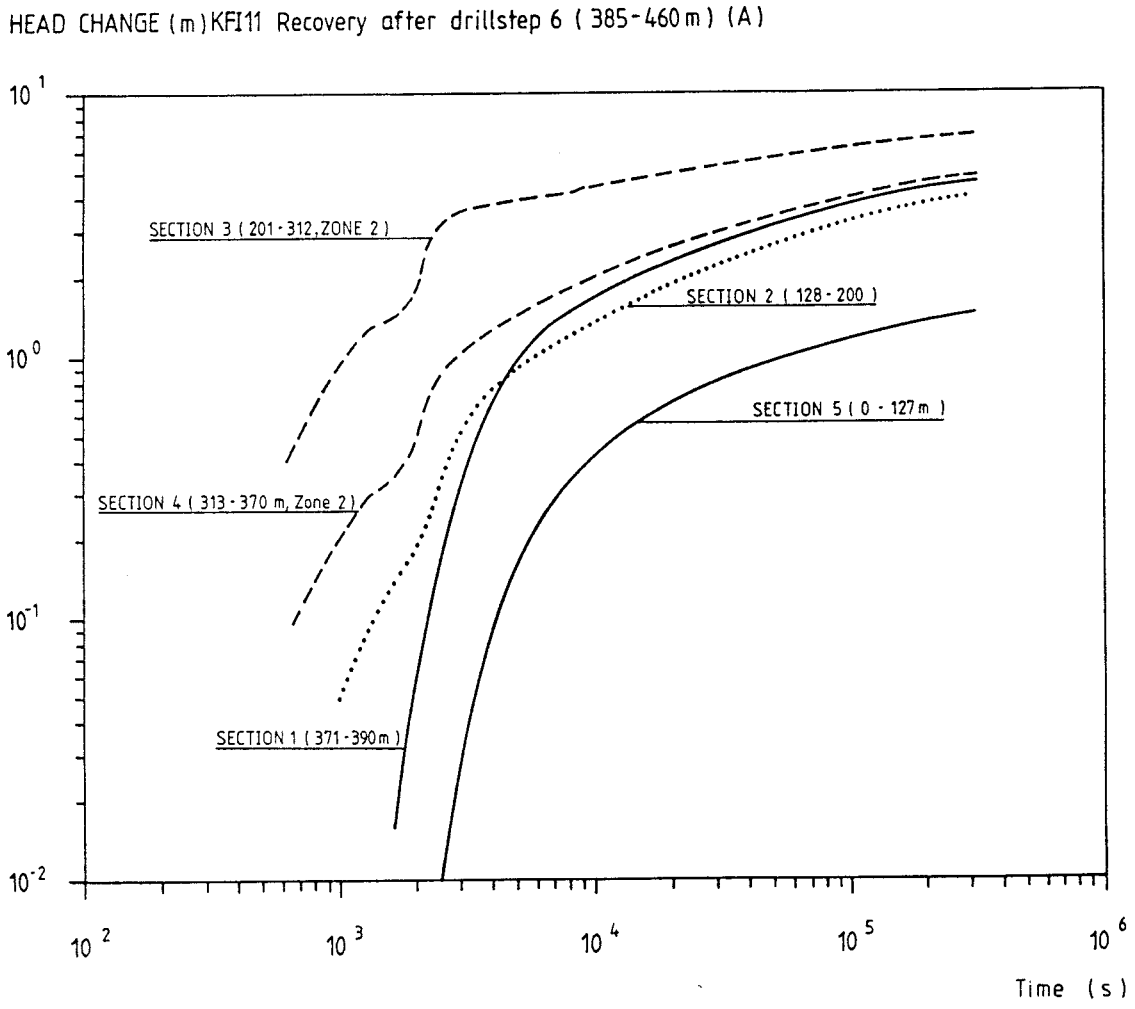

Figure 7 Recovery of groundwater head in different sections of borehole KFI11 after drillstep 6 during drilling of borehole BFI01.

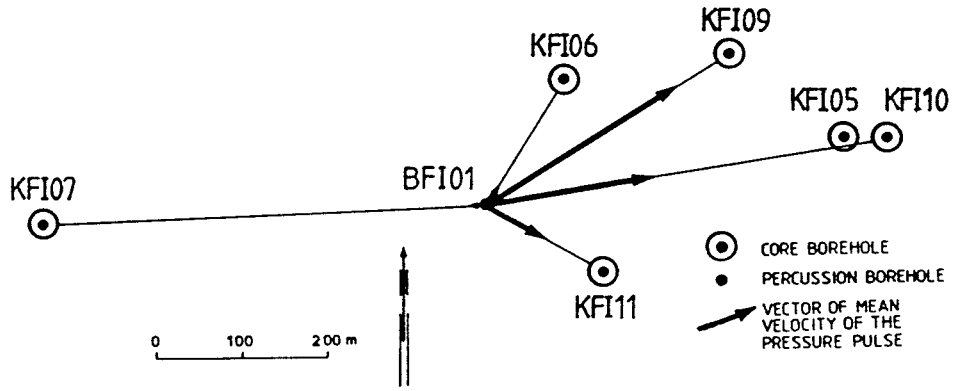

Figure 8 Vectors of the mean velocity of the propagation of the pressure pulse in different directions during drilling of borehole BFI01.

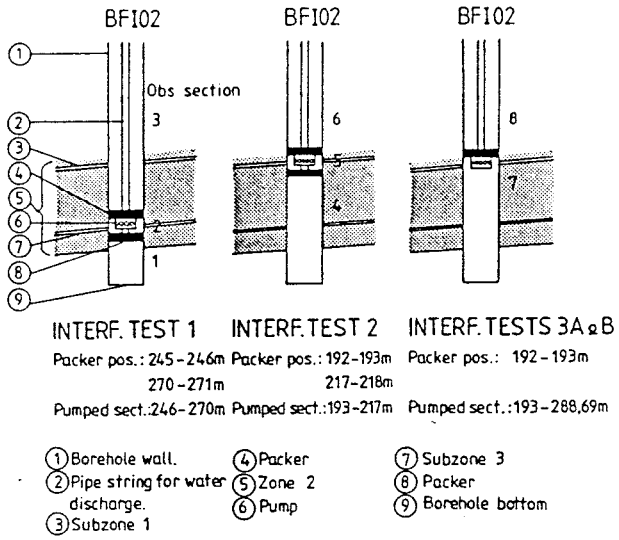

Figure 9 Schematic illustration of the equipment assembly and packer positions together with the numbering of the observation sections in the pumping borehole BFI02 during the detailed interference tests.

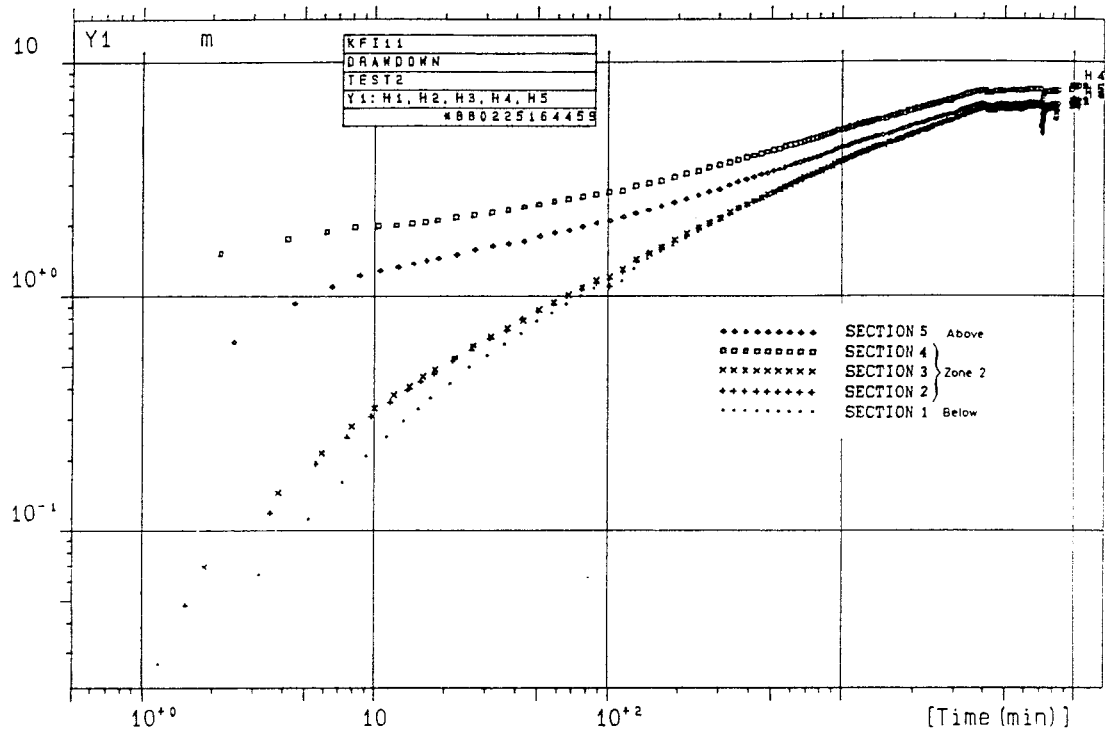

Figure 10 Drawdown responses in multiple-sections of observation borehole KFI11 during interference test 2 (uppermost subzone) in a logarithmic graph.

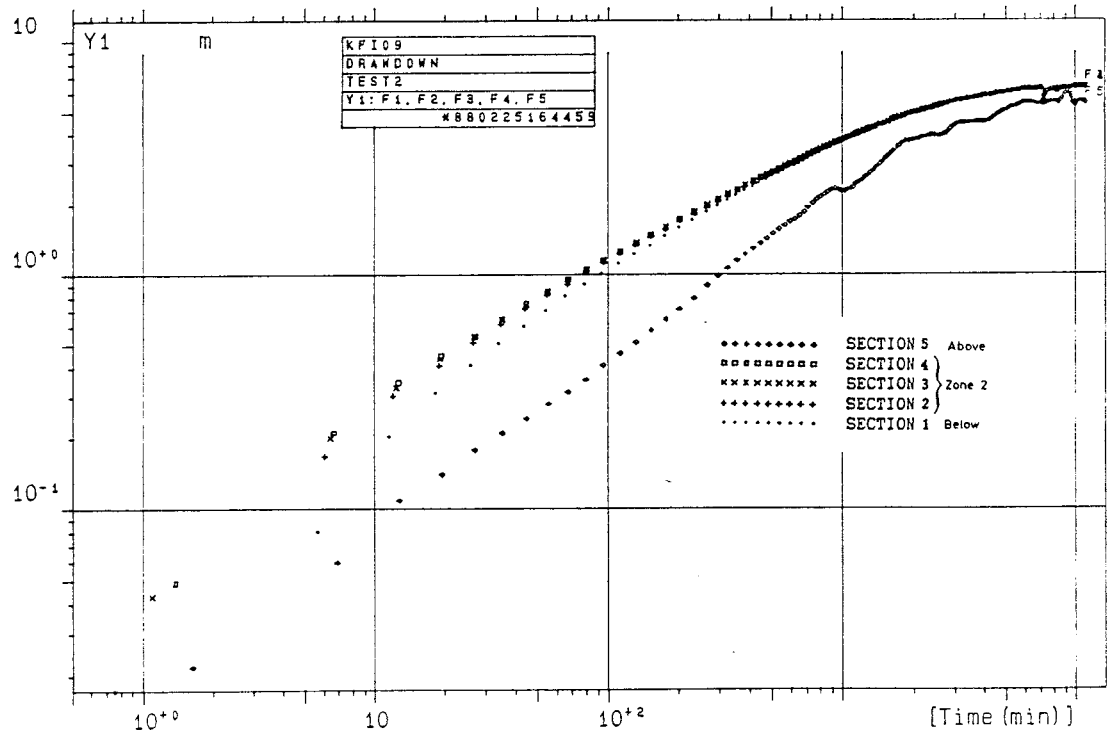

Figure 11 Drawdown responses in multiple-sections of observation borehole KFI09 during interference test 2 (uppermost subzone) in a logarithmic graph.

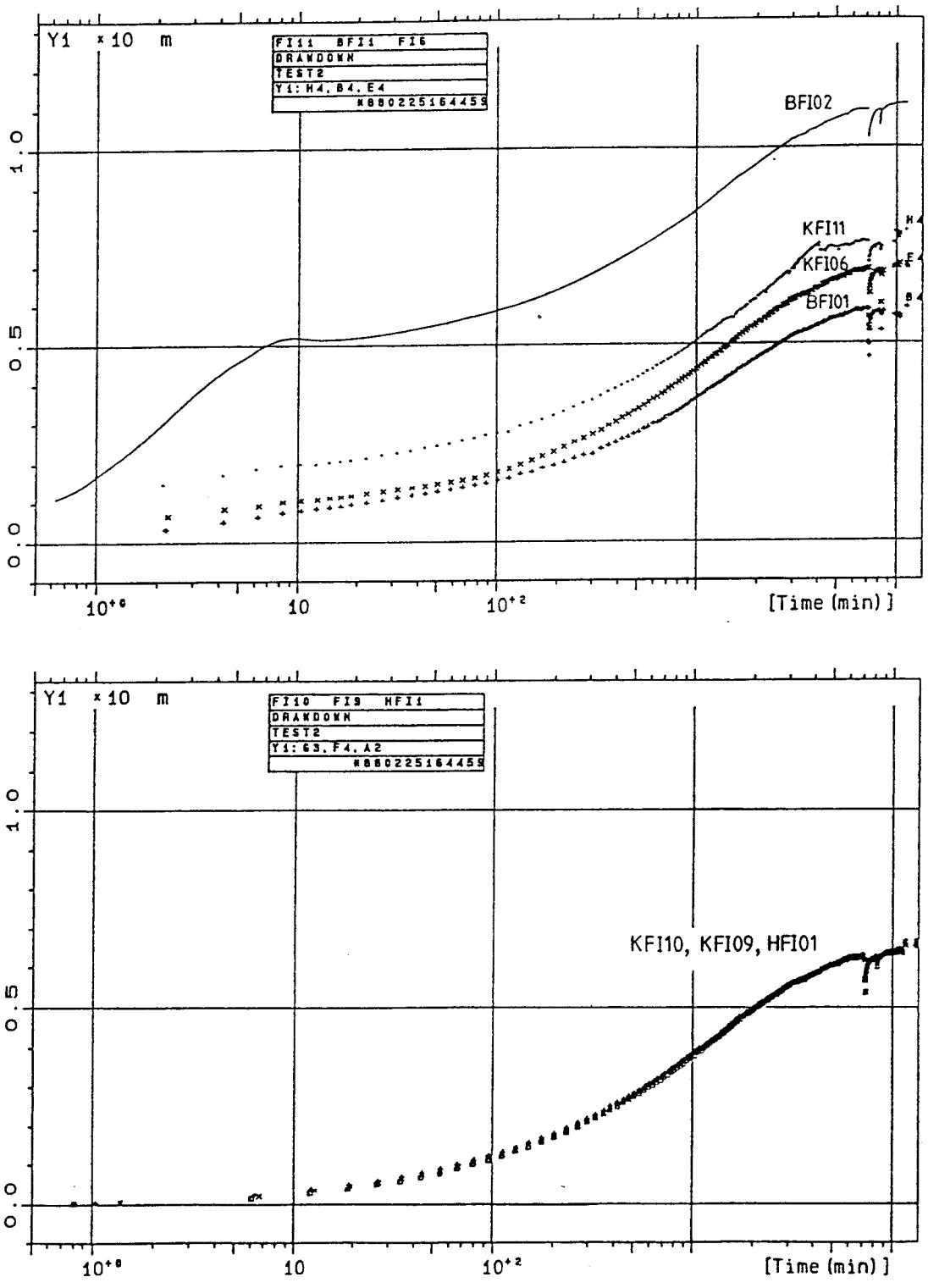

Figure 12 Drawdown of primary responses in the boreholes during interference test 2 (uppermost subzone) in a semi-logarithmic graph.

a) boreholes BFI02 (pumping borehole), BFI01, KFI06 and KFI11.

b) boreholes KFI09, KFI10 and HFI01.

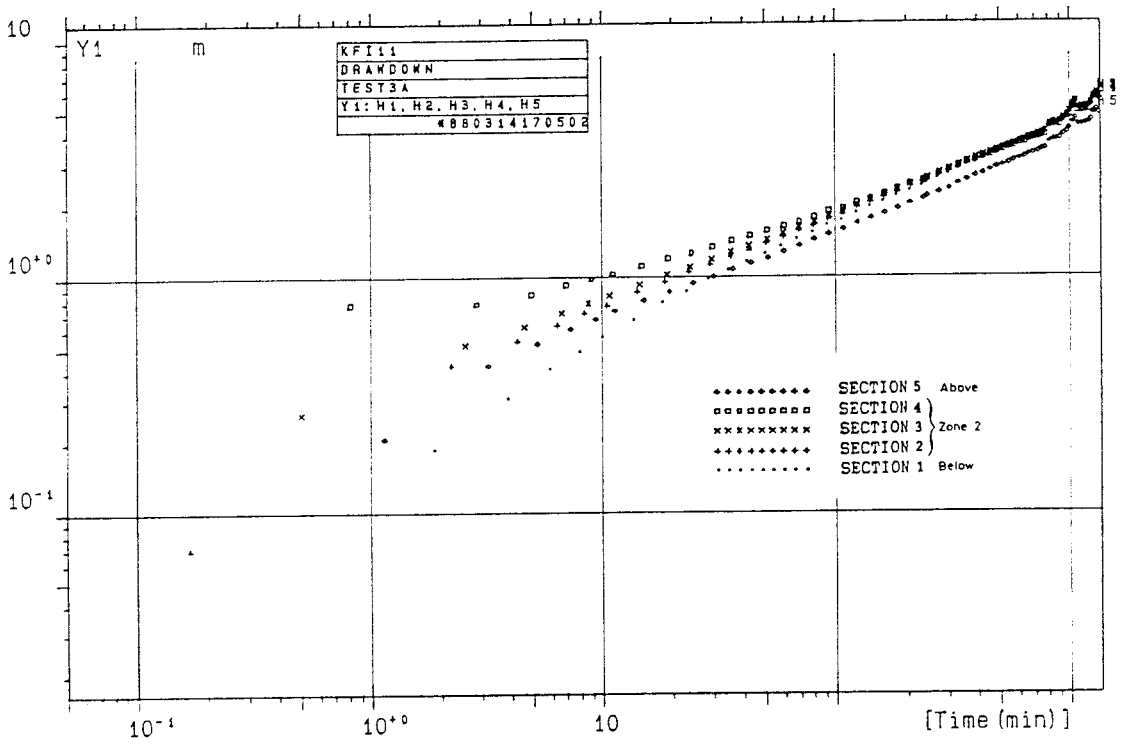

Figure 13 Drawdown responses in multiple-sections of observation borehole KFI11 during interference test 3A (entire Zone 2) in a logarithmic graph.

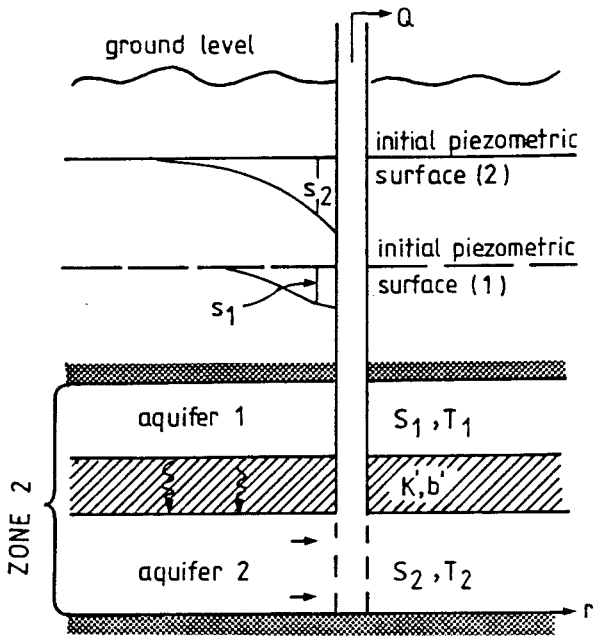

Figure 14 Schematic representation of a leaky two-aquifer system (after Hantusch, 1967).

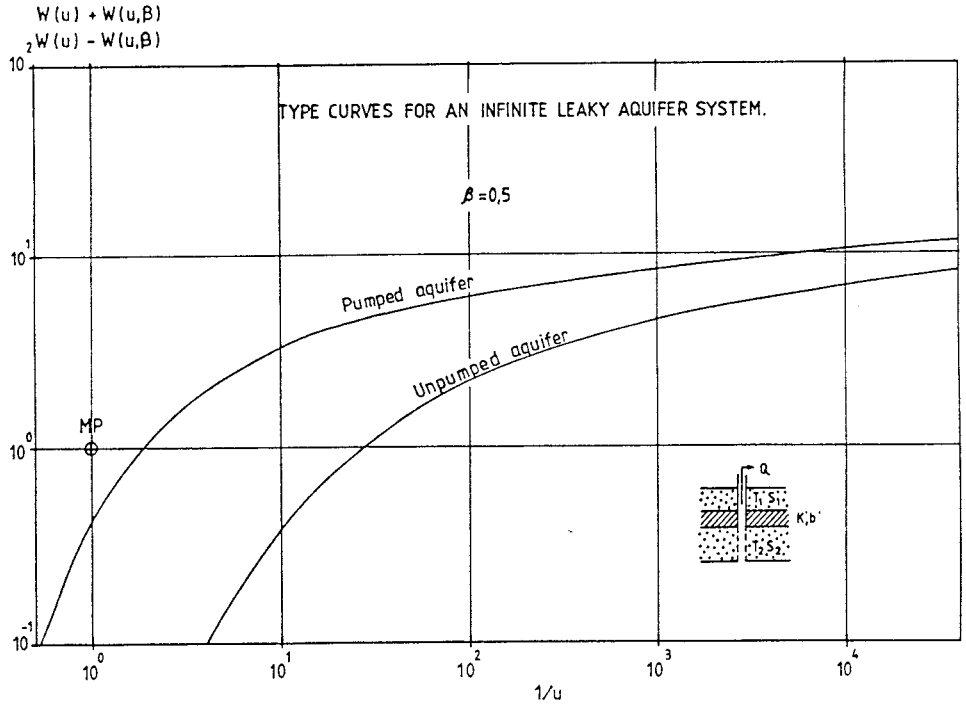

Figure 15 Examples of type curves for a leaky, infinite two-aquifer system shown in Figure 14.

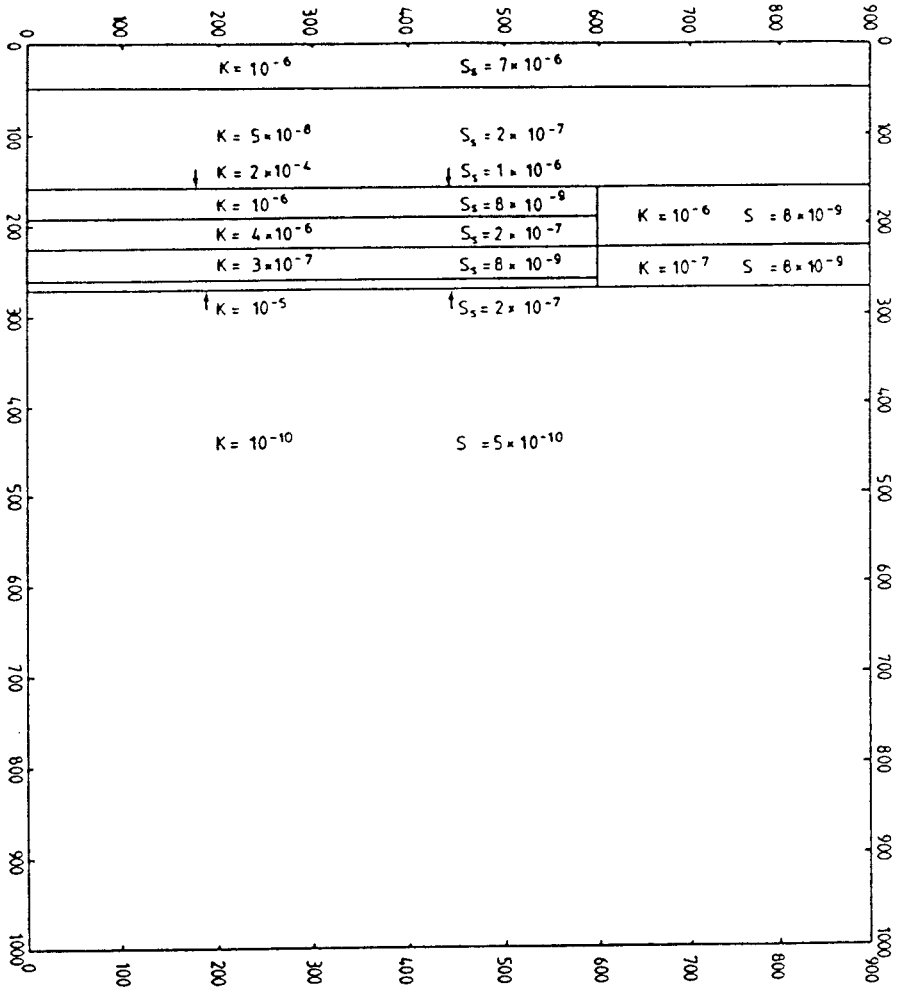

Figure 16 Parameter distribution used for the predictive numerical model prior to the interference tests.

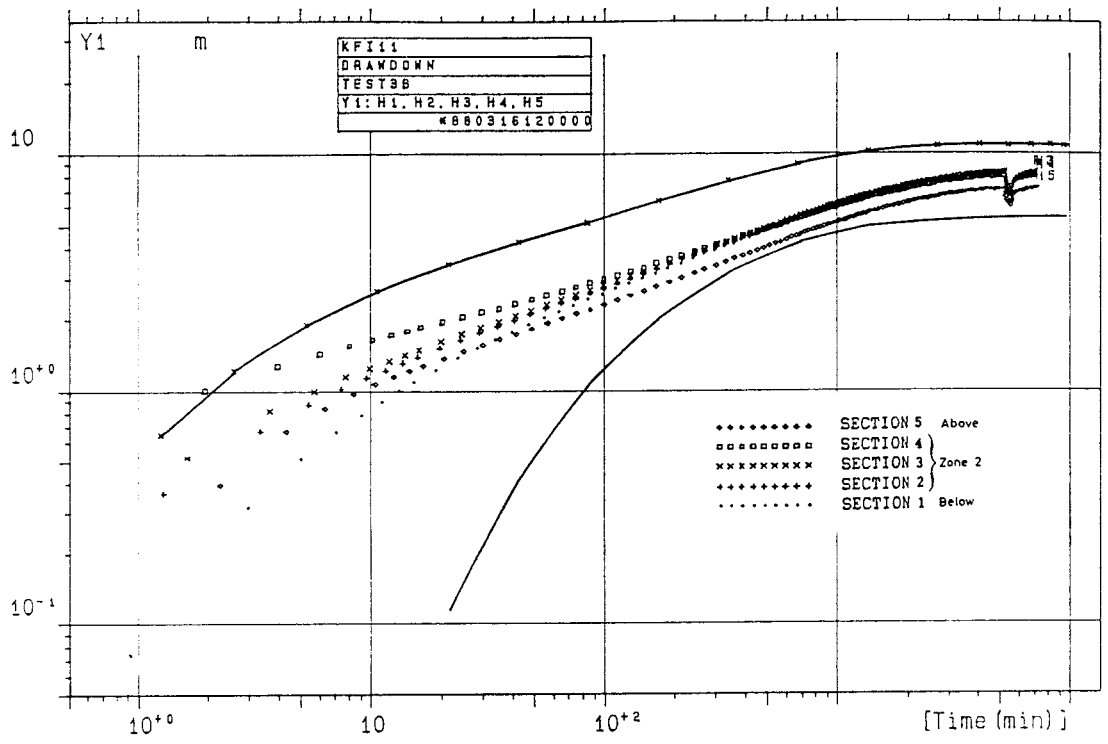

Figure 17 Predicted (solid line) and measured (primary) drawdown responses in observation borehole KFI11 during interference test 3B in BFI02.

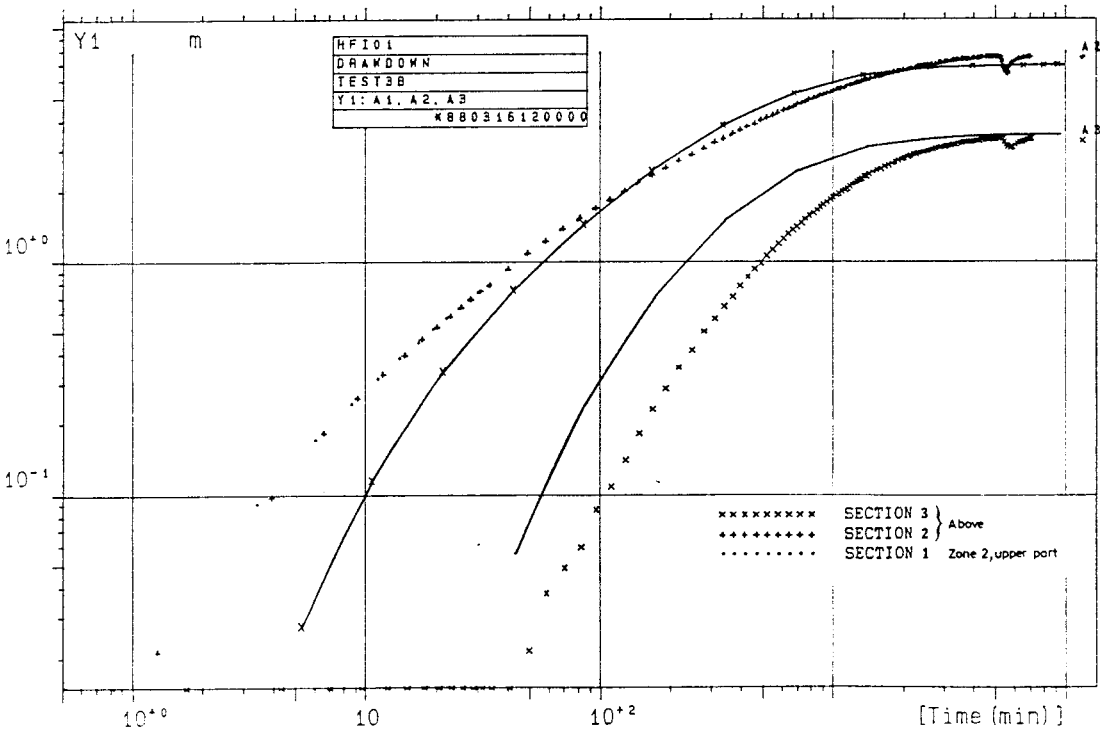

Figure 18 Predicted (solid line) and measured (primary) drawdown responses in observation borehole HFI01 during interference test 3B in BFI02.

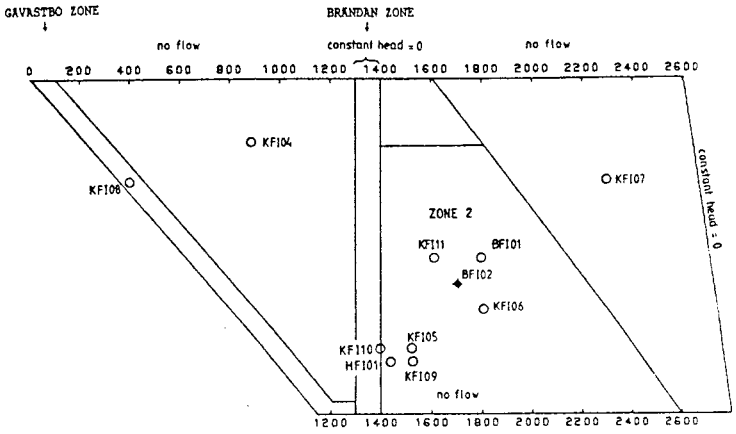

Figure 19 Layout and boundary conditions applied for the calibrated numerical model.

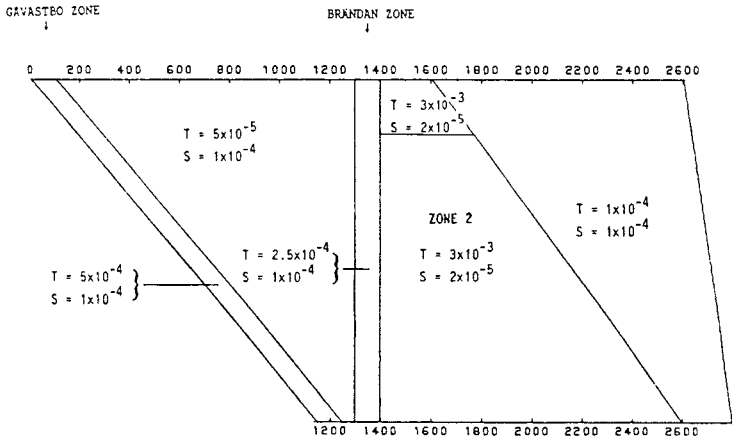

Figure 20 Parameter distribution used for the calibrated numerical model.

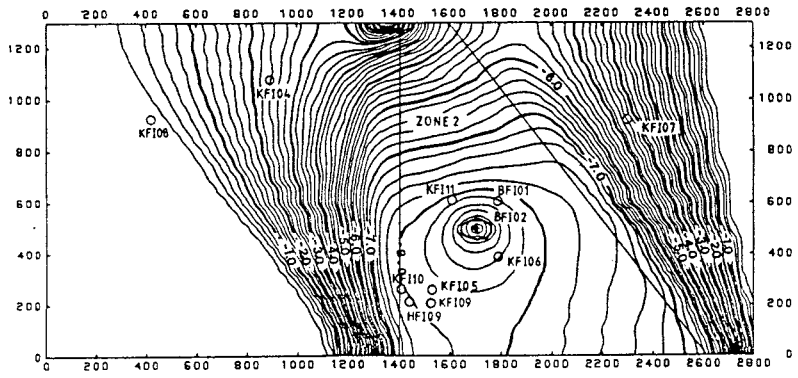

Figure 21 Contour map of the drawdown distribution near steady-state according to the calibrated numerical model. Equidistance = 0.20 m.

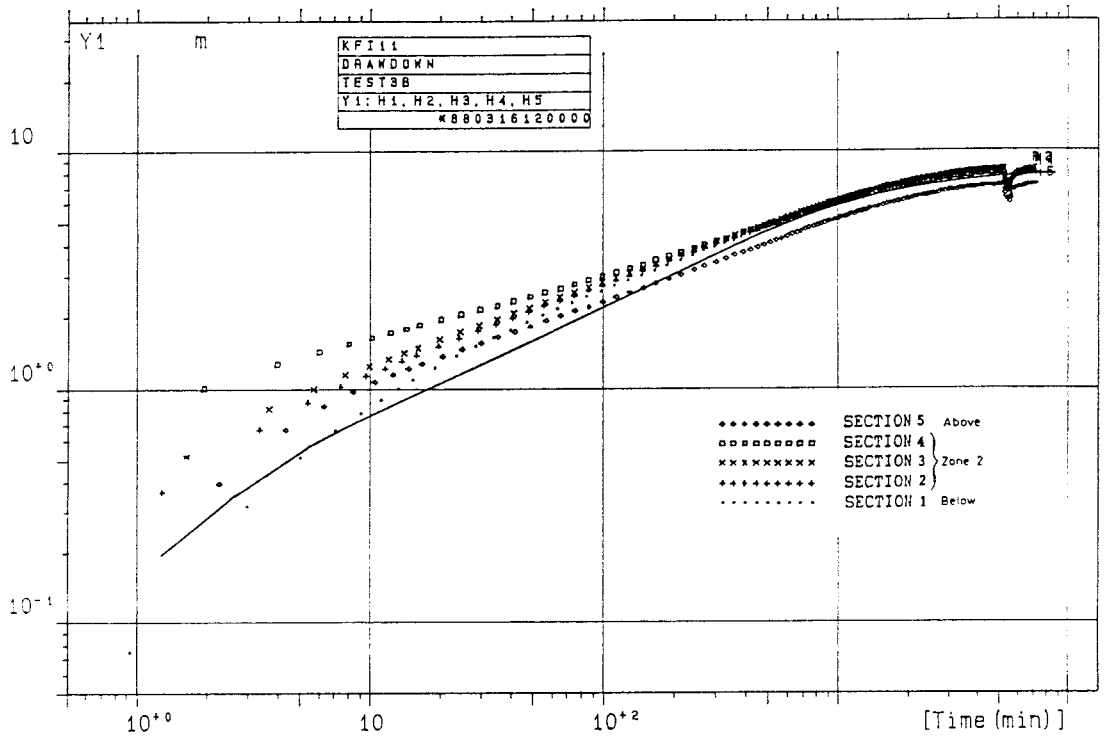

Figure 22 Predicted (solid line) and measured (primary) drawdown responses in observation borehole KFI11 during interference test 3B according to the calibrated numerical model.

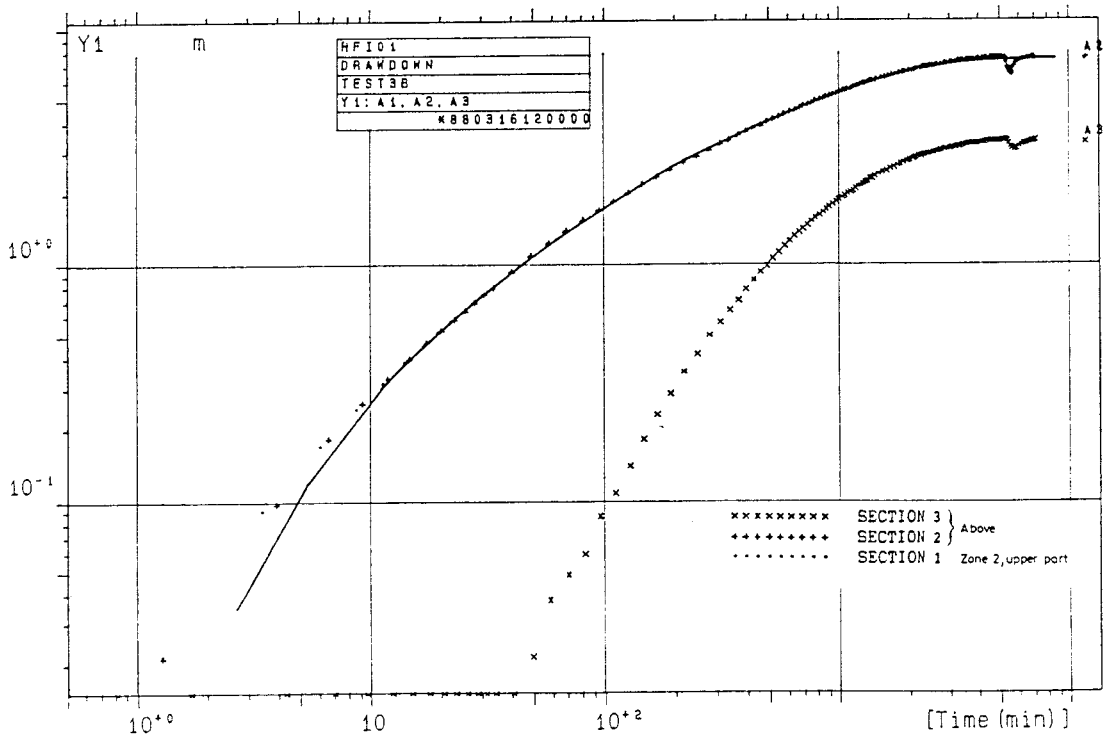

Figure 23 Predicted (solid line) and measured (primary) drawdown responses in observation borehole HFI01 during interference test 3B according to the calibrated numerical model.

CHARACTERIZATION OF FRACTURE ZONE 2, FINNSJÖN STUDY-SITE

PART 4

GROUNDWATER FLOW CONDITIONS IN A LOW ANGLE FRACTURE ZONE AT FINNSJÖN, SWEDEN

E. Gustafsson, P. Andersson

Swedish Geological Company, Uppsala, Sweden

August 1989

GROUNDWATER FLOW CONDITIONS IN A LOW ANGLE FRACTURE ZONE AT FINNSJÖN, SWEDEN.

E. GUSTAFSSON and P. ANDERSSON

Swedish Geological Company, Box 1424, S-751 44 Uppsala, Sweden

Abstract

The performance and results of a series of hydraulic head measurements and differently designed tracer tests are described. A combined interpretation of the results are utilized to estimate the natural groundwater flow conditions in a low angle major fracture zone (Zone 2) investigated at the Finnsjön study site, central eastern Sweden.

The transport of labelled flushing water used during drilling of a cored borehole was utilized to determine hydraulic connections and estimations of hydraulic parameters. The breakthrough of tracer was monitored at a distance of 440 m from the injection point with a mean residence time of 37 days. In order to determine transport parameters of the fracture zone, a tracer test was performed in conjunction with an interference test. The hydraulic fracture conductivity, flow porosity, equivalent fracture width and dispersivity were calculated for three different tracer routes. Tracer was also used to detect any bypass around the packers during the interference test. Also described are a series of groundwater flow determinations using the point dilution technique in packed-off borehole sections, carried out under natural gradient conditions.

The groundwater head measurements indicated that a pressure gradient from high to low exists between the adjacent rocks and Zone 2; where Zone 2 is located closer to the ground surface the opposite situation prevails. The upper highly conductive

part of the zone was found to have high natural flow rates, while in the lower highly conductive part the groundwater flow rates were very low, close to the rate of molecular diffusion.

1. Introduction

In order to estimate the natural groundwater flow conditions in a low angle major fracture zone located in the Brändan area, Finnsjön study site, central eastern Sweden (Fig.1), a combined interpretation of hydraulic head measurements and a series of differently designed tracer tests were utilized.. The site is located in a foliated granodiorite of Precambrian age.

Two tracer tests have been conducted. In the first, earlier discussed by Ahlbom et al. (1986, 1987), the transport of labelled flushing water used during the drilling of a cored borehole was studied. By labelling the flushing water with a suitable tracer, valuable information regarding hydraulic connections between boreholes may be obtained together with estimations of hydraulic parameters such as hydraulic conductivity and porosity.

The second tracer test, described below, has been performed in the upper, highly conductive part of Zone 2 during interference test 2 (Andersson et al.; this volume).

The specific objective of this test was primarily to investigate possible hydraulic connections between the pumped section in one borehole (BFI02) and the injection sections in the surrounding boreholes. Secondly, possible anisotropic conditions or heterogeneities were to be investigated. Ideally, determinations of the mean transport (residence) time, first arrival, hydraulic fracture conductivity, flow porosity and dispersion, should be possible from tracer arrivals originating from three directions.

Furthermore, any bypass or short-circuiting via fractures of water into borehole BFI02 from below, i.e. around the lower packer and into the pumped section, was checked by injecting labelled water just below the lower packer.

Groundwater flow determinations using the point dilution technique in packed-off borehole sections, carried out under natural gradient conditions, have also been made. The primary aim was to determine the natural groundwater flow rate in the low angle major fracture zone (Zone 2), and secondly, the flow rate in the rock and fracture zones adjacent to this major zone. The results of the dilution measurements are also compared with calculations of groundwater flow based on hydraulic tests and assumed gradients. In hydraulic tests (single hole injection tests and interference tests) the hydraulic conductivity is determined, i.e. the potential of the rock/fractures to conduct water at a certain hydraulic gradient. If a value of the natural gradient is assumed, the groundwater flow can be calculated. In some cases the gradient is determined from measurements of the hydraulic head in packed-off borehole sections, which gives a better basis for the calculations.

The point dilution technique however, provides a semi-quantitative method for in situ measurements of groundwater flow in fractures and fracture zones under natural hydraulic gradient conditions, and in the natural flow direction.

Determination of the groundwater flow by the point dilution method was first described by Kocherin in 1916 and further developed by, amongst others, Ogilvi (1958). Since then the method has been used for groundwater flow determinations in porous media (Halevy et al., 1967). Measurements in porous media, in the field and in the laboratory, have been successfully reported by several groups (e.g. Institut fur Radiohydrometrie, 1966,1967,1968,1969; Halevy et al., 1967; Carlsson, 1970 and Mälkki, 1978). Measurements in fractured media are more sparsely reported. Maini (1972) determined the groundwater flow with great accuracy in a laboratory test using a fissure model. Lewis at al. (1966) used the method in shallow fractured rock by means of tracer injections in boreholes were the dilution of tracer was measured in intermittently taken samples.

Gustafsson (1984) reported laboratory tests and measurements of groundwater flow in minor fracture zones. Further development (Gustafsson, 1986) has resulted in improved borehole point dilution equipment and field measurements in fracture zones.

2. Hydraulic head conditions

Variations of piezometric pressure were registered at different borehole sections in conjunction with the drilling of the first booster borehole, BFI01. The pressure readings obtained where converted to hydraulic (freshwater) head and utilized for studies both along the vertical length of the boreholes and laterally at different depths.

Between the different drilling steps rather long periods of undisturbed conditions prevailed thus permitting registration of the natural piezometric pressure in the borehole sections. The registration period lasted from March to November 1986. In general, 3-5 packed-off observation sections at different depths were used in each borehole for the piezometric measurements. The configuration of the observation sections in the boreholes is shown in Figure 2. The measurements were performed by a combination of automatic registration (with pressure gauge) and manual registration of water levels using thin plastic tubes or pipes in some of the boreholes (Ahlbom et al., 1987).

The general piezometric conditions were studied both in the (sub)-vertical direction along the boreholes, and along lateral directions at different depths. To allow comparison of piezometric pressures measured along the boreholes, corrections must be applied to accomodate vertical changes in density (i.e. salinity) within the boreholes (see Smellie et al., 1985; this volume). The details and the conversion of the pressure readings to average hydraulic (freshwater) head are given in Ahlbom et al. (1987).

As an example, the relative hydraulic head (potential) in three sections of borehole KFI10 is shown in Figure 3. The Figure shows the difference in (average) potential along the borehole, measured on September 15th, 1986, relative to the uppermost section (which includes the groundwater table). The Figure also shows the variations of salinity along the borehole. KFI10 penetrates both Zone 1 and Zone 2. The hydraulic head gradient is directed downward from the upper part of the borehole to Zone 1 and upward from Zone 2 to Zone 1. This indicates that the groundwater is discharged to Zone 1 from the eastern part of Zone 2 (Fig. 4). The salinity log is subdued, indicating a zone of mixed fresh water and saline water, probably due to open borehole effects.

Distribution maps showing the lateral distribution of hydraulic head within the Brändan area were constructed for three different depths: (1) groundwater table, (2) upper part of Zone 2, and (3) below Zone 2. The maps are considered schematic because of the relatively few observation points. The hydraulic head distribution in the upper part of Zone 2 is presented in Figure 4.

The results show that, in common with the shallow groundwater, the main direction of flow in the upper part of Zone 2 is towards the ENE with a small gradient (2.2 ‰) in the western part of the area. There is also a vertical component directed upward, resulting in a groundwater flow coinciding with the inclination of Zone 2, i.e. about 16 degrees towards the ENE (Tirén, this volume). In the eastern part of the area the flow is more towards the ESE, i.e. more directly towards Zone 1 compared to the shallow groundwater. However, the gradient is about the same (3.3 ‰) close to Zone 1 in both maps (Ahlbom et al., 1987). Finally, no significant deviations regarding hydraulic gradient and flow direction have been deduced below Zone 2.

Where Zone 2 is located deep below the ground surface (e.g. KFI07 and KFI11) it seems to be recharged by shallow non-saline groundwater and to a certain extent also by deep saline groundwater, i.e. a pressure gradient from high to low exists between the adjacent rocks and Zone 2, The hydraulic head gradient towards Zone 2 in the vertical direction varies between approx. 0.3 to 3.0 ‰. Since the average hydraulic conductivity of the rock just above Zone 2 is about 5 E-8 m/s, as determined from hydraulic single hole tests, the above gradients correspond to an infiltration rate of 0.5 - 5 mm/year of shallow fresh groundwater to Zone 2 from the overlying rock. This corresponds to an infiltration of 500 - 5000 m^3/year over an area of 1 km^2 (approximately the size of the Brändan rock block). However, several minor sub-vertical fracture zones, not intersected by the boreholes, are most probably increasing the rate of infiltration (see Figure 3, Tirén, this volume).

Where Zone 2 is located closer to the ground surface the opposite situation prevails, i.e. the pressure gradient is reversed thus implying that saline water is discharged from Zone 2 and the gradient is mainly directed upward. The magnitude of the upward directed flow also depends on the (vertical) hydraulic conductivity of the rock above Zone 2. Thus, in general terms, recharge to Zone 2 is likely to occur in the more deep-lying western parts of the Brändan area whereas discharge from Zone 2 probably occurs closer to the ground surface in the eastern part. The pressure gradient thus causes saline water to rise into the upper fresh water zone of the boreholes KFI05, KFI09, KFI10 and HFI01 if the boreholes are left open. This fact is also generally reflected in the salinity logs, which in these boreholes are more subdued due to mixing. Under natural flow conditions the high transmissivity in the uppermost part of Zone 2 in the subhorizontal direction (compared to the vertical direction) will prevent the saline water from rising to the surface. Instead it is discharged to Zone 1.

Knowing the hydraulic head gradient and the (total) transmissivity of Zone 2, the natural flow rate per unit horizontal width of Zone 2 may be roughly estimated. Using an average hydraulic gradient of 3.5 ‰ and a transmissivity of 3 E-3 m^2/s (see Andersson et al., this volume) the natural flow rate through a 1000 m wide horizontal section of Zone 2 will be in the order of 10 l/s or 315000 m^3/year, assuming a uniform hydraulic gradient at depth. However, groundwater flow determined in situ by the point dilution method in packed off borehole sections (see below) points out that nearly stagnant flow conditions prevail in the lower part of Zone 2, i.e. no hydraulic gradient is present below the upper boundary of Zone 2. If a groundwater flow of considerable rate only takes place in the upper highly conductive part of Zone 2, with a transmissivity of 1.4E-3 m^2/s, the total groundwater flow rate over the 1000m wide horizontal section will be approximately 150000 m^3/year.

3. Tracer tests

3.1 Flushing water tracer test

3.1.1 Design and performance

Detailed investigations of Zone 2 involved the drilling of a 390 m deep cored borehole KFI11. During drilling, flushing water was continuously pumped from a water supply well, HFI01, which had been drilled into Zone 2 at a distance of 440 metres from KFI11 (Fig. 1). The water was pumped into 5 m^3 storage tanks where it was labelled with the fluorescent dye Uranine (Sodium Fluorescein). In order to check for any hydraulic connection between the boreholes, two samples were taken during the filling of each tank, one from the incoming, unlabelled HFI01-water, and one after labelling and mixing in the storage tank. The principle design of the flushing water tracer test is shown in Figure 5.

Prior to drilling, samples for background readings of Uranine were taken in HFI01. As expected, the residual background concentration of Uranine was high since the drilling of borehole KFI09 in December 1983. The background concentration had thus increased from 0.5 ppb before drilling of KFI09, to 11 ppb before the drilling of KFI11 in October 1985. It was therefore decided to increase the initial concentration of Uranine from 1.0 ppm, which was the concentration used during drilling of KFI09, to 5 ppm.

Drilling, continuous pumping, and sampling, commenced on November 5th, 1985 and lasted for 21 days. The upper boundary of Zone 2 was breached at 224 m depth on November 13th, resulting in a total loss of flushing water. At that depth 26.2 m^3 of flushing water had been injected, of which 4.7 m^3 was returned to the ground surface. From 224 m to the hole bottom an additional 43.8 m^3 were injected into the aquifer.

The pumping and sampling of borehole HFI01 continued to March 7th, 1986 and the results from the tracer analysis are presented in Figure 6. During the 21 days of drilling there was a steady decrease in Uranine concentration from 11 ppb to 3 ppb. These samples represent the decay of Uranine remaining from the drilling of KFI09. The first breakthrough of Uranine from borehole KFI11 is recorded on December 10th, 1985. The concentration increased to a maximum of 23 ppb on January 20th, 1986 and then slowly decreased, reaching 13 ppb on March 7th, 1986 when pumping and sampling was stopped.

3.1.2 Results and interpretation

The recovery of Uranine in HFI01 on March 7th was 22 % of the total injected mass. For borehole KFI11, if only the volume injected at the depth of Zone 2 and downwards is considered, the recovery is 37%. In order to check that the Uranine originated from borehole KFI11 and not from KFI09, mass balance calculations were made as these showed that the mass from this

breakthrough represents a recovery of 130 % of flushing water from KFI09, which is impossible, the conclusion is that the breakthrough originates from the drilling of KFI11.

Estimates have been made of the hydraulic fracture conductivity, K_e, and the flow porosity $\emptyset_k$, based on the following equations:

- Radial flow, $K_e^r = ((r^2-r_w^2)\cdot\ln(r/r_w))/(2\cdot t_o\cdot\Delta h)$ (1)

- Linear flow, $K_e^l = L^2/(t_o\cdot\Delta h)$ (2)

- Flow porosity, $\emptyset_k = K/K_e$ (3)

The input data are:

- Residence time, t_o = 37 days = 3.2E6 s
- Distance between KFI11 and HFI01, r = L = 440 m
- Well radius, r_w = 0.055 m
- Head difference KFI11 - HFI01, Δh = 1.8 m
- Hydraulic conductivity of the zone K = 1.0 E-3 m/s

Contrary to the porous media case values of porosity determined in a heterogeneous rock aquifer from Equation (3) are dependent on the length of the interval where K was determined, or of the assumed thickness of the aquifer contributing to the flow. For example, in the case of one single fracture (or a few narrow spaced fractures) in a otherwise low conductive rock mass.

As can be concluded from the papers by Andersson et al. (this volume) and Tirén (this volume) the total transmissivity of Zone 2 is about 3.0 E-3 m^2/s, but the major part of the transmissivity, and hence the groundwater flow in Zone 2 is concentrated to a few (2 - 3) interconnected minor shear and fracture zones not more than one metre wide. Utilizing this knowledge the flow porosity was determined for these approxi-

mately one metre wide sub-zones where the groundwater flow of consideration actually occurs.

According to the drilling performance with continuous injection of flushing water, the residence time is estimated as the time between breaching the upper boundary of Zone 2 and when 50% of the peak concentration was reached at December 19th.

The results presented in Table 1 show that radial or linear flow assumptions differ by a factor 4 in the determination of K_e and consequently in the $\emptyset_k$-values. However, this difference is not important considering the uncertainties in the input data.

The effect of the flushing water at a large excess pressure being injected in Zone 2 during the drilling of KFI11 has also been estimated. The radius of injection, r_e, assuming isotropic condition and radial injection in Zone 2, can be determined from:

$$r_e = (V/(\pi \cdot h \cdot \emptyset_k))^{0.5} \qquad (4)$$

where V = the total volume injected into Zone 2 (m^3)
h = total width of highly conductive sub-zones in Zone 2 (m)

With V = 65 m^3 and h = 3 m, the radius of injection calculated with the two values of $\emptyset_k$ given in Table 1 is 32 m and 15 m respectively.

With the effect of r_e included in the calculations of K_e according to Equations 1 and 2, the distances r and L, respectively, will be reduced by, in the "worst" case, 32 metres. The calculations presented in Table 2A show that r_e has a small effect on the K_e-values, but it should be noted that isotropic conditions are assumed, which is not necessarily the case.

Another question is whether the flow regime is radial or linear. An estimation of the radius of influence of the pumping in HFI01 has been made based on Thiem´s equation with a drawdown of 1.1 metre and a transmissivity, T = 6.6E-4 m^2/s (Ahlbom et al., 1986). The radius of influence then becomes 280 metres. However, the natural gradient in the upper part of Zone 2 in this part of the area is in the order of 1 m/350 m (see Fig. 4) and the additional gradient caused by the pumping in borehole HFI01 is only 0.4 m/350 m at a distance of 100 m from HFI01. At a distance of 50 m from HFI01, the pumping gradient is equal to the natural gradient, thus increasing the latter to a total gradient of 2 m/350 m. The conclusion of the calculations above is that the drilling water, initially radially injected into Zone 2, a distance of approximately 30 metres, then moves under natural gradient or small pumping gradient in the order of 310-360 metres, and finally in a radially converging flow field in the order of 50-100 metres towards HFI01. In Table 2B fracture conductivity , K_e, and flow porosity, $\emptyset_k$, when considering both the effect of injection and enhanced transport velocity in the vicinity of withdrawal borehole HFI01, are presented. The values are still notably high but are within the same magnitude as the former estimates.

The use of labelled flushing water as a tracer was also shown during drilling of boreholes KFI09 and KFI10 where the existence of hydraulic connections between these boreholes and the flushing water supply well HFI01 was determined (Ahlbom et al., 1986).

The conclusions of the water flushing tracer tests is that the method can provide valuable information about hydraulic connections with a minimum of effort. Estimates of hydraulic parameters like hydraulic conductivity and porosity can be made. However, the lack of control of the radius of injection and the governing flow regime may cause errors that have to be considered.

3.2 Pulse injection tracer test

3.2.1 Design and performance

In interference test 2 (Andersson et al., 1988a) tracers were injected in section no 4 in the observation boreholes BFI01, KFI06 and KFI11, and samples were taken from the water discharging from the withdrawal borehole BFI02. In Figure 7 the relative position of the boreholes used is shown and the pumping/sampling and injection sections intersecting the upper highly conductive part of Zone 2 are marked. Basic data about the test are presented in Tables 3-5. The tracers Uranine, Iodide and Amino G Acid were injected as pulses through the pressure connection tubes in the multi-pressure probes of the Piezomac system. The tracers were injected according to the following scheme:

- Registration of natural piezometric head in the borehole sections.
- Injection of tracer slugs (50 - 125 litres) in boreholes BFI01, KFI06, and KFI11.
- Flushing with groundwater and distilled water (50 - 125 litres) in order to force the tracer some distance into the fractures and to rinse the tubing from tracer.
- Registration of piezometric head.
- Start of pumping in borehole BFI02 for the interference test when the natural piezometric head is reached in all sections.

As was expected for these highly conductive sections, the piezometric head immediately reached natural levels after the injection and flushing was completed. Pumping was then started in borehole BFI02 for a continuous water discharge during 9 days, at a capacity of 500 l/min. Sampling of the discharged water for tracer analysis was performed with automatic sampling equipment (Fig. 8). The time between the sampling events was

determined by the predicted time of first arrival; for the first day, samples were taken at every hour, followed by every second hour.

3.2.2 Methods of interpretation

The interpretation of the breakthrough curves is made assuming a prevailing homogeneous and isotropic radially converging flow field. A conceptual model of the tracer test is shown in Figure 9. The hydraulic fracture conductivity may then be determined from Darcy´s law according to Equation (1), expressed above.

Calculation of the hydraulic fracture conductivity utilizing Equation (1) requires a constant head difference Δh, i.e. a steady state. Examination of the breakthrough curves and comparison with the drawdown in the pumping and injection sections (Fig. 11 and Table 6) shows that the first arrival and mean transport time has been reached and most of the tracers have been recovered in the pumping hole long before steady-state is obtained. However, even though the drawdown is not constant, the relative head differences, especially between boreholes KFI06 - BFI02 and KFI11 - BFI02, is fairly constant during the process of tracer transport from the injection boreholes to the centrally located pumping hole BFI02 (Table 7). The error introduced by assuming constant Δh values is relatively small. For calculations of the hydraulic fracture conductivities, K_e, the values of Δh underlined in Table 7 have been used, after the addition of a correction factor (0.5 m) to obtain absolute values of Δh. In addition, the equivalent fracture width e, was determined using the expression given by Snow (1968) for laminar flow between two smooth, parallel plates:

$$e = (K_e \cdot 12\nu/g)^{0.5} \qquad (9)$$

where ν = kinematic viscosity of the water (m^2/s)

g = acceleration due to gravity (m/s^2)

The flow porosity, $\emptyset_k$, defined as the volume of rock available for transport of water (Norton and Knapp, 1977), is determined from Equation (3), assuming an equal gradient over the rock mass and the fracture, and that Darcy's law applies. As discussed in section 3.1.2, flow porosity values determined in a heterogeneous rock aquifer are dependent on the interval where the porosity is determined. The present tracer run was conducted in the upper highly conductive part of Zone 2, straddled in a 25 long borehole interval. However, hydraulic testing shows that the groundwater flow is concentrated only to a one metre wide sub-zone and thus the flow porosity is determined for that zone.

The hydraulic conductivity of the rock mass, K, used for the calculation of the flow porosity according to Equation (3) can be determined as a mean value from single hole hydraulic testing (Eqn 10), or by utilizing transmissivity values from hydraulic interference tests. In the present tracer run, data from interference test 2 (Andersson et al., this volume) was available (see Table 3B).

$$K = (T_p/L_p + T_i/L_i)/2 \qquad (10)$$

where T_p = transmissivity of pumping section (m^2/s)
T_i = transmissivity of injection section (m^2/s)
L_p = length of pumped section (m)
L_i = length of injection section (m)

Hydrodynamic dispersivity, a, is defined as the spreading in time and space of a water-soluble substance transported with the groundwater, due to the velocity distribution and the molecular diffusion in the medium. In this case the dispersivities are determined by fitting the breakthrough curves to theoretical curves according to Gelhar (1987);

$$a = 3 \cdot r \, (\Delta t/t_0)^2/64 \qquad (11)$$

where Δt is defined as depicted schematically in Figure 10.

Equation (11) takes into account the varying velocity and dispersion coefficient associated with the radial flow system and is valid for Peclet numbers Pe > 10, i.e. a/r < 0.1.

3.2.3 Results

Tracers from all boreholes reached the pumping/sampling borehole BFI02. The resulting breakthrough of the tracers is presented as normalized tracer concentrations versus time in Figure 11. In Table 8 tracer first arrivals and residence times are given.

The hydraulic fracture conductivity and the flow porosity in the upper highly conductive part of Zone 2, calculated from tracer arrivals in three directions from borehole BFI02, is presented in Table 9. The fracture conductivities are notably high, but are only a factor 5-30 higher than the hydraulic conductivity, K_{ss}, determined by hydraulic single hole tests in 0.11 m sections of borehole BFI02 (Andersson et al., 1988b). The values of hydraulic fracture conductivity determined in three directions over distances ranging 155 - 189 metres are in fairly good agreement with the value determined over a distance of about 400 metres, 1.6E-1 - 9.7E-1 m/s and 1.7E-2 - 1.5E-1 m/s respectively.

The flow porosities are also in accordance with those determined from the flushing water tracer test. The flow porosity values determined over the one metre thick sub-zone clearly shows the porosity being larger in the direction of borehole BFI01 than in the direction to the other two boreholes. A comparison between the fracture aperture calculated for one equivalent single fracture and the porosity values indicates that in the direction from KFI11 - BFI02 the transport of the tracer solute is concentrated to one or two main flow paths. In

the direction from KFI06 - BFI02 not more than 3-4 main flow paths are involved if parallel-plate fractures are assumed. However, the results indicate a larger number, 10-15, of main flow paths contributing to the solute transport in the direction from BFI01 - BFI02.

Calculated dispersivities and Peclet numbers are also presented in Table 9. According to the high Peclet numbers the tracer transport is dominated by advection, whereas dispersion is of minor importance.

The recovered mass of injected tracers was calculated after 188 hours of pumping (Table 9). The recovery was about 70% for Uranine and Amino G and 81% for Iodide. The Iodide and Uranine had not reached background values when pumping was discontinued.

In summary, the performed tracer tests indicate the upper part of Zone 2 to be fairly homogeneous. However, between boreholes BFI01 and BFI02 somewhat higher porosity flow paths and lower hydraulic fracture conductivity was determined, i.e. 5.9E-4 and 1.6E-1 m/s respectively. The corresponding values between KFI06 - BFI02 and KFI11 - BFI02 are in the range of 4.5 - 7.6 E-5 and 6.1 - 9.7E-1 m/s respectively. In all three directions the dispersivity is low, 1.3 - 3.9 m, or expressed as Peclet number , 48-118, which implies that the tracer transport in the groundwater flow paths studied, and at the distances involved, is dominated by advection whereas dispersion is of minor importance.

3.3 Bypass Test

3.3.1 Design and performance

Subsequent to the tracer pulse test a bypass test was conducted in the withdrawal borehole BFI02 during interference test 2 in order to check if there was any bypass of water from

below into the pumped section at 193 - 217 m. Uranine was injected below the lower packer as a pulse through the pressure connection tube (Fig. 8). The tracer was dissolved in groundwater and groundwater was also used to flush the tracer through the tubing.

Although Uranine was also injected in borehole BFI01 for the previously described pulse injections (Section 3.2), for the bypass test the Uranine tracer slug was introduced some 171 hours after the injection in BFI01. The peak concentration of Uranine in the pumped section in BFI02, originating from BFI01, had then already passed more than 100 hours ago and the breakthrough was on its latter declining part (Fig. 11).

3.3.2 Results

No tracer was detected in the discharged water during the 17 hours after tracer injection. Any bypass of importance, as indicated by the increasing salinity of the discharged water during interference test 2, would have been well above the detection limit and easily measurable.

When interference test 2 was finished and the packers rearranged for interference test 3, the pump was started for 10 minutes. During this time, about 65 % of the injected mass of tracer was recovered. When interference test 3 started the discharged water was sampled and the remaining part of the tracer (35%) was recovered within 5 hours.

The test performed has shown that there was no measurable bypass of water around the lower packer into the pumped section during interference test 2. Thus, the increased salinity must be due to an imposed groundwater flow in a system of fractures-/zones interconnecting the deep saline part of Zone 2 with the upper highly conductive and less saline part of the zone being pumped.

4. Tracer dilution tests

4.1 Method of groundwater flow rate determination

The point dilution method enables the determination of groundwater flow in situ, in fractures and fracture zones under natural hydraulic gradient conditions, and in the direction of the natural groundwater flow.

In this method the tracer is introduced as a homogeneous pulse into a borehole test section sealed off by rubber packers. The tracer will be diluted due to the normal groundwater from the fracture zone flowing through the borehole. The dilution of the tracer introduced is proportional to the water flow through the borehole section, and thus to the groundwater flow in the fracture zone. Within the borehole section the tracer must always be completely mixed and the concentration is measured as a function of time.

Groundwater flow rate through the borehole test section is calculated from the water volume in the test section, and the dilution as a function of time according to Equation (12). This is the solution of the equation of continuity for the dilution of a homogeneously distributed tracer solution in a constant volume V at steady-state groundwater flow.

$$Q_W = - V \cdot \ln(C/Co)/t \qquad (12)$$

where Q_W = groundwater flow rate through the borehole test section (m^3/s)

V = water volume in the borehole test section (m^3)

t = time (s)

C_O = initial tracer concentration

C = tracer concentration at time t

Dilution as a function of time is obtained from a semi-logarithmic diagram of normalized tracer concentration versus

time. In the ideal case the relation between time and logarithmic concentration is linear according to Equation (12).

As the dilution measurements aim in relating the measured groundwater flow rate through the borehole section to the rate of the undisturbed groundwater flow in the fracture zone, the flow field distortion must be taken into consideration, i.e. the degree to which the groundwater flow converges and diverges in the vicinity of the borehole test section. The groundwater specific discharge (Darcy-velocity), defined as the discharge per unit cross-sectional area perpendicular to groundwater flow, is denoted by v_f. With a correction factor, â, which accounts for the distortion of the flow lines owing to the presence of the borehole, it is possible to calculate the specific discharge according to equations (13) and (14). If the groundwater flow is not perpendicular to the borehole-axis, this also has to be accounted for (Gustafsson, 1986).

The cross-sectional area used to calculate the specific discharge is:

$$A = 2 \cdot r \cdot L \cdot \hat{a} \qquad (13)$$

Hence, the specific discharge is given by

$$v_f = Q_w/A \qquad (14)$$

The quotient Q_w/A may thus also be expressed as a volumetric flux density, Q_f, ($m^3/m^2 \cdot yr$). Figures 12 and 13 schematically shows flow lines in fissure flow and the cross-sectional area, A, defined in Equation (13).

Determination of the groundwater flow rate in each individual fissure requires either isolation of the single fissures in short test sections, or knowledge about the number of flowing fissures in the test section. Calculations of the velocity in the fissures also requires knowledge about the fissure apertures.

If the drilling has not caused any disturbances outside the borehole radius the correction factor â is 2.0 at laminar flow in a plane parallel fissure, or a homogeneous porous medium (Ogilvi, 1958). According to the formula of Ogilvi the value of â will however at least vary within â = 2÷1.5 in fractured rock (Gustafsson, 1986). Hence, the groundwater specific discharge measured in one point of a fracture zone is determined with an accuracy of +75%, according to the flow field distortion. The accuracy in flow determination is not, however, only due to the factor â, the tracer is also diluted due to changed physical and chemical properties of the labelled water in the test section compared to the native groundwater. Although the down-hole equipment may also cause disturbances, and in borehole sections of considerable length vertical currents may even be found, the equipment, tracers and concentrations used tend to eliminate most of these disturbances. Molecular diffusion of the tracer into the fractures always exists, but it can often be neglected at considerable groundwater flow in short test sections.

4.2 Measurements performed

Measurements were performed in the percussion drilled boreholes BFI01 and HFI01 from June to September 1987 in order to determine the natural groundwater flow rate in the low angle Zone 2, and secondly to establish the flow rate in the rock and fracture zones adjacent to Zone 2. The booster drilled percussion borehole BFI01, 165 mm in diameter, penetrates the entire Zone 2, in contrast to percussion borehole HFI01, 110 mm in diameter, which penetrates only the upper part of Zone 2 (Fig. 2).

The borehole test sections selected for measurement were extracted from single hole water injection tests (2 m- and 20 m sections) and checked against geophysical logging, drill cuttings, tube-wave and borehole radar measurements (Ahlbom et

al., 1986; Smellie et al., 1987; Andersson et al., 1988). The selected borehole sections are presented in Table 10.

Although most sections measured were short, 2 m, sections of considerable length, up to 180 m, were also used. In 2 m and 20 m-sections the groundwater flow rate was measured using a prototype borehole point dilution equipment with a down-hole tracer concentration measuring facility (Fig. 14). In the longer test sections (41, 45 and 180 m) equipment enabling surface sampling was used (Fig. 15). The equipment is described by Gustafsson (1986) and Gustafsson and Eriksson (1988).

From June to September 1987 the groundwater table was measured in five boreholes (BFI01, HFI01, KFI06, KFI09, KFI11) during the dilution measurements. There was a small overall rise of the groundwater table of about 0.2 m during this period, but no change of the hydraulic gradient during the individual dilution measurements could be observed.

Dilution measurements were successful in ten of twelve selected borehole sections. In borehole BFI01 the 264-266 m section could not be measured due to chemical precipitation of iron, manganese and sulphur adsorbed onto the lens and prism. The instrument was raised to the ground surface for flushing and cleaning. Unfortunately, the time schedule did not allow further attempts at this section and the instrument was lowered directly to 352-354 m. In test section 84-129 m (borehole HFI01) problems with dissolved gases in the water made it impossible to conduct any dilution measurements with the surface sampling equipment.

As an example of the measurements performed the dilution curve obtained in Borehole BFI01 sections 242-244 m and 244-246 m are shown in Figure 16.

4.3. Results

The groundwater flow rate through the borehole test section, Q_w, is calculated from the straight line part of the dilution curve (semi-logarithmic diagram). The volumetric flux density, Q_f, has been calculated with the assumption that the correction factor â=2 in the test sections. Hence, the fractures intersect the borehole at 90° angle and the drilling has not affected the rock outside the borehole radius, i.e. negligible skin.

4.3.1 Groundwater flow in borehole BFI01

The results from the dilution measurements in borehole BFI01 are presented in Figure 17 and Table 11.

In Zone 2 the groundwater flow is concentrated to the upper highly conductive part (242-246 m); in the lower highly conductive part (352-356 m) the groundwater flow is below the limit of measurement and is thus only at the rate of molecular diffusion which in this case is estimated to less than 3 E-11 m/s (Gustafsson, 1984, 1986, 1988). This confirms that the driving force, i.e the hydraulic gradient, is minimal in the lower part of Zone 2.

A low groundwater flow rate in the lower part of Zone 2 corresponds also with the results from hydrochemical investigations carried out in the boreholes KFI09 and BFI01 (Smellie et al., 1987). Below the upper, highly conductive part of Zone 2, the water has a high salinity and uniform composition which indicates that there is very little, if any, flow. In borehole KFI11 geophysical logging showed a decrease in salinity below Zone 2, possibly indicating some remaining contamination from the flushing water. This persistence of flushing water mixing may be due to the very low groundwater flow or stagnant conditions below Zone 2 (Ahlbom et al., 1988).

Above Zone 2 the groundwater flow is high in the shallow fractured and high-conductive rock (the 9 - 50 m test section). Below this rock there is almost 200 m of medium- to low-conductive rock, where the groundwater flow is low.

In Table 11 the groundwater specific discharge, calculated from the groundwater flow rate values determined with the point dilution method, v_f^d, are presented together with those calculated from hydraulic conductivities and gradients determined from hydraulic tests and piezometric measurements, v_f^g. The v_f^d and v_f^g values are in fairly good agreement in the upper part of Zone 2 as well as in the above-lying country rock. However, in the lower part of Zone 2 the specific discharge calculated from hydraulic conductivities and gradients, v_f^g, were overestimated by four orders of magnitude compared to those determined from the dilution measurements. This result indicates that determinations of the hydraulic gradient in specific groundwater flow paths from piezometric measurements from relatively few observation points can be problematical, especially when groundwater layers of different densities are involved.

4.3.2 Groundwater flow in borehole HFI01

The results of the dilution measurements in borehole HFI01 are presented in Figure 18 and Table 12.

A relatively high flow rate was obtained in the highly conductive shallow section at 38-40 m. This indicates, in similarity to BFI01, a large groundwater circulation in the shallow fractured rock. The groundwater volumetric flux density, Q_f, in the fracture zone at 38-40 m depth in HFI01 is also well in accordance with the flux determined in the highly conductive shallow rock in borehole BFI01, i.e. 12 and 14 $m^3/m^2 \cdot yr$ respectively.

In the upper part of Zone 2 the two most hydraulically conductive 2 m sections were measured (108-110 m and 112-114 m). In addition, to establish if there was any considerable flow in other fractures than these included in the highly conductive 2 m sections, a 20 m section (104-124 m) straddling these 2 m sections was also measured. Even though in the 20 m section the two 2 m-sections contribute to more than 99% of the total transmissivity, the groundwater flow rate measured in these two sections only make up 1.4% of the flow rate measured through the 20 m-section. The discrepancy is too large to be due to groundwater flow in other fractures than these included in the 2 m-sections. However, according to the drillers log and the geophysical logging, a minor discrepancy in the length determination between the hydraulic test equipment and the dilution equipment was enough to miss the hydraulically active fractures and apparently cause low flow rates in the two high-conductive 2 m-sections.

The point dilution measurement in the 20 m-section 104-124 m, however, clearly proves that the upper part of Zone 2 also at borehole HFI01 exhibits a high groundwater flow rate. Assuming that the groundwater flow rate measured in the 20 m-section is concentrated to the two straddled high-conductive 2 m-sections, the groundwater flux in the upper part of Zone 2 (4 m width) becomes 67 $m^3/m^2 \cdot yr$ at borehole HFI01, which is well in agreement with the flux at borehole BFI01, 90 $m^3/m^2 \cdot yr$.

5 Estimation of natural groundwater flow

The natural groundwater flow determined in situ by the point dilution method in packed off borehole sections points out that nearly stagnant flow conditions prevail in the lower part of Zone 2, i.e. no hydraulic gradient is present below the upper boundary of Zone 2. Groundwater flow of considerable rate only takes place in the upper highly conductive part of Zone 2. The total groundwater flow rate over a 1000 m wide horizontal section of Zone 2, calculated by extrapolation of the results

from the dilution measurements, is in the order of 150 000 - 370 000 m^3/year. This flow rate is to be compared with 150 000 - 315 000 m^3/year calculated from the hydraulic interference tests and hydraulic head measurements. The flow rate calculated by these two independent methods are in good agreement.

The rate of infiltration from the overlying rock was on the other hand calculated to only 500 - 5000 m^3/year over an area of 1 km^2, which is approximately the size of the Brändan rock block. It seems thus most reasonable that regional groundwater flow to a large extent contributes to the prevailing groundwater flow in Zone 2 at the Brändan area, even though several minor sub-vertical fracture zones which may increase the infiltration rate, were not included in the estimation of the infiltration rate.

The contribution of regional groundwater flow is further indicated by estimation of the total groundwater recharge at the Finnsjön site based on data from Carlsson and Gidlund (1983). From these data the recharge over an area of 1 km^2 has been calculated to a maximum of 150 000 m^3/year, of which the most part is circulated in the soil and the shallow, fractured and highly conductive rock, as is also shown by the dilution measurements. Hence, approximately 60 - 80 % of the groundwater flow in Zone 2 must be regionally recharged.

Knowing the groundwater flow rate over the 1000 m wide horizontal section of Zone 2 and the hydraulic gradient (0.0035), the necessary aperture width of one equivalent single fracture (with parallel planar plates representing the fracture surfaces) to discharge the assumed flow rate can be calculated. The calculated aperture was in the range 1.3E-3 - 1.7E-3 m. If the same flow rate is divided into five or ten parallel-plate fractures the aperture of the fractures are approx. 0.8E-3 m and 0.7E-3 m respectively. This makes up a total aperture of Zone 2 of 4.0E-3 m and 7.0E-3 m respectively. The aperture of Zone 2 calculated for one single equivalent fracture is to be compared with that calculated from the pulse injection of

tracers (section 3.2) in the central part of the highly conductive upper boundary of Zone 2, ranging between 5.1E-4 - 1.3E-3 m.

In the drilling water tracer test described in section 3.1.2 where tracer labelled flushing water from borehole KFI11 entered the drilling water supply well HFI01 at a distance of about 440 m (Fig. 1), the hydraulic fracture conductivity was calculated in the range of 1.7E-2 -1.5E-1 m/s depending on assumed flow regime and hydraulic gradient. Considering the uncertainties, the solitary K_e value determined over a distance of 440 metres, and the values determined in three directions over a distance of about 160 metres, are in good agreement. Furthermore, the flow porosity, Øk, was estimated in the range 6.7E-3 - 5.9E-2 in Zone 2, approximating to a thickness of 1 m. In this present work, the flow porosity calculated over the same thickness ranges between 1.0E-3 and 9.4E-3 in the upper part of Zone 2.

6 Conclusions

This investigation which includes measurements of the natural head conditions, a series of tracer tests and groundwater flow measurements has given a good picture of the groundwater flow conditions and transport parameters of the major low angle fracture zone, Zone 2.

The hydraulic head measurements show that in the deeper lying western parts of the zone, saline water from below and non-saline water from above is recharged into the zone. The vertical gradient towards Zone 2 is low, in the order of 0.3-3 ‰. Where Zone 2 is located closer to the ground surface the opposite situation prevails, i.e. the pressure gradient is reversed thus implying that saline water is discharged from Zone 2 and the gradient is mainly directed upward. The rate of infiltration from above Zone 2 was estimated to 500-5000 m^3/year over an area of 1 km^2 while the groundwater flow rate

over a 1 km wide horizontal section of Zone 2 was calculated to be in the order of 150 000-370 000 m^3/year. Thus, regional groundwater flow seems to be dominating the recharge to Zone 2.

The natural gradients are low in the Brändan area, both within Zone 2 and in the rock mass. The groundwater flow is directed towards ENE and the lateral gradients are in the order of 2.2-3.5 ‰. Groundwater flow measurements, performed with the point dilution method, shows high flow rates in the shallow fractured rock and in the upper highly conductive part of Zone 2, whereas no flow could be registered in the highly conductive lower part of the zone. This observation is also supported by geochemical investigations.

Comparison between measured and calculated groundwater flow rates shows a fairly good agreement, except for the lower highly conductive part of Zone 2. This result indicates that determinations of the hydraulic gradient in specific groundwater flow paths from piezometric measurements from relatively few observation points can be problematical, especially when groundwater layers of different densities are involved.

The tracer tests, not performed as specific tracer tests but as complements during other investigations, gave valuable information about hydraulic interconnections and transport parameters of Zone 2. The flushing water tracer test showed that the upper part of Zone 2 was hydraulically connected between boreholes KFI11 and HFI01, i.e. over a distance of 440 meters. Interconnections between boreholes KFI09, KFI10 and HFI01 could also be determined in a similar way. From the breakthrough of tracer, quantitative evaluations of transport parameters could be made. Hydraulic fracture conductivities were calculated to range between 1.7 E-2 - 1.5 E-1 m/s depending on the assumptions made regarding the flow geometry. The flow porosity was calculated over a thickness of one meter which is the approximate thickness of the upper highly conductive part of the zone. The porosities were ranging

between 6.7 E-3 - 5.9 E-2 using different flow geometry assumptions.

The results from the flushing water tracer test show good agreement with the results from the pulse injection tracer test performed in conjunction with the interference tests. From this test, performed in a smaller scale (155-190 m) with a more well defined radially converging flow geometry, also estimates of the dispersion in the upper part of Zone 2 could be made. The test also involved transport in three different directions to the pumping well thus allowing studies of the heterogeneity within the upper highly conductive part of Zone 2.

In summary, the performed tracer tests indicate the upper part of Zone 2 to be fairly homogeneous. The hydraulic fracture conductivities range between 1.6 E-1 and 9.7 E-1 m/s and the flow porosities between 1 E-3 and 9.4 E-3. The highest flow porosity was determined between boreholes BFI01 and BFI02 indicating that several flow paths are involved in the transport between these boreholes. Between boreholes KFI11 and BFI02 the results indicate that the transport is concentrated to only one or two main flow paths. The dispersivities are low in all three directions, 1.3-3.9 m, which implies that the tracer transport in the groundwater flow paths studied, and at the distances involved, is dominated by advection whereas dispersion is of minor importance.

References

Ahlbom, K., Andersson, P., Ekman, L., Gustafsson, E., Smellie, J. and Tullborg, E-L., 1986. Preliminary investigations of fracture zones in the Brändan area, Finnsjön study site. SKB Tech. Rep. 86-05.

Ahlbom, K., Andersson, P., Ekman, L. and Tirén, S., 1987. Characterization of fracture zones in the Brändan area, Finnsjön study site. SKB Tech. Rep. in prep.

Andersson, J-E., Ekman, L., Gustafsson, E., Nordquist, R., and Tirén, S., 1988a. Interference tests within the Brändan area, Finnsjön study site. SKB Stat. Rep. in prep.

Andersson, J-E., Andersson, P., Carlsten, S., Ekman, L., Eriksson, C-O., Gustafsson, E., Hansson, K. and Stenberg, L., 1988b. Documentation of borehole BFI02 within the Brändan area, Finnsjön study site. SKB Stat. Rep. in prep.

Andersson, J-E., Andersson, P. and Gustafsson, E., 1989. Effects of gas-lift pumping on hydraulic borehole conditions at Finnsjön, Sweden. , this volume.

Carlsson, L., 1970. Försök att med hjälp av utspädningsteknik bestämma grundvattnets skenbara medelströmhastighet (in swedish). Publ. A 70:2. Inst. f. vattenförsörjning och avlopp, CTH. Gothenburg.

Gelhar, L., 1987. Applications of stochastic models to solute transport in fractured rocks. SKB Tech. Rep. 87-05.

Gustafsson, E., 1983. Beräkning av grundvattenflödet i en sprickzon med hjälp av utspädningsteknik, en metodstudie (in swedish). SKB Stat. Rep. 84-06.

Gustafsson, E., 1986. Bestämning av grundvattenflödet med utspädningsteknik. Modifiering av utrustning och kompletterande mätningar (in swedish). SKB Stat. Rep. 86-21.

Gustafsson, E. and Eriksson, C-O., 1989. Characterization of fracture zones in the Brändan area, Finnsjön study site. Determination of groundwater flow by the point dilution method in packed-off sections in boreholes BFI01 and HFI01. SKB Stat. Rep. in prep.

Halevy, E., Moser, H., Zellhofer, O. and Zuber, A., 1967. Borehole dilution techniques: A critical review. Isotopes in Hydrology, p 531-564 (Proc. Symp. Vienna 1967). IAEA Vienna.

Forschungstelle für Radiohydrometrie, 1966. Jahresbericht 1965, am Institut für allgemeine und angewandte Geologie und Mineralogie der Universität Munchen.

Institut für Radiohydrometrie, 1967. Jahresbericht 1966, der Universität Munchen.

Institut für Radiohydrometrie, 1968. Jahresbericht 1967, der Universität Munchen.

Institut für Radiohydrometrie, 1969. Jahresbericht 1968, der Universität Munchen.

Lewis, D.C., Kriz, G.J. and Burgy, R.H., 1966. Tracer dilution sampling techniques to determine hydraulic conductivity of fractured rock. Water Resources Research, Vol 2, p 533-542.

Maini, Y.N.T., 1972. In situ hydraulic parameters in jointed rock - their measurement and interpretation. Doctoral thesis, Faculty of Engineering, University of London.

Mälkki, E., 1978. On interpretation of groundwater flow velocity data obtained by using point dilution method. Proc. Second Nordic IHP Meeting. Hansaari Cultural Centre, Finland.

Norton, D. and Knapp, R., 1977. Transport phenomena in hydrothermal systems: The nature of porosity. Amer. Jour. Sci. 277.

Ogilvi, N.A., 1958. Electroliceskij metod opredelenija skorostej filtracii. Bjull, O N T I, Nr 4, Gosgeoltehizdat.

Smellie, J.A.T., Larsson, N., Wikberg, P. and Carlsson, L., 1985. Hydrochemical investigations in crystalline bedrock in relation to existing hydraulic conditions: Experience from SKB testsites in Sweden. SKB Tech. Rep. 85-11.

Smellie, J.A.T., Gustafsson, E., and Wikberg, P., 1987. Groundwater sampling during and subsequent to air-flush drilling: Hydrochemical investigations at depth in fractured crystalline rock. SKB Tech. Rep. 87-31.

Smellie, J.A.T. and Wikberg, P., 1989. Hydrochemical investigations at Finnsjön, Sweden, this volume.

Snow, D.T., 1968. Rock fracture spacings, openings and porosities. J. Soil Mech. Found. Div. Am. Soc. Civ. Eng., 94.

Tirén, S., 1989. Geological setting and deformation history of a low angle fracture zone at Finnsjön, Sweden, this volume.

TABLES

Table 1 Hydraulic fracture conductivity and flow porosity from tracer breakthrough in HFI01.

Flow regime	K_e (m/s)	$\emptyset_k$
Radial flow	1.5E-1	6.7E-3
Linear flow	3.4E-2	2.9E-2

Table 2A Hydraulic fracture conductivity and flow porosity including the effect of the radius of injection influence (r_e).

Flow regime	K_e (m/s)	$\emptyset_k$
Radial flow	1.3E-1	7.7E-3
Linear flow	2.9E-2	3.4E-2

Table 2B Hydraulic fracture conductivity and flow porosity including both the effect of injection and enhanced transport velocity in the vicinity of the withdrawal borehole

Flow regime	K_e (m/s)	$\emptyset_k$
Radial flow	7.2E-2	1.4E-2
Linear flow	1.7E-2	5.9E-2

Table 3A Pumping/sampling and injection sections.

Borehole	Section (m)	Distance* (m)	T** (m^2/s)	Remarks
BFI02	193 - 217	---	1.7 E-3	pumping/sampling
BFI01	239 - 250	168	1.3 E-3	injection
KFI06	202 - 227	189	5.6 E-4	injection
KFI11	217 - 240	155	3.7 E-4	injection

* Distance to the injection sections from the pumped section in BFI02.

** Calculated from single hole water injection tests in 2 m sections. According to the interpretation of the interference test 2, T = 1.5 E-3 m^2/s in this part of Zone 2.

Table 3B Estimated hydraulic parameters of the upper part of Zone 2 from the time-drawdown analysis of interference test 2 (Andersson et al.,1988).

Route	T (m^2/s)	S
BFI01 - BFI02	1.4E-3	9.4E-6
KFI06 - BFI02	1.4E-3	2.4E-6
KFI11 - BFI02	1.4E-3	5.7E-7

Table 4 Volumes of sections and pressure connection tubing.

Borehole	L (m)	Diam. (mm)	Volumes (litres) section	tubing	total
BFI02	24	158	450	880	1330
BFI01	11	168	234.5	11.3	245.8
KFI06	25	56	48.6	2.6	51.2
KFI11	23	56	43.4	2.8	46.2

Table 5 Tracers, concentrations and volumes injected.

Borehole	Tracer	Concentration (ppm)		Volumes (litres) tracer sol.	flushing
BFI01	Uranine	10.000		125	125
KFI06	Iodide	126.900	(1 M)	50	50
KFI11	Amino G Acid	20.000		50	50

Table 6 Tracer first arrivals, t, and mean transport times, t_o.

Route	Tracer	t (hours)	t_o* (hours)
BFI01 - BFI02	Uranine	20	35
KFI06 - BFI02	Iodide	8	16
KFI11 - BFI02	Amino G Acid	5	8

t_o* = time at peak concentration, t_p, (Gelhar, 1987).

Table 7 Drawdown (meters) in pumping and injection sections.

Borehole	Drawdown (m) versus time (h)							
	0.1	1.0	5.0	10.0	15.0	33.3	66.6	100
BFI02	4.9	5.6	6.8	7.7	8.4	9.7	10.6	11.0
BFI01	0.6	1.4	2.2	3.0	3.6	4.7	5.5	5.8
KFI06	1.0	1.6	2.8	3.7	4.3	5.6	6.4	6.9
KFI11	1.8	2.6	3.6	4.4	5.0	6.2	7.5	7.5

Table 8 Relative head differences, h, (meters) between the pumping section in borehole BFI02 and the injection sections in the surrounding boreholes.

Route	h (m) versus time (h)								steady
	0.1	1.0	5.0	10.0	15.0	33.3	66.6	100	state
BFI01 - BFI02	4.3	4.2	4.6	4.7	4.8	5.0	5.1	5.2	5.2
KFI06 - BFI02	3.9	4.0	4.0	4.0	4.1	4.1	4.2	4.1	4.1
KFI11 - BFI02	3.1	3.0	3.2	3.3	3.4	3.5	3.1	3.5	3.2

Table 9 Summary of parameters calculated from pulse injection of tracers during interference test 2.

Route	BFI01-BFI02	KFI06-BFI02	KFI11-BFI02
Distance (m)	168	189	155
K_e^r (m/s)	1.6 E-1	6.1 E-1	9.7 E-1
e (m)	5.1 E-4	9.9 E-4	1.2 E-3
$\emptyset_k$ (1m section)*	9.4 E-3	1.8 E-3	1.0 E-3
$\emptyset_k$ (1m section)**	8.8 E-3	2.3 E-3	1.4 E-3
a (m)	2.4	3.9	1.3
Pe ( )	70	49	118
Recovery (%)	68	81	70

* = K in Eqn (3) determined as mean value from Eqn (10)
** = K in Eqn (3) determined from hydraulic interference test 2

Table 10 Selected borehole sections for groundwater flow measurements.

Borehole	Section	K (m/s)	Remarks
HFI01	38- 40	7.2 E-5	Fracture zone in the shallow rock
"	108-110	3.8 E-5	Upper part of Zone 2
"	112-114	1.9 E-4	"
"	104-124	2.3 E-5	"
"	84-129	1.3 E-5	Upper part of Zone 2 and affected country rock above
BFI01	242-244	3.0 E-4	Upper part of Zone 2
"	244-246	3.4 E-4	"
"	264-266	1.1 E-6	Within Zone 2
"	352-354	1.7 E-5	Lower part of Zone 2
"	354-356	3.5 E-5	"
"	9- 50	8 E-6	Highly conductive shallow rock
"	50-230	3.1 E-8	Low conductive part between shallow rock and Zone 2

Table 11 Results of point dilution measurements in borehole BFI01.

Section (m)	K (m/s)	Q_w (ml/min)	Q_f ($m^3/m^2 \cdot yr$)	v_f^d (m/s)	v_f^d (m/d)	v_f^{g*} (m/s)
9- 50	8 E-6	381.2	14.2	4.5 E-7	0.039	0.4 E-7
50-230	3.1 E-8	7.9	0.07	2.2 E-9	0.0002	8.9 E-11
242-244	3.0 E-4	169.4	131.7	4.2 E-6	0.361	0.8 E-6
244-246	3.4 E-4	61.9	48.3	1.5 E-6	0.132	0.9 E-6
352-354	1.7 E-5	no measurable flow		<3 E-11		0.5 E-7
354-356	3.5 E-5	"		<3 E-11		0.9 E-7

* calculated with I=1/200 in the uppermost section and 1/350 in the other sections

Table 12 Results of point dilution measurements in borehole HFI01.

Section (m)	K (m/s)	Q_w (ml/min)	Q_f ($m^3/m^2 \cdot yr$)	v_f^d (m/s)	v_f^d (m/d)	v_f^{g*} (m/s)
38- 40	7.2 E-5	10.4	11.7	3.7 E-7	0.0320	4.8 E-7
108-110	3.8 E-5	0.2	0.3	9.6 E-9	0.0008	2.5 E-7
112-114	1.9 E-4	1.3	1.6	5.0 E-8	0.0043	1.3 E-6
104-124	2.3 E-5	106.4	13.3	4.2 E-7	0.0365	3.1 E-7

* calculated with I=1/150

FIGURES

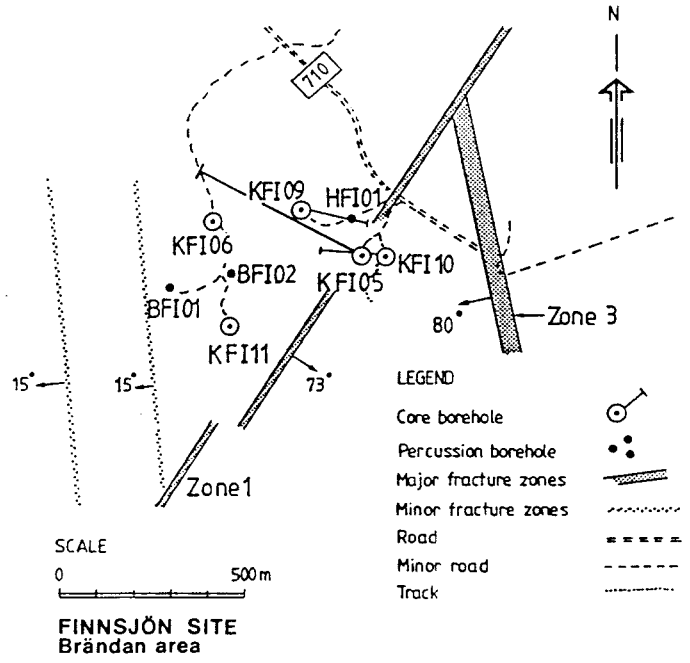

Figure 1 Map of the Finnsjön Site, Brändan area, showing borehole locations and fracture zones.

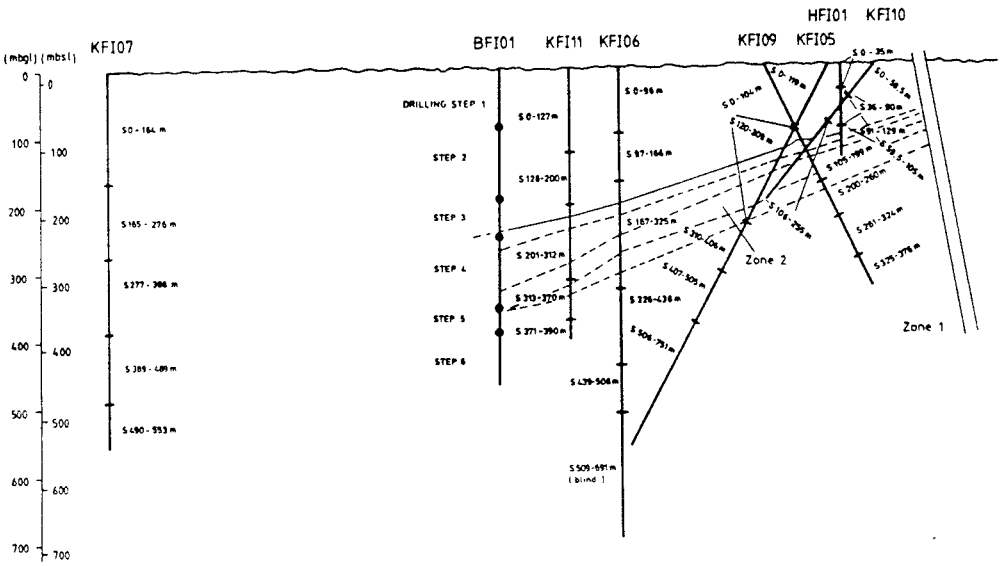

Figure 2 Packer configuration during the measurement of the undisturbed piezometric conditions and interference tests. The boreholes are projected into the profile.

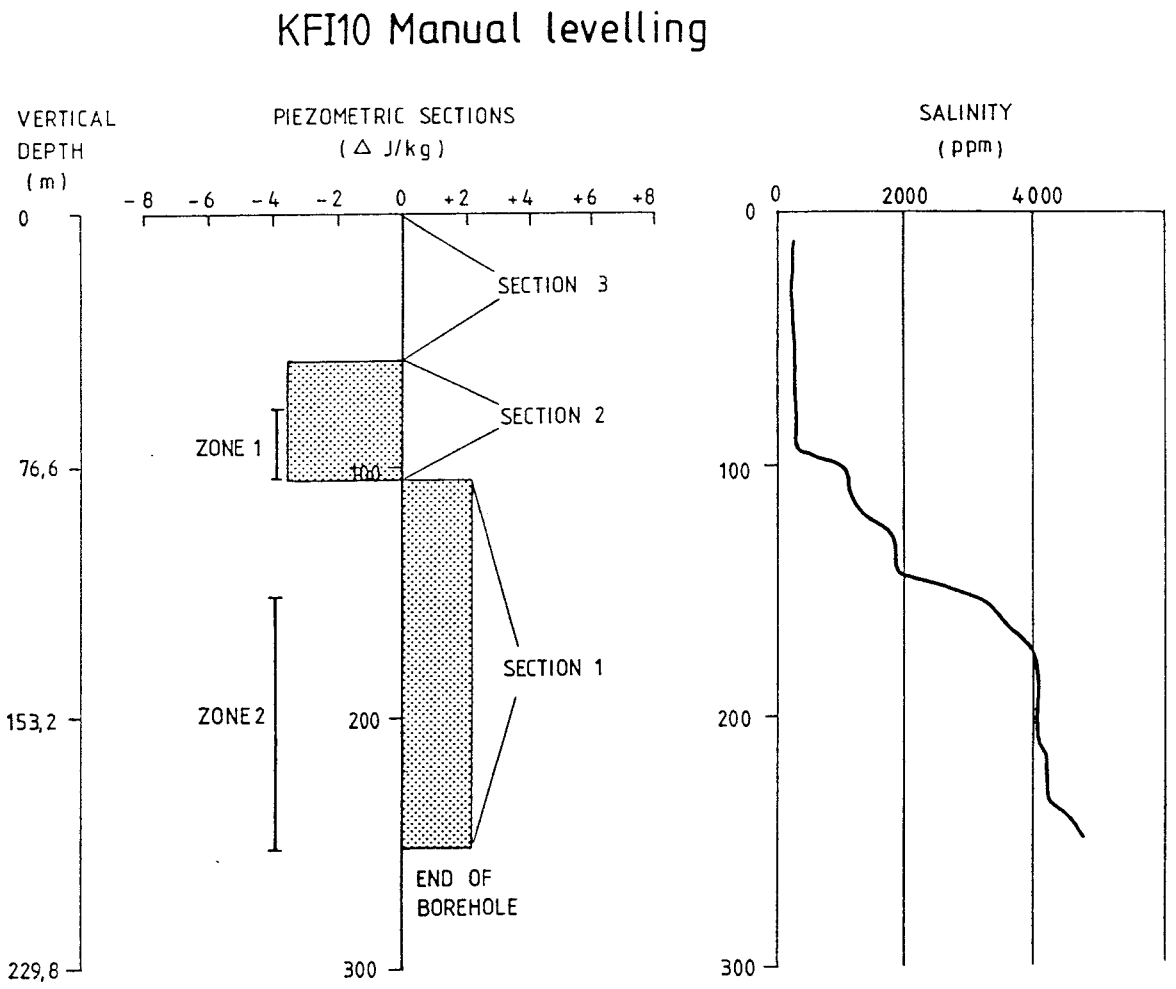

Figure 3 Vertical hydraulic head distribution in borehole KFI10.

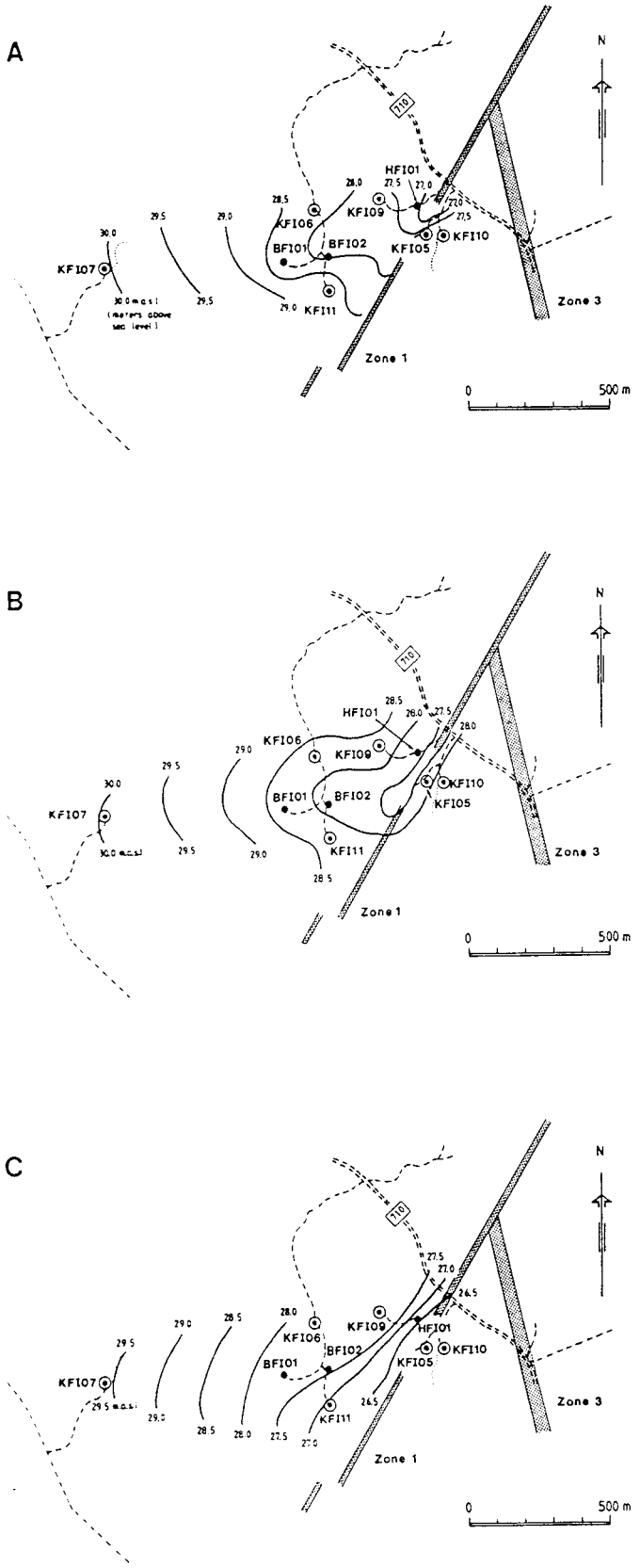

Figure 4 The groundwater head distribution in the Brändan area: A) superficially in the bedrock, B) in the upper part of Zone 2 and C) below Zone 2.

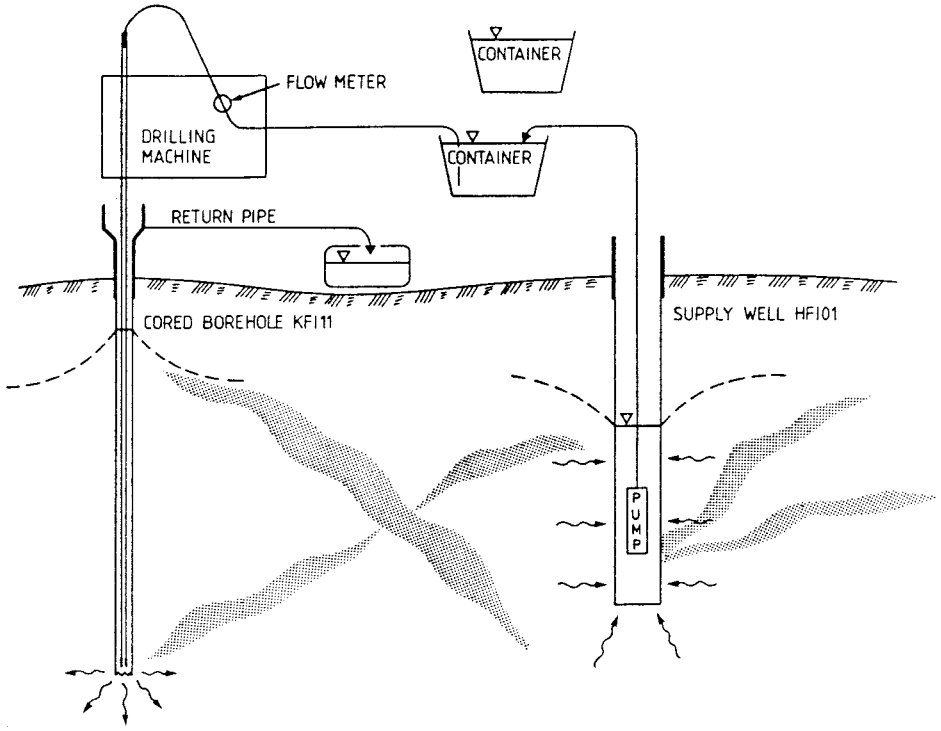

Figure 5 Schematic diagram showing the design of the drilling water tracer test.

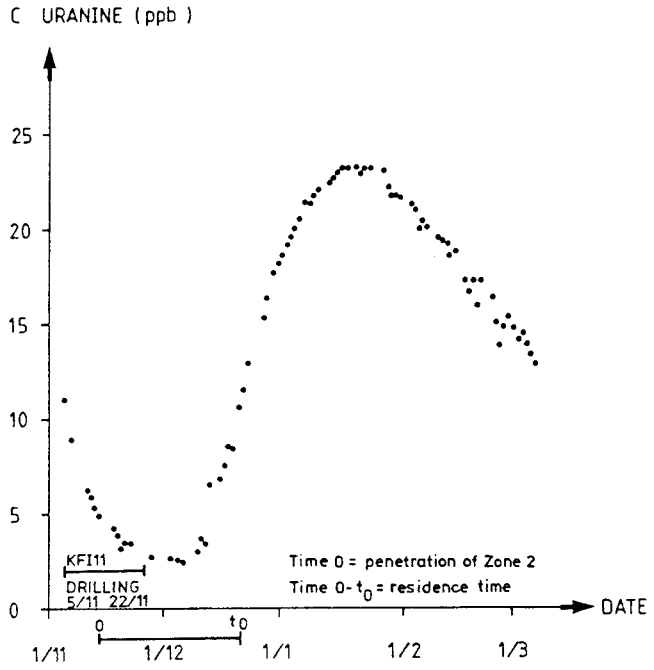

Figure 6 Breakthrough of Uranine in borehole HFI01.

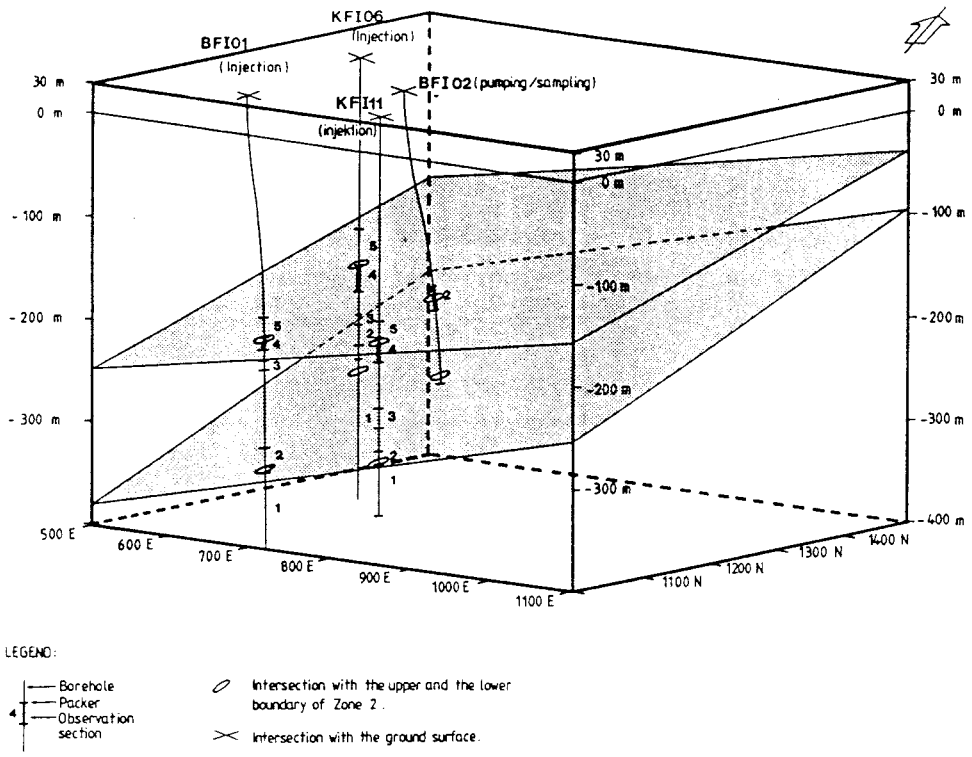

Figure 7 3-dimensional block diagram showing the positions of the boreholes used for the pulse injection of tracers in the interference test.

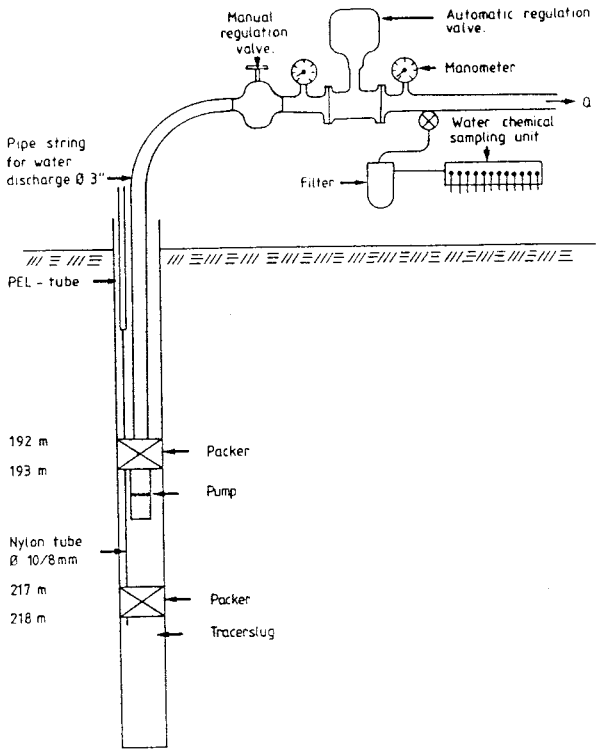

Figure 8 Packer configuration and equipment set up in borehole BFI02.

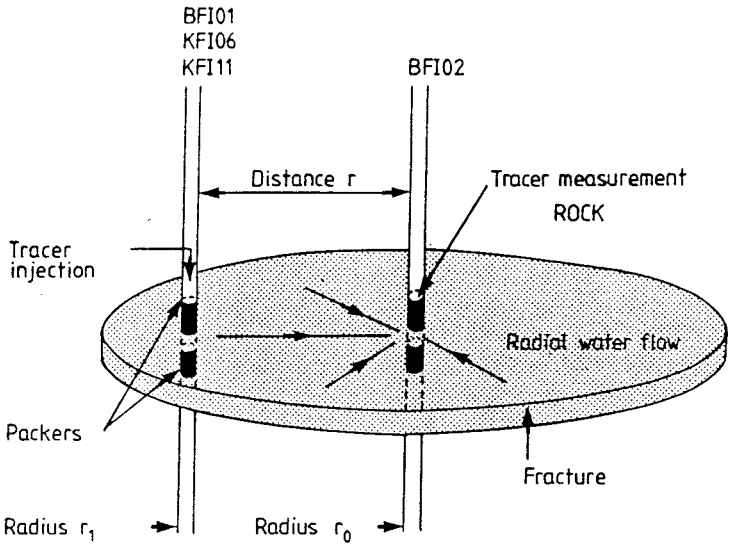

Figure 9 Conceptual model of the tracer tests.

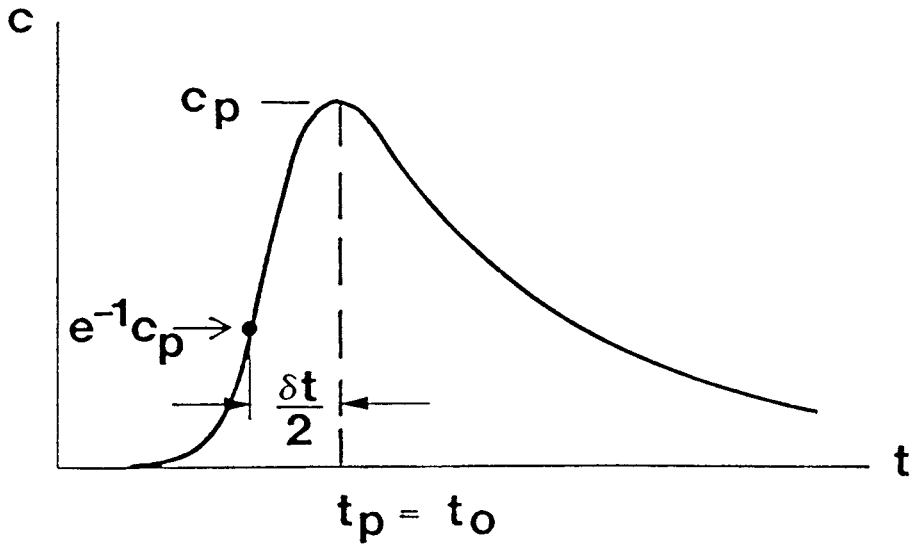

Figure 10 Schematic tracer breakthrough curve for convergent radial flow tracer test with pulse injection (Gelhar, 1987).

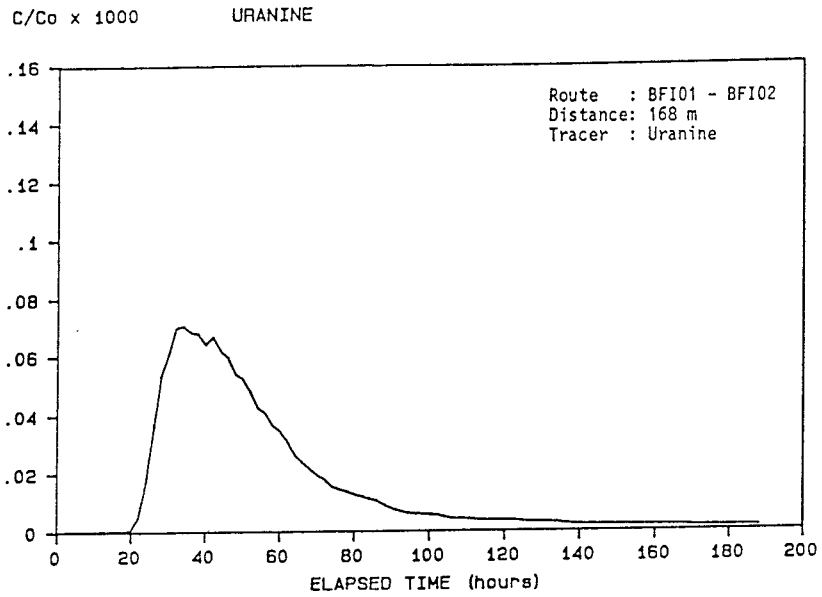

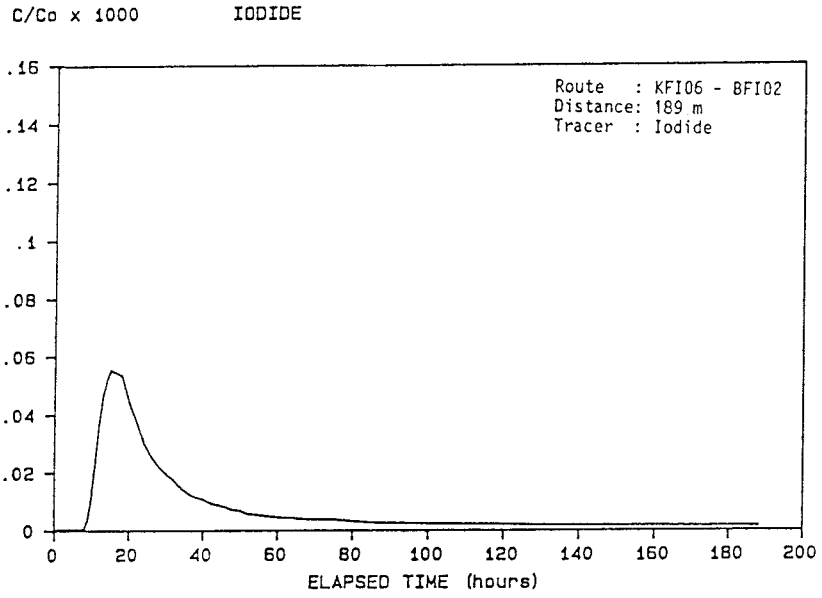

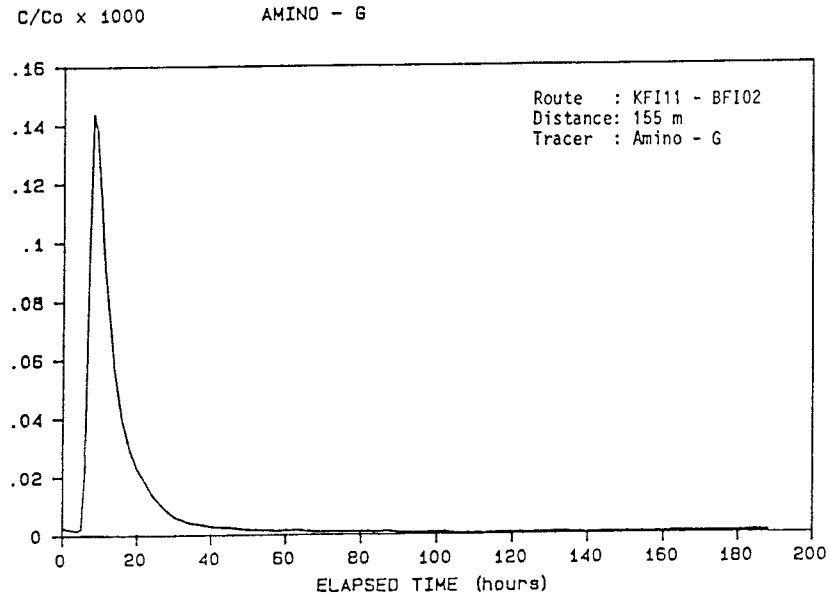

Figure 11 Breakthrough curves from pulse injections of tracers during interference test 2.

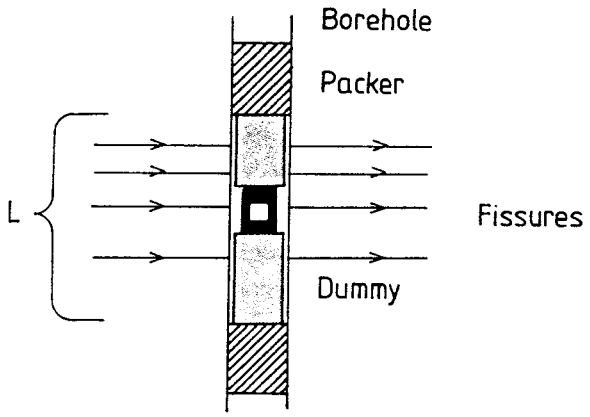

Figure 12 Schematic diagram showing the borehole test section straddling a fracture zone.

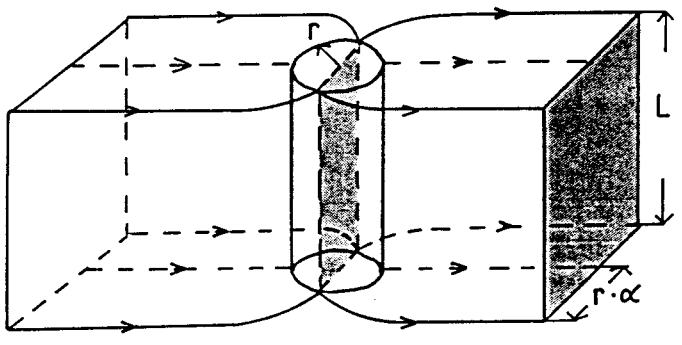

Figure 13 Schematic diagram showing flow lines converging and diverging in the vicinity of the borehole test section in the ideal case.

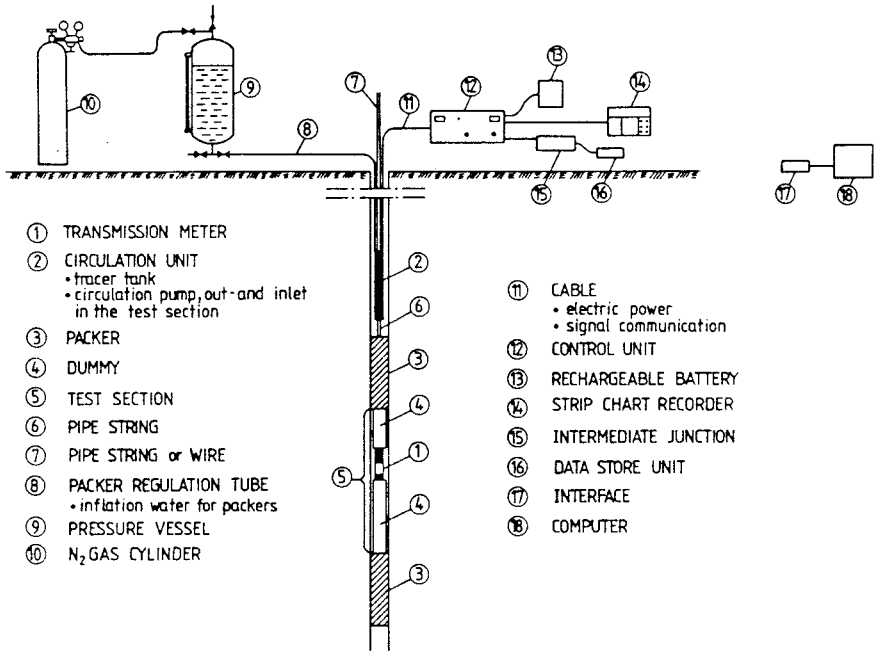

Figure 14 Borehole point dilution equipment.

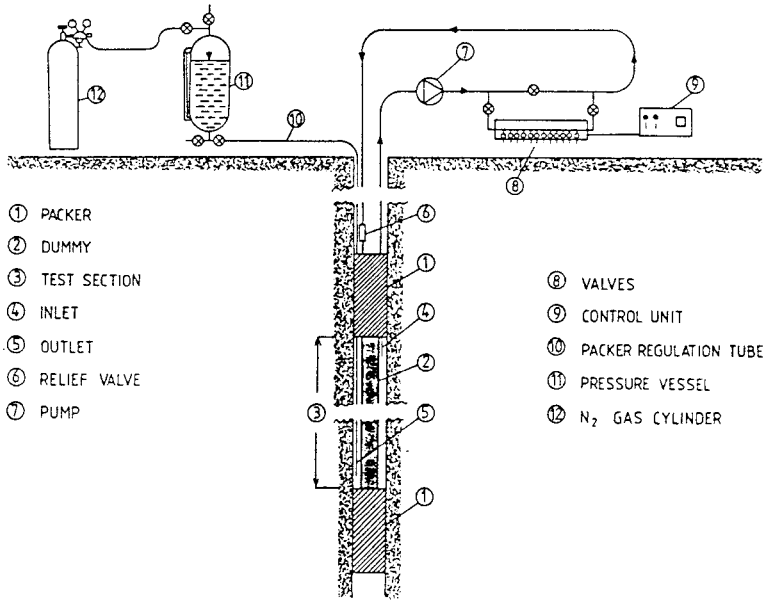

Figure 15 Surface sampling dilution equipment.

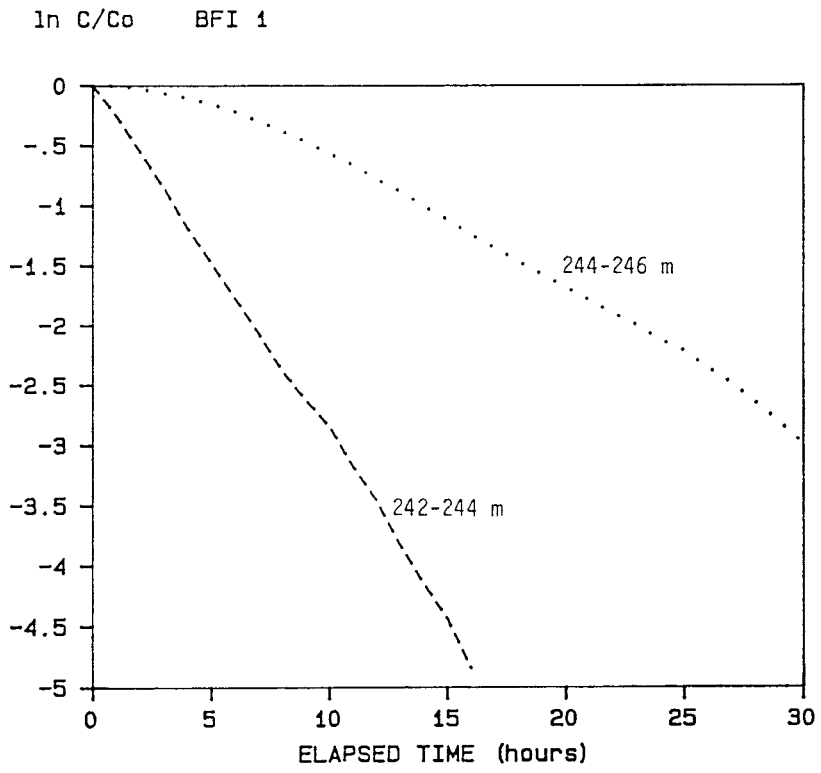

Figure 16 Dilution due to natural groundwater flow in packed-off sections of borehole BFI01.

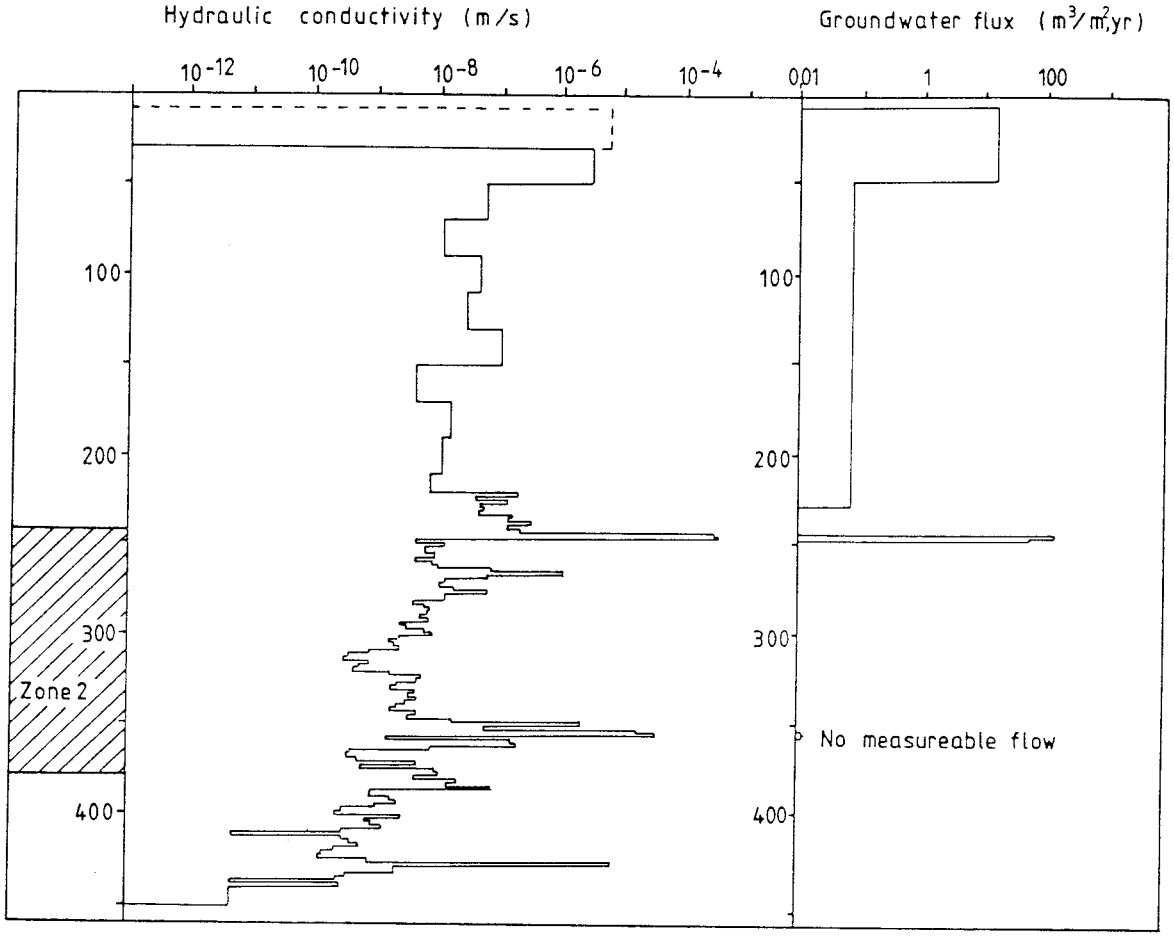

Figure 17 Results of point dilution measurements in borehole BFI01, compared with the hydraulic conductivity.

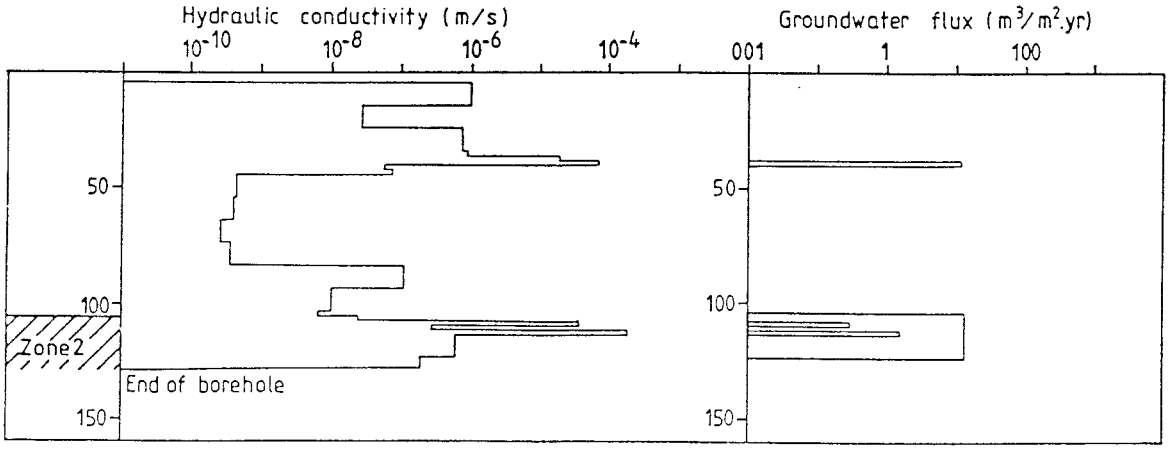

Figure 18 Results of point dilution measurements in borehole HFI01, compared with the hydraulic conductivity.

CHARACTERIZATION OF FRACTURE ZONE 2, FINNSJÖN STUDY-SITE

PART 5

HYDROCHEMICAL INVESTIGATIONS AT FINNSJÖN, SWEDEN

J.A.T. Smellie[1], P. Wikberg[2]

1 Swedish Geological Company, Uppsala, Sweden

2 Swedish Nuclear Fuel and Waste Management Company, Stockholm, Sweden

August 1989

HYDROCHEMICAL INVESTIGATIONS AT FINNSJÖN, SWEDEN.

J.A.T. SMELLIE and P. WIKBERG

Swedish Geological Company, Box 1424, 751 44 Uppsala (Sweden).
Swedish Nuclear Fuel and Waste Management Company, Box 5864,
102 48 Stockholm (Sweden)

Abstract.

Groundwaters collected from in and around a highly conductive low angle fractured zone in crystalline rock have been studied in relation to drilling and sampling methods, water quality, and the hydrogeochemical interpretation of the groundwaters.

Air-flush percussion drilling was demonstrated to be efficient down to 200-250 m; at greater depths, large amounts of drilling debris and increasing groundwater contamination from air dissolution become apparent. A stepwise drilling/sampling protocol using water-flush rotary drilling, in combination with water analysis carried out on site using a mobile laboratory, is recommended for future studies.

The chemistry of the Finnsjön groundwaters show a sharp contact between saline and non-saline compositions, this contact corresponding to a highly conductive low angle fracture zone (Zone 2. This zone is therefore a horizon along which groundwaters of contrasting age and chemistry come into contact and partially mix with one another. This mixing has produced a highly supersaturated water resulting in the precipitation of calcite. This is most evident in fractures within the more conductive, upper part of Zone 2, thus partly forming a seal between the two groundwater environments.

Comparison of the Finnsjön saline waters with other saline environments, particularly in the Fennoscandian Shield, has shown that the groundwaters are dominantly marine in origin, but with clear modifications resulting from water/rock interaction processes. Apparent radiocarbon ages range from 9 000-15 000 years in those waters recording below detection levels of tritium. These ages are considered too young and this is thought to have resulted from mainly carbon-14 dilution caused by groundwater mixing during the Holocene, when large quantities of glacial meltwater were available. This mixing process is also supported by the oxygen-18 data.

1. Introduction.

Hydrochemical investigations at the Finnsjön site have not just entailed the collection, analysis and interpretation of groundwaters from deep boreholes, but have also provided the opportunity to test and evaluate new drilling and sampling techniques which are new to the SKB (Swedish Nuclear Fuel and Waste Management Company) programme of site characterisation for radioactive waste disposal. Past experience has shown a serious lack of representative groundwater samples for hydrochemical consideration (Smellie et al, 1985). This lack of reliable data, whilst often due to technical problems or erroneous sampling from non-conductive sections of the boreholes, also illustrates the extremely complex geometry of the permeable fracture systems in crystalline bedrock, and thus the difficulty of establishing the nature and depth relation of the groundwater resevoir tapped.

Earlier studies (Smellie et al., op. cit.) have indicated that the greatest disturbances to groundwater quality are caused by:

* borehole drilling
* gas-lift pumping
* hydraulic injection tests
* water sampling
* open-hole effects
* drilling debris

To improve the quality of groundwater sampling Smellie et al. (1985) recommended air-flush percussion rotary drilling techniques. This could effectively avoid contamination of the hydro-environment normally caused by the flushing water medium during rotary drilling. If the air-flush technique is combined with a stepwise/drilling protocol, there would be the advantage of: 1) locating fairly precisely the intersection depth of the hydraulically conductive horizons, 2) obtaining representative groundwaters for the level sampled, free of contamination from any hydraulic connection with a deeper, water-filled borehole section, and 3) avoiding groundwater contamination from any long-term open-hole effects. Furthermore, confirmation of the various conductive zones for sampling purposes can be indicated by borehole geophysical methods which include radar and tubewave techniques, thus avoiding the introduction of possible contaminating water during hydraulic injection testing of the borehole (Stenberg and Olsson, 1985; Stenberg, 1986; Ahlbom et al., 1986). Such tests can be conducted subsequent to drilling and sampling.

Investigations of fracture zones at the Finnsjön study site provided the opportunity to test these air-flush techniques as an intregral part of the hydrochemical programme. During

preliminary studies of the area (Ahlbom et al., 1986) groundwater sampling was carried out during the drilling of a shallow (130 m) air-flush percussion hole, drilled to provide a source of water-flushing for the rotary core drilling programme. Sampling was crude and entailed collecting water when a conducting horizon was breached. Contamination was unavoidably present (seen as abnormal amounts of aluminum, silica and iron), but the results were promising in that the structural contact between saline and non-saline groundwater could be fairly well defined at around 100 m depth. The importance of this was subsequently realised when it was impossible to collect non-saline water from depths greater than 50 m from the same hole, due to the excess hydraulic head below the non-saline/saline contact zone.

Following these preliminary studies, a major programme was started in the Finnsjön area and this included provision for an air-flush hole solely for hydrochemical purposes.

The general geological, geophysical and hydrological characteristics of the Finnsjön site area are summarised by Ahlbom et al. (1986) and described in detail by Tiren and Andersson et al. (this volume). Earlier tectonic studies in the area (Ahlbom et al., 1986) defined and characterised three major fracture zones, Zones 1-3, two of which have been studied in detail (Fig. 1). The Brändan fracture zone (Zone 1; width of about 20 m and striking NNE with a dip of 75 degrees to the east) is topographically expressed as a minor gully traceable for more than 500 m, and from surface geophysical measurements to extend for at least 1 km, and a low angle fracture zone (Zone 2; trending north with a dip of 16 degrees to the west) defined only from borehole data.

As outlined by Ahlbom (this volume) this present phase of study in the Finnsjön area has entailed the drilling of two cored boreholes and one percussion borehole to further characterise Zone 2. All borehole locations, in relation to the major fracture zones, are illustrated in Figure 1. The air-flush hydrochemical borehole was positioned to complement studies in the main investigation area, in addition to ensuring its value in trying to obtain representative and uncontaminated groundwater samples.

This paper sets out to summarise the hydrochemical investigations carried out in the Finnsjön region during the initial stages of the SKB site characterisation programme from 1977-1982 (Hultberg et al., 1981; Laurent, 1982), and more recently within the present fracture zone project (Ahlbom et al., 1986; Smellie et al., 1987). As normal water-flush rotary drilling techniques have been widely employed, in conjunction with a single test hydrochemical hole using the air-flush percussion method, the hydrochemistry of the Finnsjön

groundwaters will be discussed in terms of: 1) quality of the sampled waters in relation to normal borehole activities, 2) the influence of air-flush percussion drilling on groundwater quality, and 3) the chemical evolution of the Finnsjön groundwaters in and around fracture Zone 2. Particular emphasis has been given to redox-sensitive parameters such as Eh and pS, environmental isotopes such as H-2, H-3, O-18, C-14, and the chemical and radiochemical behaviour of uranium.

2. Hydrochemical Borehole Location: Geological and Hydrological Considerations.

The location of the air-flush percussion hydrochemical hole in relation to the main investigation site (i.e. 200-250 m distant and positioned to intercept Zone 2 at a depth of 240 m) was based on several hydrogeological criteria. To avoid groundwater contamination from both earlier and recent drilling activities at the main site, it was important that any resulting hydrochemical data would relate to, and serve as a valuable complement, to the main investigations. To accomplish this, it was necessary to ensure a similar hydrogeological environment for extrapolation purposes. This specifically related to: 1) intersection at a predictable depth of Zone 2 which is known to represent a structural boundary between saline and non-saline groundwater, 2) to test this zone for any hydraulic response between the hydrochemical hole and the main site, and 3) to place the hole up-flow from the main site. Geological extrapolation has been facilitated by placing the hydrochemical hole within the same "tectonic block" as the main site. Such siting is important because any extrapolation between these units is likely to be complicated by inter-block transitions. Furthermore, other adjoining blocks are often characterised by different structural signatures and geology.

Figure 2 illustrates the chosen location of the percussion-borehole (BFI01) relative to estimates of total groundwater contamination relating to water loss along Zone 2 as a result of earlier borehole activities in the area. For example, borehole KFI11 recorded a total loss of 72 m3 of fluid during drilling, of which 7 m3 was lost from the bedrock surface down to Zone 2, and 65 m3 from Zone 2 to the hole bottom, most being lost along the fracture zone. Furthermore, additional fluid was introduced during the hydraulic injection tests. Thus, assuming the horizontal fracture zone to be 75 m wide, and using porosity values of 1 x 10-4 and 1 x 10-5 respectively (derived from tracer tests in the same area reported by Gustafsson and Klockars, 1981 and Ahlbom et al., 1987), contamination radii of 52 m and 165 m were indicated (Fig. 2). As a further assurance against groundwater contamination from earlier drilling

activities, and based on piezometric and hydraulic conductivity data from existing boreholes, the hole was placed up-flow from the main investigation site. The final position of the hole, although theoretically within the influence of one of the contamination estimates, was considered in practice to be suitable. A tentative groundwater flow model along a transverse section during unperturbed conditions is illustrated in Figure 3.

3. Water Quality, Sampling and Analysis.

3.1. Water quality.

The quality of groundwater chemical data depends on the quality of the groundwater sampled for analysis. Normal borehole drilling, testing and sampling methods can potentially result in groundwater contamination (Ask and Carlsson, 1984; Smellie et al., 1985). These sources include borehole drilling, gas-lift pumping, hydraulic injection tests, water sampling, open-hole effects and drilling debris. In common with earlier studies in the region, water-flush rotary drilling has been used for all drillholes comprising this present phase with the one exception of the air-flush percussion hydrochemical borehole. By experimenting with this air-flush technique, it was hoped to minimise some of the contaminating influences normally accompanying water-flush methods.

Under normal air-flush percussion drilling conditions, i.e. down to 250 m with the booster system, the penetration rate is steady and the air-flush system is efficient in removing the accumulating rock debris and borehole water. At greater depths an increase in pressure will tend to accumulate around the drillhead resulting in considerable volumes of oxygenated groundwater being flushed through the rock along breached zones of high conductivity. High positive Eh values, high uranium concentrations and low ferrous iron contents measured in groundwaters sampled from the highly conductive Zone 2 (see below) support the reality of such contamination.

The extent of drilling debris as a potential groundwater contaminant is largely unknown. It is highly plausible that the introduction of such debris during drilling can help to seal small-scale hydraulic fractures thus restricting access to certain groundwater sources. In addition, the presence of very fine debris particles in the groundwater sampled for hydrochemical characterisation can influence studies of colloids, and affect the contents of uranium (and iron if present in sufficiently small quantity) ionic complexes which may become preferentially bound to these particles and subsequently removed on filtration. Earlier reported studies

from Finnsjön (Ahlbom et al., 1986) showed that even after flushing one of the holes twice, an estimated 5 kg of rock debris was recovered out of a calculated total of 1000 kg for a 376 m long hole of diameter 56mm. Present studies (Andersson et al., this volume) showed that the amount of rock debris recovered during air-flush drilling decreased markedly with depth from 86.5 % down to 85 m, to 41.4 % down to 459 m; at approx. 250 m, which is considered to be the threshold for efficient air-flush drilling in this particular case, the recovery was 70 %. A total of about 8400 kg of debris has been calculated to have been forced into the fracture systems intercepted by the borehole, especially at depth.

The effect of rock debris on groundwater quality and sampling is not well known. Some monitoring has been carried out at Fjällveden, another test site area located just south-west of Stockholm. This showed that although the groundwater quickly became clear after commencement of pumping and a uniform particle content was soon achieved (0.01 - 0.10 mg/l), the dominant particle composition (i.e. Al, Si and Ca; Fe was sometimes also present) still suggesed the presence of drilling debris. This shows that fine debris particles introduced into and along certain hydraulic fracture zones are only partly removed during the initial surge of groundwater taken from the zone after pumping has begun. Even though the system soon stabilises and the particle content drops off, any small fluctuation in groundwater flow, for example variation in pump flow-rate during sampling, would probably reactivate particle removal. No specific studies were carried out at Finnsjön to further quantify this problem.

Groundwater contamination occurs in open boreholes by short-circuiting mechanisms occurring between the borehole and conductive horizons at different levels. Positive or negative piezometric head values of the individual horizons play an important role. Extrapolation of hydraulic measurements from the main investigation area indicate that those conductive horizons above and below Zone 2 are characterised by positive piezometric head values, and Zone 2 by negative values. Open-hole effects should therefore result in borehole water entering and contaminating Zone 2.

In order to minimise this problem a step-wise drilling/sampling method was adopted ensuring that at no juncture was any borehole length left open for long periods of time. When drilling was stopped at a suitably conducting zone, the downhole equipment was speedily installed, and the sampled groundwater analysed on site by the mobile laboratory. The groundwater analyses (see below) showed that minimal contamination resulted from open-hole effects, although short-circuiting from some of the sampled sections in the borehole

via fracture networks to deeper, more saline groundwater horizons in the bedrock, had occurred.

3.2. Sampling.

A drilling/sampling protocol was used for the air-flush percussion borehole. This differed from the main investigation site where borehole drilling by water-flush techniques was completed prior to sampling. In both cases the basic sampling and analytical equipment used was similar (Almen et al., 1986; Axelsen et al., 1986).

Essentially the groundwater is pumped up from chosen water-conducting sections in the bedrock sealed-off by inflatable rubber packers with an adjustable straddle length. A hydraulically operated piston pump is placed in connection to the packers giving a maximum flow of about 250 ml/min. It has the capacity of reducing the pressure within the sampled section by more than 1 MPa. For the main site investigations the Eh, pH, pS and pO2 values were monitored as the water passed through a flow-through cell located in the mobile laboratory at the bedrock surface. For the hydrochemical borehole investigations additional downhole measurements of Eh, pH and pS were carried out.

Following the installation of packers and downhole equipment in the borehole the pump is started and the capacity adjusted to give as high a water flow as possible without exceeding a pressure draw down of 0.5 MPa (= 50 mwc). Pumping is continued until a stable water composition is achieved, normally when the Eh values stabilise, on average after at least two days. When stability is achieved, it is often the continuous change in composition of the main constituents that determines the length of the ensuing sampling period.

The groundwater pumped up into the mobile laboratory passes through a 0.45 micron in line filter before it is collected for analysis. In special cases the water is filtered through membrane filters placed in series with 0.45, 0.2 and 0.05 micron pore sizes. The particle fractions collected on these filters are analysed for Fe, Al, Mn, S, Ca, Mg and Si. The filtrate is analysed for total and ferrous iron.

The sample volumes needed for the main constituent analyses are 1 litre untreated and 1 litre acidified by hydrochloric acid. The sample for sulphide analysis has to be collected in a 150 ml glass bottle with a ground glass stopper; preservation is by sodium hydroxide and zinc acetate. A 10 litre acidified sample is needed for the uranium, radium and radon analyses; tritium and the stable isotopes oxygen-18 and deuterium require 1 litre and 100 ml sample volumes respectively. Sample

collection for radiocarbon is less straight forward. Here the carbonate content of 130 litres of water is required to be reduced to a volume of of 1 litre by acidifying the water with hydrochloric acid, expelling the CO2 by nitrogen, and trapping it in a bottle containing sodium hydroxide through which the gas passes. However, if a tandem accelerator is available for analysis, pre-concentration is not necessary.

3.3. Analysis.

For the analysis of deep groundwaters great care has to be taken to avoid changing redox conditions during sampling and analysis. The elements analysed are those considered most important for the safety assessment of a nuclear waste repository. The main constituents, Na, K, Ca, Mg, Cl, HCO3 and SO4 indicate the groundwater residence time in the rock by showing the extent of the rock/water interaction.

The anions of this group are potential complexing agents and thus important for the calculation of waste canister corrosion, dissolution and transport of the nuclides comprising the waste. F, Br, PO4 and SiO2 are useful for identifying the origin of the water and the state of equilibrium. Fe(II), Fe(tot) and S(-II) are primarily analysed in order to describe the redox conditions and thus to support the Eh measurements. They also give information on the buffer capacity of the water.

In the field laboratory the contents of the main constituents and redox-sensitive elements are continuously analysed to achieve an immediate feed-back of the groundwater composition and stability. This allows the investigation to be constantly modified during sampling and analysis. Furthermore, this system enables the redox-sensitive elements to be analysed immediately without atmospheric contamination.

The field analyses are carried out using an ion chromatograph, by spectrophotometry, and by titration. Uranium, radium and radon are determined by neutron activation; alpha spectrometry is also used to determine uranium and the 234U/238U activity ratios. Tritium and the stable isotopes oxygen-18 and deuterium are analysed by natural decay counting and mass spectrometric methods respectively.

4. The Chemistry of the Finnsjön Groundwaters.

Groundwater chemical data at this site date back to 1977/82 when Finnsjön represented one of several areas selected for systematic study as part of a regional assessment of potential

repository bedrock environments for spent nuclear fuel (see Ahlbom; this volume). Additional groundwater data resulted from a pilot study of the fracture zone initiated in 1985, and from the present major phase of study carried out between 1986-1987. During this 10 year period a continuous appraisal of groundwater quality and sampling criteria has resulted in increasingly more reliable data becoming available for evaluation. In this respect, present emphasis has been given to those data most recently collected.

4.1. Previous hydrochemical studies.

During initial site investigations (1977-1982) a total of eight boreholes were sampled for groundwater characterisation (i.e. boreholes KFI01-KFI08; Fig. 1). These results are presented by Hultberg et al. (1981) and Laurent (1982). The chemical parameters have been discussed by Allard et al. (1983) and the geochemical association between the groundwater and fracture minerals by Tullborg and Larson (1982).

Not all data are available; for example, no Eh measurements were carried out. In general, however, the results distinguish two major types of groundwater: saline and non-saline, with the former usually increasing in extent with depth. The groundwater chemistries appear to emphasise saline groundwaters from three of the boreholes (KFI05, 6 and 8; Fig. 1) whereupon chloride concentrations ranged from 2500-5900 mg/l. Low, to below detection levels of tritium (7 to less than 3TU), coupled to old apparent radiocarbon ages (ca. 5500-10 000 years), also typify these saline waters thus establishing them as fairly representative and free from major contamination (i.e. from near-surface fresh water and drilling fluid). In contrast, KFI04 and KFI07 exhibit higher tritium (3-14 TU) and younger radiocarbon apparent ages (ca. 4000-6000 years) which, together with smaller concentrations of chloride (approx. 30-650 mg/l), indicate varying degrees of contamination or natural mixing from other sources. The two boreholes which would appear to represent non-saline water (KFI01 and KFI02) are characterised by high to very high tritium (38-50 TU) and correspondingly low radiocarbon apparent ages (ca. 2000-4000 years). These waters are thus highly contaminated by surface to near-surface derived water and not representative for the measured holes.

These waters show, therefore, that although the salinity of boreholes KFI05, KFI07 and KFI08 is beyond dispute, the remaining holes which are non-saline to weakly saline in character, may in fact prove to be more saline than originally suspected. In some respects it was therefore surprising that recent borehole logging (1985) supported the reported groundwater salinities. However, as pointed out by Gustafsson and Andersson (this volume), differences in hydraulic head

between the adjacent rocks and the low angle fracture Zone 2 can in some cases (i.e. at shallow levels) result in an upward discharge of salt water from this zone, whilst in other cases (i.e. at deeper levels) there is a recharge of fresh water down into the zone. Open boreholes would be particularly sensitive to such effects and this would account for much of the variation in salinity reported by the logging measurements.

These earlier investigations also presented trace element analyses for several of the boreholes (KFI01, KFI04, KFI05 and KFI07). Interestingly the most saline borehole (KFI05) also showed appreciable amounts of lithium and boron. Such enrichments, together with chloride, have been considered to indicate rock/water interaction processes over long periods of time (Edmunds et al., 1985).

4.2. Recent hydrochemical studies.

4.2.1. Chemical and isotopic character of the groundwaters.

The chemistry of the groundwaters resulting from recent studies (1985-1987) are summarised in Table 1 and illustrated in Figure 4. Surface recharge waters for the Finnsjön area are moderately acidic (e.g. pH 5.9), of low conductivity (e.g. 4.12 mSm), and contain only small amounts of dissolved ions. The tritium (e.g. 31+/-2 TU) and stable isotope (e.g. D = -80.5 ppt; O18 = -12.1 ppt) contents are usual for recharge meteoric waters in this part of Sweden (Saxena, 1984).

Vertical trends in groundwater chemistry from boreholes KFI09 and BFI01 (Fig. 4) show the clear distinction between the non-saline (calcium-bicarbonate type) and saline waters via a transition zone of mixing (i.e. Zone 2). This is readily indicated by the conductivity values. The pH, in contrast, shows a perceptible decrease with depth from just above Zone 2, which is contrary to that normally indicated by Swedish groundwaters at increasing depths.

Of the cations, Ca^{2+}, Na^{+} and Mg^{2+} show marked increases with depth; K^{+} is less emphasised. Of the anions, HCO_3^{-} typically decreases with depth accompanied by sympathetic increases of Cl^{-} and SO_4^{2-}; increases in Br^{-}, I^{-} and F^{-} (not plotted) are also present.

The stable isotope data show very little variation with depth and can be considered to be meteoric in origin. Radioisotope data, i.e. percentage modern carbon and tritium contents, clearly indicate the extent of the young, near-surface derived fresh water component (down to ca. 100 m depth) characterised by high amounts of modern-derived carbon (e.g. 85.30%

representing an apparent age of less than 2000 years) and significant tritium contents (8-36 TU). With increasing depth and salinity the groundwaters rapidly exhibit a reduction in modern-derived carbon (e.g. 22.60-37.45%) with minimae at the lower horizons of Zone 2 (i.e. apparent ages greater than 12 000 years). At these depths no significant tritium has been detected.

From borehole locations KFI09 to BFI01, i.e. a distance of approx. 830 m in a northwest direction, Zone 2 gently descends from a depth of 134-205 m at KFI09 to 234-353 m at BFI01. By comparing the data in Figure 4 there is some evidence that the salinity below Zone 2 increases. This is most readily seen by the conductivity values which reflect small increases in Na, Mg and Cl. Ca, K and HCO3 remain constant and SO4 shows a significant decrease. Above Zone 2, within the non-saline groundwaters, some differences are also observed. At borehole KFI09 the demarcation between non-saline and saline groundwater at the Zone 2 contact is sharp, whilst at BFI01 the transition is less distinct. This is believed to have resulted from an incursion of more saline water from depth via conducting fractures during pumping for sampling purposes.

4.2.2. Redox character of the groundwaters.

The redox conditions of the groundwaters are best defined by the Eh and the contents of ferrous iron, uranium and dissolved oxygen. Each of these parameters are individual signatures for the prevailing conditions. Oxidising groundwater conditions are characterised by dissolved oxygen, high uranium, positive Eh and low ferrous iron concentrations. Reducing conditions by an absence of oxygen, negative Eh, low uranium and high ferrous iron. Intermediate conditions are defined by no oxygen, zero Eh values and appreciable uranium and ferrous iron concentrations.

Table 2 compares the redox-sensitive parameters from the air-flush percussion borehole (BFI01) with those from the water-flush rotary borehole (KFI09) at different depths; Zone 2 is intercepted at a shallower depth by KFI09.

The most striking feature is the highly oxidising character of the groundwaters sampled from Zone 2 in borehole BFI01 compared with borehole KFI09. This is attributed to perturbations during drilling when air at high pressure was forced along the conductive fissure systems comprising Zone 2. Although a negative result from a contamination viewpoint, it is interesting to note the extent that the uranium concentrations have increased during the relatively short time period when air has affected the redox conditions (i.e. 2-6 weeks). For borehole BFI01 the Eh versus pH is plotted on a uranium stability diagram (Fig. 5). The three uppermost levels which

have not been perturbed by air intrusion plot close to the region where amorphous dioxide is the dominating solid uranium phase. Therefore the concentration of dissolved uranium is expected to be rather low. The Eh-pH relation for the perturbed borehole sections all plot in the area where uranium (V1) dominates. This is in good agreement with the artificially induced high uranium concentrations of these waters. So far no calculations have been made to utilise the data on uranium in Table 2.

The Fe(II)/Fe(tot) ratio has also been influenced varying from near unity above Zone 2 to 0.3 to 0.5 within and below the zone.

Borehole KFI09 provides a more normal situation with negative Eh readings, low uranium contents and higher activity ratio values characterising the deeper, older saline groundwaters. The iron oxidation ratios are variable due to some minor drilling water contamination.

It is worth noting here that not only are the redox conditions affected by the incursion of air into the groundwater system. A close look at the pH values show a significant reduction of pH at those levels of artificially induced high uranium content (pH 6.6 to 6.9) when compared to the other undisturbed deep levels in both BFI01 and KFI09 (pH 7.1 to 7.7). This is believed to be due to increased dissolution of carbon dioxide during percussion drilling.

4.2.3. Groundwater flow.

Using available hydrochemical data a simplistic groundwater flow model can be created in the near-vicinity of the two sampled boreholes. As indicated above, the upper (100 m) part of the rock is characterised by groundwater of calcium-bicarbonate type which has a fairly short residence time. The presence of sodium and chloride, however, shows that some water (containing ca. 1% saline water from below Zone 2) has been transported from lower levels. For example, in borehole BFI01, the sampling at 169 m shows an increase in the salinity of the water during the sampling period, confirming the possibility of conducting channels transporting saline water. A later tritium analysis than presented in Table 1 gave a value of less than 3 TU which further confirms the assumption that the groundwater sampled in this section was pumped up from deeper levels and therefore more ancient in origin. Under unperturbed conditions the sodium and chloride concentrations at this level would probably be much lower.

Within the upper part of Zone 2 the salinity increases drastically. The composition is constant throughout the

sampling period indicating that the mixing is not artifically produced by pumping. This upper part could therefore be considered as a "sump" whereupon saline water from below Zone 2 is mixed with non-saline water from above the zone. Interestingly, the mixed water in the upper part of Zone 2 has a similarly high carbonate content as the non-saline water. This implies the water has been subject to carbon dioxide diffusion after mixing with the saline water. It is not possible to decide exactly how this process has occurred; it is however obvious that the process is continuous or that it has occurred during a long period of time. Below Zone 2 the water has a constant composition which indicates that there is very little, if any, flow. This is supported by the moderate to high 234U/238U activity ratios (3-5) recorded from borehole BFI09 (Table 1) which suggest long residence times enabling a build-up of recoil-loss 234U at the rock/water interfaces.

The presence of Zone 2 thus appears to represent a structural/hydraulic boundary to the bedrock groundwater cells of circulatory movement. As a result, the downward moving non-saline water preferentially spreads out along the upper, more conductive levels of Zone 2, rather than continue to deeper levels to mix with the older saline waters. Similarly, the more sluggish upward moving saline water will do likewise. Zone 2 is therefore a horizon along which groundwaters of considerably contrasting age and chemistry come into contact and partially mix with one another.

4.2.4. Equilibrium modelling of the groundwaters.

The computer code PHREEQE has been used for groundwater modelling (Laaksoharju, 1988, written comm.). The computation of the saturation index with respect to calcite is illustrated for borehole BFI01 in Figure 6. This shows an index variation ranging from -1 to +0.5 logarithmic units. The undersaturation in the uppermost sampled section (i.e. 71-84 m) can be explained by the short residence time of the non-saline groundwaters; this, however, does not explain the undersaturation computed for the deeper sections (i.e. 284-460 m). It could be the result of drilling activities as these deeper sections tend to have low hydraulic conductivities coupled with high uranium concentrations in the sampled waters (see section 4.2.2.).

Another influencing factor are the pH values of these deeper waters which appear to be somewhat low (Table 2). It is suggested that during the percussion drilling there is an enhanced carbon dioxide concentration in the compressed air due to combustion. This results in the downhole dissolution of carbon dioxide in the groundwaters resulting in a significantly

lower pH than in the unperturbed situation. The pH values should be about half a pH unit higher.

The highest saturation index is obtained from water sampled from the upper part of Zone 2. This water has a chloride concentration of 1500 mg/l, i.e. it is diluted by a factor of three to four compared to the saline water below the zone. The supersaturation of 0.5 logarithmic units indicates that calcite is precipitating in this part of the fracture system. With time, precipitation will effectively help to seal off the upper non-saline water rockmass from the saline rockmass below.

Nordstrom and Puigdomenech (1987) using data from earlier groundwater analyses from Finnsjön have shown how the mixing of non-saline and saline water has resulted in a highly supersaturated water even though the initial starting waters are at equilibrium with respect to calcite. A similar mixing calculation is reported here from borehole KFI09 (BFI01 was not considered because of the above-mentioned perturbances) and the results are presented in Figure 7. The plotted data illustrates the fact that even though the end member waters are undersaturated, the resulting mixtures are supersaturated by a factor of 0.5 logarithmic units.

5.1. Evolution of the Finnsjön groundwaters.

The presence of deep saline waters in crystalline basement rocks is not uncommon. Occurrences have been documented from the Canadian and Fennoscandian Shield areas, and from the Carnmenellis granite in S.W. England (see Fritz and Frape, 1982; Hyyppä, 1984; Edmunds et al., 1985; Nordstrom, 1986; Ahlbom et al., 1986, Kankainen, 1986; Frape and Fritz, 1987; Puigdomenech and Nordstrom, 1987; Nurmi et al., 1988). The salinity of these waters have been attributed to one or more processes which include: a) relict ancient marine water, b) residual igneous/metamorphic fluids, c) rock/water interactions, and d) release of fluids during the mechanical rupture of fluid inclusions.

A recent study of Finnish saline groundwater occurrences in the Fennoscandian Shield (Nurmi et al., 1988) recognised four major groups: 1) brackish to saline groundwaters confined to coastal areas and occurring at shallow depths (50-200 m) below the highest postglacial Litorina Sea shore line, 2) brackish to saline groundwaters at depth (300-900 m) occurring beyond the greatest extent of the postglacial Litorina Sea shores, 3) deep (1000-2000 m) saline groundwaters and brines, and 4) very deep (to at least 11 km) brines.

The shallow, coastal brackish and saline groundwaters, occur within a narrow zone bordering the Baltic, demarcated by the

maximum extent of the Litorina marine transgressions in the period 7 500-2 500 years ago. Hästholmen, an island comprising rapakivi granite located off the southeastern coast of Finland, exemplifies such a hydrogeological environment (Hyyppä, 1984; Kankainen, 1986; Nordstrom, 1986). The geochemical and stable isotope data support a seawater origin although somewhat modified by rock/water reactions. The isotope data corresponds to that of present-day seawater in the Gulf of Finland and radiocarbon dating indicates that the mean residence time of the saline water is in the range 4 400-10 000 years, i.e. considered to be mostly groundwater derived from the Litorina Sea by infiltration, mixed with 15-20% glacial meltwater.

Inland, beyond the influence of the maximum Litorina transgressions, the deeper saline groundwaters lack a marine signature and have been compared to those less brackish waters described from the Stripa area which record apparent ages in excess of 20 000 years (Nordstrom et al., 1985). Stable isotope data for the deeper saline groundwaters in Finland fall along the meteoric water line, indicating a meteoric origin, and the present salinity of the waters are believed to mostly reflect rock/water reactions (Nurmi et al., 1988).

In Finland the further sub-division into upper and deeper saline groundwaters is mainly based on differences in salinity and stable isotope signatures. The salinity increases with depth and the isotopic composition changes, plotting consistently above the meteoric water line. The implication is that with increasing depth, mean residence times are considerably longer and that hydrothermal and metamorphic derived waters become more dominant, to the detriment of younger, meteoric-derived waters which characterise the upper horizons.

5.2. Saline groundwaters in the Finnsjön area.

The origin of the saline groundwaters in the Finnsjön area is debatable. Allard et al. (1983) have allocated a residual igneous/metamorphic fluid origin, although partial mixing with Yoldia/Litorina seawater (maximum age of 10 000 years) was not ruled out. Recent investigations by Ahlbom et al. (1986) and Piugdomenech and Nordstrom (1987) have also highlighted the complex origin to these groundwaters. The former study postulated that the saline groundwaters comprise waters resulting from the Yoldia/Litorina marine transgressions, from residual igneous/metamorphic fliuds, from fluids released from the mechanical rupture of fluid inclusions, and from rock/water interactions over long residence times. The latter study showed that the waters have Ca/Mg and Br/Cl ionic ratio values intermediate between seawater and groundwaters collected from the Stripa mine (Nordstrom et al., 1985), where the Br/Cl and

I/Cl ratios of the groundwater were found to coincide with the ionic ratios of the fluid inclusions in the Stripa granite. Thus, Piugdomenech and Nordstrom (op. cit.) suggest that fluid inclusion and micro-fracture fluid leaching may also have contributed to the groundwater salinity at Finnsjön. A further suggestion was that the groundwater chemistry has been modified by the interaction of seawater with the bedrock chemistry.

Table 3 compares the chemical ionic signatures of the Finnsjön groundwaters with other well documented saline environments. In relation to seawater, in particular Baltic seawater, Finnsjön shows significant differences in chemical composition that can be attributed to ion-exchange reactions occurring at the rock/water interfaces. This has resulted in depletions of Na, K and Mg, and a slight enrichment of Ca; some depletion of SO4 is also indicated, but bacterial reduction cannot be ruled out as a possible mechanism in this case. Compared to the other environments, notable differences exist with Hästholmen (i.e. seawater origin with some rock/water interaction), with the Canadian Shield occurrences, Kerimäki and Stripa (i.e. no trace of a marine component; salinity considered to be dominated by rock/water interaction), and with Carnmenellis (i.e. saline water resulting from rock/water interaction generated by the hydrothermal circulation of fluids deep in the bedrock). Some similarity occurs with Parainen which exhibits analogous geochemical and isotopic characteristics with typical coastal saline groundwaters (i.e. Hästholmen) but suggests greater modification from rock/water interactions.

Unpublished groundwater data from Forsmark, location of the subterranean low to intermediate radioactive waste installation 30 km east of Finnsjön, which extends for ca. 1 km under the seabed at a depth of greater than 60 m, are also presented in Table 3 for comparison. These data show a clear similarity with Hästholmen.

The geochemical differences of these documented saline groundwaters are further supported by the stable isotopic data (Fig. 8) which clearly distinguish between the marine coastal environment (Hästholmen and Forsmark) and the marine-derived but modified groundwaters of Parainen and Finnsjön. Carnmenellis and Kerimäki differ markedly from each other and also from the other plotted data. A significant number of the Stripa groundwaters plot intermediate between modified marine groundwaters and groundwaters dominated by rock/water interactions, although some overlap closely with the Kerimäki waters considered to have no marine component. Interestingly, sample HK1 from Forsmark plots within the Finnsjön field. This sample, in contrast to HK7 and HK10, originates from a steeply dipping fracture zone which is hydrogeologically distinct from the other sampled locations. The water is therefore from deeper horizons in the bedrock and represents a more modified marine

derivation, similar to that suggested by the Finnsjön data. Dilution of the saline groundwaters, particularly at shallow levels by the infiltration of fresh or saline waters through the bedrock from above, should be taken into consideration, especially when considering the substantial amounts of glacial meltwater available at various times during the period 10 000-20 000 years ago. Dilution/mixing of groundwaters can be illustrated by plotting oxygen-18 as a function of the chloride content (Fig. 9). If the Baltic Sea water is considered as diluted ocean water, then it is possible to draw a line connecting a chloride content of 19 000 mg/l (standard world oceanic chloride content and reference for oxygen-18) through typical Baltic compositions to intersect the oxygen-18 axis at a chloride content of zero. This oxygen-18 value should therefore represent non-saline water which has been mixed with the more saline Baltic waters. The obtained intersection value of -9.6 (% SMOW) for oxygen-18 does in fact correlate closely with surface recharge water values for this part of Sweden (Saxena, 1984). With the obvious exception of Carnmenellis (no marine component and only included for comparison), all data plot below this dilution line. By drawing a line from 19 000 mg/l chloride through the Finnsjön sample group, and also including HK1 from Forsmark which has been shown to be comparable in chemistry to Finnsjön, an oxygen-18 intersection value of -15.9 (% SMOW) is obtained. This indicates that the non-saline water mixed with these saline samples has a much lower oxygen-18 content than modern day precipitation waters. This non-saline water has been speculated (amongst others by Kankainen, 1986) as being derived from glacial melt resulting from the Weichselian ice sheet (Phase III some 20 000 years ago), and subsequently has mixed with the bedrock saline waters of Yoldia-Litorina origin (introduced some 2 500-8 000 years ago). These dilutions may account for the range of % modern carbon measured in saline groundwaters from both locations (Finnsjön: 19.07-40.00 %; Hästholmen: 12.94-23.78 %).

In contrast, waters from Hästholmen and Parainen, and the main bulk of the Forsmark groundwaters, are characterised by higher oxygen-18 contents. This has been interpreted as indicating that the non-saline component has mixed with the saline waters at a later stage than for the lower oxygen-18 waters. Mixing may therefore be considered a slow continuous process involving Litorina-derived saline waters in the bedrock and percolating rain/glacial melt water over a long period of time. The position of the Carnmenellis waters conforms with the known fact that up to 65 % of these waters are believed to be of recent origin.

5.3. Summary and conclusions.

Geochemical and stable isotopic signatures classify the groundwaters from Hästholmen and Forsmark (excluding HK1) as being coastal marine in origin (i.e. within the maximum extent of the Litorina sea transgressions) with minor modifications resulting from water/rock interactions. Apparent radiocarbon ages for these groundwaters range from 4 400-10 000 years at Hästholmen (Kankainen, 1986) and from 12 000-15 000 years at Forsmark. The Finnsjön area also lies below the highest postglacial Litorina Sea shoreline, but further inland. As a result the groundwaters, although still marine in origin, have been modified to a greater extent by water/rock interactions and possibly by other salt water sources; apparent radiocarbon ages range from 9 000-15 000 years in groundwaters recording below detection levels of tritium. Sample HK1 from Forsmark is anomalous in that isotopically it corresponds closely to the Finnsjön groundwaters. In addition, it is significantly older (ca. 23 000 years) than the other Forsmark groundwaters. It is believed that HK1, which is artesian and therefore less influenced by contamination and/or natural mixing processes, originates from deeper levels and therefore represents an older and more evolved saline groundwater. In this respect the Finnsjön saline groundwaters should also be expected to be older than Hästholmen and Forsmark. That they are not, is believed to be due to carbon-14 dilution, either due to groundwater mixing during the Holocene, or/and artificially induced during the recent drilling and sampling activities.

Based on the presented data, the stages of development in the Finnsjön region can be summarised as follows:

- during the melting phase of the Weichselian ice sheet (ca. 20 000 years ago) infiltration of fresh meltwater occurred either directly or by percolation through the bedrock. These waters locally mixed with existing groundwaters which may have been influenced over long periods of geological time from the accumulation of residual igneous/metamorphic fluids, limited rock/fluid interactions, and salt water sources of unknown origin; fluid inclusion influences, if present, are not considered to be important.

- during the marine transgressions of the Yoldia (ca. 8 500-9 500 years ago) and the later Litorina (ca. 2 500-7 500 years ago) the area became saturated with marine saline waters, sometimes almost totally displacing the `fresh´ water. The deeper these marine waters penetrated, or the longer the residence times, the greater the likelihood that rock/water interaction processes will modify the chemistry of the groundwaters. At Finnsjön (also HK1 from Forsmark and at Parainen) these interaction processes are more widespread.

- this mixing/dilution of rain/glacial melt water with marine-derived saline waters, prior to, during, and subsequent to the Yoldia and Litorina Sea transgressions, has also resulted in a continuous change of the groundwater isotopic signatures (i.e. % modern carbon and oxygen-18).

- following isostatic uplift and exposure of the landmass, the near-surface marine water was gradually flushed out and replaced by fresh water. The depth and extent of this flushing process has been largely dependent on the regional and local hydrogeology. In this respect the presence of major structural weaknesses (i.e. porous and permeable horizons, shears and faults etc.) will act as hydrologic barriers resulting in the entrappment of salt water at higher levels than would otherwise be expected. As sub-horizontal fracture zones are a feature of the Finnsjön (and Forsmark) area, their influence on groundwater hydraulics and chemistry has been clearly demonstrated.

The situation to-day at Finnsjön is that Zone 2 and the adjoining steeply dipping Zone 1 have effectively trapped groundwater of a high saline character at a level which is only about 100-300 m from the bedrock surface. Zone 2 represents a horizon of hydraulic mixing and the waters above and below represent extremes of composition. This local pattern can probably be extended regionally in the Finnsjön area and beyond. It can therefore be speculated that saline water exists throughout the bedrock, and its depth of occurrence is to a large degree dependent on the dip and sub-aerial extent of these large-scale sub-horizontal and near-vertical fracture/shear zones.

6. Conclusions.

Taking into consideration drilling techniques, groundwater quality and sampling methods, and the hydrochemical character and evolution of the Finnsjön groundwaters, the following conclusions can be drawn from this present study:

1) The limitations of air-flush percussion drilling have been demonstrated. The technique is only efficient down to relatively shallow depths (200-250 m); at greater depths a considerable air pressure is required to continually clear the hole from rock debris and accumulating water.

2) Increasing the air pressure also serves to extend the radius of groundwater contamination (i.e. oxygen/groundwater dissolution) further out into the host bedrock along hydraulically susceptible horizons (i.e. high conductivity coupled with a negative piezometric head) such as fracture Zone

2. Long pumping times are therefore necessary to remove these effects which have been demonstrated to significantly influence pH and the distribution of redox-sensitive elements.

3) In conjunction with a stepwise drilling/sampling protocol, rotary water-flush techniques, although still introducing contaminating fluids, are preferred, as smaller water pressures are required to drill to depths greater than 200-300 m.

4) In terms of groundwater analysis, the mobile laboratory offers the advantage of installing the downhole equipment speedily, thus minimising possible contamination from open-hole effects prior to sampling. Furthermore, analysis are rapid and changes in redox and pH in the groundwater during sampling can be offset by downhole measurements and surface in-line facilities.

5) The chemistry of the groundwaters show a sharp contact between saline and non-saline types, this contact corresponding with the highly conductive gently dipping fracture Zone 2. As a result, downward moving non-saline water preferentially spreads out along the upper, more conductive levels of Zone 2, rather than continue to deeper levels. Similarly, the more sluggish upward moving saline water will do likewise. Zone 2 is therefore a horizon along which groundwaters of considerably contrasting age and chemistry come into contact and partially mix with one another. This mixing has produced a highly supersaturated water resulting in the precipitation of calcite. This is most evident in fractures within the upper part of Zone 2, thus partly forming a seal between the two groundwater environments.

6) Comparing the Finnsjön saline groundwaters with other saline environments, particularly in the Fennoscandia Shield, has shown that the groundwaters are dominantly marine in origin, but with clear modifications resulting from water/rock interaction processes. Apparent radiocarbon ages range from 9 000-15 000 years in those waters recording below detection levels of tritium. These ages are considered too young and this is believed to be due to carbon-14 dilution, either resulting from groundwater mixing at various stages during the Holocene, or/and artificially induced during recent drilling and sampling activities.

Acknowledgements.

The authors would like to thank all those personnel, both field and laboratory staff, who have contributed to this study. This work was carried out on behalf of the Swedish Nuclear Fuel and Waste Management Company (SKB).

References.

Ahlbom, K., Andersson, P., Ekman, L., Gustafsson, E., Smellie, J.A.T. and Tullborg, E-L., 1986. Preliminary investigations of fracture zones in the Brändan area, Finnsjön study site. SKB Tec. Rep., (TR 86-05), Stockholm.

Ahlbom, K., 1989. Overview of the fracture zone project at Finnsjön, Sweden. (This volume).

Almen, K-E., Andersson, O., Fridh, B., Johansson, B-E., Sehlsted, M., Hansson, K., Olsson, O., Nilsson, G. and Wikberg, P., 1986. Site investigation - equipment for geological, geophysical, hydrogeological and hydrochemical characterisation. SKB Tec. Rep., (TR 86-16), Stockholm.

Allard, B., Larson, S-Å. and Tullborg, E-L., 1983. Chemistry of deep groundwaters from granitic bedrock. SKBF/KBS Tec. Rep., (TR 83-59), Stockholm.

Andersson, J-E., Andersson, P. and Gustafsson, E., 1989. Effects of gas-lift pumping on hydraulic borehole conditions at Finnsjön, Sweden. (This volume).

Andersson, J-E., Ekman, L., Nordqvist, R. and Winberg, A., 1989. Hydraulic testing and modelling of a low angle fracture zone at Finnsjön, Sweden. (This volume).

Ask, K. and Carlsson, L., 1984. Groundwater influence by boreholes and borehole activities in crystalline rocks - preliminary studies. SKBF/KBS Status. Rep., (AR 84-27), Stockholm.

Axelsen, K,. Wikberg, P., Andersson, L., Nederfeldt, K-G., Lund, J., Sjöström, T. and Andersson, O., 1985. Equipment for deep groundwater cgaracterisation: calibration and test run in Fjällveden. SKB Status. Rep., (AR 86-14), Stockholm.

Bruno, J., Forsythe, R. and Werme, L., 1984. Spent UO2-fuel dissolution: Tentative modelling of experimental apparent solubilities. In. Scientific Basis for Nuclear Waste Management VIII (eds. C.M. Janzen, J.A. Stone and R.C. Ewing). Boston.

Edmunds, W.M., Andrews, J.N., Burgess, W.G., Kay, R.L.K. and Lee, D.J., 1984. The evaluation of saline and thermal groundwaters in the Carnmenellis granite. Mineral. Mag., 48, 3, 407-424.

Fritz, P. and Frape, S.K., 1982. Saline groundwaters in the Canadian Shield - A first overview. Chem. Geol. 36, 179-190.

Frape, S.K., Fritz, P. and McNutt, R.H., 1984. Water-rock interaction and chemistry of groundwaters from the Canadian Shield. Geochim. Cosmochim. Acta 48, 1617-1627.

Frape, S.K. and Fritz, P., 1987. Geochemical trends for groundwaters from the Canadian Shield. In: Saline water and Gases in Crystalline Rocks (eds. P. Fritz and S.K. Frape). Geol. Assoc. Canada Spec. Paper 33, 19-38.

Gustafsson, E. and Klockars, C-E., 1981. Studies on groundwater transport in fractured crystalline rock under controlled conditions using non-radioactive tracers. SKBF/KBS Tec. Rep., (TR 81-07), Stockholm.

Gustafsson, E. and Andersson, P., 1989. Groundwater flow conditions in a low angle fracture zone at Finnsjön, Sweden. (This volume).

Hultberg, B., Larson, S-Å. and Tullborg, E-L., 1981. Grundvatten i Krystallin berggrund. (Groundwater in crystalline bedrock). SGU Unpubl. Status. Rep.

Hyyppä, J., 1984. Geochemistry of the groundwaters bedrock on Hästholmen, Loviisa. Nucl. Waste Comm. of the Finn. Power Co., Rep. YJT-84-05, Helsinki. (In Finnish; English summary).

Kankainen, T., 1986. On the age and origin of groundwater from the rapakivi granite on the island of Hästholmen. Nucl. Waste Co. Finn. Power Co. Rep. YST-86-29, Helsinki.

Kelly, W.C., Rye, R.O. and Livnat, A., 1986. Saline minewaters of the Keweenaw Peninsula, northern Michigan: their nature, origin and relation to similar deep waters in the Precambrian crystalline rocks of the Canadian Shield. Am. J. Sci., 298, 281-308.

Laurent, S., 1982. Analysis of groundwaters from deep boreholes in Kråkemåla, Sternö and Finnsjön. SKBF/KBS Tec. Rep., (TR 82-23), Stockholm.

Nordstrom, D.K., Andrews, J.N., Carlsson, L., Fontes, J-C., Moser, H. and Olsson, T., 1985. Hydrogeological and hydrogeochemical investigations in boreholes- final report of the phase I geochemical investigations of the Stripa groundwaters. Stripa Project SKB Tec. Rep., (85-06), Stockholm.

Nordstrom, D.K., 1986. Hydrogeochemical interpretation of the groundwater at the Hästholmen site, Finland. Nucl. Waste Comm. Finn. Power Comp. Rep., YJT-86-32, Helsinki.

Nurmi, P.A., Kukkonen, I.T. and Lahermo, P.W., 1988. Geochemistry and origin of saline groundwaters in the Fennoscandian Shield. Appl. Geochem., 3, 185-203.

Puigdomenech, I. and Nordstrom, D.K., 1987. Geochemical interpretation of groundwaters from Finnsjön, Sweden. SKB Tec. Rep., (TR 87-15), Stockholm.

Saxena, R.K., 1984. Surface and groundwater mixing and identification of local recharge-discharge zones from seasonal fluctuations of oxygen-18 in groundwater in fissured rock. Div. Hydrol. Uppsala Univ.

Stenberg, L. and Olsson, O., 1985. The tube wave nethod for identifying permeable fracture zones intersecting a borehole. SKBF/KBS Status. Rep., (AR 85-14), Stockholm.

Stenberg, L., 1986. Detailed investigations of fracture zones in the Brändan area, Finnsjön study site. Investigations with the tube wave method in boreholes Fi 6 and BFi 1. Swed. Geol. Co. Int. Rep., (IRAP 87002), Luleå.

Smellie, J.A.T., Larsson, N-Å,, Wikberg, P. and Carlsson, L., 1985. Hydrochemical investigations in crystalline bedrock in relation to existing hydraulic conditions: Experience from the SKB test-sites in Sweden. SKB Tec. Rep., (TR 85-11), Stockholm.

Smellie, J.A.T., Gustavsson, E. and Wikberg, P., 1987. Groundwater sampling during and subsequent to air-flush rotary drilling: hydrochemical investigations at depth in fractured crystalline rock. SKB Status. Rep., (AR 87-31), Stockholm.

Tiren, S., 1989. Geological setting and deformational history of a low angle fracture zone at Finnsjön, Sweden. (This volume).

Tullborg, E-L. and Larson, S-Å., 1982. Fissure fillings from Finnsjön and Studsvik, Sweden. SKBF/KBS Tec. Rep., (TR 82-20), Stockholm.

Figure Texts.

Fig. 1. Map of the Finnsjön Site showing borehole locations and major fracture zones.

Section A -A´, illustrated in Figure 3, is also marked.

Fig. 2. Location of hydrochemical percussion borehole BFI01 relative to estimates of groundwater contamination from earlier drilling activities in the area.

Fig. 3. Transverse hydrogeological section A - A´ (see Fig. 1 for location) showing a tentative model of groundwater flow during unperturbed conditions.

Fig. 4. Variation of pH, conductivity and selected ions with depth (Boreholes KFI09 and BFI01).

Fig. 5. Eh-pH diagram showing the stability fields of the more important U(VI), U(V) and U(IV) complexes considered relevant to groundwater compositions from crystalline bedrock environments in Sweden. The choice of thermodynamic parameters is summarised and discussed by Bruno et al. (1984). Uranium boundaries are shown for equilibria with crystalline UO2 (lower boundary) and with amorphous UO2 (upper boundary).

(See Table 2 for symbol explanation).

Fig. 6. Computation of the saturation index with respect to calcite.

(Borehole BFI01; 71 to 468 m).

Fig. 7. Mixing computation between non-saline and saline waters with respect to calcite saturation. (See text for explanation).

(Borehole KFI09; 94 to 368 m).

Fig. 8. Oxygen-18 and deuterium plot of saline groundwaters from Finnsjön compared to Forsmark and other documented saline groundwater environments. (Modified after Nurmi et al., 1988).

Data sources: Canadian Shield Brines (Frape et al., 1984; Kelly et al., 1986); Carnmenellis (Edmunds et al., 1984); Hästholmen (Kankainen, 1986); Parainen and Kerimäki (Nurmi et al., 1988); Stripa (Nordstrom et al., 1985).

Fig. 9. Oxygen-18 versus chloride plot for the Finnsjön groundwaters. Data from Forsmark, Carnmenellis, Stripa and Parainen/Kerimäki are included for comparison.

Fig. 10. Location of saline groundwater occurrences discussed in relation to the maximum extent of the Litorina transgression ca. 6500 years ago.

Table 1 Groundwater physico-chemical parameters from boreholes KFI09 and BFI01, Finnsjön.

Borehole	Surface Water	KFI09	KFI09	KFI09	KFI09	BFI01	BFI01	BFI01	BFI01	BFI01	BFI01
Sampling Int (m)	0	94	114	182	360	71-85	169-191	234-247	284-294	335-385	439-459
Date Collected	841112	850311	850224	850215	850205	860408	860507	860528	861112	860625	861025
Temperature (°C)	7.0										
pH (lab)	5.9	7.3	7.4	7.7	7.4	6.9	7.2	7.6	6.9	7.1	6.6
pH (field)	ND	7.3	7.5	7.4	7.6	6.9	7.7	7.7	6.8	7.3	7.0
Cond. (mSm)	4.12	270	656	860	1410	54	415	531	1570	1650	1660
Eh (mV)	ND	-245	-300	-212	ND	+40	-320	-270	+400	+340	+400
Alkalinity (mg/l HCO_3^-)	7	285	116	160	32	220	200	260	59	59	48
Dissolved O_2 (mg/l)	ND	0	0	0	0	0	0	0	7	2	4
Element					mg/l						
Ca	5.9	115	ND	700	1691	76	270	320	1500	1500	1600
Mg	8.81	16	ND	91	84	6.3	36	40	126	140	120
Na	2.6	415	ND	960	1510	23	610	650	1600	1700	1700
K	0.04	5.8	ND	15	7.4	3.2	6.5	8.7	15	15	13
Fe (II)	0.58	0.56	0.36	1.07	0.34	8.86	0.50	0.87	0.009	<0.01	0.005
Fe (tot)	0.97	0.56	0.35	1.08	0.35	9.01	0.51	0.90	0.022	0.01	0.016
Al	0.8	0.02	ND	0.003	0.18	0.06	0.006	0.013	0.024	0.16	0.032
Mn	0.006	0.19	0.45	0.82	0.36	0.50	0.37	0.42	1.2	1.0	0.8
SO_4	4.7	175	ND	210	326	8.3	150	140	380	400	380
F	0.13	3.4	ND	7.2	9.1	0.6	1.8	2.3	1.1	1.2	1.2
Cl	2	680	2125	2800	5150	61	1310	1500	5200	5500	5500
Br	-	2.03	ND	13.5	27.1	0.3	4.5	7.0	26.0	29.0	29.0
I	<0.01	0.01	ND	0.03	0.07	<0.002	0.020	0.035	0.070	0.120	0.120
NO_3	0.28	0.02	ND	0.019	0.01	0.006	<0.005	0.005	<0.005	<0.005	<0.005
PO_4	0.01	0.001	0.002	0.003	0.004	0.001	0.001	<0.002	<0.005	0.002	<0.005
NH_4	ND	0	ND	1.1	ND	0.15	0.34	0.63	0.46	0.71	0.35
S	ND	0.22	ND	0.44	0.03	<0.01	0.01	<0.01	0.01	<0.01	<0.01
Si	2.8	7.6	1.75	4.6	7.6	6.2	8.3	7.5	5.5	6	5.4
TOC	62	18	ND	7.5	1.0	16	12	6.9	68	4.2	18
U (ppb)	ND	2.1	ND	1.6	8.2	4.57	12.78	3.90	114.32	10.70	15.63
$^{234}U/^{238}U$	ND	4.1	ND	3.1	5.0	1.6	2.2	3.3	1.7	2.0	1.9
^{2}H (‰)	-80.5	-79.0	ND	-86.4 -86.8	-89.9	-88.2	-85.2	-85.7	-89.0	-86.9	-88.7
^{18}O (‰)	-12.1	-9.8	ND	-84.0 -10.4 -10.9 -11.0	-87.4 -11.2 -11.1	-12.0	-11.6	-11.7	-11.5	-11.8	-11.8
^{3}H (TU)	31±2	8±1	ND	<3	<3	36±3	5±2	<3	<3	<3	<3
^{14}C (% modern)	ND	ND	ND	22.60	ND	85.30	33.02	37.45	ND	19.07	28.75

ND = Not determined

Table 2: Redox-sensitive parameters of the Finnsjön groundwaters at increasing depths. (Boreholes BFI01 and KFI09).

Sample	Depth (m)	pH	Eh (mV)	Fe(II) (mg/l)	Fe(tot) (mg/l)	U (ppb)	234U/238U Activity Ratio.	Symbol (See Fig. 5)
BFI01	71- 84	6.9	+40	8.86	9.01	4.57	1.6	+
BFI01	169-192	7.7	-320	0.50	0.51	12.78	2.2	✳
BFI01*	234-247	7.7	-270	0.87	0.90	3.90	3.3	⊙
BFI01*	284-294	6.8	+400	0.009	0.022	114.32	1.7	⊡
BFI01*	335-385	7.3	+340	0.009	0.029	10.70	2.0	◬
BFI01	439-460	7.0	+400	0.005	0.016	15.63	1.9	▽
KFI09	94	7.3	-245	0.13	0.52	2.1	4.1	
KFi09*	114	7.5	-300	0.36	0.36	-	-	
KFi09*	182	7.7	-212	0.19	0.94	1.6	3.1	
KFi09	360	7.4	-	0.05	0.35	3.1	5.0	

* sampled intervals completely or mostly within Zone 2.

TABLE 3: Comparison of published ionic ratios (by weight) of saline waters with those from Finnsjön.

Sample location	Br/Cl	I/Cl x 10^6	Ca/Mg	Mg/Cl	Ca/Cl	Na/Cl	K/Cl	SO_4/Cl	^{18}O (‰ SMOW)	^{14}C (% modern)	3H (TU)
Seawater	0.00347	3.1	0.32	0.067	0.021	0.55	0.021	0.14		-	-
Baltic Seawater	0.00342	-	0.32	0.067	0.022	0.55	0.021	0.14	-6.0	-	-
Yoldia Seawater	0.00342	163	5	0.052	0.072	0.74	0.031	0.13			-
Skåne Brines	0.00550	40-53	22	0.012	0.20	0.50	0.011	0.02			-
Finnsjön											
KFI05 (384 m)	-	-	20	0.016	0.32	0.26	0.01	0.06	-11.6	40.00	5±2
KFI06 (688 m)	-	-	25	0.013	0.33	0.26	0.005	0.06	-	-	<3
KFI08 (395 m)	-	-	465	0.001	0.37	0.27	0.003	0.03	-	-	<3
KFI09 (94 m)	0.00300	14	7.2	0.023	0.17	0.61	0.009	0.26	-9.8	-	8±1
KFI09 (114 m)	-	-	-	-	-	-	-	-	-	-	-
KFI09 (182 m)	0.00970	11	20	0.030	0.25	0.34	0.005	0.08	-10.9	22.60	<3
KFI09 (360 m)	0.00526	14	20	0.016	0.32	0.29	0.001	0.06	-	-	<3
BFI01 (71-85 m)	0.00492	-	12	0.103	1.25	0.38	0.052	0.14	-12.0	85.30	36±3
BFI01 (169-191 m)	0.00340	15	8	0.027	0.21	0.47	0.005	0.11	-11.6	33.02	5±2
BFI01 (234-247 m)	0.00467	23	8	0.027	0.21	0.43	0.006	0.09	-11.7	37.45	<3
BFI01 (284-294 m)	0.00500	13	12	0.024	0.29	0.31	0.003	0.07	-11.5	-	<3
BFI01 (335-385 m)	0.00527	22	11	0.025	0.27	0.31	0.003	0.007	-11.8	19.07	<3
BFI01 (439-459 m)	0.00527	22	13	0.022	0.29	0.31	0.002	0.07	-11.8	28.75	<3
Forsmark											
HK1	0.00310	-	6	0.038	0.23	0.37	0.002	0.08	-12.2	5.70	<3
HK7a	0.00320	-	4	0.050	0.19	0.38	0.003	0.09	-9.8	22.79	3±2
HK10	0.00300	-	4	0.050	0.22	0.34	0.003	0.10	-9.3	15.75	<3
Hästholmen +											
Y1 (50.4-53.9m)	0.00367	58	3	0.160	0.40	1.54	0.064	0.71	-11.5	43.45	11.4±1.2
Y1 (122.0-125.5m)	0.00492	10	1	0.058	0.08	0.49	0.006	0.13	-	-	2.9±0.8
Y1 (174.7-178.2m)	0.00355	-	1	0.062	0.08	0.46	0.005	0.12	-8.3	20.67	10±3
Y5 (190.0-193.5m)	0.00378	-	3	0.053	0.15	0.39	0.005	0.12	-	-	-
Parainen *											
490 m	0.00540	8	6	0.035	0.19	0.41	0.010	0.10	-9.9		42.8±1.7
Keimäki *											
700 m	0.01000	187	14	0.008	0.11	0.50	0.005	-	-13.7		14.1±1.5
Stripa o											
V1 (409-506 m)	0.01032	254	905	0.0003	0.27	0.44	0.002	0.16	-12.8	-	0.7±0.1
V2 (490-493 m)	0.01109	522	228	0.001	0.19	0.49	0.002	0.20	-13.1	(13.60)	0.12±0.09
N1 (271-273 m)	0.01188	250	76	0.006	0.46	0.60	0.009	0.006	-13.0	-	0.15±0.08
Carnmenellis ⊕											
4F (380 m)	0.0034	-	14	0.019	0.27	0.26	0.008	0.01	-5.5	42.9	
Canadian Shield ϕ											
Yellow Knife (1500 m)	0.01070	-	62	0.006	0.40	0.23	0.003	-	-14.4	-	-
Thompson (1300 m)	0.01201	-	11	0.033	0.38	0.13	0.001	-	-13.2	-	-

+ Hyyppä, 1984
Kankainen, 1986
* Nurmi et al., 1988
o Nordstrom et al., 1985
⊕ Edmunds et al., 1985
ϕ Fritz and Frape, 1982

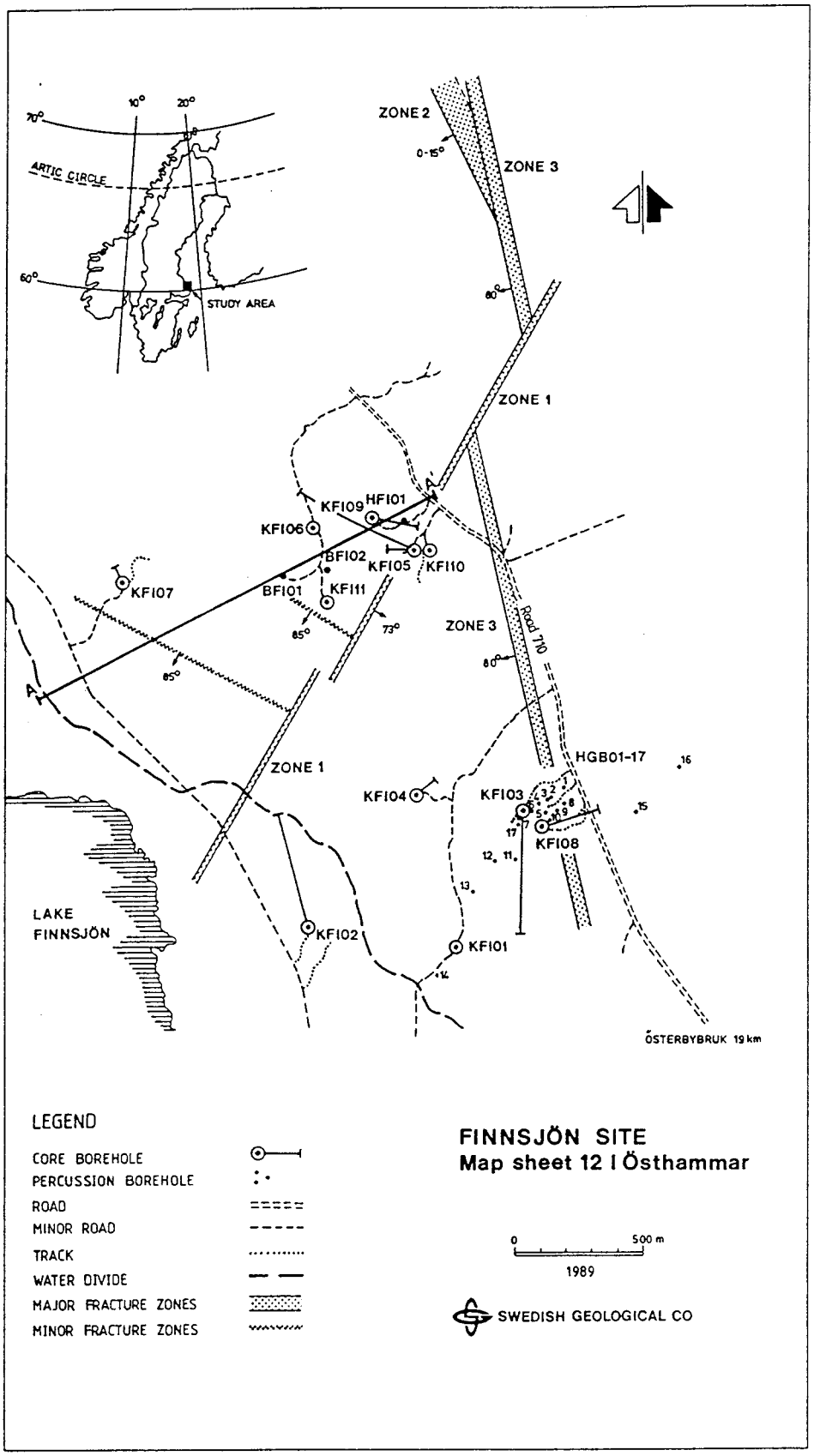

Fig. 1. Map of the Finnsjön study site showing borehole locations and major fracture zones.

Section A -A´, illustrated in Figure 3, is also marked.

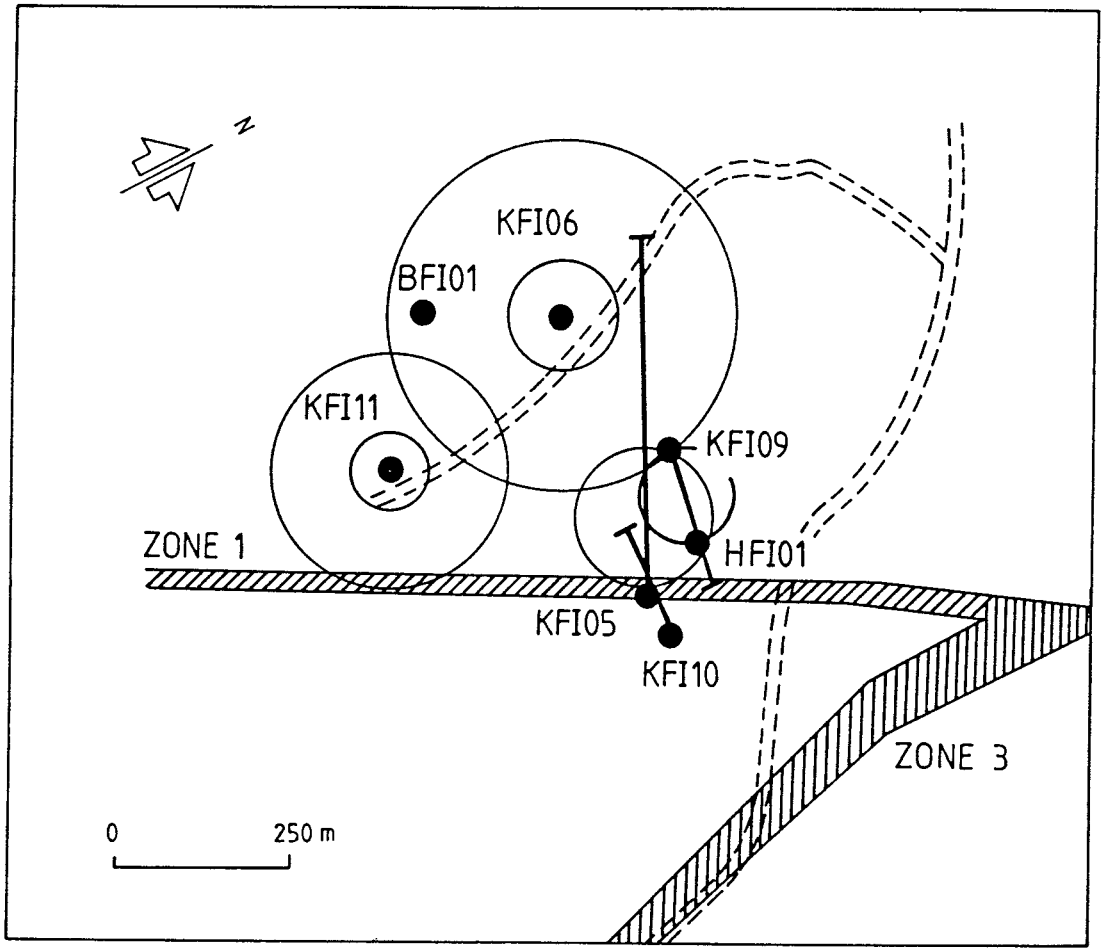

Fig. 2. Location of hydrochemical percussion borehole BFI01 relative to estimates of groundwater contamination from earlier drilling activities in the area.

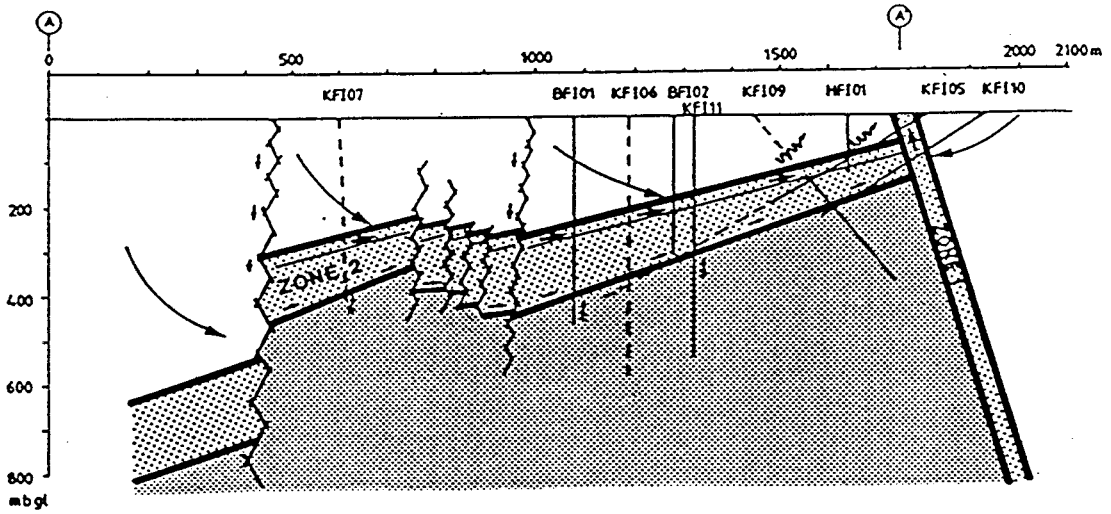

FRACTURE ZONES:

Major fracture zones Zone 1 and Zone 2 — ZONE 1,2

Minor fracture zones

SALINE AND NON SALINE WATER:

Non-saline water

Transitional water (1500-5000 mg/l Cl^-) within the major zones

Saline water (av. 5500 mg/Cl^-)

UPPER CONDUCTIVE ZONE:

Zone within large waterflow (av. 1500 mg/l Cl^-) within the major fracture zones

BOREHOLES:

Located in front of projected profile

Located behind projected profile

FLOW LINES:

Major flow lines

Minor flow lines

Recharging groundwater

HYDRAULIC HEAD:

Direction of major gradient

Direction of minor gradient

Fig. 3. Transverse hydrogeological section A - A´ (see Fig. 1 for location) showing a tentative model of groundwater flow during unperturbed conditions.

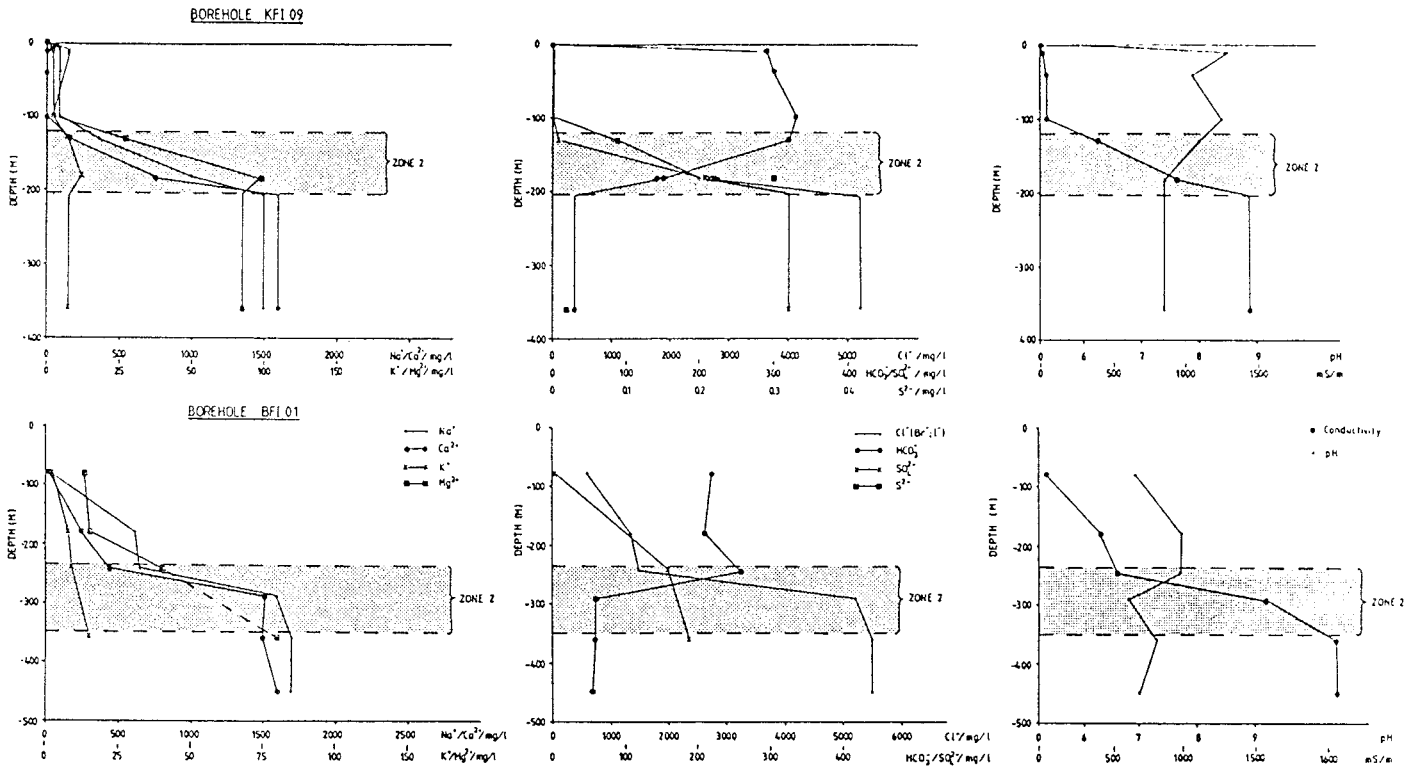

Fig. 4. Variation of pH, conductivity and selected ions with depth (Boreholes KFI09 and BFI01).

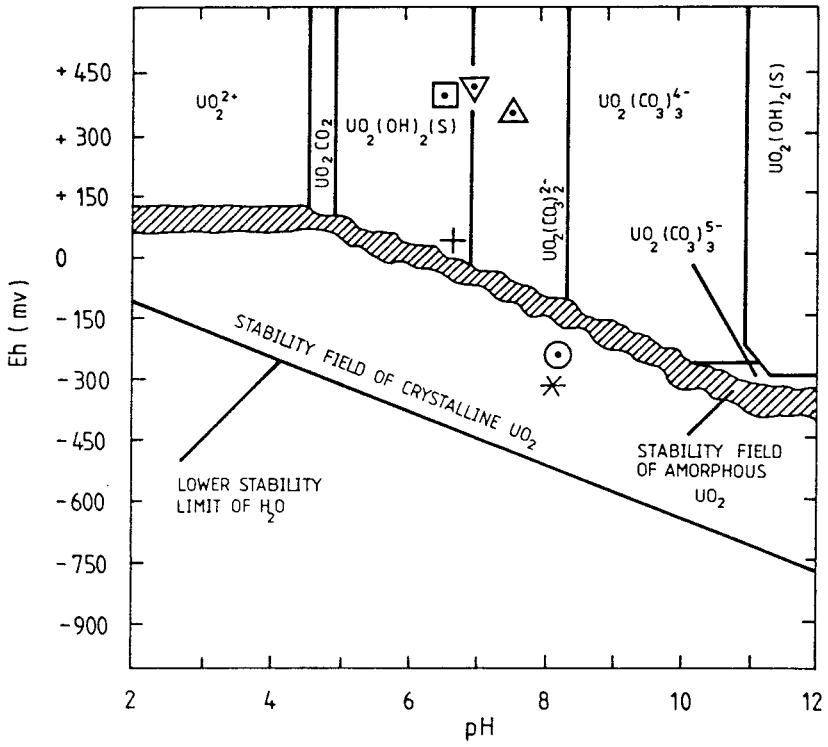

Fig. 5. Eh-pH diagram showing the stability fields of the more important U(VI), U(V) and U(IV) complexes considered relevant to groundwater compositions from crystalline bedrock environments in Sweden. The choice of thermodynamic parameters is summarised and discussed by Bruno et al. (1984). Uranium boundaries are shown for equilibria with crystalline UO2 (lower boundary) and with amorphous UO2 (upper boundary).

(See Table 2 for symbol explanation).

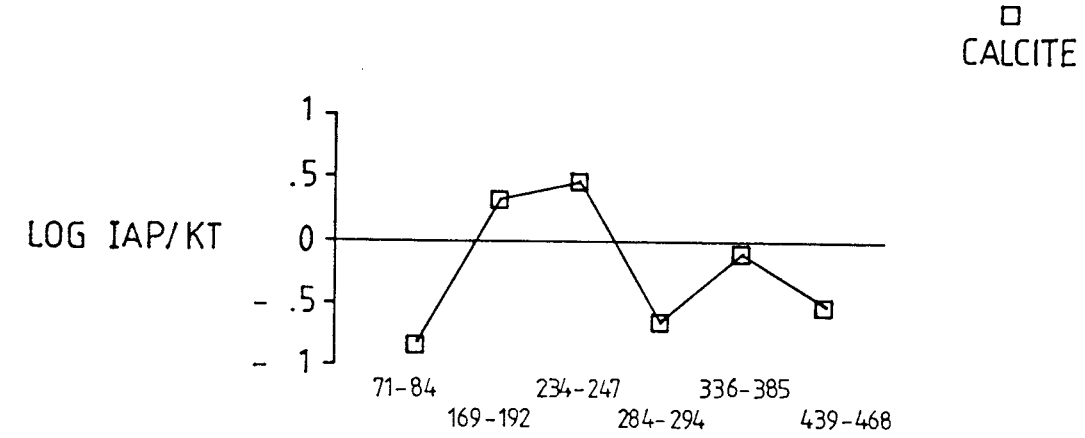

Fig. 6. Computation of the saturation index with respect to calcite.

(Borehole BFI01 from 71 to 468 m).

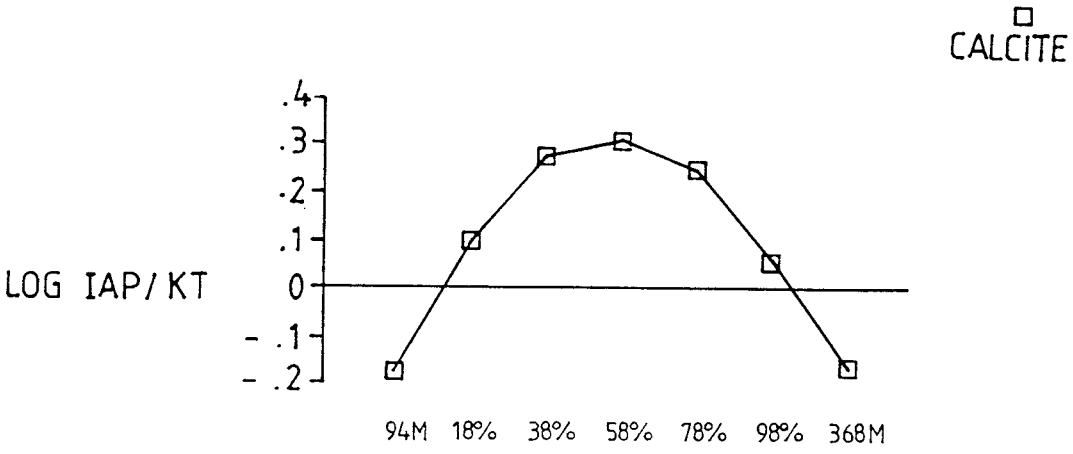

Fig. 7. Mixing computation between non-saline and saline waters with respect to calcite saturation. (See text for explanation).

(Borehole KFI09 from 94 to 368 m).

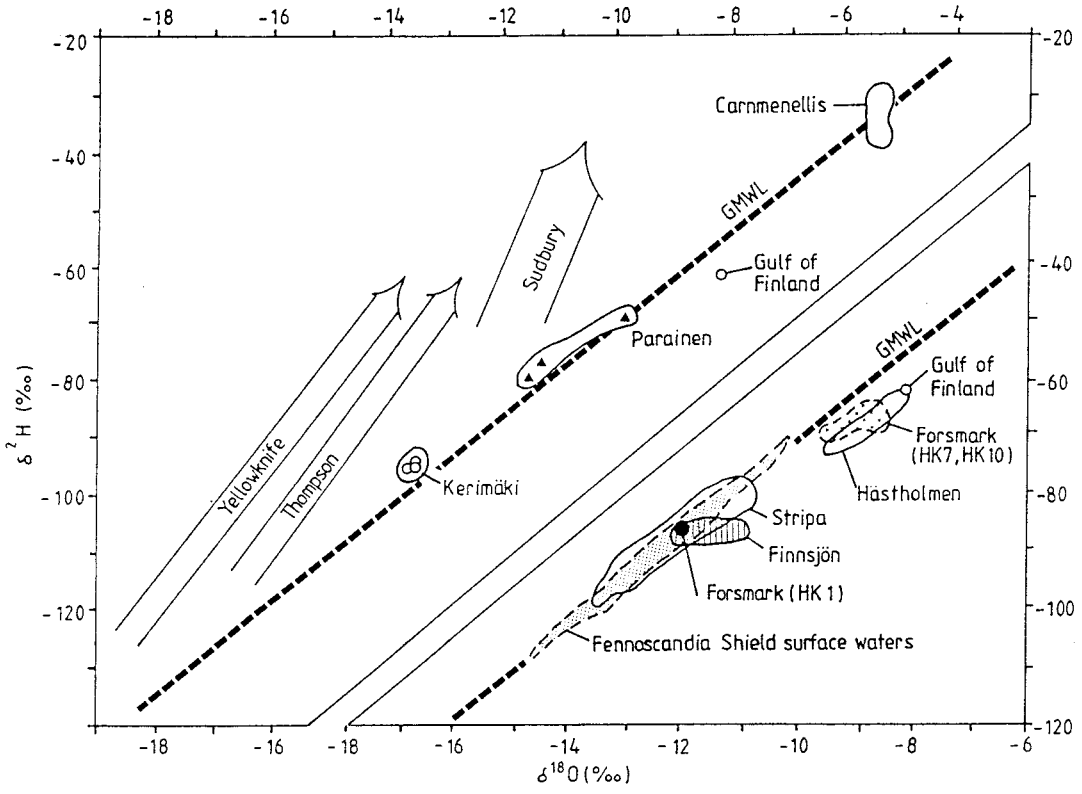

Fig. 8. Oxygen-18 and deuterium plot of saline groundwaters from Finnsjön compared to Forsmark and other documented saline groundwater environments. (Modified after Nurmi et al., 1988).

Data sources: Canadian Shield Brines (Frape et al., 1984; Kelly et al., 1986); Carnmenellis (Edmunds et al., 1984); Hästholmen (Kankainen, 1986); Parainen and Kerimäki (Nurmi et al., 1988); Stripa (Nordstrom et al., 1985).

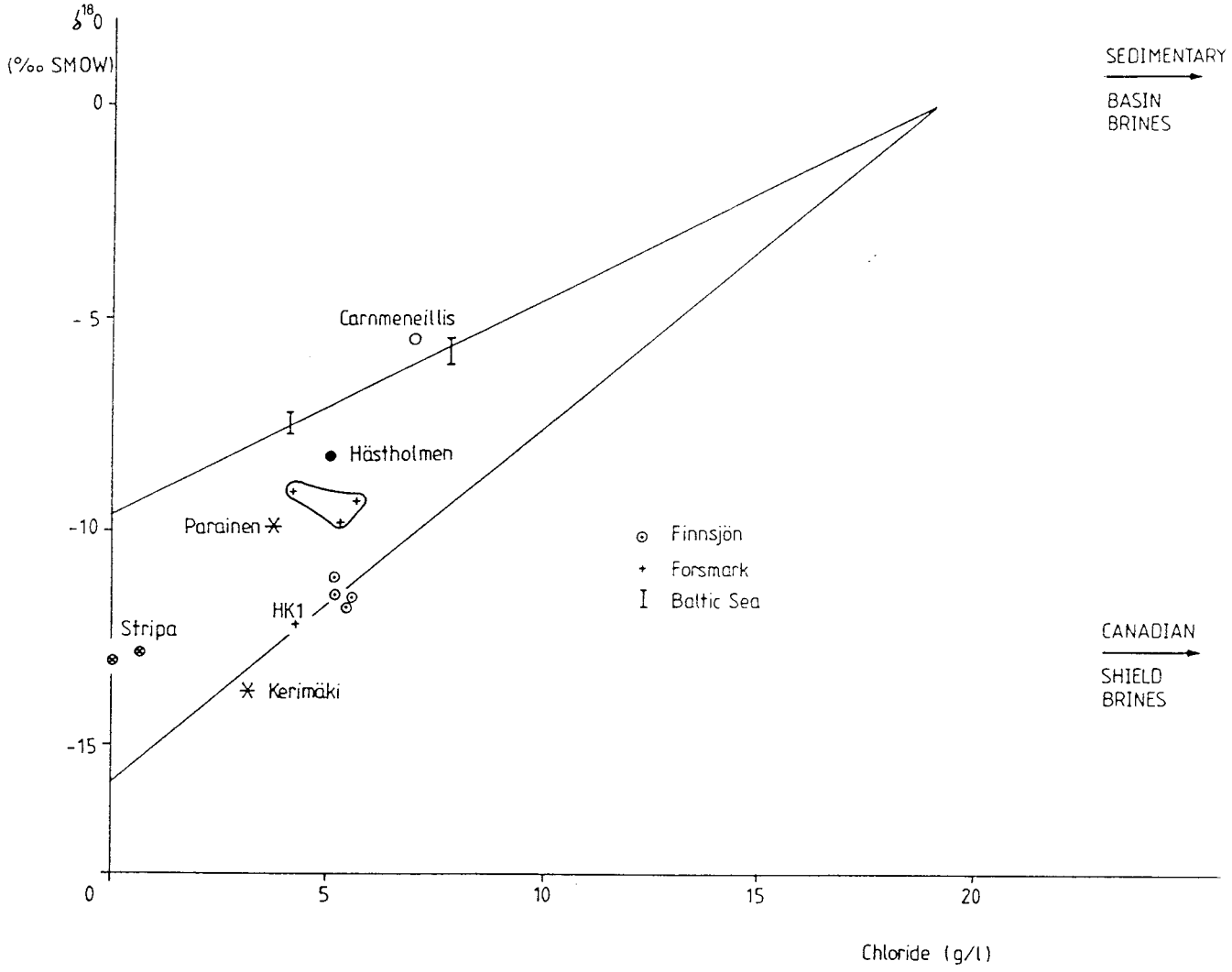

Fig. 9. Oxygen-18 versus chloride plot for the Finnsjön groundwaters. Data from Forsmark, Carnmenellis, Stripa and Parainen/Kerimäki are included for comparison.

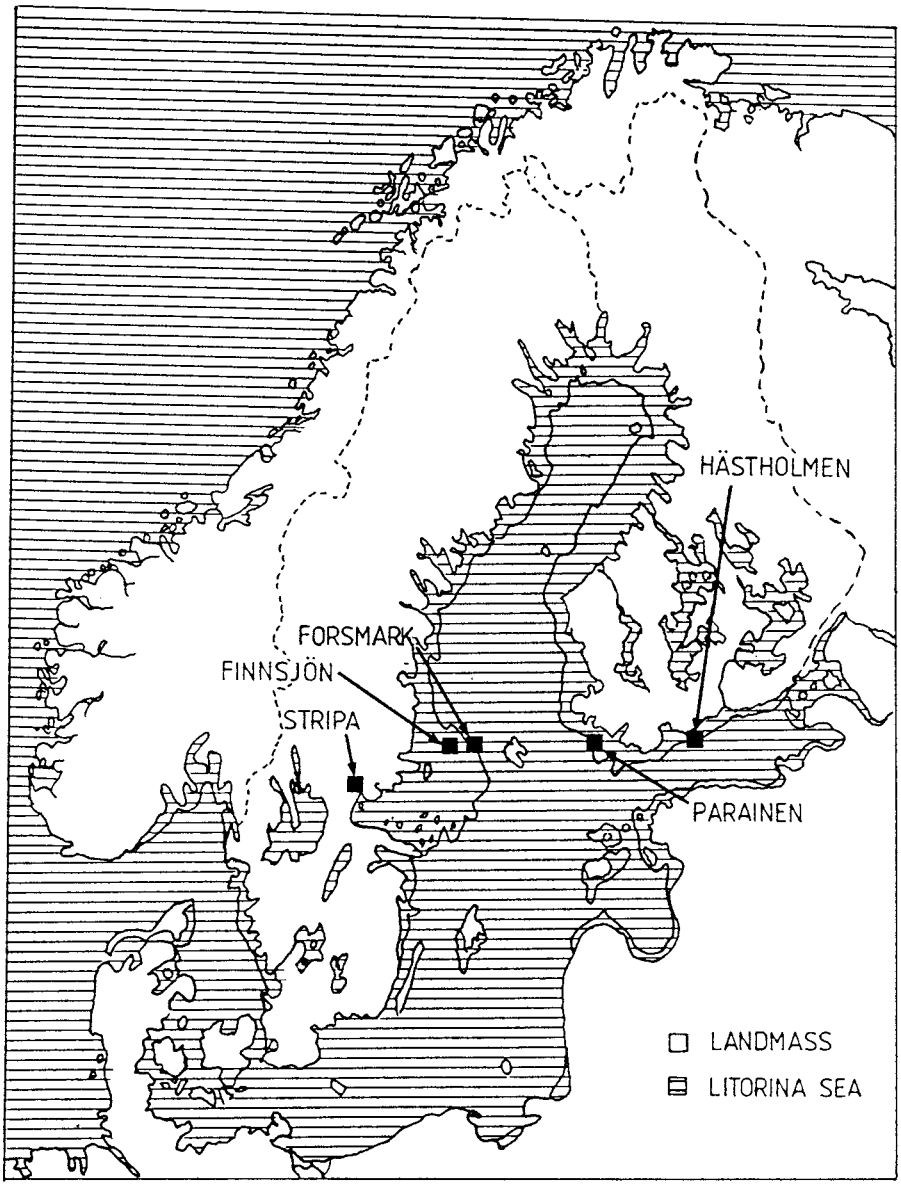

Fig. 10. Location of saline groundwater occurrences discussed in relation to the maximum extent of the Litorina transgression ca. 6500 years ago.

CHARACTERIZATION OF FRACTURE ZONE 2, FINNSJÖN STUDY-SITE

PART 6

EFFECTS OF GAS-LIFT PUMPING ON HYDRAULIC BOREHOLE CONDITIONS AT FINNSJÖN, SWEDEN

J-E. Andersson, P. Andersson, E. Gustafsson

Swedish Geological Company, Uppsala, Sweden

August 1989

EFFECTS OF GAS-LIFT PUMPING ON HYDRAULIC BOREHOLE CONDITIONS AT FINNSJÖN, SWEDEN.

J-E ANDERSSON, P. ANDERSSON and E. GUSTAFSSON

Swedish Geological Company, Box 1424, S-751 44 Uppsala (Sweden)

Abstract

The recorded volumes of flushing water used during the drilling of cored boreholes, and the amounts recovered at the surface, have been used to estimate the potential quantities of flushing water and drilling debris injected into fractures.

The results show that significant amounts of flushing water and drilling debris may be injected into fractures during drilling. For cored boreholes penetrating major fracture zones, only about 7-8% of the total volume of flushing water used was recovered at the surface. A total loss of flushing water occurred in all boreholes during penetration of these fracture zones. The recovered amounts of drilling debris were also low.

Higher percentages of drilling debris were recovered from the air-flush percussion boreholes but, on the other hand, larger total amounts of debris were lost to the rock.

During gas-lift pumping in borehole KFI10, only very small estimated amounts of the flushing water (3-4%) and drilling debris (approx. 1%) lost to the rock, were recovered. The gas-lift pumping also had a minor influence on the borehole hydraulic parameters calculated from hydraulic tests before and after pumping.

1. Introduction

During the drilling of rotary cored boreholes varying amounts of drilling debris are produced. Some of the debris is recovered at the surface by the circulating flushing water (used for cooling the drill-bit) and some will eventually be sedimented at the bottom of the borehole. However, a certain amount of the debris will most likely, together with the flushing water, be injected under high pressure (approx. 2 MPa) into the fracture systems intercepted by the borehole. Studies within the Fracture Zone Project (Ahlbom et al., 1986, 1987; Andersson et al., 1987) have examined the proportions of recovered, sedimented, and injected amounts of debris during the drilling of such boreholes. In addition, estimated amounts of the flushing water injected are also presented.

The potential amount of drilling debris injected into the fractures may eventually alter the hydraulic properties of the bedrock in the near-vicinity of the borehole by clogging, in addition to disturbing the natural chemical groundwater conditions. Furthermore, the groundwater is most certainly influenced by the injected flushing water which in most cases has a chemical composition different from that prevailing in the rock penetrated by the borehole. Since large amounts of flushing water may be injected, the groundwater environment may be severely contaminated (Smellie et al., 1985).

In order to obtain less contaminated and more representative groundwater samples, two boreholes at the Finnsjön test site (BFI01 and BFI02) were drilled using air-flush or booster drilling techniques. The amounts of drilling debris recovered at the surface and the water discharged were continuously recorded during drilling of these boreholes (Smellie et al., 1987; Ekman et al., 1988).

Efforts have been made to minimize the potential contamination effects arising from drilling debris and flushing water, and the effects on the hydraulic characteristics of the rock. One method is gas-lift pumping of the boreholes shortly after

drilling. Here, gas is injected into the borehole close to the hole bottom at an excess pressure relative to the hydrostatic pressure at that level. To cause minimum disturbance of the hydrochemical conditions, nitrogen gas is used. When introduced, water and drilling debris are forced to the surface by the rising and expanding gas bubbles thereby creating a certain clearing effect.

This clearing effect has been quantified by recovering the amounts of flushing water and drilling debris removed from borehole KFI10 (255 m) during gas-lift pumping. Furthermore, by performing and comparing transient single-hole water injection tests both before and after the gas-lift pumping in the same test intervals, it was possible to study the effects of the gas-lift pumping on the borehole hydraulic parameters (Andersson et al., 1987). A summary of the hydrochemical investigations at the Finnsjön site is presented by Smellie and Wikberg (this volume).

The location of the boreholes within the Brändan area at the Finnsjön site, together with a schematic cross-section of the area, are shown in Figures 1 and 2 respectively.

2. Records of flushing water and drilling debris

2.1 Flushing water

The chemical composition of the flushing water usually differs from that of the groundwater in the bedrock surrounding the borehole; potential contamination is therefore possible. Theoretical estimates of the flushing water volume injected into the bedrock during the drilling has been made by Smellie et al. (1985). The volumes injected were in the order of 20-130 m^3 for a 700-800 m deep cored borehole depending on the hydraulic character of the bedrock. To further study these in the Brändan area, the effects of the flushing water balance was measured during drilling of three boreholes (KFI09, KFI10 and KFI11). The supply of flushing water was derived from

groundwater pumped from percussion borehole HFI01 (Ahlbom et al., 1986; 1987).

In order to calculate the component of flushing water in a collected water sample, the drilling fluid has to be labelled with a tracer, preferably with the following qualities:

- easy to handle
- easy to detect and analyze
- non-sorbing
- low background
- no reaction with original water

In the Brändan area an organic dye was considered to be the most suitable tracer. During previous studies (boreholes KFI05 and KFI06; drilled 1978-79) the flushing water was labelled with the fluorescent dye Rhodamine WT. For this present phase the fluorescent dyes Uranine (sodium fluorescein) and Amino G Acid were chosen to minimise interference both with each other and also with the existing Rhodamine. The dye concentrations listed in Table 1 were chosen after measuring water samples from existing boreholes KFI05 and KFI06, together with samples from the percussion borehole HFI01. The governing criterium was to measure a dilution of 0.1% of the initial concentration.

The volumes of flushing water injected into the boreholes were recorded at the surface with a volumetric flow meter during the drilling operation, and the volumes recovered at the surface were collected in 1 m^3 tanks whereupon the flushing water and drilling debris contents were measured. The rate of flushing water loss in the boreholes was calculated as the volume of water lost into the bedrock over a certain borehole interval, divided by the length of the interval. Table 2 lists the total volumes injected in the boreholes, the recovered and lost volumes, and the average rate of flushing water loss over the whole borehole length.

Table 2 shows that only very small volumes of flushing water were recovered from the boreholes. The average rates of

flushing water losses presented in Table 2 are similar for the three boreholes. This is not surprising since these boreholes all penetrate major fracture zones. Table 2 also shows the depth intervals where a total loss of flushing water occurred. In boreholes KFI09 and KFI11 these depths correspond to the upper surface of Zone 2. In borehole KFI10 this depth corresponds to the upper part of Zone 1 (Fig 2).

As the rate of the flushing water loss is dependent on the hydraulic conductivity of the bedrock, this loss may provide a rough picture of the overall distribution of hydraulic conductivity distribution along the boreholes. An example is given in Figure 3 whereupon the rate of flushing water loss and the hydraulic conductivity for borehole KFI11 are plotted against borehole length. Both the total rate and the estimated rate of loss of flushing water during drilling are shown. From about 225 m to the hole bottom a total loss of flushing water occurred. The actual rates are calculated as the increments of the flushing water volume (and the water loss) divided by the length of the penetrated interval. To facilitate comparison with the hydraulic conductivity, the average rate of flushing was calculated for the same 20 m intervals. However, due to too few data regarding recovered volumes, the average rate of water loss could only be estimated over longer intervals. Thus, the two curves are not synchronous.

Figure 3 shows the location of the major high-conductivity intervals along the borehole, i.e. at about 225 m and 326 m where sharp increases of the rate of water loss occurred. These levels correspond respectively to the uppermost and lowermost parts of Zone 2 in borehole KFI11 (Tirén, this volume). Above, between and below these levels the rate of water loss was rather stable. Figure 3 also shows that the rate of water loss was high during drilling within Zone 2.

2.2 Drilling debris

Similar investigations of the amounts of drilling debris produced and recovered were performed during drilling of the cored boreholes KFI09, KFI10 and KFI11 and the two air-flush percussion boreholes BFI01 and BFI02. The calculated (dry) volume of drilling debris produced during rotary coring of a 56 mm borehole with a core diameter of 42 mm is theoretically approx. 0.11 m^3/100 m (neglecting the porosity of the rock). The corresponding figure for air-flush percussion drilling of a 165 mm diameter borehole is approx. 2.1 m^3/100 m. Using a rock density of 2716 kg/m^3 these figures correspond to 299 kg/100 m and 5704 kg/100 m of drilling debris, respectively. The difference between the produced and recovered masses thus provides an estimate of the amount of drilling debris injected into the rock (fractures and fracture zones) during drilling.

In boreholes BFI01 and BFI02 measurements of the total masses of (dry) drilling debris recovered to the surface were performed during drilling (Smellie et al., 1987; Ekman et al., 1988). From these measurements the mass lost into the rock and the recovery ratio of the drilling debris at different intervals of these boreholes was calculated. By calculating the produced mass in these two boreholes the variation of the hole diameter (as measured by the caliper log) was used. The recovery ratio is defined as the ratio between the produced and recovered masses of drilling debris.

During drilling of borehole KFI11 the recovered mass was estimated from spot measurements of the content of drilling debris in water samples (Ahlbom et al., 1987). In boreholes KFI09 and KFI10 no measurements of the recovery of drilling debris were carried out. However, in the intervals where a total loss of flushing water occurred, the amount of drilling debris injected into the rock may be estimated. The results are summarized in Table 3. For the core drilled boreholes the intervals given in Table 3 refer to the level of total loss of flushing water, whereas for the percussion boreholes the intervals refer to the upper surface of Zone 2. These two

levels coincide for all boreholes except KFI10 where this level corresponds to Zone 1.

Table 3 indicates that large amounts of debris are lost in the rock during drilling, particularly for the percussion rotary drilled boreholes because of the large bit diameter. On the other hand these boreholes show larger recovery ratios than the core drilled boreholes. The table also shows that the recovery ratios decrease significantly during drilling in the fracture zones.

3. Gas-lift pumping

Based on the above facts, clearing the boreholes from flushing water and drilling debris prior to the hydro-testing is desireable. The most common method within the Swedish programme is to apply nitrogen gas through a hose with an excess pressure at the outlet of 800 kPa at about 5-20 m above the bottom of the borehole. Water and drilling debris are then forced upward to the surface. After flushing for several hours, pumping is stopped to allow the water level to equilibrate; the whole procedure is repeated, usually 2-4 times. Gas-lift pumping between packers has also been used in order to pump a particular section of a borehole (Ahlbom et al., 1986).

In borehole KFI10 hydraulic injection tests were performed prior to the gas-lift pumping to study the effects of the pumping on the hydraulic parameters (see below). The water used for injection was also labelled with Amino G Acid and the injected volumes of water were recorded. Thus, only the recovery of the total water volumes used for the injection tests (27.2 m^3) and as flushing water (34 m^3) could be determined in this borehole. Since the gas-lift pumping was performed 8 months after the completion of the drilling, some of the flushing water should have been washed out naturally. However, the last injection tests were performed only 4 days before the gas-lift pumping. The water samples from the gas-lift pumping were analyzed for concentrations of Amino G Acid

and then dried and weighed to establish the amount of drilling debris recovered at different time intervals for a period of about 4.5 hours after starting pumping. No quantitative measurements were performed in the borehole KFI11.

The pulsating discharge during the gas-lift pumping made it somewhat difficult to calculate the recovery of flushing water. The analyses of the concentrations of Amino G Acid in borehole KFI10 (Fig. 4) showed that the injected water had been greatly diluted within some high conductive sections of the borehole, and that mixing was very poor in other sections, resulting in high peak values (spikes) with short duration of the Amino G Acid content (Andersson et al., 1987). Thus, a high sampling frequency would be required to detect all spikes. According to the measured concentrations of Amino G Acid in the water samples from borehole KFI10, the recovery of flushing water during the 5 hour long gas-lift pumping was only about 4% of the total volume of water injected in the borehole. If only the volume injected during the injection tests is considered, the recovery is 5 %.

Thus, the recovery of flushing water from borehole KFI10 was quite low. This may be expected since the borehole penetrates several highly conductive zones and thus a large dilution is probable. This is also supported by the almost constant concentration of tracer in the discharged water (approx. 0.2 ppm) that was reached after only about 30 minutes of pumping. Pumping would have to be continued for a very long time to clear the fractures entirely from flushing water. A low recovery of flushing water (3%) was also found during the gas-lift pumping in borehole KFI09 (Ahlbom et al., 1986). The pumping in this borehole was performed about one month after completion of the drilling operation.

The content of drilling debris was also measured during gas-lift pumping in boreholes KFI09 and KFI10. For the latter borehole (Fig. 5) the content of drilling debris shows a peak after approx. 5 minutes of pumping. This time corresponds roughly to the time to circulate the borehole. The content of

drilling debris then rapidly decreases to a low level (approx. 60 mg/l). This indicates that the major part of the recovered amount of drilling debris is the sedimented layer at the bottom of the borehole. Further pumping seems to have little effect.

The recovered amount of drilling debris (in relation to the estimated loss given in Table 3) during the gas-lift pumping in borehole KFI10 was estimated at only about 1% (Andersson et al., 1987). The corresponding recovery for borehole KFI09 is similar, re-inforcing the conclusion that considerable amounts of drilling debris must still remain in the fracture systems intersected by the boreholes. The estimated recovery of drilling debris in borehole KFI09 was also about 1% (Ahlbom et al., 1986).

4. Comparison of hydraulic tests before and after the gas-lift pumping

In order to quantify the effects of gas-lift pumping on the hydraulic parameters, primarily the hydraulic conductivity, single-hole injection tests were performed before and after the gas-lift pumping in borehole KFI10. To achieve the most representative conditions for comparison of the results, the tests were performed with the same equipment, by the same method, and in the same test sections. The tests are described in detail by Andersson et al. (1987).

The tests carried out prior to the gas-lift pumping were performed between November 11th and December 6th, 1985. The gas-lift pumping was made on December 10th, 1985 and the water injection tests carried out after the gas-lift pumping started on January 16th, 1986 and were completed on February 7th, 1986.

4.1 Methods and interpretation

The equipment used was the new version of the pipe string system (Almén et al., 1986a). The tests carried out prior to the gas-lift pumping had a dual purpose. Firstly, they were to be compared with tests with the umbilical hose system in the same sections. Secondly, they should also serve to allow a comparison with corresponding tests after the gas-lift pumping.

Before as well as after the gas-lift pumping, transient single-hole injection tests with constant head with two hours of injection and two hours of pressure recovery were performed in 20 m sections of borehole KFI10. In six 5 m-sections steady-state injection tests were also conducted. In this case the injection time was only 15 minutes with no pressure recovery period. Both series of tests were performed in the same test sections: eleven 20 m-sections between 10 and 230 m and a total of nine 5 m-sections: 70-75 m, 75-80 m, 95-100 m and 6 tests in the interval 205-235 m.

The transient tests before and after the gas-lift pumping were evaluated in accordance with the actual flow regime during the tests (Almén et al., 1986b). Most of the tests exhibited a spherical or steady-state flow. The hydraulic conductivity was calculated for each section for both sets of tests. In addition, the skin factor was calculated for each test section. The skin factor may be determined from the injection and recovery phases, both for pseudo-radial and spherical flow. For steady-state flow the skin factor cannot be determined.

The skin factor reflects the hydraulic conditions close to the borehole. If the borehole section is (partly) clogged, a positive value of the skin factor should result whereas a negative value should prevail if the test section is intersected by significant fractures. In addition to the hydraulic conductivity (and transmissivity) and the skin factor, the dominating flow geometry during the tests (Andersson and Persson, 1985) was interpreted for both sets of tests.

4.2 Results

The hydraulic conductivity values calculated from tests before and after the gas-lift pumping in borehole KFI10 are cross-plotted in Figure 6. As can be seen from this figure the calculated hydraulic conductivity values are very similar before and after the gas-lift pumping. All tests agree within a factor of two except in test section 210-230 m. However, due to the low injection pressures obtained in this section before and after the gas-lift pumping, both tests exceed the practical upper measurement limit of the pipe string system for a transient interpretation (Andersson et al., 1987). This 20 m-section has also been tested with successive 5 m tests. However, the sum of transmissivity from these tests is in good agreement with the total transmissivity obtained for the 20 m section.

The skin factors determined from tests before and after the gas-lift pumping are cross-plotted in Figure 7 for the same sections. This figure illustrates that the skin factors determined before and after the gas-lift pumping are rather close. The slight differences may fall within the potential error band of the interpretation. If clogging effects were significant during drilling and if the gas-lift pumping was capable of clearing the borehole sections from drilling debris, the calculated value of the skin factor would be expected to be rather high (positive) before the gas-lift pumping. The skin factor would then decrease during the pumping as a result of the clearing effect and assume a lower value after the gas-lift pumping. Provided that the hydraulic tests penetrated into the "fresh" rock fracture systems both before and after the gas-lift pumping, the calculated hydraulic conductivity values would not be expected to change significantly before and after the pumping.

As can be seen from Figure 7 there are only slight differences in the calculated skin factors. Since the skin factors generally are low (or negative) even before the gas-lift pumping, no clear indications of potential clogging effects

caused by drilling can be deduced. However, the skin factors calculated may not be indicative of permanent (non-restorable) clogging, (cf. below). Finally, the interpreted flow geometries in general, are also in close agreement between the two sets of tests.

4.3 Discussion

The results of the tests before and after the gas-lift pumping are very similar. The differences of the calculated hydraulic conductivities and skin factors are generally small. Furthermore, the interpreted flow geometries from the transient response curves are similar. Thus, the effect of the gas-lift pumping on the hydraulic parameters seems to be small. This fact may be explained in two ways. Firstly, it may be assumed that the borehole sections tested were unaffected by clogging effects even before the gas-lift pumping, which would then have a small effect on the tests after the pumping. Secondly, it may also be assumed that some of the fractures became permanently clogged by debris during drilling. The gas-lift pumping would then be incapable of clearing the fractures and only a small effect of the pumping would also be observed in this case.

In the latter case the debris may be injected so far into the rock during drilling that the skin zone created cannot be fully penetrated during the hydraulic tests. Then the skin factors determined before and after the gas-lift pumping would not be indicative of any clogging effects in fractures, since the concept of skin assumes that the skin zone is fully penetrated and the unaffected rock is reached during the test (Earlougher, 1977). Instead, the hydraulic conductivity values calculated would be less than the true conductivity representing the virgin conditions, i.e. merely representing the properties of the skin zone. If severe clogging of fractures occurred during drilling it would probably be very difficult to completely restore the natural conditions. By considering only the calculated skin factors, it is difficult to state with any confidence which of the two possibilities

discussed above is the most plausible. The results from the calculations of produced amounts of drilling debris versus recovered amounts may favour the second alternative. Further field experience on this issue is required. Transitional forms of clogging may also exist, ranging from completely restorable to permanent clogging.

5. Conclusions

The investigations show that only very small amounts (approx. 7-8%) of the total volume of flushing water used were recovered during drilling of three rotary cored boreholes at the Finnsjön site. A total loss of flushing water occurred while the fracture zones were being penetrated. The rate of water loss during drilling reflects the overall hydraulic conductivity distribution along the boreholes. The recovered amounts of drilling debris were also generally low from these boreholes, and a total loss occurred during drilling in the fracture zones. Although the proportion of recovered drilling debris was higher during air-flush percussion drilling compared to core drilling, the total amount of debris lost in the rock was also significantly higher.

During gas-lift pumping in a core drilled borehole only small proportions of flushing water were recovered, i.e. approx. 3-4% of the total volume injected into the borehole. Even smaller amounts of drilling debris (approx. 1%) were recovered. It is assumed that this amount corresponds to the debris sedimented at the bottom of the boreholes after drilling.

Furthermore, gas-lift pumping had only a minimal effect on the hydraulic parameters calculated from single-hole tests before and after the pumping. The hydraulic conductivities and skin factors calculated, as well as the flow geometries, were very similar for both sets of tests. This fact may either be explained by the inability of the gas-lift pumping to remove eventual drilling debris injected into the fractures during drilling, or alternatively, that no significant clogging

occurred before nor after the pumping. The potential effect of drilling debris on the borehole hydraulic conditions is incompletely known and should be studied further.

References

Ahlbom, K., Andersson P., Ekman, L., Gustafsson, E., Smellie, J.A.T. and Tullborg, E-L., 1986. Preliminary investigations of fracture zones in the Brändan area, Finnsjön study site. SKB Tec. Rep., (TR 86-05), Stockholm.

Ahlbom, K., Andersson, P., Ekman, L. and Tirén, S., 1987. Characterization of fracture zones within the Brändan area, Finnsjön study site. SKB Status Rep. (AR 88-09), Stockholm.

Almén, K-E., Andersson, O., Fridh, B., Johansson, B-E., Sehlstedt, M., Hansson, K., Olsson, O., Nilsson, G. and Wikberg, P., 1986. Site investigation - equipment for geological, geophysical, hydrogeological and hydrochemical characterisation. SKB Tec. Rep., (TR 86-16), Stockholm.

Almén, K-E., Andersson J-E., Carlsson, L., Hansson, K. and Larsson, N-Å., 1986. Hydraulic testing in crystalline rock. A comparative study of single-hole test methods. SKB Tec. Rep., (TR 86-27), Stockholm.

Andersson, J-E. and Persson, O., 1985. Evaluation of single hole hydraulic tests in fractured crystalline rock by steady-state and transient methods. SKB Tec. Rep., (TR 85-19), Stockholm.

Andersson, J-E., Andersson, P. and Ekman, L., 1987. Water injection tests in borehole KFI10 at the Finnsjön test site. Comparison of tests performed with two different equipment systems. The effects of gas-lift pumping on hydraulic parameters. SKB Status Rep. (AR 87-33), Stockholm.

Earlougher, R.C., 1977. Advances in well test analysis. Monograph Series. Society of Petroleum Engineers of AIME, Dallas.

Ekman, L., Andersson, J-E., Andersson, P., Carlsten, S., Eriksson, C-O., Gustafsson, E., Hansson, K. and Stenberg, L., 1988. Documentation of borehole BFI02 within the Brändan area, Finnsjön study site. SKB Status Rep. (In prep.).

Smellie, J.A.T., Larsson, N-Å., Wikberg, P. and Carlsson, L., 1985. Hydrochemical investigations in crystalline bedrock in relation to existing hydraulic conditions: Experience from the SKB test-sites in Sweden. SKB Tec. Rep., (TR 85-11), Stockholm.

Smellie, J.A.T., Gustafsson E. and Wikberg, P., 1987. Groundwater sampling during and subsequent to air-flush rotary drilling: hydrochemical investigations at depth in fractured crystalline rock. SKB Status Rep., (AR 87-31), Stockholm.

Smellie, J.A.T. and Wikberg, P., 1989. Hydrochemical investigations at Finnsjön, Sweden (This volume).

Tirén, S., 1989. Geological setting and deformational history of a low-angle fracture zone at Finnsjön, Sweden. (This volume).

Table 1 Tracers and initial concentrations (C_o).

Borehole	Tracer	C_o (ppm)
KFI05	Rhodamine WT	2
KFI06	Rhodamine WT	2
KFI09	Uranine	1.0
KFI10	Amino G Acid	2.0
KFI11	Uranine	5.0

Table 2 Approximative balance calculations of flushing water and rate of water loss in different intervals during drilling of boreholes KFI09, KFI10 and KFI11.

Borehole	Interval	Total (m^3)	Recovered (m^3)	Recovered (%)	Loss (m^3)	Loss/m (m^3/m)
KFI09	0-134	14.4	5	35	9.4	0.07
	134-375	48.1	0	0	48.1	0.20
	0-375	62.5	5	8	57.5	0.15
KFI10	0- 81	6.7	3	45	3.7	0.05
	81-255	30.5	0	0	30.5	0.18
	0-255	37.2	3	8	34.2	0.13
KFI11	0-225	26.2	4.7	18	21.5	0.10
	225-389	43.8	0	0	43.8	0.27
	0-389	70.0	4.7	7	65.3	0.17

Table 3 Recovered and lost amounts of drilling debris in different borehole intervals.

Borehole	Interval (m)	Recovered mass (kg)	Lost mass (kg)	Recovery ratio (%)	Drilling method
KFI09	0-134	not measured			DCD
	134-375	0	720	0	
KFI10	0- 81	not measured			DCD
	81-255	0	520	0	
KFI11	0-225	435	244	64	DCD
	225-389	0	489	0	
BFI01	8.4-247	11360	3180	78	AFPRD
	247-459	7164	5205	58	
BFI02	5.1-201	10400	360	97	AFPRD
	201-289	3300	1360	71	

DCD = Diamond Core Drilling
AFPRD = Air-Flush Percussion Rotary Drilling

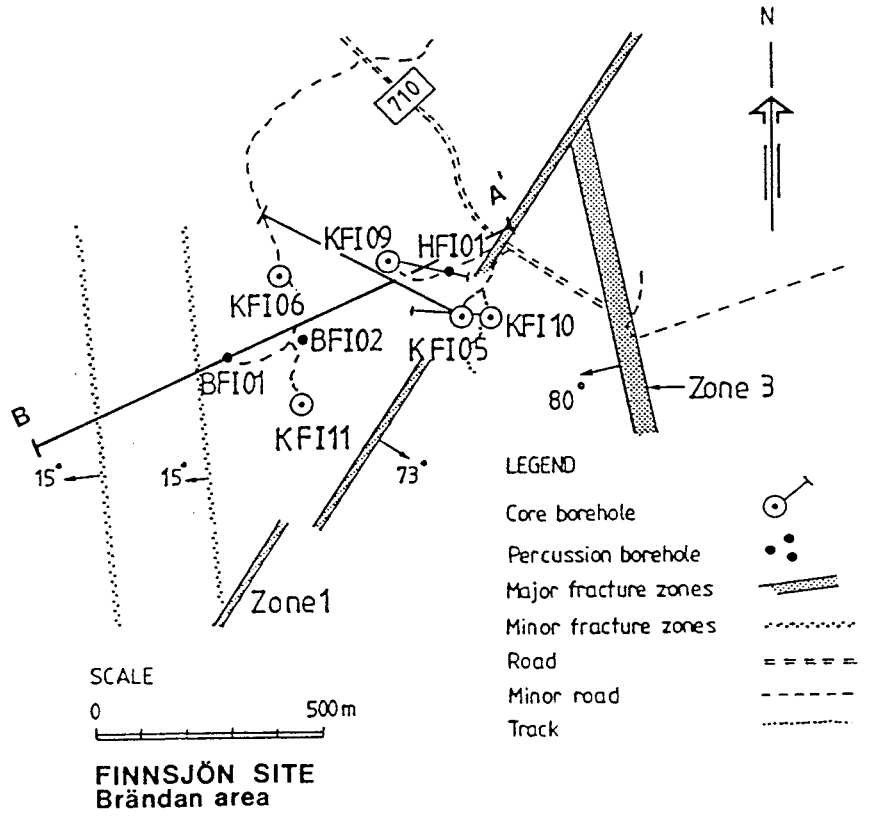

Figure 1 Borehole locations within the Brändan area.

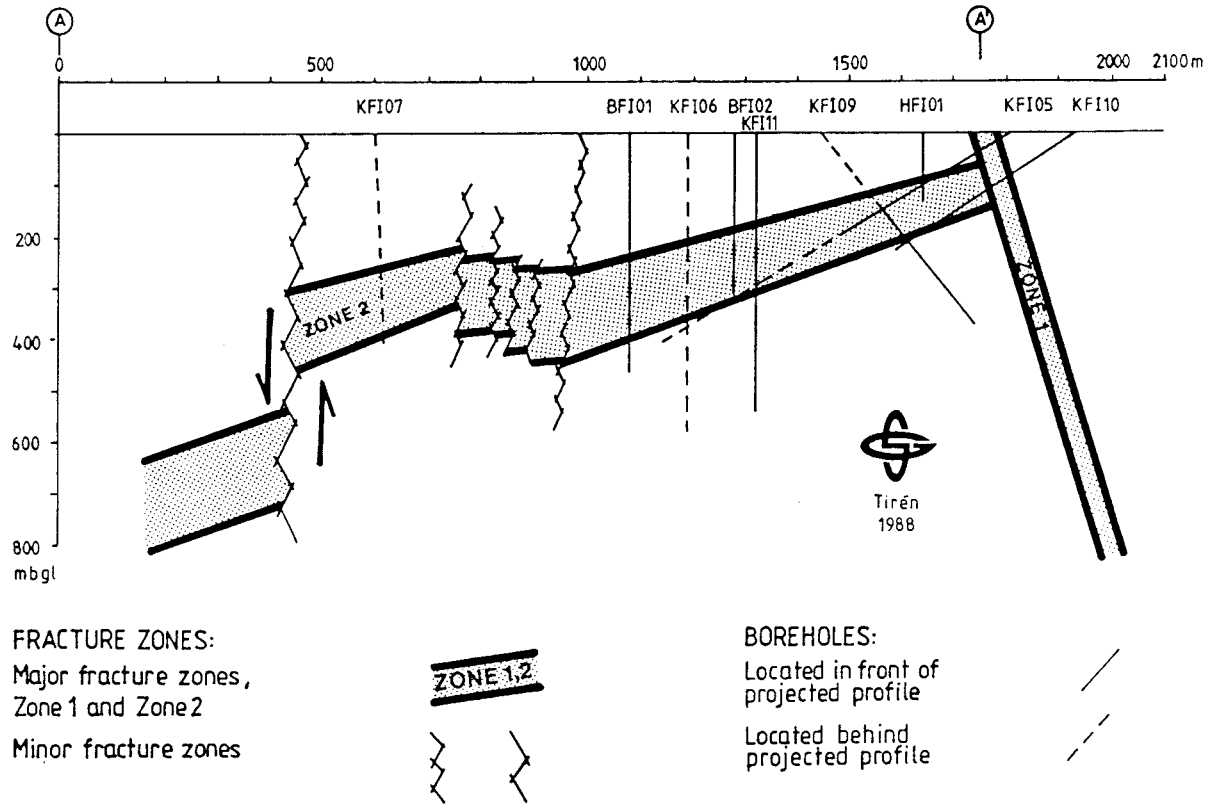

Figure 2 Schematic cross-section (B-A´) through the Brändan area.

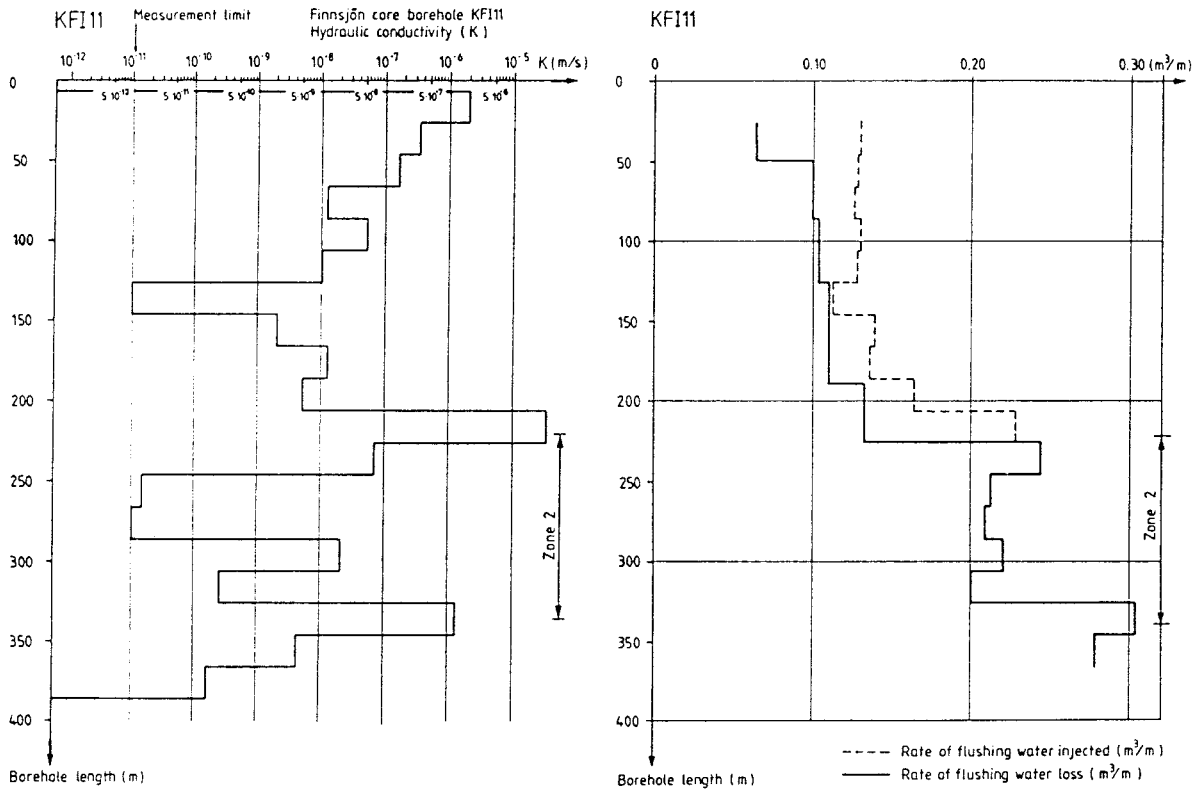

Figure 3 Flushing water loss and hydraulic conductivity versus depth in borehole KFI11.

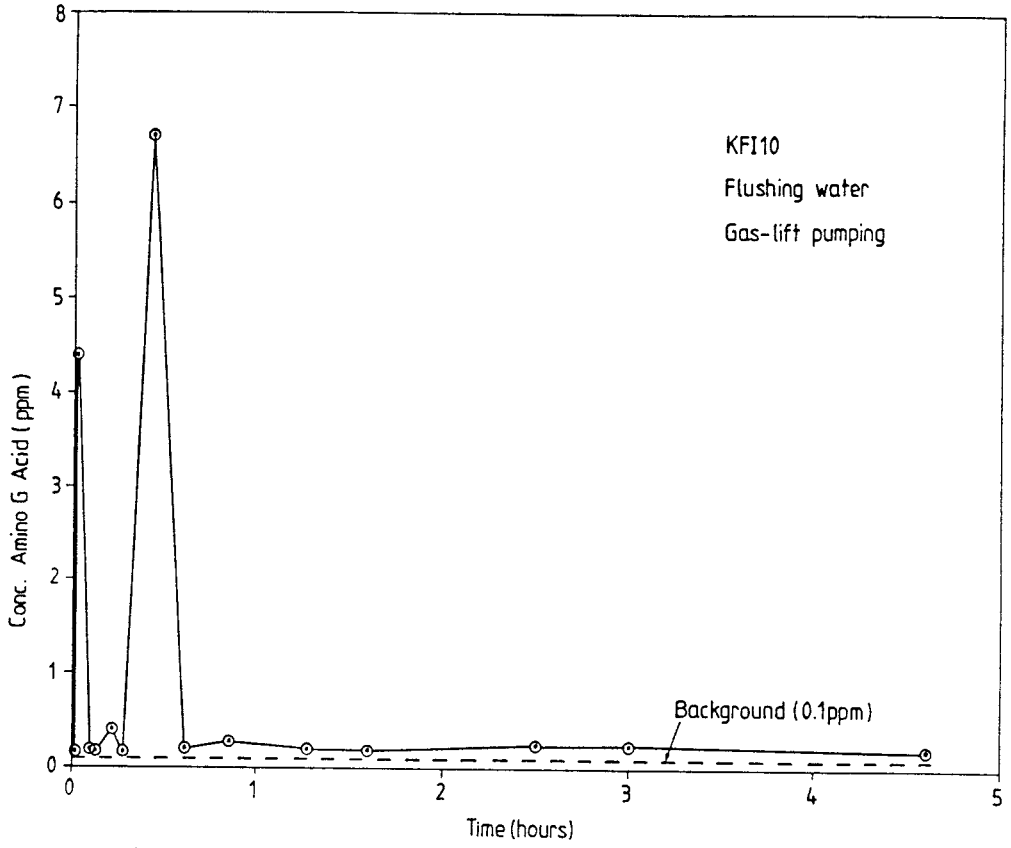

Figure 4 Concentration of Amino G Acid versus time during gas-lift pumping of KFI10.

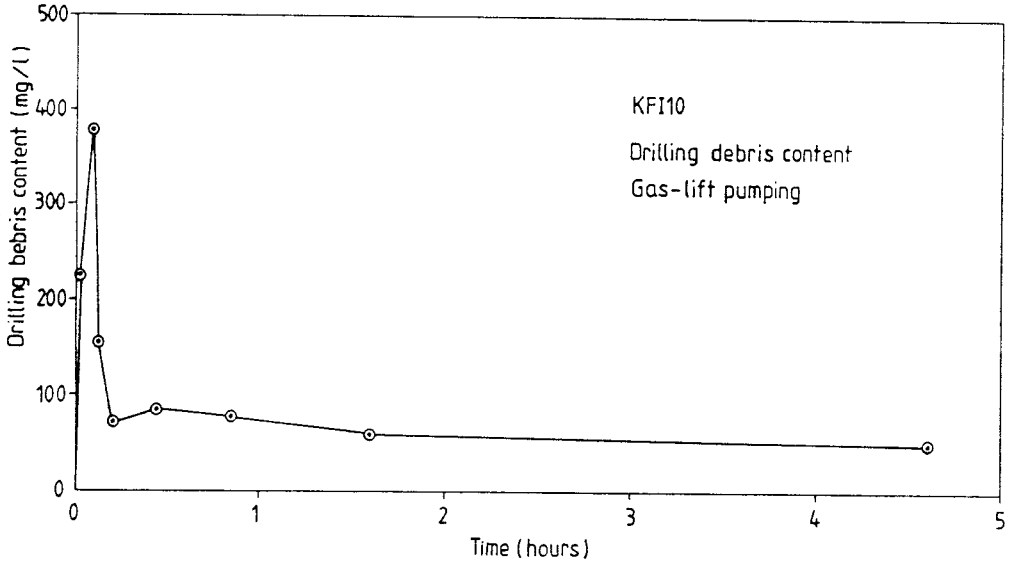

Figure 5 Drilling debris content versus time during gas-lift pumping of KFI10.

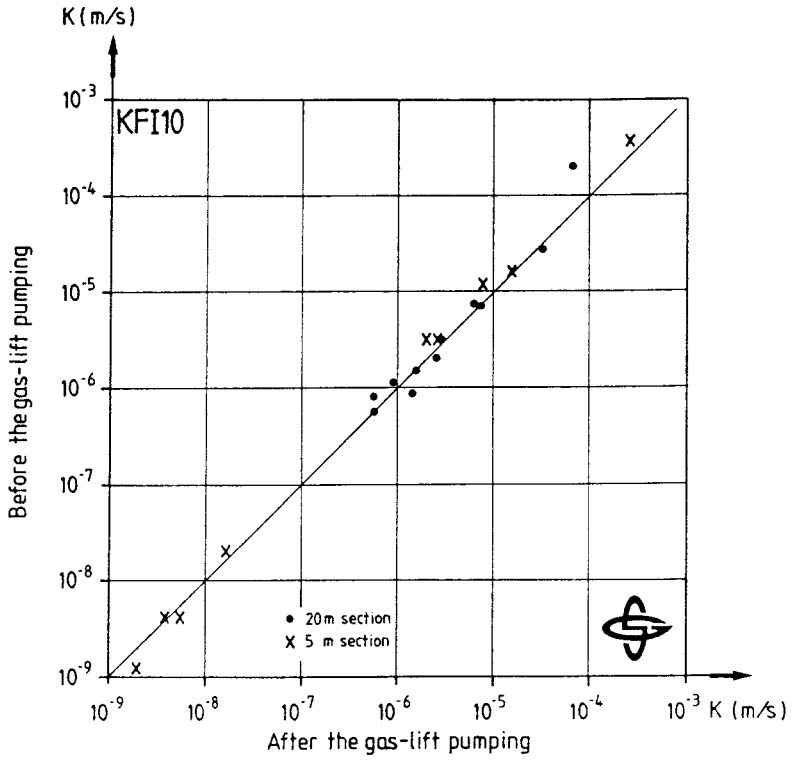

Figure 6 Cross-plot of hydraulic conductivities calculated from tests before and after gas-lift pumping.

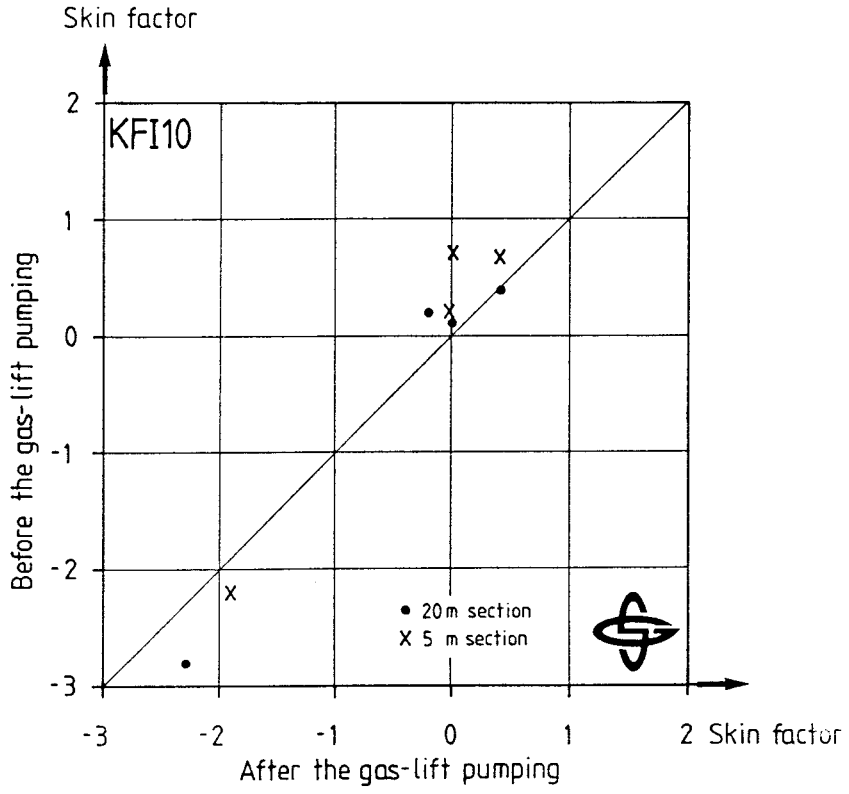

Figure 7 Cross-plot of skin factors calculated from tests before and after gas-lift pumping.

List of SKB reports

Annual Reports

1977–78
TR 121
KBS Technical Reports 1 – 120.
Summaries. Stockholm, May 1979.

1979
TR 79–28
The KBS Annual Report 1979.
KBS Technical Reports 79-01 – 79-27.
Summaries. Stockholm, March 1980.

1980
TR 80–26
The KBS Annual Report 1980.
KBS Technical Reports 80-01 – 80-25.
Summaries. Stockholm, March 1981.

1981
TR 81–17
The KBS Annual Report 1981.
KBS Technical Reports 81-01 – 81-16.
Summaries. Stockholm, April 1982.

1982
TR 82–28
The KBS Annual Report 1982.
KBS Technical Reports 82-01 – 82-27.
Summaries. Stockholm, July 1983.

1983
TR 83–77
The KBS Annual Report 1983.
KBS Technical Reports 83-01 – 83-76
Summaries. Stockholm, June 1984.

1984
TR 85–01
Annual Research and Development Report 1984
Including Summaries of Technical Reports Issued during 1984. (Technical Reports 84-01– 84-19)
Stockholm June 1985.

1985
TR 85-20
Annual Research and Development Report 1985
Including Summaries of Technical Reports Issued during 1985. (Technical Reports 85-01-85-19)
Stockholm May 1986.

1986
TR 86-31
SKB Annual Report 1986
Including Summaries of Technical Reports Issued during 1986
Stockholm, May 1987

1987
TR 87-33
SKB Annual Report 1987
Including Summaries of Technical Reports Issued during 1987
Stockholm, May 1988

1988
TR 88-32
SKB Annual Report 1988
Including Summaries of Technical Reports Issued during 1988
Stockholm, May 1989

Technical Reports

1989
TR 89-01
Near-distance seismological monitoring of the Lansjärv neotectonic fault region Part II: 1988
Rutger Wahlström, Sven-Olof Linder, Conny Holmqvist, Hans-Edy Mårtensson
Seismological Department, Uppsala University, Uppsala
January 1989

TR 89-02
Description of background data in SKB database GEOTAB
Ebbe Eriksson, Stefan Sehlstedt
SGAB, Luleå
February 1989

TR 89-03
Characterization of the morphology, basement rock and tectonics in Sweden
Kennert Röshoff
August 1988

TR 89-04
SKB WP-Cave Project
Radionuclide release from the near-field in a WP-Cave repository
Maria Lindgren, Kristina Skagius
Kemakta Consultants Co, Stockholm
April 1989

TR 89-05
SKB WP-Cave Project
Transport of escaping radionuclides from the WP-Cave repository to the biosphere
Luis Moreno, Sue Arve, Ivars Neretnieks
Royal Institute of Technology, Stockholm
April 1989

TR 89-06
SKB WP-Cave Project
Individual radiation doses from nuclides contained in a WP-Cave repository for spent fuel
Sture Nordlinder, Ulla Bergström
Studsvik Nuclear, Studsvik
April 1989

TR 89-07
SKB WP-Cave Project
Some Notes on Technical Issues
Part 1: Temperature distribution in WP-Cave: when shafts are filled with sand/water mixtures
Stefan Björklund, Lennart Josefson
Division of Solid Mechanics, Chalmers University of Technology, Gothenburg, Sweden
Part 2: Gas and water transport from WP-Cave repository Luis Moreno, Ivars Neretnieks
Department of Chemical Engineering, Royal Institute of Technology, Stockholm, Sweden
Part 3: Transport of escaping nuclides from the WP-Cave repository to the biosphere. Influence of the hydraulic cage
Luis Moreno, Ivars Neretnieks
Department of Chemical Engineering, Royal Institute of Technology, Stockholm, Sweden
August 1989

TR 89-08
SKB WP-Cave Project
Thermally incuded convective motion in groundwater in the near field of the WP-Cave after filling and closure
Polydynamics Limited, Zürich
April 1989

TR 89-09
An evaluation of tracer tests performed at Studsvik
Luis Moreno[1], Ivars Neretnieks[1], Ove Landström[2]
[1] The Royal Institute of Technology, Department of Chemical Engineering, Stockholm
[2] Studsvik Nuclear, Nyköping
March 1989

TR 89-10
Copper produced from powder by HIP to encapsulate nuclear fuel elements
Lars B Ekbom, Sven Bogegård
Swedish National Defence Research Establishment
Materials department, Stockholm
February 1989

TR 89-11
Prediction of hydraulic conductivity and conductive fracture frequency by multivariate analysis of data from the Klipperås study site
Jan-Erik Andersson[1], Lennart Lindqvist[2]
[1] Swedish Geological Co, Uppsala
[2] EMX-system AB, Luleå
February 1988

TR 89-12
Hydraulic interference tests and tracer tests within the Brändan area, Finnsjön study site The Fracture Zone Project – Phase 3
Jan-Erik Andersson, Lennart Ekman, Erik Gustafsson, Rune Nordqvist, Sven Tirén
Swedish Geological Co, Division of Engineering Geology
June 1988

TR 89-13
Spent fuel
Dissolution and oxidation
An evaluation of literature data
Bernd Grambow
Hanh-Meitner-Institut, Berlin
March 1989

TR 89-14
The SKB spent fuel corrosion program Status report 1988
Lars O Werme[1], Roy S Forsyth[2]
[1] SKB, Stockholm
[2] Studsvik AB, Nyköping
May 1989

TR 89-15
Comparison between radar data and geophysical, geological and hydrological borehole parameters by multivariate analysis of data
Serje Carlsten, Lennart Lindqvist, Olle Olsson
Swedish Geological Company, Uppsala
March 1989

TR 89-16
Swedish Hard Rock Laboratory – Evaluation of 1988 year pre-investigations and description of the target area, the island of Äspö
Gunnar Gustafsson, Roy Stanfors, Peter Wikberg
June 1989

TR 89-17

Field instrumentation for hydrofracturing stress measurements
Documentation of the 1000 m hydrofracturing unit at Luleå University of Technology

Bjarni Bjarnason, Arne Torikka
August 1989

TR 89-18

Radar investigations at the Saltsjötunnel – predicitions and validation

Olle Olsson[1] and Kai Palmqvist[2]
[1] Abem AB, Uppsala, Sweden
[2] Bergab, Göteborg
June 1989